Aberrant IL7R signaling:

the paths towards steroid resistance in pediatric T-cell acute lymphoblastic leukemia

Jordy C.G. van der Zwet

Aberrant IL7R signaling: the paths towards steroid resistance in pediatric T-cell acute lymphoblastic leukemia

Jordy C.G. van der Zwet

ISBN: 978-94-6458-129-4

Provided by thesis specialist Ridderprint, ridderprint.nl
Printing: Ridderprint
Cover design: Evelien Jagtman
Layout and design: Eduard Boxem, persoonlijkproefschrift.nl

Aberrant IL7R signaling: the paths towards steroid resistance
in pediatric T-cell acute lymphoblastic leukemia

Abberante IL7R signalering: de paden naar steroid resistentie
in kinderen met T-cell acute lymfatische leukemie

(met een samenvatting in het Nederlands)

Proefschrift

ter verkrijging van de graad van doctor aan de Universiteit Utrecht
op gezag van de rector magnificus, prof.dr. H.R.B.M. Kummeling, ingevolge het
besluit van het college voor promoties in het openbaar te verdedigen op
maandag 4 april 2022 des ochtend te 10:15 uur.

door

Jordy Clemens Gerardus van der Zwet

geboren op 21 februari 1992
te Rotterdam

Promotor:

Prof. dr. R. Pieters

Copromotor:

Dr. J.P.P. Meijerink

Dit proefschrift werd mede mogelijk gemaakt met financiele steun van NTRC
(Netherlands Translational Research Center) te Oss.

TABLE OF CONTENTS

1

Introduction

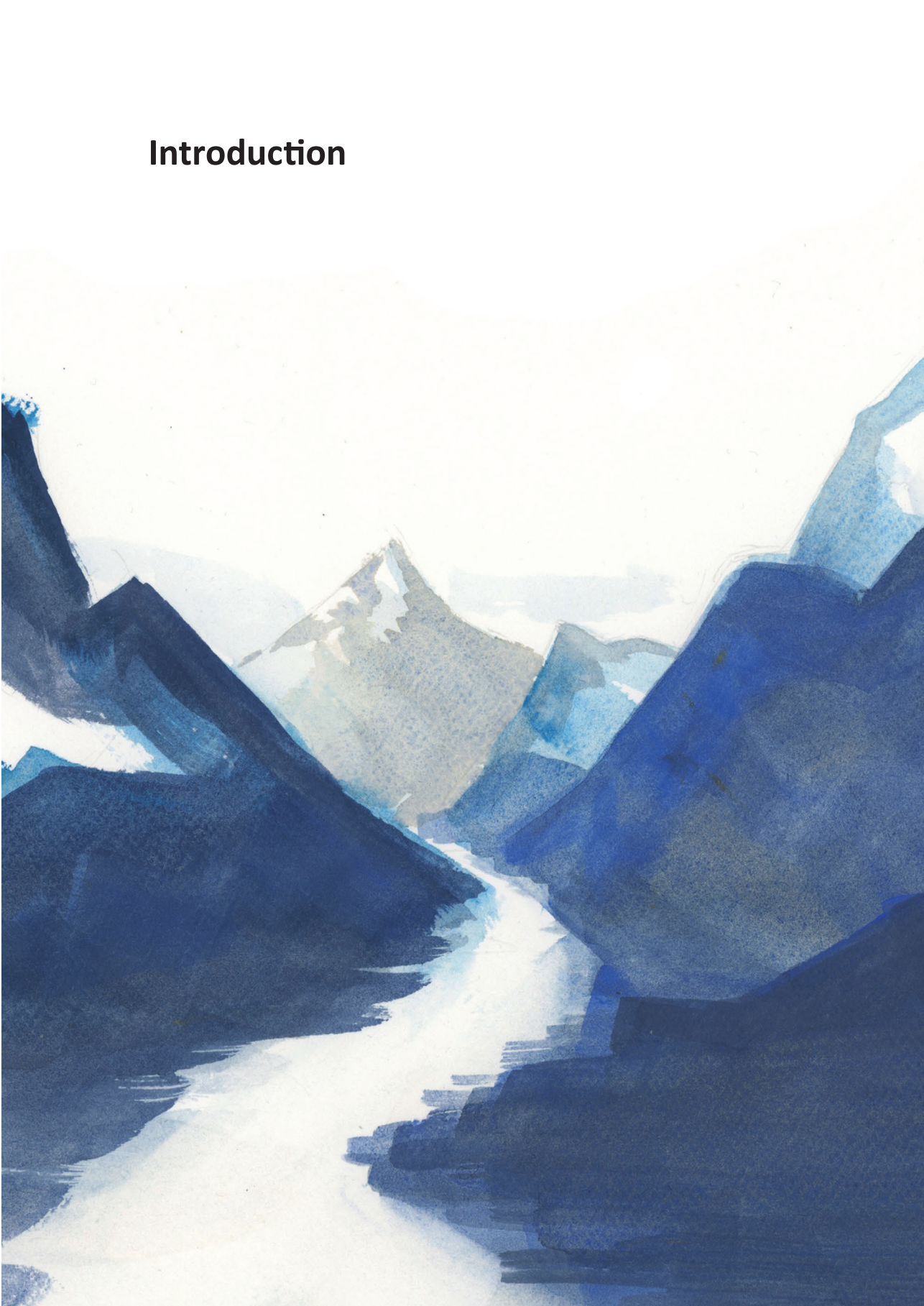

Hematopoiesis and T-cell development

The production of blood cells (hematopoiesis) is directed by a complex, yet organized network of signals, which starts with the division of pluripotent hematopoietic stem cells (HSCs) into lymphoid or myeloid progenitor cells [reviewed in (1)]. Supported and directed by environmental stimuli, these progenitor cells can further differentiate into functional blood cells of different lineages: i) myeloid progenitor cells can differentiate into red blood cells (erythrocytes), platelets (thrombocytes) and a subset of white blood cells (leukocytes) named granulocytes and monocytes, and ii) lymphoid progenitor cells can differentiate into either B- or T-lymphocytes; the agranular leukocytes that play a vital role in the human adaptive immune system.

Lymphoid progenitor cells can differentiate into mature T-cells trough the controlled, and sequential or simultaneous activation of T-cell specific genes by stimuli from the thymic microenvironment. In contrast, some genes become downregulated once the maturing T-cell successfully passes a certain differentiation step. The T-cell developmental stages within the thymus can be roughly divided into three major clusters: i) pre-T-cell committed (multipotent) cells including early T-cell progenitor cells (ETP-cells), ii) T-cell lineage committed cells that yet have to rearrange their T-cell receptor (TCR), and iii) TCR-rearranged T-cells [reviewed in (2)]. Within these clusters, smaller T-cell subsets can be distinguished based on the (co-)expression of specific cluster of differentiation (CD) markers on surface of T-cells. After successful completion of all differentiation steps, mature T-cells expressing either CD4 or CD8 leave the thymic medulla and migrate back into the peripheral blood stream to fulfill their role as functional immune cells [reviewed in (3)].

IL7R signaling in T-cell development

The graduate differentiation of intra-thymic T-cells is dependent on the presence and activation of various surface receptors and specific transcription factor genes. One of these surface receptors is the IL-7 receptor (IL7R), which can be activated by IL-7; a supporting cytokine produced by the thymic microenvironment. Interaction between IL-7 and the IL7Rα chain induces heterodimerization of the IL7Rα and γc chains, subsequently activating downstream JAK-STAT and PI3K-AKT cellular signaling pathways. These pathways (partially) facilitate the pro-survival phenotype of IL-7 activated cells by upregulation of anti-apoptotic BCL2 [reviewed in (4)]. IL7R is upregulated after the ETP-stage of T-cell development where its activation is vital for the proliferative expansion of ‘early pro-T-cells’ (late cluster i) and the survival of TCR-rearranging T-cells (cluster ii). In contrast, downregulation of IL7R in ETP-cells (early cluster i) and selected TCR-rearranged T-cells (cluster iii) is important to negatively select multipotent cells, and to allow differentiation towards functional and non-autoreactive CD4+ or CD8+ TCR-rearranged T-cells respectively [reviewed in (5)]. The differences in IL7R expression at consecutive T-cell maturation stages exemplify how surface receptors facilitate the selection and differentiation of T-cells. In addition to IL7R signaling, T-cell development

mainly depends on the NOTCH- and TCR-regulated signaling programs at specific stages of T-cell development.

Leukemogenesis and clinical characteristics

During cell differentiation and maturation, genetic errors can occur in developing leukocytes. Intrinsic and extrinsic defense mechanisms usually repair these mistakes or force defective cells into programmed cell death (apoptosis). Some mistakes however are preserved and/or potentiate a fitness advantage. When erroneous (pre-leukemic) leukocytes acquire the potential for uncontrolled cell growth and survival, leukemia arises [reviewed in (6)]. Although the acquirement of these genetic hits seems a matter of 'bad luck', it has become evident that inadequate (early) training of the immune system and (delayed) exposure to common childhood infection(s) play a role in leukemogenesis [reviewed in (7)].

Leukemia is the most common form of childhood cancer, accounting for nearly 28% of all pediatric malignancies under the age of 19 in the Netherlands (Stichting Kinderoncologie Nederland (SKION) 2003-2019 registration). Other pediatric malignancies include tumors of the central nervous system (21,6%), lymphomas (11,9%), soft tissue tumors or extraosseous sarcomas (6,6%), malignant bone tumors (5,7%), germ cell tumors (5,5%), neuroblastomas (5,3%) and renal tumors (4,7%) (SKION 2003-2019). Leukemia can originate from the lymphoid or myeloid leukocyte lineage (i.e. lymphoid leukemia versus myeloid leukemia respectively). Moreover, its onset can be rapid or slowly progressing (i.e. acute versus chronic leukemia respectively). Children predominantly present with a fast and acute expansion of leukemic blasts, which in 80% of the cases arises from the lymphoid lineage (acute lymphoblastic leukemia; ALL) (8). In 85% of pediatric ALL patients, leukemia evolves from malignant B-cell precursor lymphocytes (BCP-ALL). In the remaining 15%, ALL arises from the T-cell lineage and is therefore classified as T-cell acute lymphoblastic leukemia (T-ALL) (6). In adults, leukemia is usually slowly progressive, with chronic myeloid leukemia (CML) being the most common subtype.

Malignant expansion of 'leukemic blasts' in the bone marrow severely oppress the production of healthy erythrocytes, leukocytes and thrombocytes, which causes symptoms like fatigue, (opportunistic) infections and/or (small) hemorrhages of the skin or gums. Additionally, dissemination of leukemic cells to extra-medullary sites can cause enlargement of the liver and spleen (hepatosplenomegaly), mediastinum and lymph nodes (lymphadenopathy), or can lead to leukemic infiltration in the central nervous system (CNS), the testis and/or periosteum.

Treatment and prognosis of acute lymphoblastic leukemia

Cytostatic and cytotoxic drugs used in the Dutch Childhood Oncology Group (DCOG) ALL-11 treatment protocol include microtubules-destabilizing agents (vincristine), alkylating agents (cyclophosphamide), anthracyclines (doxorubicin, daunorubicin), anti-

metabolites (methotrexate), nucleoside analogues (6-mercaptopurine, thioguanine, cytarabine) and synthetic steroids (prednisolone and dexamethasone). The ALL-11 protocol is divided into four major treatment phases over a course of at least 2 years. The first (induction) phase starts with 7 days of systemic treatment with high-dose prednisolone. The 'prednisolone response' (i.e. how many leukemic blasts are left in the peripheral blood stream after 7 days of prednisolone treatment) is an important prognostic parameter, since a 'poor prednisolone response' is associated with inferior outcome (9, 10). Other critical risk-stratification markers include minimal residue disease (MRD) at day 33 and 79 of treatment and CNS involvement. Based on these risk-stratification markers, patients are assigned to the standard, medium or high-risk treatment arm, whereas treatment in the remaining phases is most intensive in the high-risk treatment arm. Although T-ALL patients represent only 15% of ALL patients, they comprised nearly 50% of all patients treated on ALL-10 high-risk treatment regimens (11). This disproportional distribution was likely caused by the high frequency of poor-prednisolone responders in the T-ALL patient group and the high proportion of patients with high MRD at day 79, which stratified patients to the high-risk arm (12, 13). In the ALL-11 protocol, a poor-prednisolone response excludes enrollment in the standard risk group and therefore still mandates for more intensive treatment with an associated risk for treatment-related morbidity and mortality.

Over the last decades, improved treatment regimens and risk-stratification have drastically improved the outcome of pediatric ALL patients to a 5-year overall survival (OS) of 91% (11, 14). Unfortunately, the outcome for T-ALL patients only slightly improved over the last two decades and is still inferior compared to the outcome of BCP-ALL patients (5-year OS 81% versus 93% respectively) (14, 15). This means that one out of five children with T-ALL still succumb due to relapsed or refractory disease. When T-ALL relapses despite intensive treatment, the leukemia is usually extremely chemo-resistant, resulting in a dismal outcome due to limited treatment options.Additional research is required to understand why T-ALL patients have an inferior outcome, and how treatment can be improved for this high-risk leukemic subgroup.

The role of aberrant IL7R signaling in T-cell acute lymphoblastic leukemia

T-ALL arises when genetic aberrations occur in genes involved in T-cell lineage-commitment or differentiation, whereas two types of genetic aberrations can be distinguished [reviewed in (16)]; 'Type A genetic aberrations' are driving and predominantly mutually exclusive genetic events. These aberrations mainly involve rearrangements and mutations of *MEF2C*, *HOXA*, *TLX3*, *MYB*, *TLX1*, *NKX2.1/NKX2.2*, *TAL1* or *LMO2* T-cell specific (onco)genes and facilitate a differentiation arrest at a specific stage of T-cell development (17, 18). Based on distinctive gene expression profiles, these aberrations delineate specific T-ALL subtypes: immature (ETP-ALL), TLX3, TLX1/NKX2 and TAL/LMO subtypes. 'Type B genetic aberrations' are considered as supporting genetic events that affect genes involved in cell cycle, self-renewal, TCR-signaling, differentiation

and tyrosine kinase activation. These aberrations are not mutually exclusive, although some type B events occur more frequently in specific subgroups (19). For example: mutations in *IL7Rα* or downstream signaling molecules are predominantly found ETP- and TLX3-rearranged T-ALL, and less commonly in mature T-ALL subtypes (20-22). The combination of type A and B aberrations facilitate a differentiation arrest and survival advantage of leukemic cells, leading to the malignant expansion of immature leukocytes. The expansion of T-ALL cells can also be supported by cytokines, including IL-7 [reviewed in (23)].

Over the last decade, multiple sequencing studies identified the most recurrent 'type B' genetic alterations in T-ALL (24-28). While mutations can be present in the majority of leukemic cells (clonal mutations), some mutations only occur in a very small percentage of the leukemic cells of a patient (subclonal mutations). Interestingly, the presence of certain mutations at diagnosis and/or relapse predict for outcome and chemo-sensitivity (29-32). In addition, some transcriptional abnormalities are related to treatment resistance, including an impaired transcriptional upregulation of pro-apoptotic *BIM* (a direct transcriptional target of the glucocorticoid receptor, which is pivotal for steroid-induced cell death) and high *BCL2* expression (a hallmark of ETP-ALL) in steroid resistant T-ALL (33-37).

Recently, our group performed whole-genome sequencing followed by target-exome sequencing in 146 pediatric T-ALL patients (30). This study identified that mutations in the IL7R signaling pathway (i.e. mutations of the IL7Rα chain and downstream signaling molecules like JAK1, JAK3, STAT5, AKT and RAS) were present in nearly 35% of T-ALL patients. Importantly, the presence of these mutations correlated with inferior relapse-free survival and steroid resistance. Of these mutations, *RAS* and *IL7R* mutations at relapse predict for extremely poor outcome (31). Mutations of the IL7R signaling pathway activate downstream JAK-STAT, PI3K-AKT and MAPK-ERK signaling pathways. How these genetic aberrations or activation of (specific) downstream signaling pathways contribute to steroid resistance in T-ALL is poorly understood. Additionally, physiological activation of the IL7R by IL-7 can also activate these pathways and provoke steroid resistance in T-ALL (38-40). The prognostic and therapeutic impact of aberrant IL7R signaling in T-ALL warrants further elucidation of this signaling cascade to identify its vulnerabilities for targeted therapy.

Outline of this manuscript

Physiological IL7R signaling is pivotal for the successful differentiation of healthy, immature T-cells. However, aberrant activation of this pathway in leukemic T-cells facilitates leukemogenesis and steroid resistance and contributes to the poor prognostic phenotype of T-ALL. Therefore, this thesis focuses on the molecular mechanisms that drive steroid resistance in IL7R signaling pathway mutated T-ALL patients. By dissecting the IL7R signaling cascade, we study the contribution of each individual downstream

signaling pathway to steroid resistance (**Figure 1**). By precisely unraveling the resistance mechanisms of these *paths*, we aim to identify targets for targeted therapy, which ultimately can improve current treatment strategies.

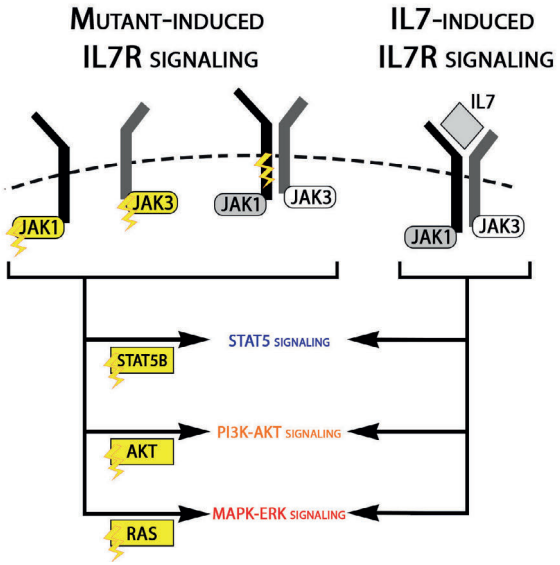

Schematic overview of mutant- and IL7-induced IL7R signaling in T-ALL. *Activating IL7R signaling mutations (i.e. mutations of the IL7Rα chain and downstream signaling molecules like JAK1, JAK3, STAT5, AKT and ERK) activate downstream STAT5, PI3K-AKT and MAPK-ERK cascades in a ligand-independent fashion (19, 30). Additionally, IL7-induced signaling also activates these downstream signaling pathways (37-39, and chapter 4 of this thesis).*

This thesis starts by providing an extensive review on all novel treatment options for T-ALL that are currently studied in a clinical or pre-clinical setting (**chapter 2**). This review includes the possible application of non-contemporary chemotherapeutics (nelarabine), immune-modulating strategies (monoclonal antibodies and CAR-T cells) and targeted small molecule inhibitors (like JAK-, MEK- and AKT-inhibitors). The extensive number of promising compounds and strategies immediately raise important questions: how do we test all novel treatment options in a limited number of patients, which patient would benefit more from drug A than drug B, and is the new drug more or less effective in combination with other (contemporary) compounds? For T-ALL patients that harbor mutations in the IL7R signaling pathway, we try to answer these and other questions in the following chapters.

In **chapter 3**, we assess the role of deletions and mutations in *NR3C1* in diagnostic T-ALL patient samples. *NR3C1* encodes for the glucocorticoid receptor, and its functionality is essential for steroid-induced cell death. In this chapter, we observe a relation between

NR3C1 aberrations and steroid resistance at disease diagnosis. Therefore, we studied the causal role of these aberrations in steroid resistance in the REH cell line model which lacks a functional NR3C1.

From **chapter 4** and onwards, we focus on aberrant IL7R signaling and study how mutations in this signaling pathway provoke steroid resistance. Chapter 4 uncovers the yet unrecognized role of MAPK-ERK signaling in steroid-resistant T-ALL. We demonstrate that mutant- or IL-7 activated MAPK-ERK signaling inactivate the pro-apoptotic molecule BIM and explored the mechanism in which this leads to steroid resistance. This chapter further elucidates the effectiveness of MEK-inhibitors and JAK1/2-inhbition to restore steroid responsiveness in steroid resistant (and MAPK-ERK activated) leukemia. Based on these results, we make important clinical recommendations for the application of MEK-inhibitors to steroid treatment in current trials and future treatment regimens.

Since functional BIM inhibits the function of anti-apoptotic Bcl2- protein family members BCL2, BCLXL and MCL1, we explore the role of these anti-apoptotic proteins in steroid-resistant T-ALL in **chapter 5**. We specifically focus on the dynamic interplay between these pro- and anti-apoptotic molecules, and observe that changes in this balance affect steroid-induced cell death. Moreover, we study the effectiveness of anti-apoptotic directed compounds (e.g. BH3-mimetics) compared to- and combined with MEK-inhibitors to improve steroid sensitivity in T-ALL.

Thus far, 'IL7-dependent' steroid resistance has been attributed to activated JAK-STAT5 signaling and subsequent upregulation of *BCL2*. Since IL-7 also induces PI3K-AKT signaling (this introduction) and MAPK-ERK signaling (chapter 4) in T-ALL, we study the specific contribution of active STAT5B signaling to steroid resistance in **chapter 6**. This chapter controversially demonstrates that isolated activation of STAT5B does not provoke steroid resistance, despite activation of various pro-survival or anti-apoptotic molecules like PIM1, and BCL2 and BCLXL respectively. Moreover, we uncover a novel, direct mechanism in which NR3C1 can influence the expression of STAT5 regulated genes.

In **chapter 7**, we study the last of three signaling pathways downstream of the IL7R: the PI3K-AKT pathway. When studying differences between wild type and mutant AKT overexpressing cell lines, we demonstrate that the cellular localization and activation mechanisms of AKT differ between both lines. Additionally, we demonstrate that these differences reflect on AKT-inhibitor sensitivity and steroid responsiveness.

Last, we reviewed the literature on how multi-omics (the integration of genomic, transcriptomic and proteomic approaches) can contribute to the precise clinical application of novel inhibitors for T-ALL patients. **Chapter 8** highlights that mutation-based patient stratification is insufficient for future personalized medicine strategies.

Importantly, this last chapter concludes how findings from pre-clinical research, as presented in chapter 4 to 7, can be translated into clinical trials and future treatment protocols to ultimately improve the outcome of pediatric T-ALL patients.

In **chapter 9**, the results and recommendations described in the previous chapters will be discussed and summarized. In the **appendices**, a layman's summary of the described work in Dutch is provided.

REFERENCES

1. Orkin SH, Zon LI. Hematopoiesis: an evolving paradigm for stem cell biology. Cell. 2008;132(4):631-44.
2. Yui MA, Rothenberg EV. Developmental gene networks: a triathlon on the course to T cell identity. Nat Rev Immunol. 2014;14(8):529-45.
3. Bonilla FA, Oettgen HC. Adaptive immunity. J Allergy Clin Immunol. 2010;125(2 Suppl 2):S33-40.
4. Jiang Q, Li WQ, Aiello FB, Mazzucchelli R, Asefa B, Khaled AR, et al. Cell biology of IL-7, a key lymphotrophin. Cytokine Growth Factor Rev. 2005;16(4-5):513-33.
5. Hong C, Luckey MA, Park JH. Intrathymic IL-7: the where, when, and why of IL-7 signaling during T cell development. Semin Immunol. 2012;24(3):151-8.
6. Pui CH, Robison LL, Look AT. Acute lymphoblastic leukaemia. Lancet. 2008;371(9617):1030-43.
7. Greaves M. Author Correction: A causal mechanism for childhood acute lymphoblastic leukaemia. Nat Rev Cancer. 2018;18(8):526.
8. Coebergh JW, Reedijk AM, de Vries E, Martos C, Jakab Z, Steliarova-Foucher E, et al. Leukaemia incidence and survival in children and adolescents in Europe during 1978-1997. Report from the Automated Childhood Cancer Information System project. Eur J Cancer. 2006;42(13):2019-36.
9. Riehm H, Reiter A, Schrappe M, Berthold F, Dopfer R, Gerein V, et al. [Corticosteroid-dependent reduction of leukocyte count in blood as a prognostic factor in acute lymphoblastic leukemia in childhood (therapy study ALL-BFM 83)]. Klinische Padiatrie. 1987;199(3):151-60.
10. Lauten M, Moricke A, Beier R, Zimmermann M, Stanulla M, Meissner B, et al. Prediction of outcome by early bone marrow response in childhood acute lymphoblastic leukemia treated in the ALL-BFM 95 trial: differential effects in precursor B-cell and T-cell leukemia. Haematologica. 2012;97(7):1048-56.
11. Pieters R, de Groot-Kruseman H, Van der Velden V, Fiocco M, van den Berg H, de Bont E, et al. Successful Therapy Reduction and Intensification for Childhood Acute Lymphoblastic Leukemia Based on Minimal Residual Disease Monitoring: Study ALL10 From the Dutch Childhood Oncology Group. J Clin Oncol. 2016;34(22):2591-601.
12. Kaspers GJ, Pieters R, Van Zantwijk CH, Van Wering ER, Van Der Does-Van Den Berg A, Veerman AJ. Prednisolone resistance in childhood acute lymphoblastic leukemia: vitro-vivo correlations and cross-resistance to other drugs. Blood. 1998;92(1):259-66.
13. Conter V, Valsecchi MG, Parasole R, Putti MC, Locatelli F, Barisone E, et al. Childhood high-risk acute lymphoblastic leukemia in first remission: results after chemotherapy or transplant from the AIEOP ALL 2000 study. Blood. 2014;123(10):1470-8.
14. Reedijk AMJ, Coebergh JWW, de Groot-Kruseman HA, van der Sluis IM, Kremer LC, Karim-Kos HE, et al. Progress against childhood and adolescent acute lymphoblastic leukaemia in the Netherlands, 1990-2015. Leukemia. 2020.
15. de Bruin O, Hagleitner MM, de Groot-Kruseman HA, Fiocco M, Karim-Kos HE, Pieters R. Outcome for Childhood T-cell Acute Lymphoblastic Leukemia (T-ALL) in the Netherlands: a Population-based study over 24-years Unpublished. 2021.
16. Van Vlierberghe P, Pieters R, Beverloo HB, Meijerink JP. Molecular-genetic insights in paediatric T-cell acute lymphoblastic leukaemia. Br J Haematol. 2008;143(2):153-68.
17. Ferrando AA, Neuberg DS, Staunton J, Loh ML, Huard C, Raimondi SC, et al. Gene expression signatures define novel oncogenic pathways in T cell acute lymphoblastic leukemia. Cancer Cell. 2002;1(1):75-87.

18. Homminga I, Pieters R, Langerak AW, de Rooi JJ, Stubbs A, Verstegen M, et al. Integrated transcript and genome analyses reveal NKX2-1 and MEF2C as potential oncogenes in T cell acute lymphoblastic leukemia. Cancer Cell. 2011;19(4):484-97.
19. Liu Y, Easton J, Shao Y, Maciaszek J, Wang Z, Wilkinson MR, et al. The genomic landscape of pediatric and young adult T-lineage acute lymphoblastic leukemia. Nat Genet. 2017;49(8):1211-8.
20. Cante-Barrett K, Spijkers-Hagelstein JA, Buijs-Gladdines JG, Uitdehaag JC, Smits WK, van der Zwet J, et al. MEK and PI3K-AKT inhibitors synergistically block activated IL7 receptor signaling in T-cell acute lymphoblastic leukemia. Leukemia. 2016;30(9):1832-43.
21. Zhang J, Ding L, Holmfeldt L, Wu G, Heatley SL, Payne-Turner D, et al. The genetic basis of early T-cell precursor acute lymphoblastic leukaemia. Nature. 2012;481(7380):157-63.
22. Zenatti PP, Ribeiro D, Li W, Zuurbier L, Silva MC, Paganin M, et al. Oncogenic IL7R gain-of-function mutations in childhood T-cell acute lymphoblastic leukemia. Nat Genet. 2011;43(10):932-9.
23. Barata JT, Durum SK, Seddon B. Flip the coin: IL-7 and IL-7R in health and disease. Nat Immunol. 2019;20(12):1584-93.
24. Armstrong SA, Look AT. Molecular genetics of acute lymphoblastic leukemia. J Clin Oncol. 2005;23(26):6306-15.
25. Belver L, Ferrando A. The genetics and mechanisms of T cell acute lymphoblastic leukaemia. Nat Rev Cancer. 2016;16(8):494-507.
26. Iacobucci I, Mullighan CG. Genetic Basis of Acute Lymphoblastic Leukemia. J Clin Oncol. 2017;35(9):975-83.
27. Van Vlierberghe P, Ferrando A. The molecular basis of T cell acute lymphoblastic leukemia. J Clin Invest. 2012;122(10):3398-406.
28. Meijerink JP, den Boer ML, Pieters R. New genetic abnormalities and treatment response in acute lymphoblastic leukemia. Semin Hematol. 2009;46(1):16-23.
29. Gutierrez A, Sanda T, Grebliunaite R, Carracedo A, Salmena L, Ahn Y, et al. High frequency of PTEN, PI3K, and AKT abnormalities in T-cell acute lymphoblastic leukemia. Blood. 2009;114(3):647-50.
30. Li Y, Buijs-Gladdines JG, Cante-Barrett K, Stubbs AP, Vroegindeweij EM, Smits WK, et al. IL-7 Receptor Mutations and Steroid Resistance in Pediatric T cell Acute Lymphoblastic Leukemia: A Genome Sequencing Study. PLoS Med. 2016;13(12):e1002200.
31. Richter-Pechanska P, Kunz JB, Hof J, Zimmermann M, Rausch T, Bandapalli OR, et al. Identification of a genetically defined ultra-high-risk group in relapsed pediatric T-lymphoblastic leukemia. Blood Cancer J. 2017;7(2):e523.
32. Jenkinson S, Koo K, Mansour MR, Goulden N, Vora A, Mitchell C, et al. Impact of NOTCH1/FBXW7 mutations on outcome in pediatric T-cell acute lymphoblastic leukemia patients treated on the MRC UKALL 2003 trial. Leukemia. 2013;27(1):41-7.
33. Bachmann PS, Gorman R, Papa RA, Bardell JE, Ford J, Kees UR, et al. Divergent mechanisms of glucocorticoid resistance in experimental models of pediatric acute lymphoblastic leukemia. Cancer Res. 2007;67(9):4482-90.
34. Bachmann PS, Piazza RG, Janes ME, Wong NC, Davies C, Mogavero A, et al. Epigenetic silencing of BIM in glucocorticoid poor-responsive pediatric acute lymphoblastic leukemia, and its reversal by histone deacetylase inhibition. Blood. 2010;116(16):3013-22.
35. Jing D, Bhadri VA, Beck D, Thoms JA, Yakob NA, Wong JW, et al. Opposing regulation of BIM and BCL2 controls glucocorticoid-induced apoptosis of pediatric acute lymphoblastic leukemia cells. Blood. 2015;125(2):273-83.
36. Jing D, Huang Y, Liu X, Sia KCS, Zhang JC, Tai X, et al. Lymphocyte-Specific Chromatin Accessibility Pre-determines Glucocorticoid Resistance in Acute Lymphoblastic Leukemia. Cancer Cell. 2018;34(6):906-21 e8.

37. Chonghaile TN, Roderick JE, Glenfield C, Ryan J, Sallan SE, Silverman LB, et al. Maturation stage of T-cell acute lymphoblastic leukemia determines BCL-2 versus BCL-XL dependence and sensitivity to ABT-199. Cancer Discov. 2014;4(9):1074-87.
38. Delgado-Martin C, Meyer LK, Huang BJ, Shimano KA, Zinter MS, Nguyen JV, et al. JAK/STAT pathway inhibition overcomes IL7-induced glucocorticoid resistance in a subset of human T-cell acute lymphoblastic leukemias. Leukemia. 2017;31(12):2568-76.
39. Meyer LK, Huang BJ, Delgado-Martin C, Roy RP, Hechmer A, Wandler AM, et al. Glucocorticoids paradoxically facilitate steroid resistance in T cell acute lymphoblastic leukemias and thymocytes. J Clin Invest. 2020;130(2):863-76.
40. Barata JT, Silva A, Brandao JG, Nadler LM, Cardoso AA, Boussiotis VA. Activation of PI3K is indispensable for interleukin 7-mediated viability, proliferation, glucose use, and growth of T cell acute lymphoblastic leukemia cells. J Exp Med. 2004;200(5):659-69.

2

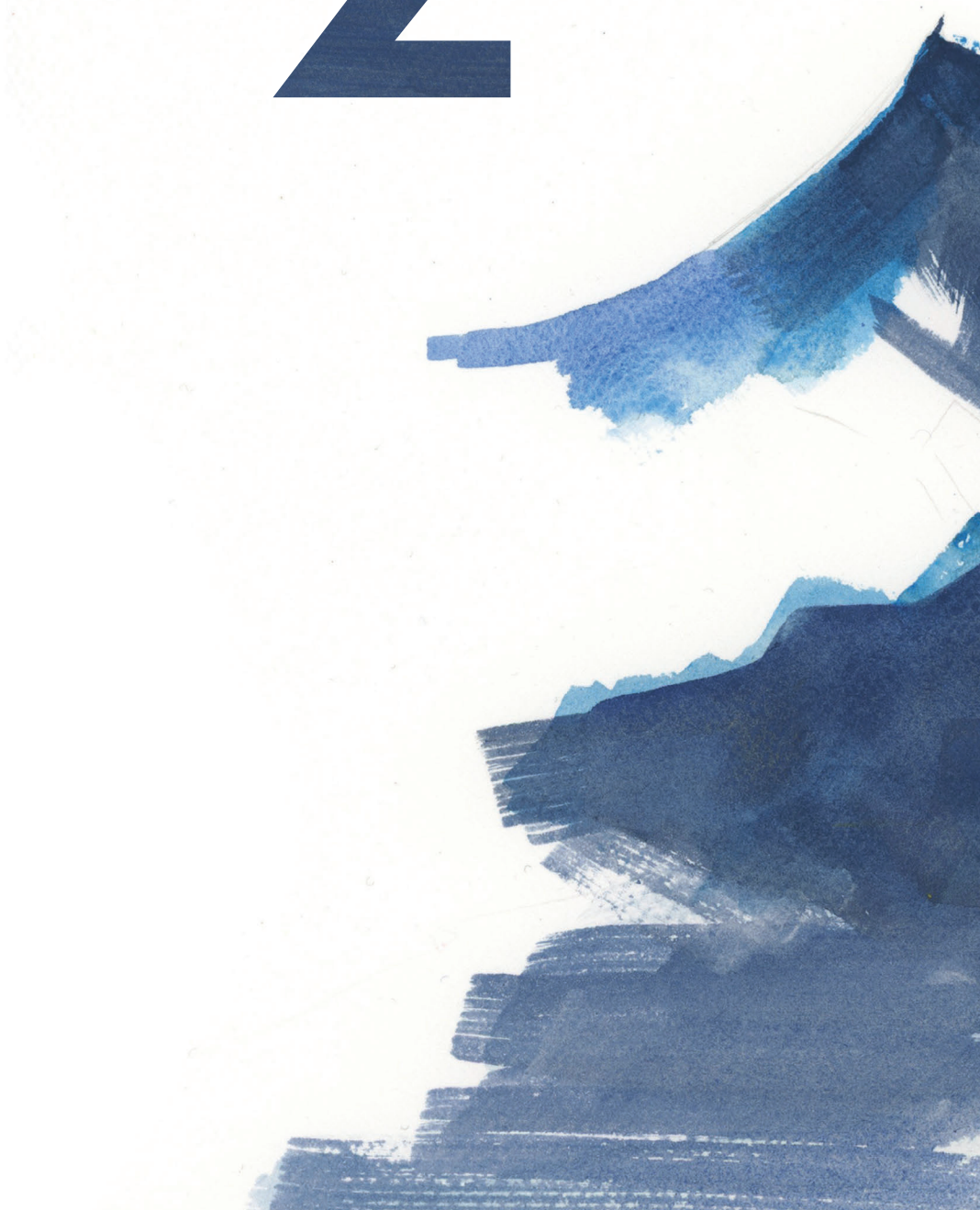

T-cell acute lymphoblastic leukemia: a roadmap to targeted therapies

Valentina Cordo'[1], Jordy C.G. van der Zwet[1], Kirsten Canté-Barrett[1], Rob Pieters[1] and Jules P.P. Meijerink[1]

[1]Princess Máxima Center for Pediatric Oncology, Utrecht, the Netherlands

Published in Blood Cancer Discovery, January 2021
DOI: 10.1158/2643-3230.BCD-20-0093

ABSTRACT

T-cell acute lymphoblastic leukemia (T-ALL) is an aggressive hematological malignancy characterized by aberrant proliferation of immature thymocytes. Despite an overall survival of 80% in the pediatric setting, 20% of T-ALL patients ultimately die from relapsed or refractory disease. Therefore, there is an urgent need for novel therapies. Molecular-genetic analyses and sequencing studies have led to the identification of recurrent T-ALL genetic drivers. This review summarizes the main genetic drivers and targetable lesions of T-ALL and gives a comprehensive overview of the novel treatments for T-ALL patients that are currently under clinical investigation or that are emerging from preclinical research.

SIGNIFICANCE

T-ALL is driven by oncogenic transcription factors that act along with secondary acquired mutations. These lesions, together with active signaling pathways, may be targeted by therapeutic agents. Bridging research and clinical practice can accelerate the testing of novel treatments in clinical trials, offering an opportunity for patients with poor outcome.

Keywords: T-ALL, targeted therapy, biomarkers, clinical trials

Abbreviations: T-ALL, T-cell acute lymphoblastic leukemia; OS, overall survival; MRD, minimal residual disease; ETP, early thymocyte progenitor; CD, cluster of differentiation; NGS, next-generation sequencing; IL7R, interleukin 7 receptor; GCR, glucocorticoid receptor; TCR, T-cell receptor; 6MP, 6-mercaptopurine; CML, chronic myeloid leukemia; CLL, chronic lymphoblastic leukemia; LBL, lymphoblastic lymphoma; Ph+, Philadelphia positive; GSI, γ-secretase inhibitor; BCP, B-cell precursor; MPN, myeloproliferative neoplasm; GvHD, graft-vs-host disease; CDK, cyclin-dependent kinase; CNS, central nervous system; NSG, NOD/Scid/IL2R-gamma null; CAR T, Chimeric antigen receptor T-cell; AML, acute myeloid leukemia; MDS, myelodysplastic syndrome.

INTRODUCTION

T-cell acute lymphoblastic leukemia (T-ALL) arises from the accumulation of genetic lesions during T-cell development in the thymus, resulting in differentiation arrest and aberrant proliferation of immature progenitors. T-ALL accounts for only 10-15% of pediatric and up to 25% of adult ALL cases (1), with an overall survival (OS) of 80% in the pediatric setting that has been achieved using a risk-based stratification towards intensive, multi-agent combination chemotherapeutic protocols (2). OS rates for adult T-ALL patients are lower than 50% due to higher treatment-related toxicities (1). Patients are assigned to standard, medium or high risk group based on initial steroid response and minimal residual disease (MRD) after the first two courses of chemotherapy (3, 4). The risk-based therapeutic regimen consists of steroids, microtubules-destabilizing agents (vincristine), alkylating agents (cyclophosphamide), anthracyclines (doxorubicin, daunorubicin), anti-metabolites (methotrexate, MTX), nucleoside analogues (6-mercaptopurine, thioguanine, cytarabine), hydrolyzing enzymes (*L*-asparaginase) and in some cases it is followed by stem cell transplantation. Some of these conventional chemotherapeutics have a lymphoid lineage-specific effect in ALL. In fact, lymphoblasts have low asparagine synthetase activity and thus they are very sensitive to exogenous asparagine depletion by *L*-asparaginase. Moreover, ALL blasts are susceptible to methotrexate treatment due to a higher accumulation of MTX-polyglutamate metabolites that increases MTX intracellular retention and its anti-leukemic effect in these cells (5). Risk-based intensification of the therapeutic regimen has greatly improved the survival rate for pediatric (6) and young adult patients treated on pediatric-based protocols (1). Nevertheless, still one out of five pediatric T-ALL patients dies within five years after first diagnosis from relapsed disease and therapy resistance (refractory disease) or from treatment-related mortalities, including toxicity and infections. Therefore, further intensification of the treatment protocol does not seem feasible for high risk patients (6) and there is an urgent need for implementation of targeted therapies. Furthermore, molecular biomarkers, in addition to MRD detection, could improve the upfront identification of high-risk patients and therefore guide the treatment of these patients with an intensified chemotherapeutic regimen or, whenever available, targeted agents. Unfortunately, such genetic biomarkers are not included in the risk stratification of newly diagnosed T-ALL patients yet.

The clinical testing of targeted agents in the oncology field has dramatically increased over the last years. Nevertheless, targeted treatment options for T-ALL patients remain limited. In fact, unlike other leukemias such as CML and Philadelphia-positive ALL (Ph^+-ALL), which are kinase-driven malignancies, the initiating events in T-ALL cause the ectopic expression of transcription factors (type A aberrations) that drive leukemogenesis. However, the additional genetic lesions that are required for full transformation into malignancy (the so-called type B mutations) potentially serve as druggable vulnerabilities. Therefore, the thorough investigation of T-ALL oncogenic

molecular pathways and their intricate RNA and protein signaling networks that sustain proliferation and survival can offer opportunities for the implementation of personalized targeted therapies (7). Potential limitations to the use of targeted drugs in pediatric T-ALL include clonal heterogeneity of the disease, resulting in only partial elimination of leukemia cells upon therapy. Therefore, resistant clones may be selected and survive under the selective pressure of treatment (8, 9). Similar resistance mechanisms have already been demonstrated for conventional chemotherapeutics such as the glucocorticoids-selected *NR3C1* mutations (10-12) and the 6-mercaptopurine (6MP)-selected *NT5C2* mutations in chemo-resistant relapsed ALL (11, 13). Already in 2017, the Innovative Therapies for Children with Cancer (ITCC) consortium advised a change in the setup of early phase pediatric clinical trials in order to accelerate the access of interesting drugs to randomized trials (14). ITCC has proposed to extrapolate data from adult clinical trials as starting point for *first-in-child* trial designs. Additionally, ITCC suggested the addition of homogeneous expansion cohorts to assess pharmacodynamic and pharmacokinetic parameters for the therapeutic agents tested and to detect early signs of antitumor activities. Furthermore, it has become evident that molecular tumor profiling is needed to study cancer heterogeneity, to understand therapy-induced mutations and the insurgence of relapse (14). **Table S1** offers an overview of current clinical trials that investigate targeted agents for T-ALL. In the following paragraphs, we summarize the main recurrent T-ALL oncogenic drivers and targetable genetic lesions and highlight the most important preclinical and clinical evidence to implement promising drugs in clinical trials for T-ALL patients. In particular, we discuss agents that target activated pathways by specific genomic lesions in T-ALL and drugs already approved for cancer treatment that are under clinical investigation for T-ALL patients. Moreover, we briefly discuss novel therapeutic options for which promising pre-clinical results were obtained in T-ALL models and that should be taken into consideration for future research. The agents discussed here include modifiers of apoptosis, inhibitors of transcriptional regulators, signal transduction, cell cycle and immunotherapies. **Figure 1** offers a visual summary of the relevant targets and therapeutic agents described throughout this review.

Oncogenic drivers and T-ALL subtypes

Historically, three main T-ALL differentiation stages were identified based on the expression of cluster of differentiation (CD) markers on the cell surface and were denoted as early/precortical, cortical and mature in analogy with the thymocytes developmental stages (15). With the rapid development of (cyto)genetic technologies and NGS in the last two decades, it was possible to identify genetic drivers that, in case of T-ALL, are transcription factors that are ectopically activated due to chromosomal rearrangements or deletions (reviewed in (7)).

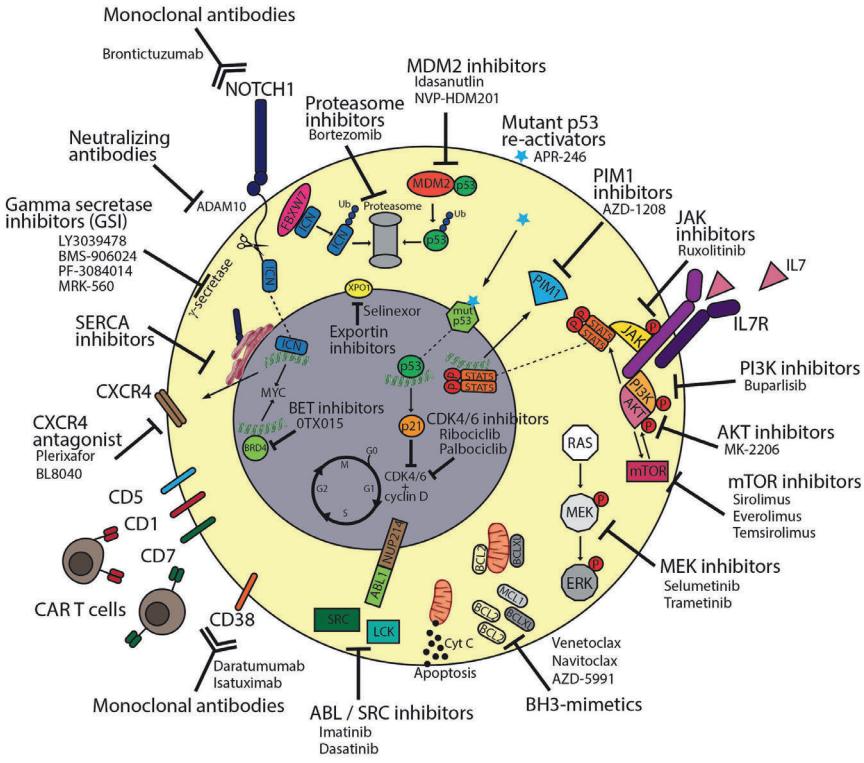

Figure 1. Targeted therapies to tackle T-ALL vulnerabilities. *Oncogenic NOTCH1 signaling can be inhibited via different strategies such as monoclonal antibodies blocking the NOTCH1 receptor itself (brontictuzumab), monoclonal antibodies blocking the ADAM10 metalloprotease that releases extracellular NOTCH1, gamma secretase inhibitors (GSI) preventing the release of intracellular ICN1, SERCA inhibitors that block the maturation of NOTCH1 and its localization on the cell surface. Since NOTCH1-mutated T-ALL cases can present higher CXCR4 surface expression, CXCR4 antagonists (plerixafor, BL8040) can be used to tackle NOTCH1-driven T-ALL as well. Immunotherapy approaches for T-ALL include monoclonal antibodies against surface CD38 (daratumumab, isatuximab) as well as CAR T-cells directed towards surface CD1, CD5, CD7 and CD38. The increased expression of anti-apoptotic BH3 proteins such as BCL2 and BCLXL can be counteracted by the use of BH3 mimetics (venetoclax, navitoclax and AZD5991). The oncogenic signaling of ABL1-fusion proteins as well as aberrant activity of Src-family kinases can be inhibited by the tyrosine kinase inhibitors imatinib and dasatinib. The aberrant IL7R signaling cascade can be tackled using multiple targeted agents including JAK inhibitors (ruxolitinib), PIM1 inhibitors (AZD-1208), PI3K inhibitors (buparlisib), AKT inhibitors (MK-2206), mTOR inhibitors (sirolimus, everolimus, temsirolimus) and MEK inhibitors (selumetinib, trametinib). APR-246 can bind mutant p53 and restore its wild-type, tumor suppressor function while MDM2 inhibitors (idasanutlin, NVP-HDM201) can prevent wild-type p53 ubiquitination and consequent degradation via the proteasome. Alternatively, tumor suppressor proteins degradation can be prevented by proteasome inhibitors (bortezomib). Increased activity of cell cycle regulators CDK4/6 can be blocked by CDK inhibitors (ribociclib, palbociclib) while aberrant transcription induced by BRD4 can be targeted by BET inhibitors (OTX015). Nuclear trafficking of oncogenic mRNA and proteins can be targeted via XPO1 inhibitors (selinexor).*

Initially using gene expression profiling (16, 17) which has been replaced by the identification of recurrent genomic abnormalities via genome sequencing (18, 19), T-ALL patients can be clustered in 4 main subtypes with characteristic oncogenic aberrations, namely early thymocyte progenitor (ETP)/immature-ALL, TLX, TLX1/NKX2.1 (originally denoted as proliferative subgroup) and TAL/LMO. **Figure 2** illustrates the main features of each subtype. The ETP–ALL group includes the most immature T-ALL cases (approximately 10% of the total T-ALL cases) that present a gene expression profile similar to hematopoietic stem cells and myeloid progenitors, with a high expression of self-renewal genes including *LMO2*, *LYL1* and *HHEX* and the anti-apoptotic *BCL2* (20). The mechanisms for high BCL2 expression in ETP-ALL are still poorly understood: the expression of this anti-apoptotic protein could reflect a stem cell-like feature of immature cells or it could be due to STAT5 activation downstream of recurrent IL7 signaling pathway mutations within this subgroup (21, 22). ETP-ALL cases show increased expression of the transcription factor *MEF2C* or genetic aberrations of *MEF2C*-associated transcription regulators such as *SPI1, RUNX1, ETV6-NCOA2* and *NKX2.5* (16). Interestingly, ETP-ALL blasts have higher mutational loads compared to blasts of other T-ALL subtypes (21, 22). In particular, while *NOTCH1* activating mutations and cell cycle regulators *CDKN2A/2B* inactivating mutations are relatively rare in ETP-ALL, recurrent activating aberrations involve kinase encoding genes, such as *FLT3*, *NRAS*, *IL7R*, *JAK1* and *JAK3* (21, 22). Additionally, recurrent 5q deletions result in deletion of the *NR3C1* locus, encoding for the glucocorticoid receptor (GCR) (22, 23). Interestingly, recent evidence demonstrated that reduced GCR expression can induce steroid resistance in T-ALL (12). Some ETP-ALL cases present genomic aberrations that activate genes of the *HOXA* locus. Such activating events have been correlated to chemo-resistance and inferior outcome in adult ETP-ALL (24).

The TLX group includes immature cases that either lack a functional T-cell receptor (TCR) or present a γ/δ TCR, in line with early or γ/δ T-cell lineage development (DN2 stage). A recent study suggests that patients with γ/δ T-ALL have higher MRD levels after induction chemotherapy compared to other T-ALL cases (25). Common genetic lesions within the TLX group include rearrangements of the transcription factor *TLX3* (16, 17), mostly as consequence of recurrent *TLX3-BCL11B* translocations (26). These aberrations result in haplo-insufficiency of the tumor suppressor *BCL11B* (27), which is a crucial regulator of the α/β lineage commitment during differentiation. Moreover, *TLX3*-rearranged T-ALL often have *NOTCH1*-activating mutations (28) and aberrations in epigenetic regulators such as PHF6 and CTCF (18). Similar to various ETP-ALL cases, some TLX patients harbor alternative *HOXA* driving events instead of *TLX3*-activating lesions (16).

The common features of the TLX1/NKX2.1 T-ALL group are genomic rearrangements involving either *TLX1* or *NKX2.1,* CD1 expression and differentiation arrest at the cortical (DN3-DP) stage of T-cell development. These cases present higher expression

of genes involved in cell cycle regulation and progression, DNA duplication and spindle assembly (16, 17). T-ALL cases with TLX1 or NKX2.1 aberrations have been associated with excellent treatment outcomes (reviewed in (7)).

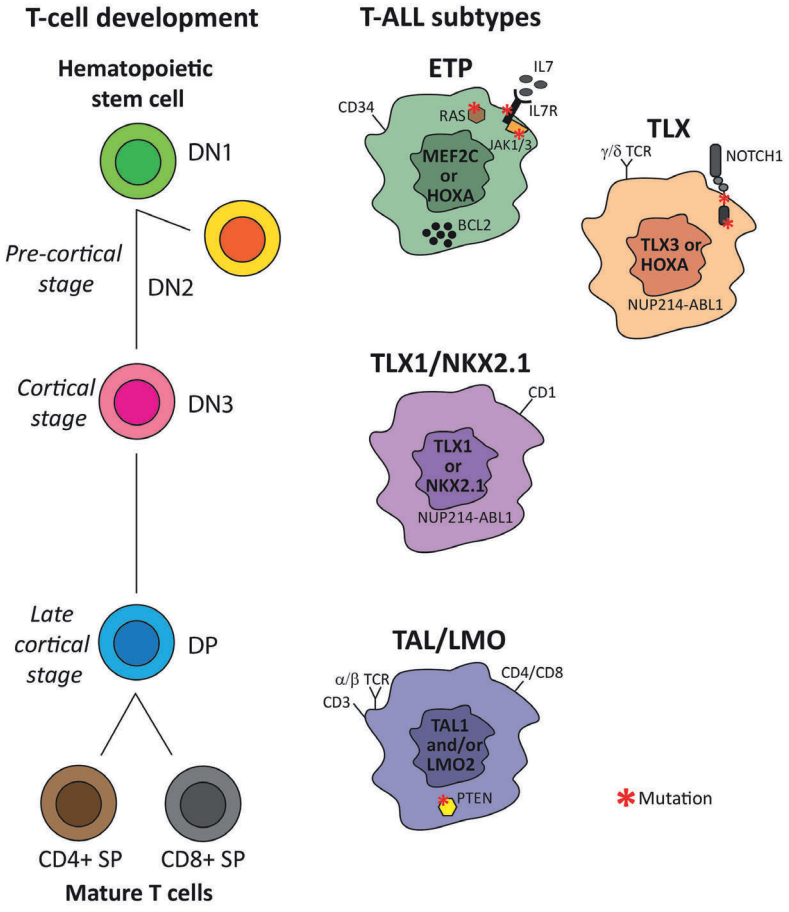

Figure 2. Thymocytes developmental stages and T-ALL subtypes. *Early thymocyte progenitor (ETP)-ALL subtype is driven by aberrant MEF2C or HOXA gene expression, present frequent mutations in the IL7 signaling cascade and shows higher BCL2 protein expression. Similarly to hematopoietic progenitors, ETP-ALL blasts express stem cell markers such as CD34. The TLX subgroup, driven by either TLX3 or HOXA activating events, often present NOTCH1 mutations and, in some cases, expression of the γ/δ T-cell receptor (TCR), in analogy to the pre-cortical γ/δ T-cell progenitors (DN2 stage). The TLX1/NKX2.1 subgroup is driven by either NKX2.1 or TLX1 aberrations. TLX–rearranged cases can present the oncogenic NUP214-ABL1 fusion. The TAL/LMO subgroup, driven by the expression of the oncogenes TAL1 and LMO2, includes the most mature T-ALL cases. As for late cortical (SP) T-cell progenitors, TAL/LMO blasts express mature T-cell surface markers such as CD4, CD8, CD3 and α/β TCR and often present PTEN mutations.*

The TAL/LMO T-ALL subgroup comprises nearly half of all pediatric T-ALL patients and it is characterized by ectopic expression of *TAL1* (either via translocation or *SIL-TAL1* deletion), *TAL2, LYL1, LMO1, LMO2* or *LMO3* (driven by *TCRB* or *TCRAD* rearrangements) (16, 17). Immuno-phenotypes of TAL/LMO patients mostly resemble late cortical (CD4+ SP or CD8+ SP) T-cell development stages. *PTEN* mutations are most common in this subgroup and have been associated with poor outcome (29). In addition, *PIK3R1* or *PIK3CG* activating lesions are frequent within this cluster (30, 31). Moreover, *TAL1*-rearranged cases often have mutations in the ubiquitin-specific protease USP7 that regulates MDM2 and TP53 stability (18).

Current and novel possibilities for targeted therapy

In the following paragraphs, we will discuss various classes of drugs and biological agents that provide novel strategies for targeted treatment. These are classified as modifiers of apoptosis, inhibitors of transcription regulation, signal transduction, cell cycle and immunotherapies

Modifiers of apoptosis

BH3 mimetics

Encouraged by significant responses of the BCL2 inhibitor venetoclax (ABT-199) in chronic lymphatic leukemia (CLL) (32), BH3 mimetics became of great interest for the treatment of various hematological malignancies. The sensitivity towards BH3 mimetics can be determined by BH3 profiling, a functional screening method that determines the 'priming of death' state in cells by measuring specific BCL2 family member (*e.g.* BCL2, BCLXL and/or MCL1) dependencies (33). BH3 profiling of T-ALL cell lines and patient blasts identified a dependency on BCL2 in ETP-ALL and BCLXL in the remaining subtypes of T-ALL (34). Consequently, immature/ETP-ALL cells are most responsive to venetoclax while other T-ALL subtypes are more sensitive to navitoclax (ABT-263) treatment, respectively (34, 35). The BCL2/BCLW/BCLXL inhibitor navitoclax induces significant cell death in both T-ALL and BCP-ALL PDX models (36), but it can induce severe thrombocytopenia *in vivo*. First reports on pediatric and adult relapsed/refractory T-ALL patients treated with venetoclax alone or combined with navitoclax showed promising results (37, 38). However, various resistance mechanisms towards venetoclax treatment have been reported in several hematological malignancies including T-ALL, such as acquired *BCL2* mutations, altered mitochondrial fitness or MCL1 upregulation (36, 39-41). Combination treatment of venetoclax with other BH3 mimetics or PI3K/AKT/mTOR inhibitors significantly increases cell toxicity and overcomes venetoclax-induced resistance (39, 40). The MCL1 inhibitor S63845 also induces efficient cell death in various T-ALL cell lines as single treatment (39), therefore serving as an interesting alternative to venetoclax, especially given the limited dependency on BCL2 in most T-ALL patients (34). Measuring BCL2 family dependencies can enable guided application of different BH3 mimetics for individualized medicine. In addition, the mitochondrial priming for

apoptosis correlates with clinical responses in ALL and predicts for chemo-sensitivity, empowering the use of BH3 profiling as a functional screen in pediatric leukemia (42).

Transcriptional regulator inhibitors

NOTCH1 inhibitors

Over 70% of T-ALL cases present *NOTCH1*-activating mutations *(gain-of-function)* and up to 25% of patients harbor mutations in the *FBXW7* gene (18), which mediates the proteasomal degradation of NOTCH1. Gamma-secretase inhibitors (GSI) have been extensively studied as potential treatment for NOTCH1-activated tumors. Despite promising pre-clinical results, GSI failed during clinical trials due to insufficient efficacy (even in presence of *NOTCH1* mutations) and excessive gastro-intestinal toxicity caused by the concomitant inhibition of NOTCH2 in the gut epithelium (reviewed in (43)). Preclinical data showed that simultaneous administration of corticosteroid can relieve gastro-intestinal toxicity and enhance the GSI anti-tumor activity (44). Current clinical trials are investigating whether combined GSI and dexamethasone administration could be an effective therapeutic approach (NCT02518113, NCT01363817). As an alternative strategy, Habets and co-workers showed a safe, selective GSI-targeting of NOTCH1 signaling in T-ALL using a PSEN1 inhibitor (MRK-560) (45). While intestinal epithelial cells express both PSEN1 and PSEN2 subunits of the γ-secretase proteolytic complex, T-ALL cells only express PSEN1. *In vivo* preclinical data showed that γ-secretase inhibition by MRK-560 has anti-leukemic activity without causing intestinal toxicity in T-ALL patient-derived mouse xenografts, offering a promising alternative therapeutic approach for NOTCH1-activated T-ALL cases (45). It is fair to question whether, despite high prevalence of *NOTCH1* mutations in T-ALL, GSI is a valid strategy to efficiently and safely target this mutant protein and the consequent altered transcriptional program.

Additional strategies to block aberrant NOTCH1 signaling include monoclonal antibodies (46) or SERCA (sarco-endoplasmic reticulum Ca^{2+}-ATPase) inhibitors that blocks NOTCH1 protein maturation by preventing its localization on the cell membrane (47). Other approaches to tackle oncogenic NOTCH1 involve the targeting of molecules that are activated upon NOTCH1-induced signaling. For example, it has been reported that GSI-resistant T-ALL cells express lower levels of the anti-apoptotic protein MCL1. Since MCL1 can counteract the inhibition of BCL2 and BCLXL, cells with lower MCL1 expression are vulnerable to navitoclax treatment (48). At last, another emerging druggable player within NOTCH1 oncogenic signaling is CXCR4 (CD184), the chemokine receptor for CXCL12 that is released by stromal cells in the thymus. CXCR4 is upregulated in NOTCH1-driven T-ALL and promotes survival and proliferation in the bone marrow niche (reviewed in (49)). Therefore, CXCR4 antagonists, which are already largely used in the clinic to promote stem cells mobilization into the bloodstream, could be repurposed as therapeutic option for leukemic patients. In fact, the novel CXCR4 inhibitor BL8040 is now in phase II clinical trial for relapsed T-ALL/LBL patients (**Table S1**). Together these

studies show that there is potential for targeting mutant NOTCH1 or its downstream signaling.

BET inhibitors

Bromodomain (BRD)-containing proteins affect gene transcription via binding to acetylated histones. Their functions include remodeling of the chromatin, modifying histones and modulating transcription itself (50). The bromodomain and extraterminal (BET) family of BRD-containing proteins consists of four members: BRD2, BRD3, BRD4 and the testis-specific BRDT. One of the first small molecules developed to selectively inhibit BET proteins was JQ1 (50). In leukemia, BRD4-activity can drive aberrant MYC expression. Since *MYC* is an important and direct NOTCH1-target gene (51), *NOTCH1*-mutated T-ALL cases have increased MYC expression. In preclinical T-ALL models, JQ1 competes with BRD4, resulting in reduced MYC expression, decreased cell proliferation and impaired tumor growth (52). Moreover, JQ1 treatment can synergize with vincristine (53) and also with the BCL2 inhibitor venetoclax (54). Interestingly, T-ALL cells that acquire resistance to γ-secretase inhibitors remain responsive to BRD4 inhibition by JQ1 (55), indicating that *NOTCH1*-mutated patients could benefit from BET inhibitor treatment. In addition to *MYC*, JQ1 also lowers the transcription of another important NOTCH1 target gene, the IL7 receptor (*IL7R*) (56). Moreover, another BRD4-dependent transcription factor, ETS1 can cooperate with NOTCH1 during leukemogenesis. Since Ets1 deletion sensitizes T-ALL cells to GSI (57), targeting NOTCH1 transcriptional cofactors could offer an alternative strategy to treat NOTCH1-driven T-ALL cases.

Cancer cells often use super-enhancer structures to restore and sustain oncogene expression. Guo and colleagues (58) showed that JQ1-resistant leukemic cells can restore MYC expression via enhancer remodeling. However, combined BET and CDK7 (transcriptional regulator) inhibition in JQ1-resistant cells effectively abrogates MYC expression. Pharmacological targeting of CDK7 results in decreased enhancer activity in T-ALL and epigenetic reprogramming, in particular for NOTCH1-related enhancers that are not affected by GSI treatment (59). CDK7 inhibition also effectively disrupts the TAL1 super-enhancer (60), highlighting that disruption of oncogenic transcription complexes may be an effective approach for T-ALL treatment when direct targeting of mutant genes, proteins or pathways is not possible. Therefore, the investigation of the epigenetic state of leukemia cells can provide additional insights to guide the use of targeted treatments. Despite promising results in preclinical models, JQ1 has a very short half-life that limits its applicability as therapeutic agent *in vivo*. Nevertheless, several novel BET inhibitors have been developed by multiple companies and they are currently under investigation in oncology trials, highlighting the great interest in these epigenetic drugs and their potential application (61) . Among these novel agents, OTX015 was proven effective in preclinical leukemia models (62).

Signal transduction inhibitors

ABL1 / Src-family kinases inhibitors

Differently from B-ALL cases, T-ALL patients with *ABL1* fusions are rare (18, 63). The most common *ABL1* aberration in T-ALL is the *NUP214-ABL1* fusion due to an episomal amplification of the 9q34 region, which was one of the few discovered T-ALL lesions that can be directly targeted by a kinase inhibitor (63). Usually, *NUP214-ABL1* rearrangements are particularly present at the sub-clonal level (64). Novel *ZBTB16-ABL1* and *ZMIZ1-ABL1* fusions have been identified in rare T-ALL cases ((65) and unpublished observations), resulting in sensitivity towards imatinib and dasatinib treatment in preclinical models (65). Interestingly, in 2017, Bourquin and colleagues identified a subgroup of T-ALL patients that are highly sensitive to dasatinib treatment *in vitro* despite the absence of *ABL1* aberrations, suggesting a role for SRC kinase as putative novel target for therapy (66). Other studies proposed the lymphocytic specific kinase LCK, which is often highly expressed in T-ALL, as prime dasatinib target in T-ALL (67, 68). Based on these pre-clinical data, patients presenting high SRC phosphorylation and/or increased LCK expression could potentially benefit from dasatinib treatment. Therefore, in addition to genomic analyses, further investigation of the phospho-proteome could highlight aberrantly activated proteins (7) that could serve as biomarkers for dasatinib responsiveness when *ABL1* abnormalities are not present.

JAK inhibitors

JAK-STAT pathway activation in T-ALL is mainly observed in the context of IL7-induced signaling or caused by activating mutations in the *IL7R* gene or in genes encoding downstream effectors (*e.g. JAK1*, *JAK3* or *STAT5*) that are recurrently found at diagnosis (18, 21, 69). Active JAK-STAT signaling leads to the upregulation of various anti-apoptotic and pro-survival proteins including BCL2 and PIM1 and contributes to steroid resistance (21, 70, 71). Ruxolitinib, an FDA-approved JAK1/2-inhibitor for the treatment of myeloproliferative neoplasms (MPNs) and graft-versus-host disease (GvHD) blocks JAK-STAT signaling regardless of the presence of mutations (72). In T-ALL, ruxolitinib shows efficacy in IL7-responsive T-ALL and ETP-ALL (69). Ruxolitinib treatment can synergize with dexamethasone treatment to overcome IL7-induced steroid resistance in both T-ALL and ETP-ALL patients. Multiple trials are under way to test the efficacy of ruxolitinib for JAK-mutated T-ALL (**Table S1**) or Philadelphia-like BCP-ALL with CRLF2-rearrangements and/or JAK mutations (NCT2723994, NCT03117751 and NCT02420717), despite the fact that the clinical responses to ruxolitinib in MPNs seem rather limited (73). This indicates that the role of JAK inhibitors should be carefully considered in future treatment regimens of T-ALL.

PIM1 inhibitors

When exploring alternative treatment options for aberrant JAK-STAT signaling, *PIM1* was identified as a direct STAT5 transcriptional target gene that is also upregulated by

physiological IL7-induced signaling (71, 74, 75). Expression of the pro-survival PIM1 kinase is mainly observed in pre-cortical T-ALL, with the highest expression in the TLX and ETP-ALL subtypes (71, 74, 76, 77). This is in agreement with the higher occurrence of activating mutations in the IL7R signaling pathway in these T-ALL subtypes, including *JAK1/3* and *STAT5B* mutations (3, 18, 21, 22). PIM1 inhibition has proven efficacy in T-ALL using *in vitro* and *in vivo* models, with an increased effect observed for ETP-ALL blasts (74, 77). Both phospho-STAT5 and PIM1 expression levels can be used as a predictive biomarker for response to JAK inhibitors (74). PIM1 inhibition paradoxically results in enhanced MAPK-ERK signaling, and may explain the observed synergy of combined PIM1 and MEK inhibitors treatment (74, 78). Additionally, synergistic effects of PIM1 inhibitors in combination with venetoclax or dexamethasone have been observed (77, 79) indicating that PIM1 could be a valuable therapeutic target to counteract unfavorable hallmarks of immature /ETP-ALL cases such as high BCL2 expression and steroid resistance.

PI3K-AKT-mTOR inhibitors

High PI3K-AKT-mTOR signaling is frequently observed in T-ALL and can be caused by a variety of cellular events, including activating mutations in *PI3K* or *AKT*, inactivating lesions in the tumor suppressor gene *PTEN* or by post-translational modification of these molecules (21, 30, 31, 80). *PTEN* inactivating events are predominantly observed in T-ALL patients that belong to the TAL/LMO subtype. PTEN loss is associated with poor prognosis in T-ALL, resulting in higher risk of disease relapse (29, 30, 80, 81). Additionally, IL7R-signaling mutations that frequently occur in ETP-ALL and TLX subtypes also activate the downstream PI3K-AKT pathway and correlate with steroid resistance and inferior event-free survival (3, 21). Pan-PI3K inhibitors have shown higher efficacy in inhibiting cell growth and survival of T-ALL cell lines compared to inhibitors that target only specific catalytic subunit(s) of PI3K (82). Preclinical *in vitro* studies demonstrate synergy between PI3K-inhibitors and several chemotherapeutic agents including doxorubicin, nelarabine and glucocorticoids (21, 83, 84). Moreover, dual PI3K/mTOR inhibitors seem to be even more effective and also synergize with a wide range of chemotherapeutics (84-87).

The effects of first generation allosteric mTOR inhibitors rapamycin (sirolimus) and rapalogues RAD001 (everolimus) and CCI-779 (temsirolimus) have been largely investigated in T-ALL (85, 88, 89). These inhibitors only target mTORC1 and can paradoxically activate AKT via PI3K-mTORC2 in some cell types (reviewed in (90)). Second generation ATP-competitive dual mTORC1/mTORC2 inhibitors are more efficient in inducing apoptosis in T-ALL blasts since they also interfere with more downstream PI3K-AKT-mTOR signaling effectors, including a strong inhibition of 4EBP1 phosphorylation (91). The stronger cytotoxic effects and broad PI3K-AKT pathway regulation of dual-inhibitors (*e.g.* PI3K/mTOR and mTORC1/mTORC2 inhibitors) compared to PI3K- or

mTORC1-only inhibitors provides evidence that dual inhibitors are more suitable for future clinical trials (90, 92).

Alternatively, the oncogenic signaling of the PI3K-AKT-mTOR axis can also be targeted by direct AKT inhibition. The allosteric AKT inhibitor MK-2206 inhibits AKT and impairs downstream activation of mTORC1, mTORC2, GSK3 and FOXO in various T-ALL cell lines (93). Additionally, MK-2206 synergizes with steroids in primary T-ALL patient samples (21, 93). ATP-competitive AKT inhibitors like AZD5363 also demonstrate cytotoxic effect against T-ALL cells *in vitro* (94).

MEK inhibitors

The presence of mutations in *N*- and *K-RAS* genes at diagnosis, which strongly activate the MAPK-ERK signaling, predicts for inferior outcome in both BCP- and T-ALL patients (81, 95-97). Additionally, a high prevalence of these mutations in ALL patients is found at relapse (10). Although not significantly enriched in relapsed T-ALL, the presence of *RAS* mutations in relapsed pediatric T-ALL patients predicts for extremely poor outcome (98). *MAPK-ERK* activating mutations, which may be selected under the pressure of treatment, can contribute to steroid resistance (3, 21, 99). MEK inhibitors induce cell death in *RAS*-mutant cells and synergize with glucocorticoids in primary T-ALL patient cells and *in vivo* BCP-ALL models (21, 96, 100, 101). These findings led to the ongoing SeluDex trial that combines the MEK inhibitor selumetinib with dexamethasone for the treatment of relapsed adult and pediatric BCP- and T-ALL patients (NCT03705507; **Table S1**). As IL7R and JAK1 signaling mutations strongly activate downstream MEK-ERK signaling, in addition to the JAK-STAT and PI3K-AKT pathways, and strongly provoke steroid resistance in T-ALL (21), patients having such IL7R signaling mutations should also become eligible for selumetinib treatment.

Cell cycle inhibitors

CDK inhibitors

More than 70% of T-ALL cases downregulate CDKN2A/B (18), negative regulators of cyclin-dependent kinases (CDK) 4/6, either via recurrent gene deletions, sporadic mutations or promoter hypermethylation (102). Therefore, the CDK4/6 inhibitors palbociclib and ribociclib could be potential therapeutic options for T-ALL patients. Palbociclib induces cell cycle arrest in T-ALL cells and can suppress leukemia progression in animal models (103). Moreover, another preclinical study proved that the CDK4/6 inhibitor ribociclib can act synergistically with glucocorticoids and mTOR inhibitors in both T-ALL cell lines and murine models (89). Current phase I clinical trials for relapsed/refractory pediatric ALL (**Table S1**) are investigating the tolerability of the combination of ribociclib with everolimus and dexamethasone (NCT03740334) or the addition of palbociclib to the standard re-induction chemotherapeutic regimen (NCT03792256). Other aberrations involving cell cycle regulators include overexpression of the NOTCH1

target Cyclin D3, and CDK6 (18, 19, 21, 65, 98). Moreover, deletions of CDKN1B ($p27^{KIP1}$), which is a negative regulator of Cyclin E-CDK2 complex, have been reported in about 13% of T-ALL patients (18). Therefore, inhibitors targeting CDK2 might be of interest for the treatment of T-ALL as well. In 2017, Moharram and colleagues reported the efficacy of the CDK1/2/5/9 inhibitor dinaciclib in preclinical T-ALL models (104). Despite the promising results, a clinical trial had already showed only transient effect of dinaciclib treatment for adult leukemia patients (105).

Nelarabine

Active cell cycle may increase the sensitivity to nucleoside analogues treatment. Nelarabine is a purine nucleoside analogue that inhibits DNA synthesis and showed higher efficacy in T-ALL compared to other malignancies. Whether this is an exclusive T-ALL effect still remains debatable. Nevertheless, T-lymphoblasts show higher accumulation of nelarabine active metabolite ara-G with consequent increased cytotoxicity compared to other hematopoietic cells (106), making T-ALL cells more susceptible to this treatment. At the moment, it is the only novel drug approved for the treatment of relapsed T-ALL/LBL cases. As single agent for relapsed or refractory T-ALL in children and young adults, nelarabine had a response rate of over 50% (107). In adults these response rates were somewhat lower (36% achieved complete remission), but they still provided encouraging results for relapsed cases by inducing clinical remissions that facilitated access to stem cell transplantation (108). However, nelarabine treatment can have significant neurologic side effects depending on other central nervous system-directed therapy, in particular in children older than 10 years of age (109). The results of nelarabine safety and efficacy trials in T-cell acute lymphoblastic leukemia/lymphoma patients highlight considerable single agent activity in the relapse setting that facilitates disease control. Moreover, nelarabine can be combined with other drugs with non-overlapping toxicities. The Children's Oncology Group recently published the results of a randomized phase III trial investigating the addition of nelarabine to the chemotherapeutic treatment for newly diagnosed pediatric and young adult T-ALL patients. The increased disease free-survival rate as well as the decreased CNS relapse incidence without excessive toxicity, supports the inclusion of nelarabine into frontline therapy for pediatric T-ALL, especially for high-risk cases (110).

Drugs targeting mutant p53

Mutations that inactivate p53 are rare in T-ALL patients at diagnosis (1-6%) but show an increased incidence at relapse and correlate with poor prognosis (18, 98). A recent study showed that p53-mutant sub-clones that were detected at first relapse can give rise to clonal p53 mutations detectable in post-stem cell transplantation relapses. Furthermore, in these patients, p53 mutations correlated with an extremely short time-to-relapse (111). Various re-activators of mutant p53 that induce restoration of the wild-type conformation are in preclinical investigation (112). Interestingly, leukemic blasts from a T-ALL patient who relapsed after stem cell transplantation, showed sensitivity *ex vivo*

to the p53 re-activator APR-246 (111). APR-246 already showed promising results for p53-mutant patients affected by other hematological malignancies (NCT00900614) and could be a suitable option for T-ALL patients that relapse after stem cell transplantation and present with p53 mutations.

Drugs targeting wild-type p53

P53 signaling pathway can be impaired despite the presence of wild-type p53 by overexpression of physiological p53 inhibitors such as MDM2 or MDM4. In fact, p53 activity can be restored by targeting the E3 ubiquitin-ligase MDM2. The MDM2 antagonist idasanutlin disrupts the MDM2-p53 interaction and prevents p53 degradation. Currently, idasanutlin has reached phase I/II clinical trial investigation for pediatric ALL (NCT04029688). Furthermore, another MDM2 inhibitor, NVP-HDM201, is currently investigated in a phase I/II clinical trial for wild-type p53 tumors, including relapsed ALL (NCT02143635). Lastly, the MDM2/MDM4 stapled peptide ALRN-6924 has reached clinical investigation in pediatric patients with relapsed ALL (NCT03654716).

Immunotherapies

Antibody-based therapy

Monoclonal antibodies can be applied in immunotherapies and have entered various trials for T-cell lymphoma (reviewed and summarized in (113)). Surprisingly, only a few have been considered in the treatment of ALL such as anti-CD38 antibodies. CD38 is a transmembrane receptor that is expressed on subsets of myeloid, lymphoid and some non-hematological cells. The anti-CD38 monoclonal antibody daratumumab was initially developed for multiple myeloma and was approved by the FDA in 2015 and the EMA in 2016 as a single agent for relapsed/refractory multiple myeloma patients. CD38 is also a promising target for T-ALL as it is robustly and consistently expressed on T-ALL and ETP-ALL blasts at diagnosis, during chemotherapy treatment, and at relapse (114). Moreover, daratumumab displayed great efficacy in 14 out of 15 patient-derived xenograft models in NOD/Scid/IL2R-gamma null (NSG) mice (114). Of note, the cytotoxic efficacy of daratumumab in NSG mice—that do not have B, T, NK cells, and complement factors—seems therefore independent of T-cell mediated or complement-dependent cytotoxicity. CD38 expression on regulatory B and T-cells as well as on myeloid suppressor cells results in their depletion by daratumumab, which could boost anti-tumor responses (115). Clinical trials will reveal whether daratumumab has an even higher efficacy than that observed in NSG mice, as both T-cell mediated toxicity and repression of regulatory cells will be active in T-ALL patients. Recently, daratumumab has been successfully administered for compassionate use to three CD38-positive ALL patients who experienced multiple relapses, with one patient that relapsed after an allogeneic stem cell transplantation (116). Two patients had T-ALL while the third had a CD19/CD22-negative pre B-ALL and all three achieved an MRD-negative remission after daratumumab treatment. Trials combining daratumumab treatment with standard

chemotherapy for pediatric and young adult ALL patients are in phase II (NCT03384654; EudraCT 2017-003377-34). Another anti-CD38 monoclonal antibody that is under clinical investigation is isatuximab. An isatuximab trial for adult T-ALL patients in the USA was closed prematurely due to lack of response, while the NCT03860844 trial for pediatric patients with refractory/relapsed acute leukemia is still ongoing.

Pre-clinical evidences suggest that TCR-expressing T-ALL blasts can be targeted by anti-CD3 antibodies. In fact, the activation of persistent TCR signaling induced by antibodies engaging CD3, leads to cell death *in vitro* and *in vivo* (117), suggesting a novel targeted therapeutic option for T-ALL cases that present TCR expression.

Cellular therapy

Genetically engineered autologous chimeric antigen receptor T-cells (CAR T) have been used successfully as therapy for various malignancies including relapsed ALL. An extensive review recently addressed the challenges and potential solutions for the use of CAR T-cells in T-cell malignancies and lists all currently ongoing trials (118). Initially, the challenge to harvest sufficient mature T-cells from patients with T-cell malignancies without any lymphoblast contamination hampered the development of CAR T-cells against T-ALL/LBL. Most of the CAR T therapies developed so far are dependent on harvesting sufficient autologous and healthy T-cells from a single patient. The production of allogenic CAR T-cells would eliminate this challenge by using genetically modified T-cells from a healthy donor (reviewed in (119)). Additionally, the fratricide effect – the paradigm that CAR T-cells share the same surface markers with their malignant T-cell targets – would rapidly self-extinguish the CAR T-cells. After the first approval of the anti-CD19 CAR T for the treatment of pediatric relapsed B-ALL patients, many different surface proteins have been investigated for the development of novel CAR T therapies directed towards T-cell malignancies, including CD5, CD7, CD1 and CD38. One of the advantages of anti-CD5 CAR T-cells is the rapid internalization of CD5 from their cell surface, resulting in a limited and transient fratricide effect (120). Nevertheless, the internalization of CD5 can happen on blasts as well, offering an escape mechanism for leukemia cells that needs to be taken into account. Currently, a phase I anti-CD5 CAR T-cell trial is ongoing for patients with CD5-positive T-ALL or T-cell lymphoma (NCT03081910). As CD5 is expressed on most T-ALL subtypes while it is absent or expressed at low levels on ETP-ALL cells, there is need for additional CAR T-cells that can target ETP-ALL as well. CD7 is a promising target on T-lymphoblasts but is also highly expressed on effector T-cells. To minimize the fratricide effect, the CRISPR-Cas9 gene editing technology has been used to remove the endogenous *CD7* gene from these CAR T cells (121). A clinical trial using these modified anti-CD7 CAR T-cells for treating CD7-positive T-ALL/LBL has been designed (NCT03690011). However, since CD7 is expressed on all thymocytes and T-cells, patients receiving CD7 CAR T-cell treatment risk a lifelong T-cell depletion and immunodeficiency that might impair a broad use in the clinic. In order to avoid such side effects and to regulate the activity

of these cellular therapies, some CARs have been designed to express an inducible suicide gene (*e.g.* caspase 9) that can be selectively activated upon administration of a small molecule (reviewed in (122)). As an alternative strategy to target CD7, a second generation, fratricide-resistant anti-CD7 CAR T-cells have been developed using T cells from healthy donors (UCART7) (123). These CAR T-cells have been genetically altered to be not only *CD7* deficient, but also to lack the *TCRAD* gene to eliminate the risk for an allogenic CAR T-cell mediated graft-versus-host disease (GvHD). Of note, such an allogenic product can be immediately available for treatment of multiple patients as an "off-the-shelf" product. Promising results on the use of another allogeneic anti-CD7 CAR T cells have been recently presented at the American Association for Cancer Research virtual meeting in April 2020. Dr X. Wang reported the preliminary exciting data on the efficacy of a single infusion of TruUCAR™ GC027 (Gracell Biotechnologies) after 6 days of lympho-depleting chemotherapy in 5 adult refractory/relapsed T-ALL patients enrolled in a phase I clinical trial in China (ChiCTR1900025311). Four patients achieved complete response at day 28 with manageable cytokine release syndrome and absence of neurotoxicities and GvHD, while one patient that had received the lowest CAR T dose relapsed. Three out of four patients remained in complete remission at day 161 of follow-up. Future evaluations will investigate the duration of the remissions induced by this treatment (124).

CD1a is another promising target for refractory or relapsed cortical T-ALL (125). Moreover, CD1a is only expressed during the proliferative phase of thymocyte development and not on immature progenitor cells or mature T-cells, limiting the risk of complete immunodeficiency after treatment. Recently, the development of fratricide-resistant anti-CD1a CAR T-cells for the treatment of CD1a-positive T-ALL has been reported (125). However, since CD1-positive cortical T-ALL patients have been associated with excellent outcomes, it is not known what percentage of relapsed T-ALL patients will express CD1 and thus benefit from such a CAR T therapy.

As discussed in the previous session, CD38 is widely expressed on T-lymphoblasts, thus the development of anti-CD38 CAR T has also been pursued (126). Recently, the treatment of a relapsed adult B-ALL patient was reported with the occurrence of serious side effects including cytokine release syndrome and damage to lung and liver tissues that also express the CD38 antigen (127). Therefore, caution and accurate target choices are warranted to extend the repertoire of safe and effective CAR T-cell treatments.

Other promising targeted treatments in development

Oncology drug development is constantly growing, and several potential novel candidates have been recently put into the spotlight. New potentially promising compounds that should be kept in consideration for upcoming studies will be discussed below**.**

OBI-3424 is a *first-in-class* targeted treatment for liquid and solid tumors that overexpress the Aldo-Keto Reductase 1 c3 (AKR1C3) enzyme such as castrate-resistant prostate cancer and hepatocellular carcinoma. AKR1C3 is also expressed in T-ALL, with the exclusion of *TLX1/3*-rearranged cases (128). OBI-3424 is a pro-drug that releases a potent DNA-alkylating component upon intracellular reduction by AKR1C3. This agent has shown promising cytotoxic activity in T-ALL cell lines and patient-derived xenografts that express AKR1C3 (128). In September 2017, OBI-3424 received FDA orphan drug designation for AKR1C3-expressing tumors including ALL, and it is currently investigated in a phase I/II clinical trial for solid tumors (NCT03592264).

Selinexor (KPT-330) is a selective inhibitor of Exportin-1 (XPO1) which has recently been approved in combination with dexamethasone for the treatment of refractory/relapsed multiple myeloma. XPO1 is the key player in nuclear export of receptors (*e.g*. NR3C1), tumor suppressor proteins (*e.g.* p53 and pRB) but also oncogenic mRNAs transcribed from *MDM2, BCL2* and *MYC*, which will be retained in the nucleus upon XPO1 inhibition. Selinexor treatment is currently investigated in a phase I clinical trial for relapsed pediatric acute leukemia (NCT02091245). Furthermore, the second generation XPO1 inhibitor, *eltanexor* (KPT-8602) can induce cytotoxicity and apoptosis in ALL models and can enhance the efficacy of dexamethasone treatment (129).

Histone deacetylases (HDAC) are key enzymes in chromatin remodeling and epigenetic gene regulation. HDACs are frequently overexpressed in cancer, including T-ALL. T-ALL patient samples demonstrate higher HDAC1 and HDAC4 but lower HDAC5 levels compared to B-ALL (130). The pan-HDAC inhibitor *panobinostat* has shown anti-leukemic activity in T-ALL preclinical models (131) and it is under clinical investigation for relapsed acute leukemia (**Table S1**). The same applies for *vorinostat***,** which is already approved for the treatment of refractory/relapsed cutaneous T-cell lymphoma.

Additional epigenetic regulators that can be pharmacologically targeted are DNA methyltransferases. DNA methyltransferase inhibitors *decitabine* and *azacitidine* induce chromatin hypomethylation with a consequent alteration in gene transcription. They have been approved for the treatment of myelodysplastic syndromes and they are currently investigated in early phase clinical trials for pediatric ALL patients (**Table S1**). In 2016, Lu and colleagues showed that decitabine pre-treatment enhanced chemo-sensitivity of preclinical models of ETP-ALL (132). One year later, the successful treatment of a relapsed adult ETP-ALL patient with decitabine was reported (133), therefore offering a promising opportunity for salvage therapy of ETP-ALL cases.

An alternative way to target oncogenic signaling pathways is by tackling protein stability or degradation. Cancer cells become addicted to the rapid elimination of tumor suppressor proteins or may require higher protein turnover to sustain their metabolism. Therefore, processes involved in protein degradation can provide leukemia-specific

vulnerabilities that can be effectively targeted. *Bortezomib*, a *first-in-class* proteasome inhibitor, is approved for the treatment of refractory multiple myeloma. It inhibits the 26S subunit of the proteasome, impairing protein degradation that results in cell cycle arrest and eventually apoptosis. A recent report of the Children's Oncology Group highlights the safety of bortezomib during re-induction chemotherapy for pediatric relapsed ALL, and provided encouraging results for T-ALL, with an increase in patients achieving complete remission (134). Another way of altering protein stability and activity is through inhibition of the Nedd8-activating enzyme (NAE). NAE is an ubiquitin-like (UBL) protein that regulates the activity and the protein-protein interactions of NF-kB and cullins, which are essential cell cycle regulators (135). Preclinical data showed that the NAE inhibitor *pevonedistat* (MLN4924) can induce cell cycle arrest and apoptosis in T-ALL models (135). Both bortezomib and pevonedistat are currently under clinical investigation for ALL patients (**Table S1**).

Aurora kinases (AURK) are mitotic regulators often overexpressed in cancer, including pediatric ALL (136). AURKA inhibitor alisertib (MLN8237) had shown promising results for both ALL and lymphoma cells *in vitro* (137). Unfortunately, a phase II clinical trial from the Children's Oncology Group reported objective response after alisertib single agent treatment in less than 5% of the pediatric patients with recurrent/refractory advanced solid tumor or acute leukemia (138). Recent evidence elucidates a role for AURKB in inhibiting proteasomal degradation of MYC, thus stabilizing this oncogenic protein (139). *In vitro* treatment of T-ALL cells with the AURKB inhibitor barasertib (AZD1152) leads to reduced MYC protein levels (139) and enhanced cell death (139, 140). Furthermore, AZD1152 can act in synergy with vincristine (139).

CONCLUSIONS

The outcome for children diagnosed with T-ALL has dramatically improved in the last decades. Nevertheless, therapy resistance, disease relapse, treatment-related death and long-term detrimental side effects for cancer survivors remain serious issues to be solved. Additionally, the lack of predictive biomarkers at diagnosis remain an unmet need for T-ALL patients. In this review, we presented an overview of the current state of drug development and ongoing clinical trials that are of interest for the T-ALL field, integrating preclinical evidence and clinical data. Several molecular tumor profiling protocols have been initiated in Europe (*e.g.* MOSCATO-01, iTHER, ESMART) (141) to identify actionable lesions for targeted treatment in specific subgroups of patients. This highlights the importance of bridging preclinical research with clinical practice to accelerate the use of promising novel drugs in effective new treatment combinations for T-ALL patients.

Acknowledgements. This study was supported by grants of the Dutch Cancer Society (KWF Kankerbestrijding) grant number KWF2016_10355 (VC), Foundation 'Kinderen Kankervrij' (KiKa): KiKa-219 (JZ) and KiKa-295 (KCB).

Contribution of authors. VC, JvdZ, KCB and JM wrote the manuscript. RP provided critical input and revised the manuscript.

Disclosures. None.

REFERENCES

1. Patel AA, Thomas J, Rojek AE, Stock W. Biology and Treatment Paradigms in T Cell Acute Lymphoblastic Leukemia in Older Adolescents and Adults. Curr Treat Options Oncol. 2020;21(7):57.
2. Pui CH, Evans WE. Treatment of acute lymphoblastic leukemia. N Engl J Med. 2006;354(2):166-78.
3. Cante-Barrett K, Spijkers-Hagelstein JA, Buijs-Gladdines JG, Uitdehaag JC, Smits WK, van der Zwet J, et al. MEK and PI3K-AKT inhibitors synergistically block activated IL7 receptor signaling in T-cell acute lymphoblastic leukemia. Leukemia. 2016;30(9):1832-43.
4. Pui CH, Pei D, Coustan-Smith E, Jeha S, Cheng C, Bowman WP, et al. Clinical utility of sequential minimal residual disease measurements in the context of risk-based therapy in childhood acute lymphoblastic leukaemia: a prospective study. Lancet Oncol. 2015;16(4):465-74.
5. Masson E, Relling MV, Synold TW, Liu Q, Schuetz JD, Sandlund JT, et al. Accumulation of methotrexate polyglutamates in lymphoblasts is a determinant of antileukemic effects in vivo. A rationale for high-dose methotrexate. J Clin Invest. 1996;97(1):73-80.
6. Jeha S, Pei D, Choi J, Cheng C, Sandlund JT, Coustan-Smith E, et al. Improved CNS Control of Childhood Acute Lymphoblastic Leukemia Without Cranial Irradiation: St Jude Total Therapy Study 16. J Clin Oncol. 2019;37(35):3377-91.
7. van der Zwet JCG, Cordo V, Cante-Barrett K, Meijerink JPP. Multi-omic approaches to improve outcome for T-cell acute lymphoblastic leukemia patients. Adv Biol Regul. 2019;74:100647.
8. Waanders E, Gu Z, Dobson SM, Antic Z, Crawford JC, Ma X, et al. Mutational landscape and patterns of clonal evolution in relapsed pediatric acute lymphoblastic leukemia. Blood Cancer Discov. 2020;1(1):96-111.
9. Dobson SM, Garcia-Prat L, Vanner RJ, Wintersinger J, Waanders E, Gu Z, et al. Relapse-Fated Latent Diagnosis Subclones in Acute B Lineage Leukemia Are Drug Tolerant and Possess Distinct Metabolic Programs. Cancer Discov. 2020;10(4):568-87.
10. Oshima K, Khiabanian H, da Silva-Almeida AC, Tzoneva G, Abate F, Ambesi-Impiombato A, et al. Mutational landscape, clonal evolution patterns, and role of RAS mutations in relapsed acute lymphoblastic leukemia. Proc Natl Acad Sci U S A. 2016;113(40):11306-11.
11. Li B, Brady SW, Ma X, Shen S, Zhang Y, Li Y, et al. Therapy-induced mutations drive the genomic landscape of relapsed acute lymphoblastic leukemia. Blood. 2020;135(1):41-55.
12. Wandler AM, Huang BJ, Craig JW, Hayes K, Yan H, Meyer LK, et al. Loss of glucocorticoid receptor expression mediates in vivo dexamethasone resistance in T-cell acute lymphoblastic leukemia. Leukemia. 2020;34(8):2025-37.
13. Tzoneva G, Perez-Garcia A, Carpenter Z, Khiabanian H, Tosello V, Allegretta M, et al. Activating mutations in the NT5C2 nucleotidase gene drive chemotherapy resistance in relapsed ALL. Nat Med. 2013;19(3):368-71.
14. Moreno L, Pearson ADJ, Paoletti X, Jimenez I, Geoerger B, Kearns PR, et al. Early phase clinical trials of anticancer agents in children and adolescents - an ITCC perspective. Nat Rev Clin Oncol. 2017;14(8):497-507.
15. Bene MC, Castoldi G, Knapp W, Ludwig WD, Matutes E, Orfao A, et al. Proposals for the immunological classification of acute leukemias. European Group for the Immunological Characterization of Leukemias (EGIL). Leukemia. 1995;9(10):1783-6.
16. Homminga I, Pieters R, Langerak AW, de Rooi JJ, Stubbs A, Verstegen M, et al. Integrated transcript and genome analyses reveal NKX2-1 and MEF2C as potential oncogenes in T cell acute lymphoblastic leukemia. Cancer Cell. 2011;19(4):484-97.

17. Ferrando AA, Neuberg DS, Staunton J, Loh ML, Huard C, Raimondi SC, et al. Gene expression signatures define novel oncogenic pathways in T cell acute lymphoblastic leukemia. Cancer Cell. 2002;1(1):75-87.
18. Liu Y, Easton J, Shao Y, Maciaszek J, Wang Z, Wilkinson MR, et al. The genomic landscape of pediatric and young adult T-lineage acute lymphoblastic leukemia. Nat Genet. 2017;49(8):1211-8.
19. Seki M, Kimura S, Isobe T, Yoshida K, Ueno H, Nakajima-Takagi Y, et al. Recurrent SPI1 (PU.1) fusions in high-risk pediatric T cell acute lymphoblastic leukemia. Nat Genet. 2017;49(8):1274-81.
20. Coustan-Smith E, Mullighan CG, Onciu M, Behm FG, Raimondi SC, Pei D, et al. Early T-cell precursor leukaemia: a subtype of very high-risk acute lymphoblastic leukaemia. Lancet Oncol. 2009;10(2):147-56.
21. Li Y, Buijs-Gladdines JG, Cante-Barrett K, Stubbs AP, Vroegindeweij EM, Smits WK, et al. IL-7 Receptor Mutations and Steroid Resistance in Pediatric T cell Acute Lymphoblastic Leukemia: A Genome Sequencing Study. PLoS Med. 2016;13(12):e1002200.
22. Zhang J, Ding L, Holmfeldt L, Wu G, Heatley SL, Payne-Turner D, et al. The genetic basis of early T-cell precursor acute lymphoblastic leukaemia. Nature. 2012;481(7380):157-63.
23. La Starza R, Barba G, Demeyer S, Pierini V, Di Giacomo D, Gianfelici V, et al. Deletions of the long arm of chromosome 5 define subgroups of T-cell acute lymphoblastic leukemia. Haematologica. 2016;101(8):951-8.
24. Bond J, Marchand T, Touzart A, Cieslak A, Trinquand A, Sutton L, et al. An early thymic precursor phenotype predicts outcome exclusively in HOXA-overexpressing adult T-cell acute lymphoblastic leukemia: a Group for Research in Adult Acute Lymphoblastic Leukemia study. Haematologica. 2016;101(6):732-40.
25. Pui CH, Pei D, Cheng C, Tomchuck SL, Evans SN, Inaba H, et al. Treatment response and outcome of children with T-cell acute lymphoblastic leukemia expressing the gamma-delta T-cell receptor. Oncoimmunology. 2019;8(8):1599637.
26. Su XY, Della-Valle V, Andre-Schmutz I, Lemercier C, Radford-Weiss I, Ballerini P, et al. HOX11L2/TLX3 is transcriptionally activated through T-cell regulatory elements downstream of BCL11B as a result of the t(5;14)(q35;q32). Blood. 2006;108(13):4198-201.
27. Gutierrez A, Kentsis A, Sanda T, Holmfeldt L, Chen SC, Zhang J, et al. The BCL11B tumor suppressor is mutated across the major molecular subtypes of T-cell acute lymphoblastic leukemia. Blood. 2011;118(15):4169-73.
28. Zuurbier L, Homminga I, Calvert V, te Winkel ML, Buijs-Gladdines JG, Kooi C, et al. NOTCH1 and/or FBXW7 mutations predict for initial good prednisone response but not for improved outcome in pediatric T-cell acute lymphoblastic leukemia patients treated on DCOG or COALL protocols. Leukemia. 2010;24(12):2014-22.
29. Paganin M, Grillo MF, Silvestri D, Scapinello G, Buldini B, Cazzaniga G, et al. The presence of mutated and deleted PTEN is associated with an increased risk of relapse in childhood T cell acute lymphoblastic leukaemia treated with AIEOP-BFM ALL protocols. Br J Haematol. 2018;182(5):705-11.
30. Zuurbier L, Petricoin EF, 3rd, Vuerhard MJ, Calvert V, Kooi C, Buijs-Gladdines JG, et al. The significance of PTEN and AKT aberrations in pediatric T-cell acute lymphoblastic leukemia. Haematologica. 2012;97(9):1405-13.
31. Gutierrez A, Sanda T, Grebliunaite R, Carracedo A, Salmena L, Ahn Y, et al. High frequency of PTEN, PI3K, and AKT abnormalities in T-cell acute lymphoblastic leukemia. Blood. 2009;114(3):647-50.
32. Roberts AW, Davids MS, Pagel JM, Kahl BS, Puvvada SD, Gerecitano JF, et al. Targeting BCL2 with Venetoclax in Relapsed Chronic Lymphocytic Leukemia. N Engl J Med. 2016;374(4):311-22.

33. Butterworth M, Pettitt A, Varadarajan S, Cohen GM. BH3 profiling and a toolkit of BH3-mimetic drugs predict anti-apoptotic dependence of cancer cells. Br J Cancer. 2016;114(6):638-41.
34. Chonghaile TN, Roderick JE, Glenfield C, Ryan J, Sallan SE, Silverman LB, et al. Maturation stage of T-cell acute lymphoblastic leukemia determines BCL-2 versus BCL-XL dependence and sensitivity to ABT-199. Cancer Discov. 2014;4(9):1074-87.
35. Peirs S, Matthijssens F, Goossens S, Van de Walle I, Ruggero K, de Bock CE, et al. ABT-199 mediated inhibition of BCL-2 as a novel therapeutic strategy in T-cell acute lymphoblastic leukemia. Blood. 2014;124(25):3738-47.
36. Suryani S, Carol H, Chonghaile TN, Frismantas V, Sarmah C, High L, et al. Cell and molecular determinants of in vivo efficacy of the BH3 mimetic ABT-263 against pediatric acute lymphoblastic leukemia xenografts. Clin Cancer Res. 2014;20(17):4520-31.
37. Lacayo NJ, Pullarkat VA, Stock W, Jabbour E, Bajel A, Rubnitz J, et al. Safety and Efficacy of Venetoclax in Combination with Navitoclax in Adult and Pediatric Relapsed/Refractory Acute Lymphoblastic Leukemia and Lymphoblastic Lymphoma. Blood. 2019;134(Supplement_1):285-.
38. La Starza R, Cambò B, Pierini A, Bornhauser B, Montanaro A, Bourquin JP, et al. Venetoclax and Bortezomib in Relapsed/Refractory Early T-Cell Precursor Acute Lymphoblastic Leukemia. JCO Precision Oncology. 2019(3):1-6.
39. Li Z, He S, Look AT. The MCL1-specific inhibitor S63845 acts synergistically with venetoclax/ABT-199 to induce apoptosis in T-cell acute lymphoblastic leukemia cells. Leukemia. 2019;33(1):262-6.
40. Choudhary GS, Al-Harbi S, Mazumder S, Hill BT, Smith MR, Bodo J, et al. MCL-1 and BCL-xL-dependent resistance to the BCL-2 inhibitor ABT-199 can be overcome by preventing PI3K/AKT/mTOR activation in lymphoid malignancies. Cell Death Dis. 2015;6:e1593.
41. Chen X, Glytsou C, Zhou H, Narang S, Reyna DE, Lopez A, et al. Targeting Mitochondrial Structure Sensitizes Acute Myeloid Leukemia to Venetoclax Treatment. Cancer Discov. 2019;9(7):890-909.
42. Ni Chonghaile T, Sarosiek KA, Vo TT, Ryan JA, Tammareddi A, Moore Vdel G, et al. Pretreatment mitochondrial priming correlates with clinical response to cytotoxic chemotherapy. Science. 2011;334(6059):1129-33.
43. Takebe N, Nguyen D, Yang SX. Targeting notch signaling pathway in cancer: clinical development advances and challenges. Pharmacol Ther. 2014;141(2):140-9.
44. Samon JB, Castillo-Martin M, Hadler M, Ambesi-Impiobato A, Paietta E, Racevskis J, et al. Preclinical analysis of the gamma-secretase inhibitor PF-03084014 in combination with glucocorticoids in T-cell acute lymphoblastic leukemia. Mol Cancer Ther. 2012;11(7):1565-75.
45. Habets RA, de Bock CE, Serneels L, Lodewijckx I, Verbeke D, Nittner D, et al. Safe targeting of T cell acute lymphoblastic leukemia by pathology-specific NOTCH inhibition. Sci Transl Med. 2019;11(494).
46. Agnusdei V, Minuzzo S, Frasson C, Grassi A, Axelrod F, Satyal S, et al. Therapeutic antibody targeting of Notch1 in T-acute lymphoblastic leukemia xenografts. Leukemia. 2014;28(2):278-88.
47. Marchesini M, Gherli A, Montanaro A, Patrizi L, Sorrentino C, Pagliaro L, et al. Blockade of Oncogenic NOTCH1 with the SERCA Inhibitor CAD204520 in T Cell Acute Lymphoblastic Leukemia. Cell Chem Biol. 2020.
48. Dastur A, Choi A, Costa C, Yin X, Williams A, McClanaghan J, et al. NOTCH1 Represses MCL-1 Levels in GSI-resistant T-ALL, Making them Susceptible to ABT-263. Clin Cancer Res. 2019;25(1):312-24.

49. Tsaouli G, Ferretti E, Bellavia D, Vacca A, Felli MP. Notch/CXCR4 Partnership in Acute Lymphoblastic Leukemia Progression. J Immunol Res. 2019;2019:5601396.
50. Filippakopoulos P, Qi J, Picaud S, Shen Y, Smith WB, Fedorov O, et al. Selective inhibition of BET bromodomains. Nature. 2010;468(7327):1067-73.
51. Palomero T, Lim WK, Odom DT, Sulis ML, Real PJ, Margolin A, et al. NOTCH1 directly regulates c-MYC and activates a feed-forward-loop transcriptional network promoting leukemic cell growth. Proc Natl Acad Sci U S A. 2006;103(48):18261-6.
52. Roderick JE, Tesell J, Shultz LD, Brehm MA, Greiner DL, Harris MH, et al. c-Myc inhibition prevents leukemia initiation in mice and impairs the growth of relapsed and induction failure pediatric T-ALL cells. Blood. 2014;123(7):1040-50.
53. Loosveld M, Castellano R, Gon S, Goubard A, Crouzet T, Pouyet L, et al. Therapeutic targeting of c-Myc in T-cell acute lymphoblastic leukemia, T-ALL. Oncotarget. 2014;5(10):3168-72.
54. Peirs S, Frismantas V, Matthijssens F, Van Loocke W, Pieters T, Vandamme N, et al. Targeting BET proteins improves the therapeutic efficacy of BCL-2 inhibition in T-cell acute lymphoblastic leukemia. Leukemia. 2017;31(10):2037-47.
55. Knoechel B, Roderick JE, Williamson KE, Zhu J, Lohr JG, Cotton MJ, et al. An epigenetic mechanism of resistance to targeted therapy in T cell acute lymphoblastic leukemia. Nat Genet. 2014;46(4):364-70.
56. Ott CJ, Kopp N, Bird L, Paranal RM, Qi J, Bowman T, et al. BET bromodomain inhibition targets both c-Myc and IL7R in high-risk acute lymphoblastic leukemia. Blood. 2012;120(14):2843-52.
57. McCarter AC, Gatta GD, Melnick A, Kim E, Sha C, Wang Q, et al. Combinatorial ETS1-dependent control of oncogenic NOTCH1 enhancers in T-cell leukemia. Blood Cancer Discov. 2020;1(2):178-97.
58. Guo L, Li J, Zeng H, Guzman AG, Li T, Lee M, et al. A combination strategy targeting enhancer plasticity exerts synergistic lethality against BETi-resistant leukemia cells. Nature communications. 2020;11(1):740.
59. Kloetgen A, Thandapani P, Ntziachristos P, Ghebrechristos Y, Nomikou S, Lazaris C, et al. Three-dimensional chromatin landscapes in T cell acute lymphoblastic leukemia. Nat Genet. 2020;52(4):388-400.
60. Kwiatkowski N, Zhang T, Rahl PB, Abraham BJ, Reddy J, Ficarro SB, et al. Targeting transcription regulation in cancer with a covalent CDK7 inhibitor. Nature. 2014;511(7511):616-20.
61. Cochran AG, Conery AR, Sims RJ, 3rd. Bromodomains: a new target class for drug development. Nat Rev Drug Discov. 2019;18(8):609-28.
62. Astorgues-Xerri L, Vazquez R, Odore E, Rezai K, Kahatt C, Mackenzie S, et al. Insights into the cellular pharmacological properties of the BET-inhibitor OTX015/MK-8628 (birabresib), alone and in combination, in leukemia models. Leuk Lymphoma. 2019;60(12):3067-70.
63. Graux C, Cools J, Melotte C, Quentmeier H, Ferrando A, Levine R, et al. Fusion of NUP214 to ABL1 on amplified episomes in T-cell acute lymphoblastic leukemia. Nat Genet. 2004;36(10):1084-9.
64. Graux C, Stevens-Kroef M, Lafage M, Dastugue N, Harrison CJ, Mugneret F, et al. Heterogeneous patterns of amplification of the NUP214-ABL1 fusion gene in T-cell acute lymphoblastic leukemia. Leukemia. 2009;23(1):125-33.
65. Chen B, Jiang L, Zhong ML, Li JF, Li BS, Peng LJ, et al. Identification of fusion genes and characterization of transcriptome features in T-cell acute lymphoblastic leukemia. Proc Natl Acad Sci U S A. 2018;115(2):373-8.
66. Frismantas V, Dobay MP, Rinaldi A, Tchinda J, Dunn SH, Kunz J, et al. Ex vivo drug response profiling detects recurrent sensitivity patterns in drug-resistant acute lymphoblastic leukemia. Blood. 2017;129(11):e26-e37.

67. Serafin V, Capuzzo G, Milani G, Minuzzo SA, Pinazza M, Bortolozzi R, et al. Glucocorticoid resistance is reverted by LCK inhibition in pediatric T-cell acute lymphoblastic leukemia. Blood. 2017;130(25):2750-61.
68. Shi Y, Beckett MC, Blair HJ, Tirtakusuma R, Nakjang S, Enshaei A, et al. Phase II-like murine trial identifies synergy between dexamethasone and dasatinib in T-cell acute lymphoblastic leukemia. Haematologica. 2020.
69. Maude SL, Dolai S, Delgado-Martin C, Vincent T, Robbins A, Selvanathan A, et al. Efficacy of JAK/STAT pathway inhibition in murine xenograft models of early T-cell precursor (ETP) acute lymphoblastic leukemia. Blood. 2015;125(11):1759-67.
70. Delgado-Martin C, Meyer LK, Huang BJ, Shimano KA, Zinter MS, Nguyen JV, et al. JAK/STAT pathway inhibition overcomes IL7-induced glucocorticoid resistance in a subset of human T-cell acute lymphoblastic leukemias. Leukemia. 2017;31(12):2568-76.
71. de Bock CE, Demeyer S, Degryse S, Verbeke D, Sweron B, Gielen O, et al. HOXA9 Cooperates with Activated JAK/STAT Signaling to Drive Leukemia Development. Cancer Discov. 2018;8(5):616-31.
72. Verstovsek S, Kantarjian H, Mesa RA, Pardanani AD, Cortes-Franco J, Thomas DA, et al. Safety and efficacy of INCB018424, a JAK1 and JAK2 inhibitor, in myelofibrosis. N Engl J Med. 2010;363(12):1117-27.
73. Greenfield G, McPherson S, Mills K, McMullin MF. The ruxolitinib effect: understanding how molecular pathogenesis and epigenetic dysregulation impact therapeutic efficacy in myeloproliferative neoplasms. J Transl Med. 2018;16(1):360.
74. Padi SKR, Luevano LA, An N, Pandey R, Singh N, Song JH, et al. Targeting the PIM protein kinases for the treatment of a T-cell acute lymphoblastic leukemia subset. Oncotarget. 2017;8(18):30199-216.
75. Ribeiro D, Melao A, van Boxtel R, Santos CI, Silva A, Silva MC, et al. STAT5 is essential for IL-7-mediated viability, growth, and proliferation of T-cell acute lymphoblastic leukemia cells. Blood Adv. 2018;2(17):2199-213.
76. La Starza R, Messina M, Gianfelici V, Pierini V, Matteucci C, Pierini T, et al. High PIM1 expression is a biomarker of T-cell acute lymphoblastic leukemia with JAK/STAT activation or t(6;7)(p21;q34)/TRB@-PIM1 rearrangement. Leukemia. 2018;32(8):1807-10.
77. De Smedt R, Peirs S, Morscio J, Matthijssens F, Roels J, Reunes L, et al. Pre-clinical evaluation of second generation PIM inhibitors for the treatment of T-cell acute lymphoblastic leukemia and lymphoma. Haematologica. 2019;104(1):e17-e20.
78. Lin YW, Beharry ZM, Hill EG, Song JH, Wang W, Xia Z, et al. A small molecule inhibitor of Pim protein kinases blocks the growth of precursor T-cell lymphoblastic leukemia/lymphoma. Blood. 2010;115(4):824-33.
79. De Smedt R, Morscio J, Reunes L, Roels J, Bardelli V, Lintermans B, et al. Targeting cytokine- and therapy-induced PIM1 activation in preclinical models of T-cell acute lymphoblastic leukemia and lymphoma. Blood. 2020;135(19):1685-95.
80. Mendes RD, Sarmento LM, Cante-Barrett K, Zuurbier L, Buijs-Gladdines JG, Povoa V, et al. PTEN microdeletions in T-cell acute lymphoblastic leukemia are caused by illegitimate RAG-mediated recombination events. Blood. 2014;124(4):567-78.
81. Trinquand A, Tanguy-Schmidt A, Ben Abdelali R, Lambert J, Beldjord K, Lengline E, et al. Toward a NOTCH1/FBXW7/RAS/PTEN-based oncogenetic risk classification of adult T-cell acute lymphoblastic leukemia: a Group for Research in Adult Acute Lymphoblastic Leukemia study. J Clin Oncol. 2013;31(34):4333-42.
82. Lonetti A, Cappellini A, Sparta AM, Chiarini F, Buontempo F, Evangelisti C, et al. PI3K pan-inhibition impairs more efficiently proliferation and survival of T-cell acute lymphoblastic leukemia cell lines when compared to isoform-selective PI3K inhibitors. Oncotarget. 2015;6(12):10399-414.

83. Lonetti A, Antunes IL, Chiarini F, Orsini E, Buontempo F, Ricci F, et al. Activity of the pan-class I phosphoinositide 3-kinase inhibitor NVP-BKM120 in T-cell acute lymphoblastic leukemia. Leukemia. 2014;28(6):1196-206.
84. Lonetti A, Cappellini A, Bertaina A, Locatelli F, Pession A, Buontempo F, et al. Improving nelarabine efficacy in T cell acute lymphoblastic leukemia by targeting aberrant PI3K/AKT/mTOR signaling pathway. J Hematol Oncol. 2016;9(1):114.
85. Chiarini F, Fala F, Tazzari PL, Ricci F, Astolfi A, Pession A, et al. Dual inhibition of class IA phosphatidylinositol 3-kinase and mammalian target of rapamycin as a new therapeutic option for T-cell acute lymphoblastic leukemia. Cancer Res. 2009;69(8):3520-8.
86. Hall CP, Reynolds CP, Kang MH. Modulation of Glucocorticoid Resistance in Pediatric T-cell Acute Lymphoblastic Leukemia by Increasing BIM Expression with the PI3K/mTOR Inhibitor BEZ235. Clin Cancer Res. 2016;22(3):621-32.
87. Gazi M, Moharram SA, Marhall A, Kazi JU. The dual specificity PI3K/mTOR inhibitor PKI-587 displays efficacy against T-cell acute lymphoblastic leukemia (T-ALL). Cancer Lett. 2017;392:9-16.
88. Batista A, Barata JT, Raderschall E, Sallan SE, Carlesso N, Nadler LM, et al. Targeting of active mTOR inhibits primary leukemia T cells and synergizes with cytotoxic drugs and signaling inhibitors. Exp Hematol. 2011;39(4):457-72 e3.
89. Pikman Y, Alexe G, Roti G, Conway AS, Furman A, Lee ES, et al. Synergistic Drug Combinations with a CDK4/6 Inhibitor in T-cell Acute Lymphoblastic Leukemia. Clin Cancer Res. 2017;23(4):1012-24.
90. Benjamin D, Colombi M, Moroni C, Hall MN. Rapamycin passes the torch: a new generation of mTOR inhibitors. Nat Rev Drug Discov. 2011;10(11):868-80.
91. Yun S, Vincelette ND, Knorr KL, Almada LL, Schneider PA, Peterson KL, et al. 4EBP1/c-MYC/PUMA and NF-kappaB/EGR1/BIM pathways underlie cytotoxicity of mTOR dual inhibitors in malignant lymphoid cells. Blood. 2016;127(22):2711-22.
92. Martelli AM, Chiarini F, Evangelisti C, Cappellini A, Buontempo F, Bressanin D, et al. Two hits are better than one: targeting both phosphatidylinositol 3-kinase and mammalian target of rapamycin as a therapeutic strategy for acute leukemia treatment. Oncotarget. 2012;3(4):371-94.
93. Simioni C, Neri LM, Tabellini G, Ricci F, Bressanin D, Chiarini F, et al. Cytotoxic activity of the novel Akt inhibitor, MK-2206, in T-cell acute lymphoblastic leukemia. Leukemia. 2012;26(11):2336-42.
94. Lynch JT, McEwen R, Crafter C, McDermott U, Garnett MJ, Barry ST, et al. Identification of differential PI3K pathway target dependencies in T-cell acute lymphoblastic leukemia through a large cancer cell panel screen. Oncotarget. 2016;7(16):22128-39.
95. Irving J, Matheson E, Minto L, Blair H, Case M, Halsey C, et al. Ras pathway mutations are prevalent in relapsed childhood acute lymphoblastic leukemia and confer sensitivity to MEK inhibition. Blood. 2014;124(23):3420-30.
96. Jerchel IS, Hoogkamer AQ, Aries IM, Steeghs EMP, Boer JM, Besselink NJM, et al. RAS pathway mutations as a predictive biomarker for treatment adaptation in pediatric B-cell precursor acute lymphoblastic leukemia. Leukemia. 2018;32(4):931-40.
97. Driessen EM, van Roon EH, Spijkers-Hagelstein JA, Schneider P, de Lorenzo P, Valsecchi MG, et al. Frequencies and prognostic impact of RAS mutations in MLL-rearranged acute lymphoblastic leukemia in infants. Haematologica. 2013;98(6):937-44.
98. Richter-Pechanska P, Kunz JB, Hof J, Zimmermann M, Rausch T, Bandapalli OR, et al. Identification of a genetically defined ultra-high-risk group in relapsed pediatric T-lymphoblastic leukemia. Blood Cancer J. 2017;7(2):e523.

99. Aries IM, van den Dungen RE, Koudijs MJ, Cuppen E, Voest E, Molenaar JJ, et al. Towards personalized therapy in pediatric acute lymphoblastic leukemia: RAS mutations and prednisolone resistance. Haematologica. 2015;100(4):e132-6.
100. Matheson EC, Thomas H, Case M, Blair H, Jackson RK, Masic D, et al. Glucocorticoids and selumetinib are highly synergistic in RAS pathway-mutated childhood acute lymphoblastic leukemia through upregulation of BIM. Haematologica. 2019;104(9):1804-11.
101. Kerstjens M, Driessen EM, Willekes M, Pinhancos SS, Schneider P, Pieters R, et al. MEK inhibition is a promising therapeutic strategy for MLL-rearranged infant acute lymphoblastic leukemia patients carrying RAS mutations. Oncotarget. 2017;8(9):14835-46.
102. Jang W, Park J, Kwon A, Choi H, Kim J, Lee GD, et al. CDKN2B downregulation and other genetic characteristics in T-acute lymphoblastic leukemia. Exp Mol Med. 2019;51(1):4.
103. Sawai CM, Freund J, Oh P, Ndiaye-Lobry D, Bretz JC, Strikoudis A, et al. Therapeutic targeting of the cyclin D3:CDK4/6 complex in T cell leukemia. Cancer Cell. 2012;22(4):452-65.
104. Moharram SA, Shah K, Khanum F, Marhall A, Gazi M, Kazi JU. Efficacy of the CDK inhibitor dinaciclib in vitro and in vivo in T-cell acute lymphoblastic leukemia. Cancer Lett. 2017;405:73-8.
105. Gojo I, Sadowska M, Walker A, Feldman EJ, Iyer SP, Baer MR, et al. Clinical and laboratory studies of the novel cyclin-dependent kinase inhibitor dinaciclib (SCH 727965) in acute leukemias. Cancer Chemother Pharmacol. 2013;72(4):897-908.
106. Kurtzberg J, Ernst TJ, Keating MJ, Gandhi V, Hodge JP, Kisor DF, et al. Phase I study of 506U78 administered on a consecutive 5-day schedule in children and adults with refractory hematologic malignancies. J Clin Oncol. 2005;23(15):3396-403.
107. Berg SL, Blaney SM, Devidas M, Lampkin TA, Murgo A, Bernstein M, et al. Phase II study of nelarabine (compound 506U78) in children and young adults with refractory T-cell malignancies: a report from the Children's Oncology Group. J Clin Oncol. 2005;23(15):3376-82.
108. Gokbuget N, Basara N, Baurmann H, Beck J, Bruggemann M, Diedrich H, et al. High single-drug activity of nelarabine in relapsed T-lymphoblastic leukemia/lymphoma offers curative option with subsequent stem cell transplantation. Blood. 2011;118(13):3504-11.
109. Malone A, Smith OP. Nelarabine toxicity in children and adolescents with relapsed/refractory T-ALL/T-LBL: can we avoid throwing the baby out with the bathwater? Br J Haematol. 2017;179(2):179-81.
110. Dunsmore KP, Winter SS, Devidas M, Wood BL, Esiashvili N, Chen Z, et al. Children's Oncology Group AALL0434: A Phase III Randomized Clinical Trial Testing Nelarabine in Newly Diagnosed T-Cell Acute Lymphoblastic Leukemia. J Clin Oncol. 2020;38(28):3282-93.
111. Hoell JI, Ginzel S, Kuhlen M, Kloetgen A, Gombert M, Fischer U, et al. Pediatric ALL relapses after allo-SCT show high individuality, clonal dynamics, selective pressure, and druggable targets. Blood Adv. 2019;3(20):3143-56.
112. Bykov VJN, Eriksson SE, Bianchi J, Wiman KG. Targeting mutant p53 for efficient cancer therapy. Nat Rev Cancer. 2018;18(2):89-102.
113. Ghione P, Moskowitz AJ, De Paola NEK, Horwitz SM, Ruella M. Novel Immunotherapies for T Cell Lymphoma and Leukemia. Current hematologic malignancy reports. 2018;13(6):494-506.
114. Bride KL, Vincent TL, Im SY, Aplenc R, Barrett DM, Carroll WL, et al. Preclinical efficacy of daratumumab in T-cell acute lymphoblastic leukemia. Blood. 2018;131(9):995-9.
115. Krejcik J, Casneuf T, Nijhof IS, Verbist B, Bald J, Plesner T, et al. Daratumumab depletes CD38+ immune regulatory cells, promotes T-cell expansion, and skews T-cell repertoire in multiple myeloma. Blood. 2016;128(3):384-94.

116. Ofran Y, Ringelstein-Harlev S, Slouzkey I, Zuckerman T, Yehudai-Ofir D, Henig I, et al. Daratumumab for eradication of minimal residual disease in high-risk advanced relapse of T-cell/CD19/CD22-negative acute lymphoblastic leukemia. Leukemia. 2020;34(1):293-5.
117. Trinquand A, Dos Santos NR, Tran Quang C, Rocchetti F, Zaniboni B, Belhocine M, et al. Triggering the TCR Developmental Checkpoint Activates a Therapeutically Targetable Tumor Suppressive Pathway in T-cell Leukemia. Cancer Discov. 2016;6(9):972-85.
118. Fleischer LC, Spencer HT, Raikar SS. Targeting T cell malignancies using CAR-based immunotherapy: challenges and potential solutions. J Hematol Oncol. 2019;12(1):141.
119. Depil S, Duchateau P, Grupp SA, Mufti G, Poirot L. 'Off-the-shelf' allogeneic CAR T cells: development and challenges. Nat Rev Drug Discov. 2020;19(3):185-99.
120. Mamonkin M, Rouce RH, Tashiro H, Brenner MK. A T-cell-directed chimeric antigen receptor for the selective treatment of T-cell malignancies. Blood. 2015;126(8):983-92.
121. Gomes-Silva D, Srinivasan M, Sharma S, Lee CM, Wagner DL, Davis TH, et al. CD7-edited T cells expressing a CD7-specific CAR for the therapy of T-cell malignancies. Blood. 2017;130(3):285-96.
122. Brandt LJB, Barnkob MB, Michaels YS, Heiselberg J, Barington T. Emerging Approaches for Regulation and Control of CAR T Cells: A Mini Review. Front Immunol. 2020;11:326.
123. Cooper ML, Choi J, Staser K, Ritchey JK, Devenport JM, Eckardt K, et al. An "off-the-shelf" fratricide-resistant CAR-T for the treatment of T cell hematologic malignancies. Leukemia. 2018;32(9):1970-83.
124. Wang X, Li S, Gao L, Yuan Z, Wu K, Liu L, et al. Abstract CT052: Clinical safety and efficacy study of TruUCAR™ GC027: The first-in-human, universal CAR-T therapy for adult relapsed/refractory T-cell acute lymphoblastic leukemia (r/r T-ALL). Cancer Research. 2020;80(16 Supplement):CT052-CT.
125. Sanchez-Martinez D, Baroni ML, Gutierrez-Aguera F, Roca-Ho H, Blanch-Lombarte O, Gonzalez-Garcia S, et al. Fratricide-resistant CD1a-specific CAR T cells for the treatment of cortical T-cell acute lymphoblastic leukemia. Blood. 2019;133(21):2291-304.
126. Gao Z, Tong C, Wang Y, Chen D, Wu Z, Han W. Blocking CD38-driven fratricide among T cells enables effective antitumor activity by CD38-specific chimeric antigen receptor T cells. J Genet Genomics. 2019;46(8):367-77.
127. Guo Y, Feng K, Tong C, Jia H, Liu Y, Wang Y, et al. Efficiency and side effects of anti-CD38 CAR T cells in an adult patient with relapsed B-ALL after failure of bi-specific CD19/CD22 CAR T cell treatment. Cell Mol Immunol. 2020;17(4):430-2.
128. Evans K, Duan J, Pritchard T, Jones CD, McDermott L, Gu Z, et al. OBI-3424, a Novel AKR1C3-Activated Prodrug, Exhibits Potent Efficacy against Preclinical Models of T-ALL. Clin Cancer Res. 2019;25(14):4493-503.
129. Verbeke D, Demeyer S, Prieto C, de Bock CE, De Bie J, Gielen O, et al. The XPO1 Inhibitor KPT-8602 Synergizes with Dexamethasone in Acute Lymphoblastic Leukemia. Clin Cancer Res. 2020.
130. Moreno DA, Scrideli CA, Cortez MA, de Paula Queiroz R, Valera ET, da Silva Silveira V, et al. Differential expression of HDAC3, HDAC7 and HDAC9 is associated with prognosis and survival in childhood acute lymphoblastic leukaemia. Br J Haematol. 2010;150(6):665-73.
131. Waibel M, Vervoort SJ, Kong IY, Heinzel S, Ramsbottom KM, Martin BP, et al. Epigenetic targeting of Notch1-driven transcription using the HDACi panobinostat is a potential therapy against T-cell acute lymphoblastic leukemia. Leukemia. 2018;32(1):237-41.
132. Lu BY, Thanawala SU, Zochowski KC, Burke MJ, Carroll WL, Bhatla T. Decitabine enhances chemosensitivity of early T-cell precursor-acute lymphoblastic leukemia cell lines and patient-derived samples. Leuk Lymphoma. 2016;57(8):1938-41.

133. El Chaer F, Holtzman N, Binder E, Porter NC, Singh ZN, Koka M, et al. Durable remission with salvage decitabine and donor lymphocyte infusion (DLI) for relapsed early T-cell precursor ALL. Bone Marrow Transplant. 2017;52(11):1583-4.
134. Horton TM, Whitlock JA, Lu X, O'Brien MM, Borowitz MJ, Devidas M, et al. Bortezomib reinduction chemotherapy in high-risk ALL in first relapse: a report from the Children's Oncology Group. Br J Haematol. 2019;186(2):274-85.
135. Han K, Wang Q, Cao H, Qiu G, Cao J, Li X, et al. The NEDD8-activating enzyme inhibitor MLN4924 induces G2 arrest and apoptosis in T-cell acute lymphoblastic leukemia. Oncotarget. 2016;7(17):23812-24.
136. Hartsink-Segers SA, Zwaan CM, Exalto C, Luijendijk MW, Calvert VS, Petricoin EF, et al. Aurora kinases in childhood acute leukemia: the promise of aurora B as therapeutic target. Leukemia. 2013;27(3):560-8.
137. Park SI, Lin CP, Ren N, Angus SP, Dittmer DP, Foote M, et al. Inhibition of Aurora A Kinase in Combination with Chemotherapy Induces Synthetic Lethality and Overcomes Chemoresistance in Myc-Overexpressing Lymphoma. Targeted oncology. 2019;14(5):563-75.
138. Mosse YP, Fox E, Teachey DT, Reid JM, Safgren SL, Carol H, et al. A Phase II Study of Alisertib in Children with Recurrent/Refractory Solid Tumors or Leukemia: Children's Oncology Group Phase I and Pilot Consortium (ADVL0921). Clin Cancer Res. 2019;25(11):3229-38.
139. Jiang J, Wang J, Yue M, Cai X, Wang T, Wu C, et al. Direct Phosphorylation and Stabilization of MYC by Aurora B Kinase Promote T-cell Leukemogenesis. Cancer Cell. 2020;37(2):200-15. e5.
140. Goto H, Yoshino Y, Ito M, Nagai J, Kumamoto T, Inukai T, et al. Aurora B kinase as a therapeutic target in acute lymphoblastic leukemia. Cancer Chemother Pharmacol. 2020;85(4):773-83.
141. Harttrampf AC, Lacroix L, Deloger M, Deschamps F, Puget S, Auger N, et al. Molecular Screening for Cancer Treatment Optimization (MOSCATO-01) in Pediatric Patients: A Single-Institutional Prospective Molecular Stratification Trial. Clin Cancer Res. 2017;23(20):6101-12.

Supplemental Table 1. Relevant clinical trials investigating targeted therapies for T-ALL treatment

Therapeutic agent	Target	Association with T-ALL subtype / outcome	Clinical trial identifier and year posted on clinicaltrials.gov	Tumor type	Phase and status	Results
BH3 mimetics						
Venetoclax (ABT-199)	Higher BCL2 expression	Higher in ETP-ALL	NCT03236857 (p, ya); 2017	R/R malignancies	I (R)	
			NCT03808610 (a); 2019	R/R ALL (with low dose chemotherapy)	I/II (R)	
Navitoclax (ABT-263)	Higher BCL2 and BCLXL expression		NCT00406809 (a); 2006	R/R lymphoid malignancies	I/II (C)	Acute thrombocytopenia and neutropenia observed (1)
			NCT03181126 (p, a); 2017	R/R ALL or LBL (with chemotherapy)	I (A)	
AZD-5991	Higher MCL1 expression		NCT03218683 (a); 2017	R/R hematological malignacies (also with venetoclax)	I (A)	
NOTCH1 inhibitors	*NOTCH1* activating mutations	Favorable outcome				
Brontictuzumab (OMP-52M51)			NCT01703572 (a); 2012	R/R lymphoid malignancies	I (C)	
γ-secretase inhibitors						
LY3039478			NCT02518113 (p, a); 2015	T-ALL/T-LBL (with dexamethasone)	I/II (C)	
BMS-906024			NCT01363817 (a); 2011	R/R T-ALL/LBL (alone or in combination with dexamethasone)	I (C)	
PF-3084014			NCT00878189 (ya; a); 2009	R/R T-ALL/LBL and solid tumors	I (C)	Preliminary anti T-ALL activity (2)
CXCR4 inhibitors						
Plerixafor (AMD3100)			NCT01319864 (p, a); 2011	R/R ALL, AML and MSD (with cytarabine and etoposide)	I (C)	No response in ALL patients (3)
BL-8040			NCT02763384 (a); 2016	R/R T-ALL/T-LBL (with nelarabine)	II (R)	
BET inhibitors	BRD4 activity aberrant Myc activity					
OTX015 (MK-8628)			NCT01713582 (a); 2012	R/R acute leukemia and MM	I (C)	
GSK525762			NCT٠١٩٤٣٨٥١ (a); ٢٠١٣	R/R hematological malignancies	I/II (C)	
ABL/SRC inhibitors	*ABL1* fusions					
Dasatinib			NCT03117751 (p); 2017	Dx ALL/LL (with chemotherapy)	II/III (R)	
Imatinib			NCT02551718 (p, a); 2015	R/R acute leukemia	N/A (R)	

JAK1/2 inhibitor	*IL7Rα, JAK1/3* and *STAT5B* mutations	Higher in ETP-ALL Associated with steroid resistance				
Ruxolitinib			NCT01251965 (ya, a); 2010	R/R ALL/AML	I/II (T)	No clinical benefit *
			NCT03613428 (p, a); 2018	R/R ETP-ALL (with chemotherapy)	I/II (NR)	
			NCT03117751 (p); 2017	Dx ALL/LL (with chemotherapy)	II/III (R)	
			NCT03515200 (p, ya); 2018	R/R ALL (with chemotherapy)	I (T)	
Pan-PI3K inhibitors						
Buparlisib (BMK120)	*PIK3R1 and PIK3CA/D mutations* *AKT mutations and PTEN deletions*	Poor prognosis, therapy failure and relapse	NCT01396499 (a); 2011	R/R acute leukemia	I (C)	
			NCT01833169 (a); 2013	PIK3-activated solid and hematological malignancies	II (C)	
Selective-PI3K inhibitors						
Duvelisib (IPI-145, γ/δ inhibitor)			NCT02711852 (a); 2016	R/R hematological malignancies	II (A)	
Idelalisib (CAL-101, δ inhibitor)			NCT03742323 (a); 2018	R/R ALL	I/II (R)	
mTOR inhibitors						
Everolimus (rapamycin, RAD001)			NCT00968253 (p, a); 2009	R/R ALL (with chemotherapy)	I/II (C)	The combination is well tolerated with moderate activity in T-ALL (4)
			NCT01523977 (p, ya); 2012	R/R ALL (with chemotherapy)	I (C)	Combination is feasible (5)
			NCT00874562 (p, a); 2009	R/R ALL (with corticosteroids)	I (C)	
			NCT03740334 (p,a); 2018	R/R ALL (with dexamethasone and ribociclib)	I (R)	
Temsirolimus (CCI-799)			NCT00084916 (a); 2004	R/R leukemia	II (C)	
			NCT01403415 (p, ya); 2011	>2 relapses ALL/LBL (with re-induction chemotherapy)	I (C)	Excessive toxicity (6)
Dual PI3K/mTOR inhibitors			NCT01756118 (a); 2012	R/R acute leukemia	I (A)	
Dactolisib (NVP-BEZ235)						
AKT inhibitors			NCT01231919 (p, ya); 2010	R/R solid tumors or leukemia	I (C)	
MK-2206 (allosteric)						

MEK inhibitors						
Selumetinib	*NRAS / KRAS* mutations	Higher in ETP-ALL Associated with steroid resistance	NCT03705507 (p, a); 2018	R/R ALL (with dexamethasone)	I/II (R)	
Trametinib			NCT00920140 (a); 2009	R/R leukemias	I/II (C)	
			NCT02551718 (p, a); 2015	R/R acute leukemias	N/A (R)	
Binimetinib (MEK162)			NCT01885195 (a); 2013	RAS/RAF/MEK-activated malignancies	II (C)	
CDK4/6 inhibitors						
Ribociclib (LEE011)	CDKN2A/B downregulation CDKN1B deletions CCND3 upregulation	Lower incidence in ETP-ALL	NCT02187783 (a); 2014	CDK4/6-activated tumors	II (C)	
			NCT03740334 (p, a); 2018	R/R ALL (with dexamethasone and everolimus)	I (R)	
			NCT02813135 (p); 2016	R/R cancer	I/II (R)	
Palbociclib (PD-332991)			NCT03792256 (p); 2019	R/R ALL/LL (with re-induction chemotherapy)	I (R)	
			NCT03132454 (ya, a); 2017	R/R leukemia (with sorafenib, decitabine or dexamethasone)	I (R)	
			NCT03515200 (p, ya); 2018	R/R ALL (with chemotherapy)	I (T)	
Purine analog	Rapid DNA synthesis					
Nelarabine			NCT02551718 (p, a); 2015	R/R acute leukemia	N/A (R)	
			NCT00866671 (p, ya); 2009	R/R T-ALL/LBL with ≥2 prior treatments	IV (C)	The risk–benefit profile is positive (7)
			NCT00408005 (p, ya); 2006	Dx T-ALL/LBL	III (A)	Increased disease-free survival rate (8)
MDM2 inhibitors	MDM2 overexpression					
Idasanutlin			NCT04029688 (p, ya); 2019	R/R acute leukemia or solid tumors (with chemotherapy or venetoclax)	I/II (R)	
HDM201			NCT02143635 (a); 2014	p53-wild type advanced tumors, including ALL	I (C)	
ALRN-6924			NCT03654716 (p, ya); 2018	pediatric cancer, including R/R ALL	I (R)	
Immunotherapy						
Daratumumab	CD38 expression		NCT00501826 (p, a); 2007	T-ALL/T-LBL (with chemotherapy)	II (R)	
			NCT03384654 (p); 2017	R/R ALL/LBL (with chemotherapy)	II (R)	
Isatuximab			NCT03860844 (p); 2019	R/R ALL or AML (with chemotherapy)	II (R)	

CAR T						
Anti-CD5 CAR T	CD5 expression		NCT03081910 (p, a); 2017	R/R T-cell malignancies	I (R)	
Anti-CD7 CAR T	CD7 expression		NCT03690011 (p, a); 2018	R/R T-cell malignancies	I (NR)	
OTHER DRUGS						
XPO1 inhibitor	Nuclear export of oncogenic proteins/mRNA					
Selinexor (KPT-330)			NCT02212561 (p, ya); 2014	R/R ALL, AML or MSD	I (C)	Drug is safe and has promising activity (9)
			NCT02091245 (p, ya); 2014	R/R ALL and AML	I (A)	
HDAC inhibitors	High HDAC expression and activity					
Panobinostat			NCT00723203 (a); 2008	R/R ALL or AML	II (T)	Lack of efficacy *
			NCT02518750 (p); 2015	R/R T-ALL/LBL (with bortezomib and chemotherapy)	II (T)	Slow accrual *
			NCT01321346 (p); 2011	R/R acute leukemias (with cytarabine) and lymphomas	I (C)	
Vorinostat			NCT03117751 (p); 2017	Newly diagnosed ALL/LBL (with chemotherapy)	II/III (R)	
			NCT01483690 (p, ya); 2011	R/R ALL (with decitabine and chemotherapy)	I/II (T)	Excessive toxicity *
			NCT02553460 (p); 2015	Dx ALL (with bortezomib and chemotherapy)	I/II (R)	
Methyltransferase inhibitors	DNA methyltransferases activity					
5-Azacitidine			NCT02551718 (p,a); 2015	R/R acute leukemias	N/A (R)	
			NCT01861002 (p); 2013	R/R ALL or AML (with chemotherapy)	I (C)	
Decitabine			NCT02551718 (p, a); 2015	R/R acute leukemias	N/A (R)	
			NCT01483690 (p, ya); 2011	R/R ALL (with vorinostat and chemotherapy)	I/II (T)	Excessive toxicity *
			NCT00349596 (p, a); 2006	R/R ALL	I (C)	
			NCT03132454 (ya, a); 2017	R/R ALL or AML (with palbociclib)	I (R)	

Proteasome inhibitors						
Bortezomib	Rapid protein turnover and degradation of tumor suppressors proteins		NCT02518750 (p); 2015	R/R T-ALL/LBL (with panobinostat and chemotherapy)	II (T)	Slow accrual *
			NCT02553460 (p); 2015	Dx ALL (with vorinostar and chemotherapy)	I/II (R)	
			NCT02551718 (p, a); 2015	R/R acute leukemias	N/A (R)	
			NCT00440726 (p); 2007	R/R ALL (with chemotherapy)	I/II (C)	
			NCT04224571 (p, ya); 2020	R/R ALL (with chemotherapy)	II (R)	
			NCT00873093 (p, a); 2009	1st relapse ALL/LBL (with chemotherapy)	II (C)	Promising results for T-ALL (10)
			NCT02112916 (p, ya); 2014	Dx T-ALL-LBL (with chemotherapy)	III (A)	
			NCT03590171 (p); 2018	R ALL (with chemotherapy)	II (R)	
			NCT03117751 (p); 2017	Dx ALL/LBL (with chemotherapy)	II/III (R)	
			NCT03643276 (p); 2018	Dx ALL (with chemotherapy)	III (R)	
NAE inhibitor						
Pevonedistat (MLN49243)			NCT03349281 (ya, a); 2017	R/R ALL (with chemotherapy)	I (R)	
AURK inhibitors	AURK overexpression					
Alisertib			NCT01154816 (p, ya); 2010	R/R ALL, AML and solid tumors	II (C)	Response rate <5% as single treatment (11)
AT-9283			NCT01431664 (p); 2011	R/R acute leukemia	I (C)	No efficacy as single treatment (12)

1. Wilson WH, O'Connor OA, Czuczman MS, LaCasce AS, Gerecitano JF, Leonard JP, *et al.* Navitoclax, a targeted high-affinity inhibitor of BCL-2, in lymphoid malignancies: a phase 1 dose-escalation study of safety, pharmacokinetics, pharmacodynamics, and antitumour activity. Lancet Oncol **2010**;11(12):1149-59 doi 10.1016/S1470-2045(10)70261-8.
2. Papayannidis C, DeAngelo DJ, Stock W, Huang B, Shaik MN, Cesari R, *et al.* A Phase 1 study of the novel gamma-secretase inhibitor PF-03084014 in patients with T-cell acute lymphoblastic leukemia and T-cell lymphoblastic lymphoma. Blood Cancer J **2015**;5:e350 doi 10.1038/bcj.2015.80.
3. Cooper TM, Sison EAR, Baker SD, Li L, Ahmed A, Trippett T, *et al.* A phase 1 study of the CXCR4 antagonist plerixafor in combination with high-dose cytarabine and etoposide in children with relapsed or refractory acute leukemias or myelodysplastic syndrome: A Pediatric Oncology Experimental Therapeutics Investigators' Consortium study (POE 10-03). Pediatr Blood Cancer **2017**;64(8) doi 10.1002/pbc.26414.
4. Daver N, Boumber Y, Kantarjian H, Ravandi F, Cortes J, Rytting ME, *et al.* A Phase I/II Study of the mTOR Inhibitor Everolimus in Combination with HyperCVAD Chemotherapy in Patients with Relapsed/Refractory Acute Lymphoblastic Leukemia. Clin Cancer Res **2015**;21(12):2704-14 doi 10.1158/1078-0432.CCR-14-2888.
5. Place AE, Pikman Y, Stevenson KE, Harris MH, Pauly M, Sulis ML, *et al.* Phase I trial of the mTOR inhibitor everolimus in combination with multi-agent chemotherapy in relapsed childhood acute lymphoblastic leukemia. Pediatr Blood Cancer **2018**;65(7):e27062 doi 10.1002/pbc.27062.
6. Rheingold SR, Tasian SK, Whitlock JA, Teachey DT, Borowitz MJ, Liu X, *et al.* A phase 1 trial of temsirolimus and intensive re-induction chemotherapy for 2nd or greater relapse of acute lymphoblastic leukaemia: a Children's Oncology Group study (ADVL1114). Br J Haematol **2017**;177(3):467-74 doi 10.1111/bjh.14569.

7.	Zwaan CM, Kowalczyk J, Schmitt C, Bielorai B, Russo MW, Woessner M*, et al.* Safety and efficacy of nelarabine in children and young adults with relapsed or refractory T-lineage acute lymphoblastic leukaemia or T-lineage lymphoblastic lymphoma: results of a phase 4 study. Br J Haematol **2017**;179(2):284-93 doi 10.1111/bjh.14874.
8.	Dunsmore KP, Winter SS, Devidas M, Wood BL, Esiashvili N, Chen Z*, et al.* Children's Oncology Group AALL0434: A Phase III Randomized Clinical Trial Testing Nelarabine in Newly Diagnosed T-Cell Acute Lymphoblastic Leukemia. J Clin Oncol **2020**;38(28):3282-93 doi 10.1200/JCO.20.00256.
9.	Alexander TB, Lacayo NJ, Choi JK, Ribeiro RC, Pui CH, Rubnitz JE. Phase I Study of Selinexor, a Selective Inhibitor of Nuclear Export, in Combination With Fludarabine and Cytarabine, in Pediatric Relapsed or Refractory Acute Leukemia. J Clin Oncol **2016**;34(34):4094-101 doi 10.1200/JCO.2016.67.5066.
10.	Horton TM, Whitlock JA, Lu X, O'Brien MM, Borowitz MJ, Devidas M*, et al.* Bortezomib reinduction chemotherapy in high-risk ALL in first relapse: a report from the Children's Oncology Group. Br J Haematol **2019**;186(2):274-85 doi 10.1111/bjh.15919.
11.	Mosse YP, Fox E, Teachey DT, Reid JM, Safgren SL, Carol H*, et al.* A Phase II Study of Alisertib in Children with Recurrent/Refractory Solid Tumors or Leukemia: Children's Oncology Group Phase I and Pilot Consortium (ADVL0921). Clin Cancer Res **2019**;25(11):3229-38 doi 10.1158/1078-0432.CCR-18-2675.
12.	Vormoor B, Veal GJ, Griffin MJ, Boddy AV, Irving J, Minto L*, et al.* A phase I/II trial of AT9283, a selective inhibitor of aurora kinase in children with relapsed or refractory acute leukemia: challenges to run early phase clinical trials for children with leukemia. Pediatr Blood Cancer **2017**;64(6) doi 10.1002/pbc.26351.

List of clinical trials investigating the targeted agents described in this review. The clinical trials listed were chosen based on the following two selection criteria: the targeted drug investigated belongs to one of the categories of agents described in the text (modifiers of apoptosis, inhibitors of transcription regulation, signal transduction, cell cycle or immunotherapies) and the trial includes T-ALL patients.

* Source: https://clinicaltrials.gov/

Abbreviations: p= pediatric, ya= young adult, a= adults; ALL= acute lymphoblastic leukemia, LBL= lymphoblastic lymphoma, AML= acute myeloid leukemia, MDS= myelodysplastic syndrome, MM= multiple myeloma, Dx= newly diagnosed, R/R= refractory/relapsed; N/A= not applicable, R= recruiting, A= active, C= completed, T= terminated, NR= not yet recruiting.

3

Recurrent *NR3C1* aberrations at first diagnosis relate to steroid resistance in pediatric T-cell acute lymphoblastic leukemia patients

Jordy C.G. van der Zwet[1], Willem Smits[1], Jessica G.C.A.M Buijs-Gladdines[1], Rob Pieters [1] and Jules P.P. Meijerink[1]

[1] Princess Máxima Center for Pediatric Oncology, Utrecht, the Netherlands

Published in HemaSphere, January 2021
doi: 10.1097/HS9.0000000000000513, PMID: 33364552

ABSTRACT

The glucocorticoid receptor *NR3C1* is essential for steroid-induced apoptosis, and deletions of this gene have been recurrently identified at disease relapse for acute lymphoblastic leukemia (ALL) patients. Here, we demonstrate that recurrent NR3C1 inactivating aberrations – including deletions, missense- and nonsense mutations – are identified in 7% of pediatric T-ALL patients at diagnosis. These aberrations are frequently present in early thymic progenitor (ETP)-ALL patients and relate to steroid resistance. Functional modelling of NR3C1 aberrations in preB-ALL and T-ALL cell lines demonstrate that aberrations decreasing NR3C1 expression are important contributors to steroid resistance at disease diagnosis. Relative *NR3C1* mRNA expression in primary diagnostic patient samples however does not correlate with steroid response.

INTRODUCTION

Synthetic steroids also denoted as glucocorticoids remain cornerstone chemotherapeutic drugs in the treatment of acute lymphoblastic leukemia (ALL). Insufficient response to glucocorticoids during induction therapy remains an important predictor for inferior outcome in pediatric ALL, particularly for T-cell ALL (T-ALL) (1, 2). Activation of the glucocorticoid receptor (NR3C1) leads to its cytoplasmic-to-nuclear translocation, facilitating its function as a transcription factor resulting in cell death (3). Steroid treatment may therefore provide selective pressure of leukemic cells to acquire genetic events that reduces a functional steroid response resulting in therapy failure and relapse, as was recently demonstrated in an elegant T-ALL mouse model (4). An alternative underlying mechanism may include inhibitory phosphorylation of NR3C1 that impairs its nuclear localization and transactivation potential to activate important downstream target genes including *BIM* and *NR3C1* itself (5, 6). Low NR3C1 levels, the failure to upregulate *NR3C1* as a positive feedback loop following steroid exposure or epigenetic silencing of *BIM* have all been linked to steroid resistance (7, 8). Inactivation of NR3C1 by mutations or entire gene deletions have also been identified in leukemic cell lines (9) and are reported in about six percent of ALL patients at relapse (10-12). In particular, over 16 percent of ETV6-RUNX1-positive preB-ALL patients have acquired *NR3C1* deletions at relapse (13). Point mutations or small insertion/deletion mutations in *Nr3c1* were also identified in 18 percent of dexamethasone-resistant relapsed samples in the previously mentioned T-ALL mouse model (4).

In our previous integrated study on pediatric T-ALL patients where we combined genetic data with clinical data including outcome and therapy response of diagnostic biopsies, activating IL7R signaling mutations were identified as an important contributor to steroid resistance (14). In addition, physiological IL7R signaling can also raise cellular steroid resistance (15). Here, we observe that *NR3C1* aberrations are already recurrently present in pediatric T-ALL as early as at first diagnosis. Moreover, we confirm that NR3C1 abnormalities relate to steroid resistance and may facilitate disease selection under first-line induction therapy resulting in relapse.

MATERIALS AND METHODS

Patient samples

Primary diagnostic bone marrow or peripheral blood samples were used from a total of 146 primary pediatric T-ALL patients in this study: 72 enrolled on the Dutch Childhood Oncology Group (DCOG) protocols ALL-7/8 (n=30)(16, 17) or ALL-9 (n=42) (18) and 74 patients enrolled on the German Co-Operative Study Group for Childhood Acute Lymphoblastic Leukemia study (COALL-97, n=74)(19) with a median follow up of 67 and 52 months, respectively. The patients' parents or legal guardians provided informed consent to use leftover diagnostic material for research in accordance with the Institutional Review Board of the Erasmus MC Rotterdam and the Declaration of Helsinki. Leukemia cells were harvested from blood or bone marrow samples and enriched to a purity of at least 90% (16-19). Screening for *NR3C1* mutations and LOH was performed by Ion Torrent sequencing, array-CGH and/or multiplex ligation probe amplification analyses (MLPA) as previously described (14). Transcriptional *NR3C1* expression of primary patient material was determined using U133plus 2.0 arrays. Prednisolone LC50 was determined by performing a four-day MTT-assay, with the prednisolone concentration ranging from 0,008 to 250 µg/ml.

Constructs and transduction

For REH cells, gateway multi-site recombination (Invitrogen) was used for gateway cloning of lentiviral expression vectors by using a Gateway-adapted lentiviral pLEGO-iC2 destination vector (Addgene) as previously described (14). The entry vectors existed of (1) *attL1/attR5*-flanked doxycycline-inducible promoter (third generation, Clontech); (2) *attL5/attL4*-NR3C1 (wild-type or mutant) cDNA sequence; (3) *attR4/attR3*-flanked DDK-tag followed by a stop codon, WPRE sequences, and a constitutive pSFFV promoter; and (4) tetracycline (doxycycline)-induced transcriptional activator protein-Thosea asigna virus 2A-truncated Nerve Growth Factor Receptor reporter. For the shRNA experiments in REH and SUP-T1 cells, lentiviral transduction was performed with PLKO.1-puro lentiviral shRNA constructs directed against the human *NR3C1* gene that were selected from the MISSION T shRNA Library (Sigma-Aldrich).

Western blot

Protein extraction and subsequent blotting procedure on REH or SUP-T1 cells were performed as previously described (14). Primary antibodies used for western blotting: DKDDDDK Tag (Cell Signaling Technologies, CST #2368) and β-actin (#ab6276).

Real-time quantitative PCR

RNA was isolated with TRIzol reagent (Thermo Fisher Scientific). RTQ-PCR reactions were performed by using the DyNAmo HS SYBR Green qPCR Kit (Thermo Fisher Scientific) under 1X conditions, supplemented with 4mM $MgCl_2$ using the CFX384 Touch-Time PCR Detection System (Biorad). Expression levels were calculated relative

to the expression of the GAPDH house hold gene. Primers used are: *GAPDH* Fw primer 5'-GTCGGAGTCAACGGATT-3', *GAPDH* Rev primer 5'-AAGCTTCCCGTTCTCAG-3'; *GILZ* Fw primer 5'-TGGCCATAGACAACAAGAT-3', *GILZ* Rev primer 5'-TTGCCAGGGTCTTCAA-3', *FKBP5* Fw primer 5'-GAATGGTGAGGAAACGC-3', *FKPB5* Rev primer 5'-ATGCCTCCATCTTCAAATAA-3', *SGK1* Fw primer 5'-GGAGCCTGAGCTTATGAAT-3', *SGK1* Rev primer 5'-TTCCGCTCCGACATAATA-3'.

Statistical tests

Associations between NR3C1 mutational/deletion status and transcriptional *NR3C1* expression or *in-vitro* prednisolone LC50 were calculated by using the Mann-Whitney test. Survival analysis for relapse-free survival in our patient cohort was calculated using the log-rank (Mantel-Cox) test. For all tests, $p<0.05$ was used as significance level.

RESULTS

Recurrent *NR3C1* aberrations in T-ALL patients at diagnosis

In our initial patient cohort for which we combined results from sequencing and LOH analyses (14), we identified six out of 69 (9%) diagnostic patient biopsies that harbor *NR3C1* deletions (n=4) or carried heterozygous missense mutations (n=2; G323V and K777N). To substantiate these findings, we screened an additional cohort of 77 diagnostic pediatric T-ALL patient samples (totaling 146 patients) for *NR3C1* mutations and/or LOH using Ion Torrent sequencing, array-CGH and/or multiplex ligation probe amplification analyses (MLPA). We identified two additional patients with *NR3C1* deletions and three patients who harbored *NR3C1* mutations. A heterozygous single nucleotide insertion resulting in a premature frameshift in the protein coding domain (E116fs) was identified in one patient whereas a second patient had a heterozygous G568W missense mutation. The third patient had acquired three mutations including two missense mutations (N130D and R386L) and a nonsense mutation (G371X) that truncates the NR3C1 protein before the DNA binding and ligand binding domains. Thus, we identified six patients having *NR3C1* deletions (4%) and five other patients with newly identified missense or nonsense *NR3C1* mutations (3%) in a total of 146 diagnostic T-ALL patient samples (**Figure 1, supplemental table 1**).

Four out of six *NR3C1*-deleted patients were classified as early T-cell progenitor acute lymphoblastic leukemia (ETP-ALL) based on unsupervised cluster analysis of gene expression data (20). These *NR3C1* deletions occurred in the context of larger 5q deletion (**Figure 2a**), which is consistent with the observation that ETP-ALL patients frequently harbor interstitial or terminal 5q deletions (21). One patient (#1944) had a *TLX1* translocation and co-clustered with the TLX cluster, and in contrast to ETP-ALL patients had a relative small deletion on 5q that includes the *NR3C1* locus. For one patient its cluster had not been determined.

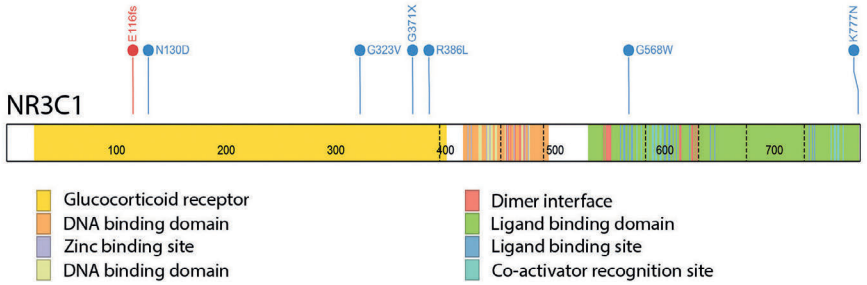

Figure 1. **Schematic overview of the NR3C1 protein**. *Missense mutations (blue) and frameshift (red) mutations as found in our cohort of 146 T-ALL patients have been indicated.*

In relation to outcome, none of the *NR3C1* deleted patients relapsed, while three out of five patients with a *NR3C1* mutation relapsed. In addition to small patient numbers, no significant difference in survival was observed compared to patients that lack *NR3C1* aberrations (**Figure 2b**). As a consequence of *NR3C1* deletions, *NR3C1* expression levels were significantly lower for *NR3C1* deleted patients compared to wild-type patients (**Figure 2c**, p=0.0017). Interestingly, no correlation was found between the relative *NR3C1* expression and *in-vitro* steroid response as measured for 83 treatment-naïve patient samples (**Figure 2d**). This indicates that relative basal *NR3C1* mRNA expression levels in patient biopsies are not predictive for steroid responsiveness of primary T-ALL patients at diagnosis. This is in line with previous observations that steroid responsiveness is largely determined by the ability to upregulate steroid response genes including *NR3C1* itself and pro-apoptotic *BIM* following steroid exposure (22, 23). Therefore, steroid responsiveness seems independent of a certain *NR3C1* expression threshold. Upon measuring actual steroid-induced cytotoxicity, we found that patients with *NR3C1* aberrations overall had a significantly inferior *in-vitro* steroid response compared to *NR3C1* wild-type patients (**Figure 2e**, p=0.0078). Four *NR3C1*-aberrant patients were completely resistant *in-vitro*, and four had an intermediate *in-vitro* response to prednisolone.

NR3C1 levels determine steroid response levels

To further investigate the relationship between NR3C1 expression and steroid responsiveness, we used the REH cell line that lacks expression of a functional glucocorticoid receptor (24). For this, we stably transduced REH cells with a doxycycline-inducible *NR3C1* expression construct (denoted as REH^{NR3C1}). Restoration of wild-type NR3C1 expression following doxycycline induction effectuated a highly sensitive prednisolone response in REH^{NR3C1} cells (**Figure 3a**).

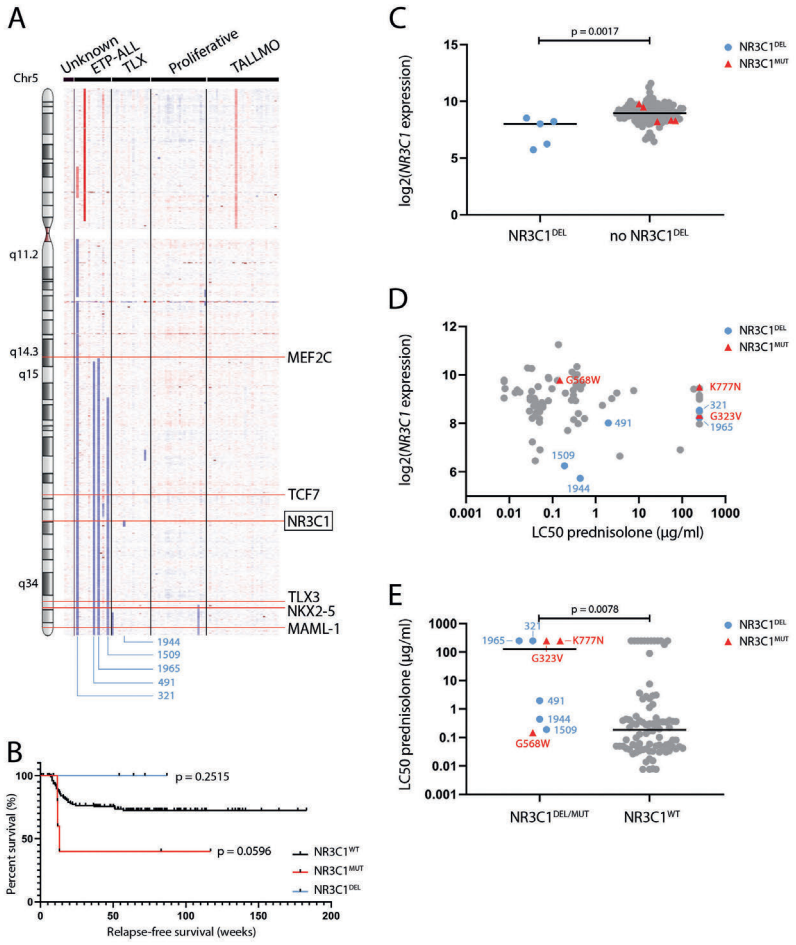

Figure 2. Characteristics and steroid response of NR3C1 aberrations in primary T-ALL patient samples *(***a***) Array-CGH data of 92 diagnostic biopsies from pediatric T-ALL patients. Patients are horizontally orientated and T-ALL subtypes are indicated as determined by gene expression profiling. Deleted regions of the five NR3C1-deleted patients detected by Array-CGH are characterized by the larger blue lesions around the 5q31 locus.* (**b**)*. Kaplan Meier survival analysis of 146 T-ALL patients who have been treated with different treatment protocols (see* **supplemental table 1***). The survival for of either NR3C1 deleted or NR3C1 mutated patients was compared to patients that lack NR3C1 aberrations and analyzed using the log-rank (Mantel-Cox) test.* (**c**) *Median NR3C1 expression of 116 diagnostic biopsies from pediatric T-ALL patients determined by U133plus 2 arrays. NR3C1 deleted cases (blue dots) had significant lower NR3C1 expression levels compared to non-NR3C1 deleted cases (including NR3C1 mutated patients highlighted by red triangles) (Mann-Whitney test, p=0.0017).* (**d**) *Matched NR3C1 expression data to in-vitro prednisolone response of 83 diagnostic biopsies from pediatric T-ALL patients.* (**e**) *In-vitro prednisolone response of 96 diagnostic biopsies from pediatric T-ALL patients. Patients that harbor NR3C1 aberrations (deletion (blue dots) or mutation (red triangles)) were significantly more resistant to prednisolone compared to NR3C1 wild-type patients (Mann-Whitney test, p=0.0078).*

To explore whether reductions in NR3C1 levels would proportionally diminish the steroid response, we knocked-down NR3C1 expression in REH^{NR3C1} cells by introducing four IPTG-inducible *NR3C1*-directed short-hairpin RNA (shRNA) lentiviral constructs. Partial knock-down of NR3C1 upon IPTG treatment in doxycycline-induced REH^{NR3C1} cells reduced the sensitivity to prednisolone treatment. For these derivative REH^{NR3C1} lines, knockdown by short-hairpin constructs led to pronounced NR3C1 knockdown and steroid insensitivity (**Figure 3b-c**). As a control, no reduction in steroid cytotoxicity was observed for REH^{NR3C1} cells that were transduced with shRNA construct (sh5) directed against the 3' UTR of the normal *NR3C1* gene, which was absent in the lentiviral *NR3C1* expression construct.

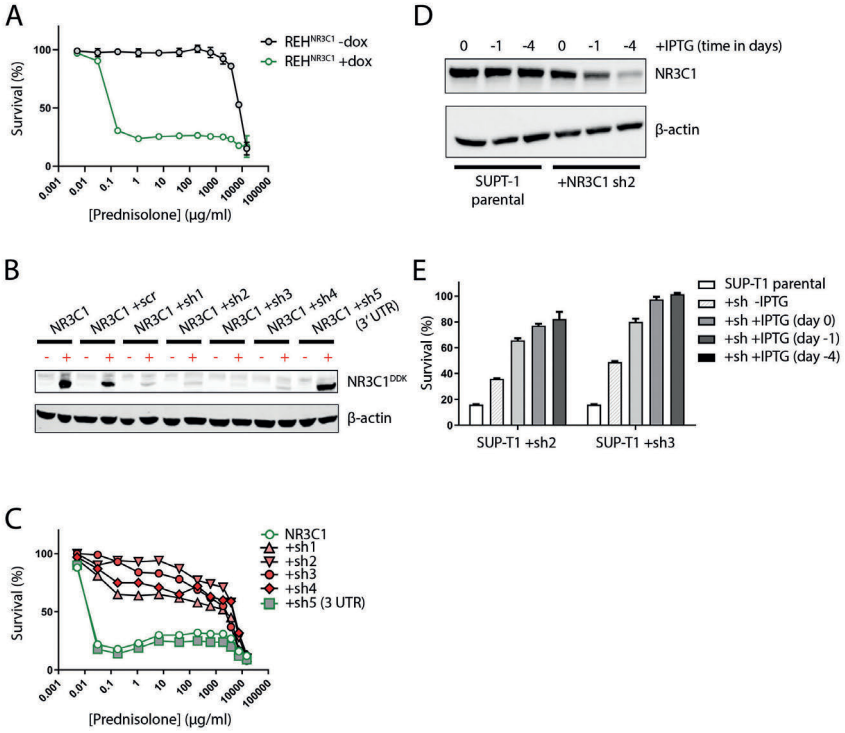

Figure 3. **NR3C1 expression levels predict steroid response in REH cells** *(***a***) Steroid response curves for doxycycline-induced (+dox) or non-induced (-dox) steroid resistant REH cells following 96-hour exposure to serial dilutions of prednisolone. Cell survival was determined by flowcytomery-measured cell counts. REH cells were transfected with a doxycycline-inducible NR3C1 wild-type construct. (***b-c***) Steroid response curves and NR3C1 protein levels and steroid response curves of NR3C1-REH cells (e.g. doxycycline-induced REH NR3C1 wild-type cells) that have been transduced with NR3C1-directed lentiviral shRNA constructs (sh1-4). Control shRNA construct sh5 is directed against the 3'UTR of NR3C1, which is not included in the NR3C1 expression construct.* **(d-e***) Steroid response curves and (endogenous or short-hairpin reduced) NR3C1 protein levels of steroid sensitive SUP-T1 cells. shRNA constructs were induced by IPTG 4 days or 1 day prior to – or at the start (day 0) of steroid treatment. Steroid response was determined after 96 hours by flowcytometry-measured cell counts.*

To further visualize the relationship between NR3C1 protein level and steroid sensitivity in a T-ALL context, we transduced steroid-sensitive SUP-T1 T-ALL cells with *NR3C1*-directed shRNA lentiviral constructs sh2 or sh3. Timed activation of these shRNA constructs by addition of IPTG (e.g. 4 or 1 days prior- or at the start of prednisolone treatment) demonstrated that a gradual increase in NR3C1 knockdown augmented steroid resistance (**Figure 3d-e**). These results highlight an interdependency between NR3C1 expression and steroid response within a specific cellular context.

***NR3C1* mutations and steroid response**

We then used the same REH model to study the functional consequences of the identified *NR3C1* missense (K777N, G323V or N130D) or G371X nonsense mutation on steroid responsiveness. REH cells were stably transduced with either of these mutant *NR3C1* expression constructs, resulting in expression of mutant NR3C1 receptors following doxycycline induction (**Figure 4a**). Using these bulk transduced lines, expression of K777N, G323V or N130D mutant molecules elicited an efficient transcriptional steroid response, as demonstrated by the upregulation of specific NR3C1 target genes such as *GILZ*, *FKBP5* and *SGK1* after steroid treatment (**Figure 4b**). Moreover, the functionally of these mutations was reflected by their steroid responsiveness, since these mutations were equally sensitive steroid response compared to REH^{NR3C1} cells (**Figure 4c).** As expected, expression of the truncating G371X mutant was totally ineffective to restore a steroid response (**Figure 4b-c**).

DISCUSSION

In this study, we found that relative *NR3C1* mRNA expression levels in primary diagnostic patient samples do not correlate with steroid response. Interindividual differences in other factors that contribute to steroid resistance may influence the steroid response at diagnosis. For example, IL7R signaling mutations, epigenetic silencing of the *BIM* locus or overexpression of BCL2 have all been associated with steroid resistance (8, 14, 25-27). Thus, the relative *NR3C1* mRNA level is not useful as a predictive biomarker for clinical steroid responsiveness for patients at diagnosis *per sé*. However, for experiments performed within a specific and controlled cellular context such as REH or SUP-T1 cells, we observed a strong interdependency between NR3C1 levels and steroid response levels, in line with previous findings by others (4, 28).

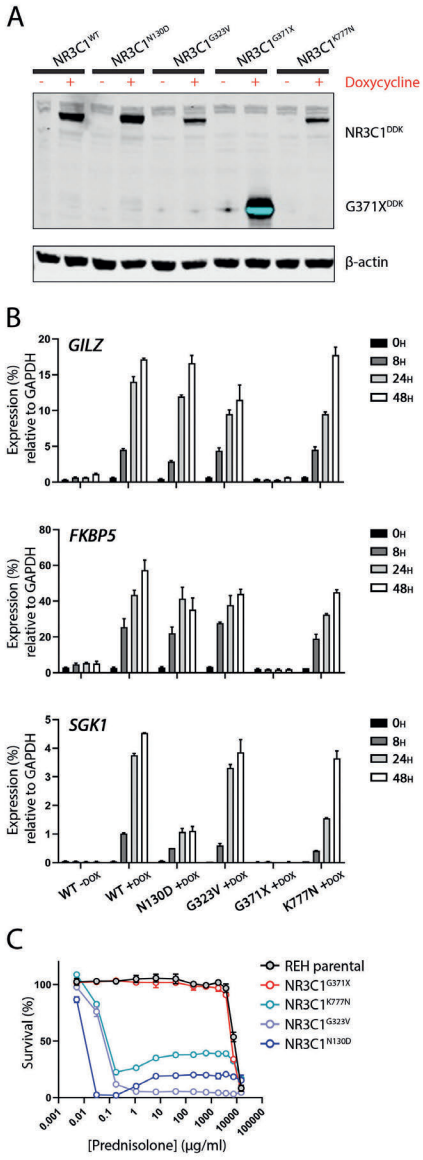

Figure 4. **Non-truncated NR3C1 missense mutations induce efficient steroid-induced cell death**
*(***a***) Western blot results of total NR3C1 levels for REH cell lines transfected with doxycycline-inducible NR3C1 or mutant NR3C1-constructs as indicated. (***b***) Transcriptional steroid response of REH cells that have been transfected with doxycycline-inducible wild-type or mutant NR3C1 constructs. Doxycycline-induced cells were treated with 250µg/ml prednisolone. Expression of glucocorticoid receptor target genes GILZ, FKBP5 and SGK1 was determined at 8, 24 and 48 hours following prednisolone treatment. (***c***) Steroid response curves of REH parental and REH cells transfected with doxycycline-inducible mutant NR3C1 constructs.*

Loss of NR3C1 expression due to mutations, deletions or other mechanisms that occur under the pressure of steroid treatment (4) explain the relative increased incidence of *NR3C1* deletions and mutations at disease relapse (10, 11, 13). However, our study demonstrates that heterozygous *NR3C1* deletions or truncating mutations are already present in diagnostic biopsies of approximately 5% of pediatric T-ALL patients and associate with steroid resistance. This may suggest that natural steroid hormones that normally shape the immune system (29, 30) already elicits a strong selection pressure on (pre)leukemic cells before actual diagnosis of disease.

We identified *NR3C1* missense mutations in four T-ALL patients (including one patient that also harbored a truncating mutation). The missense mutations tested in REH cells demonstrated an efficient transcriptional steroid response and seemed equally effective as the wild-type NR3C1 molecule in effectuating steroid-induced apoptosis. This is in contrast to a recent functional screening using a similar experimental approach in REH cells, demonstrating that (distinct) relapse-enriched *NR3C1* mutations in ALL did confer steroid resistance (31). This indicates that *NR3C1* missense mutations found at relapse are selected during therapy and cause resistance towards synthetic steroids, while mutations at diagnosis do not necessarily drive steroid resistance *per sé*. The N130D mutation co-occurred with the truncating G371X mutation in one of our patients, and may therefore represent a passenger mutation rather than reflecting a steroid resistance driving mutation.

The steroid sensitive phenotype of our mutant NR3C1 overexpressing cells somewhat contradict the intermediate or steroid resistant phenotype of corresponding primary patient blasts. Since induced expression of mutant NR3C1 molecules exceeds the physiological level as normally expressed in ALL blasts, we cannot exclude the possibility that subtle effects of the studied NR3C1 mutations on steroid responsiveness are masked. This may be exemplified by the T-ALL patient harboring the K777N mutation, since this mutation was also preserved at relapse. In contrast to the controlled context of REH cells, many other factors are influential in the steroid sensitivity of leukemic blasts. The presence of mutant NR3C1 may therefore synergize with other (epi)genetic aberrations at disease diagnosis. Regardless of a supporting or causal role, the presence of *NR3C1* mutations related to steroid resistance in our cohort, and 3 out of 4 patients with missense *NR3C1* mutations relapsed during therapy.

In conclusion, approximately 7 percent of patients that are diagnosed with T-ALL already harbor NR3C1 inactivating events that influence their leukemic response to steroid treatment.

Acknowledgements. This study was supported by grants of the Foundation “Kinderen Kankervrij” (KiKa): KiKa-82 (WS) and KiKa-219 (JvdZ).

Contribution of authors. J.C.G. van der Zwet participated in the research design, the performance of the research and writing of the paper. W. Smits and J.C.G. Buijs-Gladdines participated in the performance of the research. R. Pieters participated in writing of the paper. J.P.P. Meijerink participated in the research design, supervision of the research and writing of the paper.

Disclosures. None.

REFERENCES

1. Riehm H, Reiter A, Schrappe M, Berthold F, Dopfer R, Gerein V, et al. [Corticosteroid-dependent reduction of leukocyte count in blood as a prognostic factor in acute lymphoblastic leukemia in childhood (therapy study ALL-BFM 83)]. Klinische Padiatrie. 1987;199(3):151-60.
2. Griffin TC, Shuster JJ, Buchanan GR, Murphy SB, Camitta BM, Amylon MD. Slow disappearance of peripheral blood blasts is an adverse prognostic factor in childhood T cell acute lymphoblastic leukemia: a Pediatric Oncology Group study. Leukemia. 2000;14(5):792-5.
3. Weikum ER, Knuesel MT, Ortlund EA, Yamamoto KR. Glucocorticoid receptor control of transcription: precision and plasticity via allostery. Nat Rev Mol Cell Biol. 2017;18(3):159-74.
4. Wandler AM, Huang BJ, Craig JW, Hayes K, Yan H, Meyer LK, et al. Loss of glucocorticoid receptor expression mediates in vivo dexamethasone resistance in T-cell acute lymphoblastic leukemia. Leukemia. 2020;17 Feb. [Epub ahead of print].
5. Miller AL, Garza AS, Johnson BH, Thompson EB. Pathway interactions between MAPKs, mTOR, PKA, and the glucocorticoid receptor in lymphoid cells. Cancer Cell Int. 2007;7:3.
6. Piovan E, Yu J, Tosello V, Herranz D, Ambesi-Impiombato A, Da Silva AC, et al. Direct reversal of glucocorticoid resistance by AKT inhibition in acute lymphoblastic leukemia. Cancer Cell. 2013;24(6):766-76.
7. Gruber G, Carlet M, Turtscher E, Meister B, Irving JA, Ploner C, et al. Levels of glucocorticoid receptor and its ligand determine sensitivity and kinetics of glucocorticoid-induced leukemia apoptosis. Leukemia. 2009;23(4):820-3.
8. Jing D, Huang Y, Liu X, Sia KCS, Zhang JC, Tai X, et al. Lymphocyte-Specific Chromatin Accessibility Pre-determines Glucocorticoid Resistance in Acute Lymphoblastic Leukemia. Cancer Cell. 2018;34(6):906-21 e8.
9. Schmidt S, Irving JA, Minto L, Matheson E, Nicholson L, Ploner A, et al. Glucocorticoid resistance in two key models of acute lymphoblastic leukemia occurs at the level of the glucocorticoid receptor. FASEB J. 2006;20(14):2600-2.
10. Mullighan CG, Phillips LA, Su X, Ma J, Miller CB, Shurtleff SA, et al. Genomic analysis of the clonal origins of relapsed acute lymphoblastic leukemia. Science. 2008;322(5906):1377-80.
11. Irving JA, Bloodworth L, Bown NP, Case MC, Hogarth LA, Hall AG. Loss of heterozygosity in childhood acute lymphoblastic leukemia detected by genome-wide microarray single nucleotide polymorphism analysis. Cancer Res. 2005;65(8):3053-8.
12. Irving JA, Enshaei A, Parker CA, Sutton R, Kuiper RP, Erhorn A, et al. Integration of genetic and clinical risk factors improves prognostication in relapsed childhood B-cell precursor acute lymphoblastic leukemia. Blood. 2016;128(7):911-22.
13. Kuster L, Grausenburger R, Fuka G, Kaindl U, Krapf G, Inthal A, et al. ETV6/RUNX1-positive relapses evolve from an ancestral clone and frequently acquire deletions of genes implicated in glucocorticoid signaling. Blood. 2011;117(9):2658-67.
14. Li Y, Buijs-Gladdines JG, Cante-Barrett K, Stubbs AP, Vroegindeweij EM, Smits WK, et al. IL-7 Receptor Mutations and Steroid Resistance in Pediatric T cell Acute Lymphoblastic Leukemia: A Genome Sequencing Study. PLoS Med. 2016;13(12):e1002200.
15. Delgado-Martin C, Meyer LK, Huang BJ, Shimano KA, Zinter MS, Nguyen JV, et al. JAK/STAT pathway inhibition overcomes IL7-induced glucocorticoid resistance in a subset of human T-cell acute lymphoblastic leukemias. Leukemia. 2017;31(12):2568-76.

16. Kamps WA, Bokkerink JP, Hahlen K, Hermans J, Riehm H, Gadner H, et al. Intensive treatment of children with acute lymphoblastic leukemia according to ALL-BFM-86 without cranial radiotherapy: results of Dutch Childhood Leukemia Study Group Protocol ALL-7 (1988-1991). Blood. 1999;94(4):1226-36.
17. Kamps WA, Bokkerink JP, Hakvoort-Cammel FG, Veerman AJ, Weening RS, van Wering ER, et al. BFM-oriented treatment for children with acute lymphoblastic leukemia without cranial irradiation and treatment reduction for standard risk patients: results of DCLSG protocol ALL-8 (1991-1996). Leukemia. 2002;16(6):1099-111.
18. Veerman AJ, Kamps WA, van den Berg H, van den Berg E, Bokkerink JP, Bruin MC, et al. Dexamethasone-based therapy for childhood acute lymphoblastic leukaemia: results of the prospective Dutch Childhood Oncology Group (DCOG) protocol ALL-9 (1997-2004). Lancet Oncol. 2009;10(10):957-66.
19. Escherich G, Troger A, Gobel U, Graubner U, Pekrun A, Jorch N, et al. The long-term impact of in vitro drug sensitivity on risk stratification and treatment outcome in acute lymphoblastic leukemia of childhood (CoALL 06-97). Haematologica. 2011;96(6):854-62.
20. Homminga I, Pieters R, Langerak AW, de Rooi JJ, Stubbs A, Verstegen M, et al. Integrated transcript and genome analyses reveal NKX2-1 and MEF2C as potential oncogenes in T cell acute lymphoblastic leukemia. Cancer Cell. 2011;19(4):484-97.
21. La Starza R, Barba G, Demeyer S, Pierini V, Di Giacomo D, Gianfelici V, et al. Deletions of the long arm of chromosome 5 define subgroups of T-cell acute lymphoblastic leukemia. Haematologica. 2016;101(8):951-8.
22. Bouillet P, Metcalf D, Huang DC, Tarlinton DM, Kay TW, Kontgen F, et al. Proapoptotic Bcl-2 relative Bim required for certain apoptotic responses, leukocyte homeostasis, and to preclude autoimmunity. Science. 1999;286(5445):1735-8.
23. Ramdas J, Liu W, Harmon JM. Glucocorticoid-induced cell death requires autoinduction of glucocorticoid receptor expression in human leukemic T cells. Cancer Res. 1999;59(6):1378-85.
24. Bachmann PS, Gorman R, Papa RA, Bardell JE, Ford J, Kees UR, et al. Divergent mechanisms of glucocorticoid resistance in experimental models of pediatric acute lymphoblastic leukemia. Cancer Res. 2007;67(9):4482-90.
25. Bachmann PS, Piazza RG, Janes ME, Wong NC, Davies C, Mogavero A, et al. Epigenetic silencing of BIM in glucocorticoid poor-responsive pediatric acute lymphoblastic leukemia, and its reversal by histone deacetylase inhibition. Blood. 2010;116(16):3013-22.
26. Jing D, Bhadri VA, Beck D, Thoms JA, Yakob NA, Wong JW, et al. Opposing regulation of BIM and BCL2 controls glucocorticoid-induced apoptosis of pediatric acute lymphoblastic leukemia cells. Blood. 2015;125(2):273-83.
27. Autry RJ, Paugh SW, Carter R, Shi L, Liu J, Ferguson DC, et al. Integrative genomic analyses reveal mechanisms of glucocorticoid resistance in acute lymphoblastic leukemia. Nature Cancer. 2020;1(3):329-44.
28. Grausenburger R, Bastelberger S, Eckert C, Kauer M, Stanulla M, Frech C, et al. Genetic alterations in glucocorticoid signaling pathway components are associated with adverse prognosis in children with relapsed ETV6/RUNX1-positive acute lymphoblastic leukemia. Leuk Lymphoma. 2016;57(5):1163-73.
29. Sacedon R, Vicente A, Varas A, Jimenez E, Munoz JJ, Zapata AG. Early maturation of T-cell progenitors in the absence of glucocorticoids. Blood. 1999;94(8):2819-26.
30. Pazirandeh A, Xue Y, Prestegaard T, Jondal M, Okret S. Effects of altered glucocorticoid sensitivity in the T cell lineage on thymocyte and T cell homeostasis. FASEB J. 2002;16(7):727-9.
31. Li B, Brady SW, Ma X, Shen S, Zhang Y, Li Y, et al. Therapy-induced mutations drive the genomic landscape of relapsed acute lymphoblastic leukemia. Blood. 2020;135(1):41-55.

Supplemental Table 1. *Diagnostic primary T-ALL patient samples characteristics.*

Online link to Table S1: https://tinyurl.com/Chap3-SuppTable1-Jordy-vd-Zwet

4

[1]Princess Máxima Center for Pediatric Oncology, Utrecht, the Netherlands
[2]Biomolecular Mass Spectrometry and Proteomics, Bijvoet Center of Biomolecular Research and Utrecht Institute for Pharmaceutical Sciences, Utrecht University, Utrecht, the Netherlands
[3]Netherlands Translational Research Center B.V., Oss, the Netherlands
[4]Institute of Cancer Genetics, Columbia University Medical Center, New York, New York 10032, USA
[5]Children's Research Center, University Children's Hospital Zurich, Zurich, Switzerland
[6]KU Leuven Center for Human Genetics & VIB Center for Cancer Biology, Leuven, Belgium
[7]Newcastle University, Newcastle upon Tyne, United Kingdom

MAPK-ERK is a central pathway in T-cell acute lymphoblastic leukemia that drives steroid resistance

Jordy C.G van der Zwet[1], Jessica G.C.A.M. Buijs-Gladdines[1], Valentina Cordo'[1], Donna O. Debets[2], Willem K. Smits[1], Zhongli Chen[1], Jelle Dylus[3], Guido J.R. Zaman[3], Maarten Altelaar[2], Koichi Oshima[4], Beat Bornhauser[5], Jean-Pierre Bourquin[5], Jan Cools[6], Adolfo A. Ferrando[4], Josef Vormoor[1,7], Rob Pieters[1], Britta Vormoor[1] and Jules P.P. Meijerink[1]

Published in Leukemia, May 2021
doi: 10.1038/s41375-021-01291-5, PMID: 34007050

ABSTRACT

(Patho-)physiological activation of the IL7-receptor (IL7R) signaling contributes to steroid resistance in pediatric T-cell acute lymphoblastic leukemia (T-ALL). Here, we show that activating IL7R pathway mutations and physiological IL7R signaling activate MAPK-ERK signaling, which provokes steroid resistance by phosphorylation of BIM. By mass spectrometry, we demonstrate that phosphorylated BIM is impaired in binding to BCL2, BCLXL and MCL1, shifting the apoptotic balance towards survival. Treatment with MEK inhibitors abolishes this inactivating phosphorylation of BIM and restores its interaction with anti-apoptotic BCL2-protein family members. Importantly, the MEK inhibitor selumetinib synergizes with steroids in both IL7-dependent and IL7-independent steroid resistant pediatric T-ALL PDX samples. Despite the anti-MAPK-ERK activity of ruxolitinib in IL7-induced signaling and JAK1 mutant cells, ruxolitinib only synergizes with steroid treatment in IL7-dependent steroid resistant PDX samples but not in IL7-independent steroid resistant PDX samples. Our study highlights the central role for MAPK-ERK signaling in steroid resistance in T-ALL patients, and demonstrates the broader application of MEK inhibitors over ruxolitinib to resensitize steroid-resistant T-ALL cells. These findings strongly support the enrollment of T-ALL patients in the current phase I/II SeluDex trial (NCT03705507) and contributes to the optimization and stratification of newly designed T-ALL treatment regimens.

Keywords: T-cell acute lymphoblastic leukemia, glucocorticoid response, steroid resistance, MAPK-ERK signaling, MEK inhibition, BIM

INTRODUCTION

T-cell acute lymphoblastic leukemia (T-ALL) is a high-risk hematological malignancy of early developing T-cells and represents 15 percent of children that present with ALL. T-ALL patients comprised nearly 40% of patients that were treated in the high-risk treatment arm of the Dutch Childhood Oncology Group (DCOG) ALL-10 protocol (1). To date, cure-rates of 75-80 percent are achieved (2-4), indicating that therapy still fails in one out of 4-5 children with T-ALL. T-ALL patients that suffer from relapse have a dismal outcome due to acquired resistance to a wide range of chemotherapeutics. Synthetic glucocorticoids (also denoted as steroids) including prednisolone and dexamethasone are cornerstone drugs in the treatment of both T-ALL and B-cell precursor-ALL (BCP-ALL). Resistance to steroids is a frequent problem in T-ALL that historically predicts for poor outcome and is used for risk-stratification in many treatment protocols including the DCOG ALL-11 protocol (3, 5, 6).

The gene coding for the pro-apoptotic molecule BIM (7)–a BH3-only member of the BCL-2 protein family–is an important direct transcriptional target of the glucocorticoid receptor (NR3C1). Upon steroid treatment, BIM is upregulated to mediate steroid-induced death of lymphoid cells (8-12). In contrast, anti-apoptotic BCL2 is downregulated in lymphoblasts treated with steroids (8). Upregulation of BIM changes the dynamic balance between pro- and anti-apoptotic BCL-2 family members, resulting in the release and activation of the pro-apoptotic effector molecules BAK and BAX, which triggers apoptosis (13-15). Various mechanisms have been described that may impair the activation or function of BIM, hence resulting in steroid resistance. These mechanisms rely on the activation of specific kinases (*e.g.* AKT, ERK, p38 or JNK) that can either impair the transcription of *BIM*, or alter its function, cellular localization and/or proteasomal degradation (10, 11, 16-24).

Aberrant activation of the interleukin-7 (IL7) signaling pathway is frequently observed in T-ALL (25-27). Physiological activation of the pathway is induced when IL7 binds to its cognate receptor, which results in the activation of downstream JAK-STAT and PI3K-AKT pathways. We previously demonstrated that mutations in the IL7R signaling pathway are associated with steroid resistance and inferior relapse-free survival (28). Mutations in the IL7Rα chain or downstream signaling molecules activate the JAK-STAT and PI3K-AKT signaling pathways in a ligand-independent manner (28). In contrast to physiological IL7R signaling in normal T-cells, IL7R-signaling mutations also strongly activate MAPK-ERK signaling, albeit its significance is currently unknown. Physiological IL7R signaling in T-ALL cells from patients can also raise steroid resistance, further providing evidence for crosstalk between the IL7- and steroid-induced signaling pathways independent of the presence of specific activation mutations (29). To date, this so-called 'IL7-dependent steroid resistant' phenotype is attributed to STAT5 activation and subsequent upregulation of *BCL2* (30). *BCL2* upregulation also occurs as a result of

IL7-induced PI3K-AKT pathway activation in T-ALL (25). However, the activation of the MAPK-ERK pathway in IL7-induced signaling in T-ALL has not been studied yet, and its contribution to steroid resistance remains poorly understood.

This study reveals that the MAPK-ERK pathway is aberrantly activated downstream of mutant- and physiological IL7R-signaling. As a result, steroid-induced pro-apoptotic BIM is inactivated through phosphorylation, which changes the apoptotic threshold and drives MAPK-ERK induced steroid resistance. Our results demonstrate the broader efficacy of MEK inhibitors over the JAK1/2 inhibitor ruxolitinib to resensitize steroid-resistant T-ALL cells.

MATERIALS AND METHODS

Functional screening of SUPT-1 cell lines
JAK1, IL7R and NRAS mutant or wild-type molecules were stably expressed through lentiviral transduction of SUPT-1 cells. Viability during cytotoxicity screens was determined after four days by methylthiazolyldiphenyl-tetrazolium bromide (MTT, Sigma Aldrich). Details concerning lentiviral transduction and purification of cell lines, cytotoxicity screens and RTQ-PCR can be found in the supplemental materials and method.

Functional screening of PDX cells
Cytotoxicity screens of PDX samples was performed as previously described (28) in the presence or absence of 25 ng/ml IL7 (R&D Systems). PDX cells were plated at a concentration of $1x10^6$ cells/ml, and viability after four days was measured by ATPlite 1Step (Perkin Elmer, Groningen, The Netherlands).

Co-immuno-precipitation and mass spectrometry
Dynabeads (Thermo Fisher Scientific) were linked to the immunoprecipitation antibody of interest, briefly incubated and subsequently crosslinked to BS^3 (2,5 mM) to avoid co-elution of the antibody. After overnight incubation each sample was eluted with Laemmli sample buffer (without dithiothreitol) and heated for 10' at 50°C. Antibodies used for immunoprecipitation of target proteins: BIM (#2933; Cell Signaling), MCL1 (#AHO0102; Thermo Fisher Scientific) and BCL2 (#551051; BD Pharmingen™). For mass spectrometry, proteins were digested by trypsin (Promega) and peptides were analyzed by LC-MS/MS using an Agilent 1290 system coupled to a Q-exactive HF-X (Thermo Fisher Scientific). iBAQ quantification was performed, representing protein abundance in each sample. Details concerning protein isolation in non-IP experiments, the western-blotting procedure and mass spectrometry procedures and analysis can be found in the supplemental materials and methods.

RESULTS

Steroid resistant IL7R and JAK1 mutants activate the MAPK-ERK signaling pathway
To explore the mechanisms driving IL7R-signaling mediated steroid resistance, we generated doxycycline-inducible SUPT-1 cell lines that express wild-type or mutant IL7R or downstream signaling components. Whereas expression of wild-type IL7R ($IL7R^{WT}$) or the non-cysteine mutant $IL7R\alpha^{V253GPSL}$ did not affect the sensitive steroid response of SUPT1 cells, expression of cysteine mutant $IL7R\alpha^{PILLT240\text{-}244RFCPH}$, $IL7R\alpha^{PIL240\text{-}242QSPSC}$ or $IL7R\alpha^{LT243\text{-}244LMCPT}$ strongly raised cellular resistance (**Figure 1a-b**). We observed activation of the downstream MAPK-ERK signaling in these three steroid resistant lines expressing mutant IL7Rα isoforms in contrast to the wild-type and the non-cysteine IL7Rα mutant lines (**Figure 1c**). Notably, MAPK-ERK activation has not been observed in physiological IL7 signaling in normal T-cells (31). Validation of MAPK-ERK activation in other steroid sensitive ($JAK1^{WT}$) or steroid resistant ($JAK1^{R724H}$, $JAK1^{T901A}$, $NRAS^{WT}$ or $NRAS^{G12D}$) derivate SUPT-1 lines demonstrated strong MAPK-ERK activation in all steroid resistant lines (28). As the inducibility of all doxycycline-inducible cell lines exceeded 85 percent (data not shown), differences in MAPK-ERK signaling among various cell lines reflect quantitative differences. Of note, MAPK-ERK pathway activation seemed linked to changes in the apparent molecular weight of the pro-apoptotic BIM-EL and BIM-L isoforms (**Figure 1c**). Phosphorylation of the pro-apoptotic BIM-S isoform was not observed.

IL7 can induce steroid resistance and MAPK-ERK activation in T-ALL PDX cells
Our observed relationship between mutant IL7R signaling, MAPK-ERK pathway activation and steroid response suggests that MAPK-ERK signaling may represent a major determinant for steroid resistance, including steroid resistance that is induced by physiological IL7 signaling. We therefore examined the steroid response of 46 patient-derived xenografts (PDX) samples (including 9 matched diagnostic-relapse PDX pairs) in the absence and presence of IL7. Steroid sensitivity was measured as Area Under the Curve (AUC) to quantify cytotoxic responses over a 4-log dynamic range of prednisolone concentrations. The steroid sensitivity of 34 PDX samples was not affected by addition of IL7. However, 12 samples demonstrated an AUC increase of more than 1.5 fold in the presence of IL7 compared to cells cultured in the absence of IL7 (**Figure 1d, supplemental figure 1a**). This indicates that ligand-dependent IL7R activation can induce steroid resistance in 26% of our T-ALL PDX cohort.

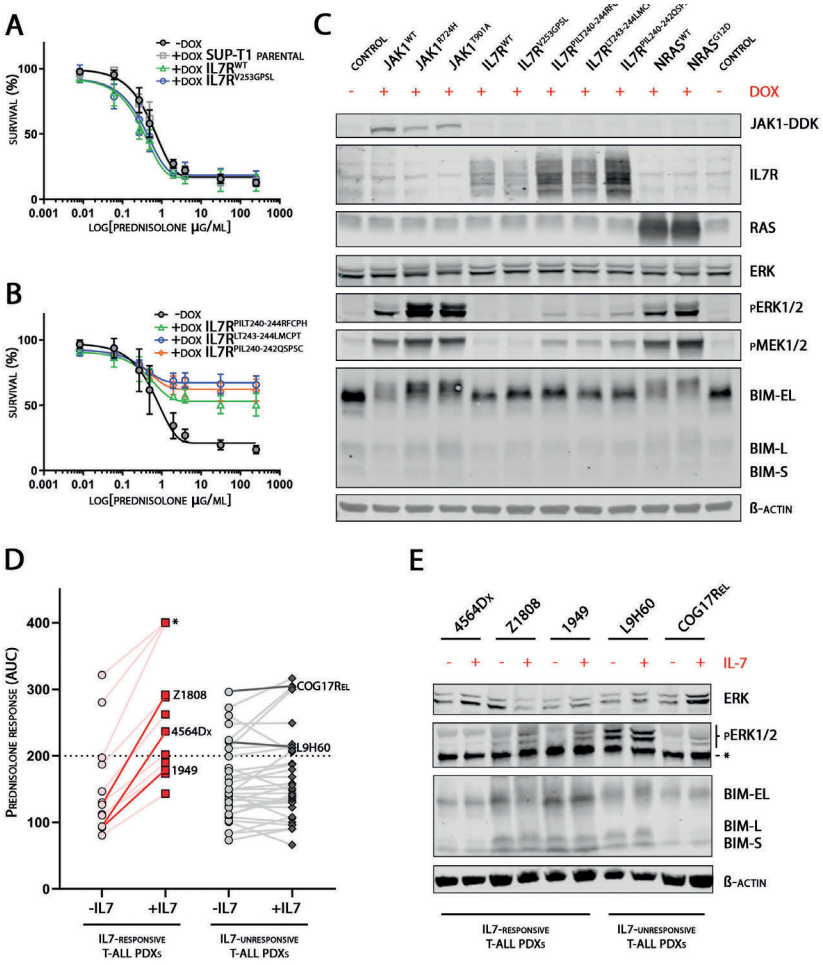

Figure 1. IL7R signaling mutations and physiological IL7-signaling activates MAPK-ERK signaling in T-ALL. *(**A**) Cell toxicity screening of doxycycline-induced SUPT-1 parental (grey), IL7R^{WT} (green) and IL7R^{V253GPSL} (blue) mutant cells. As negative control for the mutant cell lines, the average survival of both cell lines is illustrated in the -DOX condition (dark grey). Cells were treated with prednisolone (range 0.00822 – 250 µg/ml) for four days. (**B**) Cell toxicity screening of doxycycline-induced IL7R$^{PILT240-244RFCPH}$ (green), IL7R$^{LT243-244LMCPT}$ (blue) and IL7R$^{PIL240-242QSPSC}$ (orange) cysteine-mutant cells. As negative control for the mutant cell lines, the average survival of both cell lines is illustrated in the -DOX condition (dark grey). Cells were treated with prednisolone (range 0.00822 – 250 µg/ml) for four days. (**C**) Western blot of JAK1 (DDK-tagged), IL7R and NRAS overexpressing cells to study downstream MAPK-ERK pathway activation. (**D**) Cell toxicity screening of 46 T-ALL PDX samples in IL7 treated and untreated condition. Area Under the Curve (AUC) values represent steroid response (range 3.16nM-31.6µM prednisolone). The 'IL7-responsive'group was defined by an >1.5 fold increase in prednisolone AUC in the IL7 treated condition. Starred samples represent extreme resistant samples with AUC >400, since an AUC of 400 represent the maximum AUC in a 4-log dynamic concentration range of prednisolone. (**E**) Western blot of selected T-ALL PDX samples to study downstream MAPK-ERK pathway activation in response to IL7. *off-target band.*

We then studied whether IL7-induced signaling can activate the MAPK-ERK pathway alike IL7R signaling mutations. For this, we selected 3 PDX samples that became more resistant to steroids following IL7 exposure (denoted as IL7-dependent steroid resistant samples), and 2 steroid resistant PDX samples for which the steroid sensitivity was not affected by IL7 (denoted as IL7-independent steroid resistant samples) (**Supplemental figure 1b-c)**. Interestingly, we observed increased ERK phosphorylation after 30 minutes of IL7 exposure in IL7-dependent and IL7-indendent steroid resistant PDX samples (**Figure 1e**, **supplemental figure 1d)**. In some of these samples, higher molecular weight isoforms of BIM-L and BIM-EL were observed in relation to (IL7-induced) MAPK-ERK signaling. In addition to mutant IL7R signaling, we reveal that physiological IL7 signaling also activates the MAPK-ERK pathway in T-ALL. MAPK-ERK signaling may therefore represent a major cause for IL7-induced steroid resistance.

MAPK-ERK signaling drives phosphorylation of BIM isoforms

The presence of higher molecular weight BIM-EL and BIM-L isoforms in MAPK-ERK activated and steroid resistant cell lines and T-ALL PDX samples suggest a common post-translational modification of BIM downstream of activated MAPK-ERK signaling. To study if this modification was due to protein phosphorylation, we treated whole cell lysates of doxycycline-induced SUPT-1 $JAK1^{R724H}$ cells *ex-vivo* with lambda phosphatase in the presence of limiting concentrations of phosphatase inhibitors. Induction of $JAK1^{R724H}$ resulted in high phosphorylation of ERK and higher molecular weight forms for BIM-EL and BIM-L, which were reduced to single and lower molecular isoforms upon phosphatase treatment similar to non-induced control cells (**Figure 2a,** only BIM-EL isoform is displayed). Therefore, we conclude that these higher molecular weight BIM isoforms were due to phosphorylation. To investigate whether BIM is phosphorylated downstream of activated MAPK-ERK signaling, we performed an *in-vitro* phosphorylation assay with human active (MEK-activated) recombinant ERK1 and human recombinant BIM-L (**Figure 2b**). Only in the presence of ERK1 and 100μM ATP, BIM was phosphorylated, concluding that ERK is directly responsible for the phosphorylation of pro-apoptotic BIM. We validated this result by treating wild-type and mutant JAK1 SUPT-1 cells with the MEK-inhibitor CI1040 (**Figures 2c**). In both JAK mutated lines, phosphorylation of ERK and BIM-EL and BIM-L isoforms were effectively blocked upon CI1040 treatment. Similar findings were observed for three cysteine-mutant IL7Rα lines following CI1040 treatment, while BIM remained unphosphorylated in wild-type IL7Ra cells irrespective of MEK inhibitor treatment (**Supplemental figure 2a**). Both clinically relevant MEK inhibitors selumetinib and trametinib also effectively blocked BIM phosphorylation in a dose-dependent manner at concentrations that did not induce cytotoxicity (**Figure 2d-e, supplemental figure 2b-d)**. Therefore, we conclude that phosphorylation of BIM follows MAPK-ERK pathway activation and can be effectively blocked by MEK inhibitors.

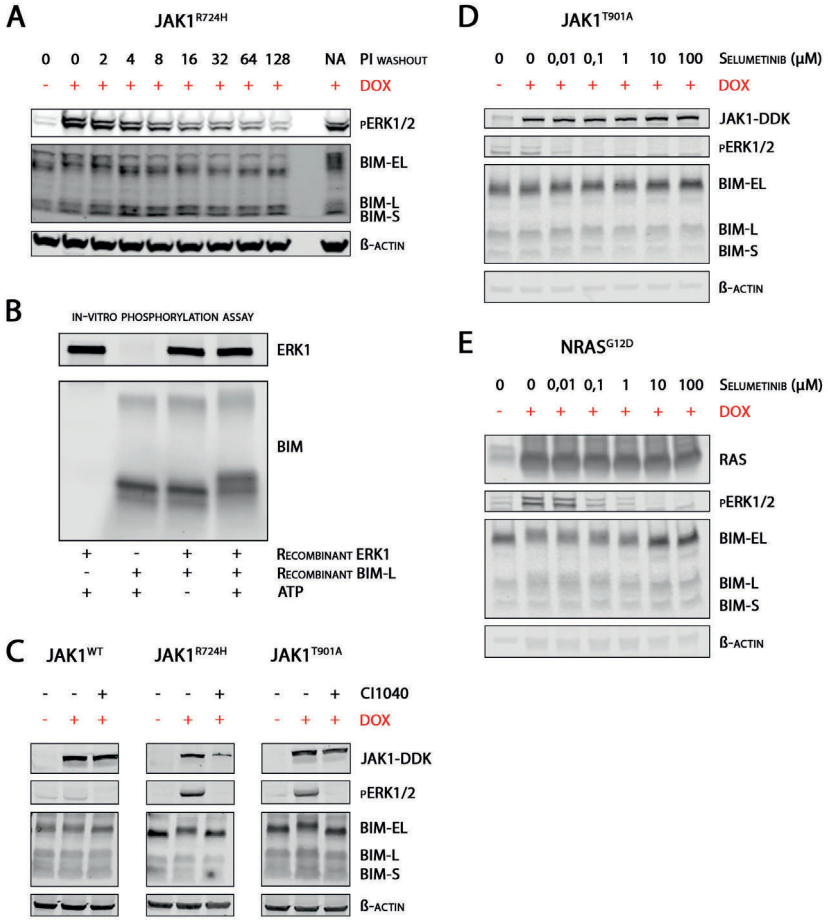

Figure 2. Pro-apoptotic BIM is phosphorylated downstream of activated MAPK-ERK signaling. *(**A**) Western blot of JAK1^{R724H} overexpressing cells (+DOX) treated with lambda phosphatase during cell lysis. A standard phosphatase inhibitor (PI) cocktail used for cell lysis was diluted 0 to128 times to study the effect of lambda phosphatase in absence of phosphatase inhibitors. A lambda phosphatase untreated sample with standard PI cocktail levels (last lane, PI dilution 'NA') was used as a control. (**B**) In-vitro phosphorylation assay between recombinant ERK1 and BIM-L in a 1:3 kinase: substrate weight ratio. The kinase reaction was performed in the presence and absence of 100µM ATP (lane 1, 3 and 4). (**C**) Western blot of wild-type and mutant JAK1 cells that were induced (second lane in each individual blot) and treated with 2µM of MEK inhibitor CI1040 (third lane in each individual blot). (**D and E**) Protein phosphorylation of ERK and BIM at increasing concentration of MEK inhibitor selumetinib (range 0-100µM) in JAK1^{T901A} and NRAS^{G12D} overexpressing cells.*

The transcriptional steroid response is intact in SUPT-1 steroid resistant lines
BIM, among other genes, represents an important transcriptional target gene of the glucocorticoid receptor (NR3C1) (8-10, 12, 18, 21, 32). Failure to upregulate *BIM* has been linked to steroid resistance in pediatric ALL patients and ALL PDX samples (8, 17, 18, 33). To establish whether transcriptional activation of *BIM* is impaired as a potential steroid resistance mechanism downstream of mutant IL7R signaling, we measured *BIM* expression in the presence and absence of steroid treatment in SUPT-1 cells with and without expression of mutant JAK1 or IL7Rα molecules (**Figures 3a-b**). In the absence of doxycycline, where cells do not express mutant molecules (i.e. steroid sensitive phenotype), all cell lines underwent a 4 to 10-fold increase in *BIM* expression following overnight exposure to prednisolone. Doxycycline-induced expression of mutant (and steroid resistant) JAK1 or IL7Rα molecules also resulted in a robust upregulation of *BIM* following steroid treatment. This was also confirmed at the protein level, where steroid treatment led to increased BIM levels independently of MAPK-ERK signaling (**Figure 3c**). This indicates that the transcriptional response of NR3C1 upon steroid exposure remains intact in steroid resistant IL7R and JAK1 mutant lines, which hints that phosphorylation of BIM may drive MAPK-ERK-dependent steroid resistance. Notably, MCL1 levels also increased following prednisolone exposure in all lines tested, indicating that *MCL1* might represent a novel and direct transcriptional target gene of NR3C1 (**Figure 3c**).

Phosphorylation of BIM impairs its binding to anti-apoptotic BCL-2 family members
BIM can bind to anti-apoptotic family members including BCL2, BCLW, BCLXL and MCL1 to antagonize their pro-survival activities (7, 34-37). We hypothesized that phosphorylation of BIM is causative for MAPK-ERK dependent steroid resistance in T-ALL by directly impairing the binding of BIM to anti-apoptotic family members. We therefore performed a qualitative unbiased mass spectrometry analysis of BIM-immunoprecipitation eluates from non-induced and doxycycline-induced $NRAS^{G12D}$ cells. As a result, we identified 23 proteins that consistently bound to unphosphorylated BIM in three replicate experiments (**Supplemental table 1**). Between eluates, we observed variation in BIM protein abundancy (quantified by the BIM iBAQ value; **Supplemental figure 3a, supplemental table 1**). This variation could easily be explained by differences in immunoprecipitation efficiency, but could also be caused by potential proteasomal degradation of phosphorylated BIM (11, 22, 23). By treating $NRAS^{G12D}$ overexpressing cells with the proteasomal inhibitor bortezomib, we indeed observed moderate increased BIM protein levels, whereas MCL1 stabilization confirmed effective inhibition of the proteasome (**Supplemental figure 3b**). To correct our analysis for technical differences and proteasomal degradation, we normalized the iBAQ value of each individual protein to the BIM iBAQ value within each sample (**Supplemental table 1**). Since the *BIM* gene is a direct target gene of the glucocorticoid receptor, mass spectrometry and subsequent normalization was also performed on BIM-immunoprecipitation eluates of prednisolone-treated $NRAS^{G12D}$ cells. This qualitative mass spectrometry approach demonstrated that five out of 23 proteins consistently decreased direct protein-protein

interaction with BIM upon its phosphorylation (**Figure 4a, supplemental table 1**). With the exception of Aurora Kinase A (AURKA), the other four proteins represent BCL-2-family members, that is BCLXL, BCL2, MCL1 and BMF.

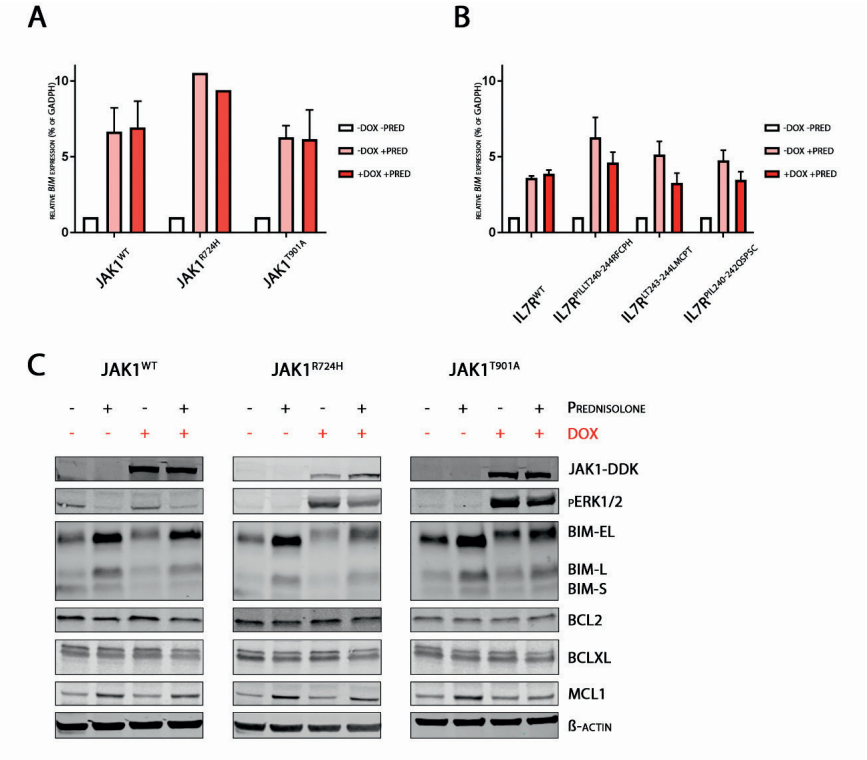

Figure 3. Steroid-dependent expression of *BIM* is not impaired in MAPK-ERK activated cell lines. *(***A-B***) Relative BIM expression levels (mean and SD of triplicates) of wild-type and mutant JAK1 and IL7R cell lines. Expression was normalized to GAPDH expression. BIM expression of non-induced cells that were not treated with prednisolone was used as baseline (relative expression=1). RT-QPCR was performed on both doxycycline-induced and non-induced samples that were treated overnight with prednisolone (250 µg/ml). (***C***) Pathway signaling and BH3-protein family members were studied in steroid-treated (250 µg/ml prednisolone) and untreated wild-type and mutant JAK1 cells.*

To validate the finding that phosphorylation impairs the capability of BIM to bind anti-apoptotic BCL-2 family members, we performed BIM-immunoprecipitation in steroid-sensitive ($JAK1^{WT}$) and steroid-resistant ($JAK1^{T901A}$, $JAK1^{R724H}$ and the $NRAS^{G12D}$) cell lines (**Figures 4b-c**, **supplemental figures 4a-b**). As expected, (non-phosphorylated) BIM effectively binds MCL1, BCL2 and BCLXL in all these lines under non-induced, steroid-sensitive conditions. Moreover, steroid-dependent BIM upregulation further enhanced capturing of MCL1, BCL2 and BCLXCL proteins (lane 5 and 6). Following

doxycycline-induced expression of mutant JAK1 or NRAS molecules and subsequent BIM phosphorylation, BIM decreased its binding to all three anti-apoptotic molecules (compare lanes 7 and 8 to 5 and 6, respectively). Reciprocal immunoprecipitation experiments for BCL2 or MCL1 using the $NRAS^{G12D}$ line also confirmed reduced binding to BIM isoforms following BIM phosphorylation (**Supplemental figures 4c-d)**. We therefore conclude that phosphorylation of BIM impairs its interaction with anti-apoptotic BCL-2 family members, which drives steroid resistance. Following inhibition of the proteasome, which slightly elevated BIM protein levels, we did not observe enhanced binding of BIM to BCL2 (**Supplemental figure 4e**). This confirms that phosphorylation of BIM results in loss-of-binding to anti-apoptotic molecules, rather than indirectly due to proteasomal degradation. Unfortunately, we were unable to identify the BIM phospho-motif responsible for this loss-of-binding effect, since phosphorylation at known Ser55, Ser69, Thr56 and Thr112 was not observed in our SUPT-1 cell lines with activated MAPK-ERK signaling (data not shown).

To explore therapeutic options for this MAPK-ERK-induced steroid resistance mechanism, we studied to what extend JAK or MEK inhibitors are able to prevent phosphorylation of BIM and to restore its binding to anti-apoptotic family members. For this, BIM was precipitated in lysates from doxycycline-induced $JAK1^{T901A}$ and $NRAS^{G12D}$ lines that were treated with the JAK1/2-inhibitor ruxolitinib or the MEK inhibitor selumetinib. Treatment with either ruxolitinib or selumetinib abolished MAPK-ERK and consequential phosphorylation of BIM in JAK1 mutant cells, whereas the effect of selumetinib was independent on active JAK1 signaling (**Supplemental figure 5a**; lanes 5 and 6). As expected, selumetinib but not ruxolitinib abolished MAPK-ERK activation and subsequent phosphorylation of BIM in doxycycline-induced $NRAS^{G12D}$ cells (**Supplemental figure 5b**; lanes 5 and 6). Restoration of non-phosphorylated BIM in both lines restored its binding to MCL1, BCL2 and BCLXL (**Figures 4d-e**, lanes 4, 5 and 6). Treatment with selumetinib or ruxolitinib also prevented phosphorylation of BIM upon IL7 exposure in the T-ALL PDX sample Z1808 (**Supplemental figure 5c**). We therefore conclude that the adverse effects of MAPK-ERK pathway activation downstream of active IL7R/JAK signaling can be blocked by both JAK and MEK inhibitors, while MAPK-ERK activation by mutations downstream of the IL7R or JAK molecules can only be blocked by MEK inhibitors.

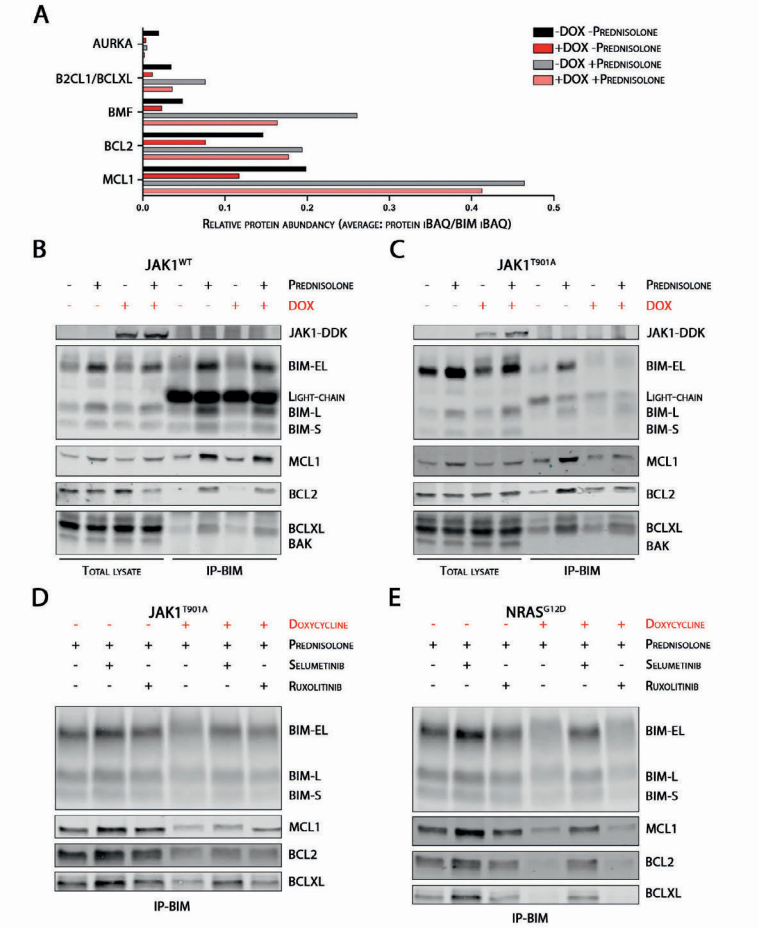

Figure 4. Phosphorylation of BIM directly impairs its binding to anti-apoptotic proteins, which is prevented by pharmacological inhibition of MAPK-ERK signaling. *(***A***) Protein abundancy of five proteins identified by qualitative mass spectrometry that lost binding to BIM upon BIM phosphorylation in prednisolone untreated and treated conditions. Relative protein abundancy was determined by the ratio of protein abundancy in each individual sample (protein iBAQ) versus total BIM protein abundancy in each individual sample (BIM iBAQ). Bars represent the average of the replicates (n=3) in NRAS^{G12D} SUPT-1 cells. The comparison between –dox –prednisolone versus +dox –prednisolone and –dox +prednisolone versus +dox +prednisolone illustrate the loss of binding of these five proteins. Samples were induced by doxycycline and/or treated with 250 µg/ml prednisolone for 24 hours before BIM immunoprecipitation. (***B-C***) BIM-immunoprecipitation of wild-type JAK1 and JAK1^{T90A1} mutant cells. Lane 1-4: total lysate of induced and non-induced cells incubated overnight in the absence or presence of 250 µg/ml prednisolone. Lane 5-6: BIM-immunoprecipitation of corresponding samples, studying differences in the binding of BIM to anti-apoptotic BCL2 family members (MCL1, BCL2 and BCLXL). (***D-E***) BIM-immunoprecipitation of JAK1^{T901A} and NRAS^{G12D} mutant cells. In addition to doxycycline-induction and prednisolone treatment (250 µg/ml prednisolone), samples were treated with either 2µM ruxolitinib or 10µM selumetinib. Corresponding total lysate blots are presented in* **supplemental figure 4a-b**.

MEK-ERK inhibition enhances steroid responsiveness

To elaborate on the clinical application of these targeted compounds in T-ALL, we first tested the cytotoxic efficacy of ruxolitinib or MEK inhibitors selumetinib, trametinib and binimetinib in 46 T-ALL PDX samples. In the absence of IL7, none of the PDX samples tested responded to single ruxolitinib treatment, while the majority of these samples demonstrated a robust response to all three MEK inhibitors (**Figure 5a**). Since ruxolitinib seems effective in PDX-models when tested *in-vivo* (29, 38), we hypothesized that its therapeutic effect may be dependent on IL7-enhanced survival and/or proliferation pathways. We therefore studied the relationship between IL7-dependent viability and ruxolitinib sensitivity in six IL7-dependent steroid resistant PDX samples (**Supplemental figure 6a**). These PDX cells were more viable when cultured in the presence of IL7 (**Supplemental table 2**), and became sensitive to ruxolitinib treatment (**Supplemental figure 6a**). Importantly, we observed a significant correlation (p=0.0039) between increased ruxolitinib sensitivity and the level of IL7-enhanced viability (**Figure 5b, supplemental figure 6a**). This was not observed for six IL7-independent steroid resistant PDX samples that remained insensitive to ruxolitinib even in the presence of IL7 (**Supplemental table 2, supplemental figure 6b**). Therefore, we conclude that the therapeutic effect of ruxolitinib is dependent on IL7-enhanced cell viability. This may limit the therapeutic application of ruxolitinib, since only a minority of T-ALLs exploit IL7-signaling to provoke steroid resistance (**Figure 1d**). Cellular sensitivity towards selumetinib was independent on IL7-enhanced viability (**Figure 5b**, **supplemental figure 6a**).

We then investigated whether pharmacological inhibition of MAPK-ERK signaling could synergize with prednisolone in steroid-resistant T-ALL cells. For this, we combined prednisolone treatment with selumetinib or ruxolitinib in the six IL7-independent steroid-resistant PDX samples and the six IL7-dependent steroid resistant PDX samples (**Figure 5c, supplemental figure 7a-b, supplemental table 3**). Combination treatment with prednisolone and selumetinib was highly synergistic in both IL7-dependent and IL7-independent steroid resistant samples. This highlights that MAPK-ERK signaling is a central driver in both IL7-dependent and IL7-independent steroid resistance mechanisms in T-ALL. Selumetinib was also synergistic in PDX cells under steroid-sensitive conditions (*e.g.* IL7-dependent cells that were tested in the absence of IL7). In addition to all IL7-dependent steroid resistant samples, only one IL7-independent steroid resistant sample demonstrated synergy between prednisolone and ruxolitinib in the presence of IL7 (PDX COG17R, purple dots, **Figure 5c**). Interestingly, synergy between prednisolone and ruxolitinib was also observed in one IL7-dependent steroid resistant sample in the absence of IL7 (PDX Z1808, green dots, **Figure 5c**). For both samples in their respective conditions, we did observe STAT5 activation and subsequent BCL2 upregulation (**Supplemental figure 1b**). However, both samples also heavily benefitted from combined prednisolone and selumetinib treatment (- or + IL7 lanes for PDX COG17R, +IL7 lane for PDX Z1808). Therefore, these results highlight that MEK

inhibitors are superior over the JAK1/2 inhibitor ruxolitinib, since MEK-inhibitors can resensitize steroid-resistant T-ALL patients that are insensitive to ruxolitinib treatment.

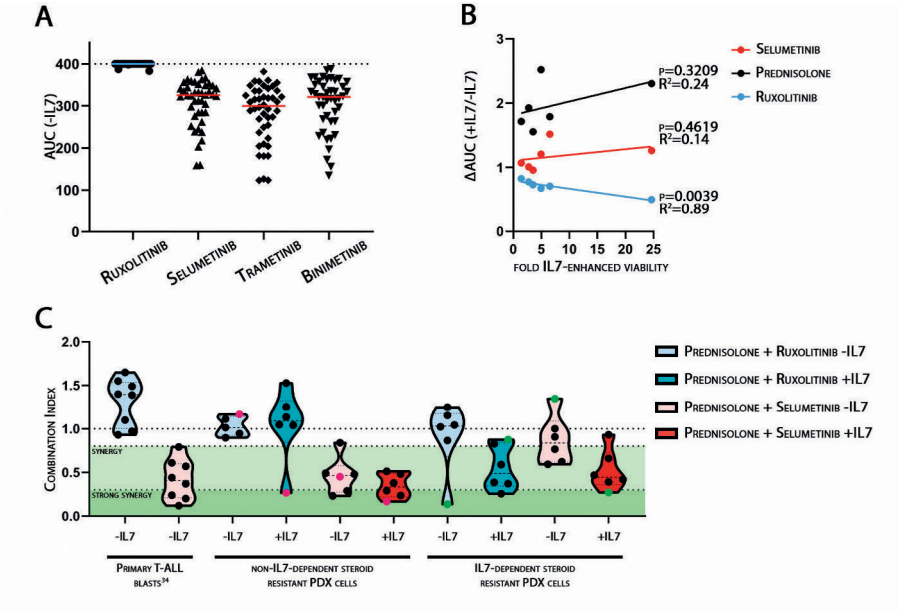

Figure 5. MEK-inhibitors synergize with steroid treatment in IL7-dependent and IL7-independent steroid-resistant T-ALL. *(**A**) Cell toxicity screening of 46 T-ALL PDX samples for ruxolitinib (JAK-inhibitor), selumetinib, trametinib or binimetinib (MEK inhibitors) in IL7 untreated condition. Cell viability is illustrated by AUC, whereas an AUC of 400 represent the maximum AUC in a 4-log dynamic concentration range of each specific inhibitor. (**B**) Correlation between IL7-enhanced cell viability and altered drug sensitivity in the presence of IL7 in six 'IL7-dependent steroid resistant' PDX samples. 'IL7-dependent steroid resistant' PDX samples were defined by an increase in prednisolone AUC by >1,5 fold in the presence of IL7 with a minimal AUC of 175 in the presence of IL7. Y-axis represent delta AUC, defined by the ratio between the AUC of the specific drug in the presence and absence of IL7. X-axis represent the magnitude of IL7-enhanced viability in each individual sample relative to viability in the absence of IL7 (Supplemental figure 5a). Linear regression (R^2) and p-values conclude a significant correlation between IL7-enhanced viability and ruxolitinib sensitivity. (**C**) The combination Index (CI) of T-ALL PDX samples, treated with prednisolone and ruxolitinib (blue) or selumetinib (red) treatment in the absence (light colored) or presence (dark colored) of IL7. The synergy value of each sample illustrated is an average CI score, calculated over the complete therapeutic window of the combination treatment (Supplemental figure 6a-b). Synergy was defined by a CI between 0.3 and 0.8, whereas strong synergy was defined by a CI <0.3. PDX COG17 was highlighted by the purple dots, whereas PDX Z1808 was highlighted by the green dots.*

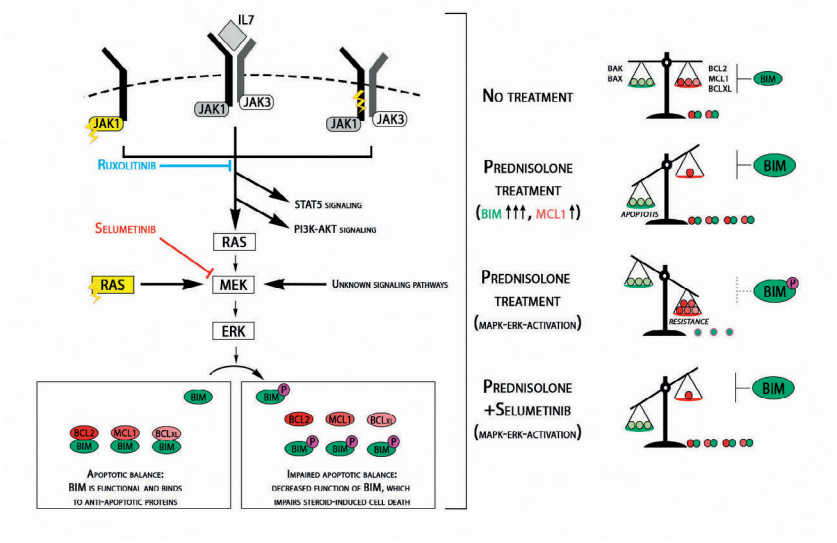

Figure 6. Schematic overview of MAPK-ERK-induced steroid resistance. *Cysteine IL7Rα mutations, JAK1 mutations, and physiological IL7 signaling can activate the MAPK-ERK signaling pathway in T-ALL. Additionally, the MAPK-ERK pathway can be activated by RAS mutations or unknown (i.e. non-IL7) signaling pathways. Activated ERK phosphorylates the pro-apoptotic molecule BIM, which normally binds to anti-apoptotic Bcl-2 family proteins (BCL2, BCLXL and MCL1).*

DISCUSSION

In the last two decades, major improvements have been made in the treatment of pediatric T-ALL. Certain genetic aberrations, like recurrent IL7R pathway mutations, are related to drug resistance and inferior outcome (28, 39, 40). Here, we demonstrate that both ligand- and mutation-induced IL7R signaling activates the MAPK-ERK pathway in cell lines and pediatric T-ALL PDX samples. Activated MEK-ERK phosphorylates pro-apoptotic BIM, which impairs its binding to anti-apoptotic proteins, resulting in steroid resistance. We demonstrate that MEK inhibitors effectively abolish this resistance mechanism and synergize with steroid treatment (**Figure 6**). These data highlight an opportunity for treatment with MEK inhibitors in MAPK-ERK activated T-ALL during steroid therapy. Moreover, treatment with MEK inhibitors could prevent selection of cells that harbor MAPK-ERK-activating mutations during steroid treatment. The latter specifically accounts for *IL7Rα, JAK1* and *NRAS* mutations (28), especially since *IL7Rα* and *NRAS* mutations have been identified as predictors for extremely poor outcome for relapsed T-ALL patients (41). Interestingly, we observed synergy between MEK inhibitor selumetinib and prednisolone in both IL7-dependent and IL7-independent PDX samples. This implies that the application of MEK inhibitors in T-ALL is not limited to specific T-ALL patient subgroups or certain genetic aberrations, but that the MAPK-ERK pathway may be a central convergence point that is activated downstream of multiple important signaling pathways in T-ALL.

MAPK-ERK activation induces phosphorylation of BIM-EL and BIM-L isoforms. BIM-EL consists of exons 2-6, with exon 3 containing at least three serine residues (Ser-59, Ser-69 and Ser-77) that are known sites for phosphorylation by ERK (11, 22, 42). Although BIM-L lacks exon 3, we observed that this isoform is also subjected to phosphorylation that can be abolished by MEK inhibitor treatment. Phosphorylation of the pro-apoptotic BIM-S isoform, which only consists of exons 5 and 6, was not observed in our models. Therefore, we predict that one or multiple residues on BIM exon 4 can also be subjected to ERK-dependent phosphorylation as also observed in other studies (22, 42, 43).

We identified Aurora Kinase A (AURKA) as a BIM-interacting protein, which lost interaction upon BIM phosphorylation. It has been reported that AURKA – in contrast to ERK – specifically phosphorylates BIM-EL during mitosis (44, 45). Our mass spectrometry data however demonstrated that the interaction between unphosphorylated BIM and AURKA already drastically decreases upon steroid treatment. This decreased interaction might be caused by the downregulation of *AURKA* as a result of steroid treatment, as is observed in a BCP-ALL xenograft model (46). Down-regulation of AURKA in steroid-treated leukemia implies that AURKA does not actively contribute to steroid resistance, which would exclude AURKA inhibitors as therapeutic agents to reverse steroid resistance.

In addition to MAPK-ERK signaling, activation of the IL7R also leads to activation of the PI3K-AKT and JAK-STAT pathways, highlighting the complexity of IL7R signaling. Like MEK inhibitors, JAK and AKT inhibitors also seem promising to restore steroid sensitivity (28, 38). Early T-cell progenitor (ETP) ALL patient cells are intrinsically more resistant to steroid treatment than non-ETP-ALL cells, frequently bear JAK-STAT activating mutations and are responsive to JAK1/2-inhibitor ruxolitinib (38). Moreover, combination treatment of ruxolitinib and dexamethasone enhances steroid-induced cell death in IL7-dependent steroid resistant T-ALL cells due to IL7-induced JAK-STAT activation (29). We confirm these findings and demonstrate that IL7-dependent steroid resistant T-ALL cells can benefit from synergistic effects of ruxolitinib on steroid-induced cytotoxicity in the presence of IL7. Moreover, we demonstrate that ruxolitinib also effectively blocks active MAPK-ERK signaling in IL7-dependent T-ALL PDX cells and JAK1 mutant T-ALL cells. The synergistic effect between JAK1/2-inhibition and steroids may therefore (in part) depend on the consequential inhibition of downstream MAPK-ERK signaling (38, 47).

With the exception of sample Z1808 that displays high STAT5 pathway activation in the absence of IL7 (*i.e.* IL7-induced signaling), we did not observe synergy between ruxolitinib and steroids in the remaining five IL7-dependent steroid resistant PDX samples in the absence of IL7. Our data suggests that the effect of ruxolitinib is limited to leukemic cells that utilize IL7-induced signaling to boost cell viability. In *in-vivo* PDX models that depend on active proliferation of leukemia cells, treatment with JAK1/2

inhibitors have been demonstrated to be effective and synergistic when combined with steroids. This effect might depend on the presence of stromal cells as main source for IL7 production. Our data however suggests the majority of non-proliferating cells will not respond to ruxolitinib treatment: (quiescent) leukemia cells in low-IL7-containing niches in patients may therefore not benefit from combined ruxolitinib and steroid treatment, limiting the curative application of ruxolitinib. This may be exemplified by the limited effect of ruxolitinib treatment in myeloproliferative neoplasms – a disease characterized by dominant mutational driven JAK-STAT pathway activation –, since molecular remission upon ruxolitinib treatment is usually not achieved in these patients (48). A similar dependency on IL7-enhanced viability is not a prerequisite for the synergistic effects of MEK inhibitors on steroid-induced cytotoxicity, and selumetinib was effective in all T-ALL PDX samples regardless of IL7-induced signaling. As the MAPK-ERK pathway is often activated downstream of active JAK-signaling, MEK inhibitors may provide a valuable alternative for ruxolitinib in JAK-STAT-activated neoplasms. Therefore, our data indicates that care should be taken implementing ruxolitinib in clinical practice for T-ALL.

In addition to our findings in T-ALL, the presence of RAS mutations in BCP-ALL at diagnosis predict for resistance to chemotherapeutic treatment and early relapse (49). RAS mutations are enriched in relapsed BCP-ALL, frequently arising from minor subclones already present at diagnosis. MEK inhibitors also provide strong synergy with dexamethasone treatment in RAS-mutated BCP-ALL by enhancing functional BIM levels (50). Additionally, inhibition of the MAPK-ERK signaling cascade in ALL may enhance steroid sensitivity via the upregulation of p53 (51). Results from these and other studies formed the basis of the phase I/II SeluDex trial (CT03705507) for mutant N/KRAS- (or FLT3, PTPN11 or cCBL) relapsed/refractory BCP-ALL and T-ALL patients (28, 50). Our data indicates that *JAK1* and *IL7Rα* mutations could be included in the 'RAS-activating mutations panel' in the current SeluDex trial. As the MAPK-ERK pathway may represent a central junction for more signaling pathways than (mutant) IL7R-signaling, the effect of combined MEK inhibitor and steroid treatment seems beneficial for a large group of T-ALL patients.

In conclusion, MAPK-ERK pathway inhibitors – and in particular MEK inhibitors – potentiate steroid-induced cell death by preventing the inactivation of (steroid-induced) pro-apoptotic BIM. Our data highlight the importance of MAPK-ERK signaling in T-ALL, since the synergistic effect of MEK inhibitors with steroids is not limited to IL7-induced signaling or the presence of specific activating (mutational) events. By expanding the inclusion criteria for the current SeluDex trial, the clinical effect of MEK inhibitors may be studied for more relapsed/refractory T-ALL patients to substantiate the potential use of combined MEK inhibitor and steroid therapy in future (first-line) treatment regimens.

Acknowledgements. This study was sponsored by grants of the foundation “Kinderen Kankervrij”; KiKa-219 (JvdZ), KiKa-92, KiKa-295 (WKS), the Chemotherapy Foundation (AAF) and NIH grants P30 CA013696 (Flow Cytometry Shared Resource and Genomics Shared Resource, Herbert Irving Comprehensive Cancer Center) and R35 CA210065 (AAF). This research was part of the Netherlands X-omics Initiative and partially funded by NWO, project 184.034.019.

Contribution of authors. JvdZ designed study, performed research and wrote manuscript. JBG, VC, DD, WKS, ZC and JD performed research. GZ, MA, KO, BB, J-PB, JC and AAF performed research, and provided critical input. JV, RP and BV provided critical input and wrote manuscript. JM designed and supervised the study and wrote manuscript.

Disclosures. JV and BV: Cancer Research United Kingdom alliance funding from AstraZeneca for SeluDex trial (NCT03705507).

REFERENCES

1. Pieters R, de Groot-Kruseman H, Van der Velden V, Fiocco M, van den Berg H, de Bont E, et al. Successful Therapy Reduction and Intensification for Childhood Acute Lymphoblastic Leukemia Based on Minimal Residual Disease Monitoring: Study ALL10 From the Dutch Childhood Oncology Group. J Clin Oncol. 2016;34(22):2591-601.
2. Conter V, Valsecchi MG, Parasole R, Putti MC, Locatelli F, Barisone E, et al. Childhood high-risk acute lymphoblastic leukemia in first remission: results after chemotherapy or transplant from the AIEOP ALL 2000 study. Blood. 2014;123(10):1470-8.
3. Lauten M, Moricke A, Beier R, Zimmermann M, Stanulla M, Meissner B, et al. Prediction of outcome by early bone marrow response in childhood acute lymphoblastic leukemia treated in the ALL-BFM 95 trial: differential effects in precursor B-cell and T-cell leukemia. Haematologica. 2012;97(7):1048-56.
4. Reedijk AMJ, Coebergh JWW, de Groot-Kruseman HA, van der Sluis IM, Kremer LC, Karim-Kos HE, et al. Progress against childhood and adolescent acute lymphoblastic leukaemia in the Netherlands, 1990-2015. Leukemia. 2020.
5. Kaspers GJ, Pieters R, Van Zantwijk CH, Van Wering ER, Van Der Does-Van Den Berg A, Veerman AJ. Prednisolone resistance in childhood acute lymphoblastic leukemia: vitro-vivo correlations and cross-resistance to other drugs. Blood. 1998;92(1):259-66.
6. Lauten M, Stanulla M, Zimmermann M, Welte K, Riehm H, Schrappe M. Clinical outcome of patients with childhood acute lymphoblastic leukaemia and an initial leukaemic blood blast count of less than 1000 per microliter. Klinische Padiatrie. 2001;213(4):169-74.
7. O'Connor L, Strasser A, O'Reilly LA, Hausmann G, Adams JM, Cory S, et al. Bim: a novel member of the Bcl-2 family that promotes apoptosis. EMBO J. 1998;17(2):384-95.
8. Jing D, Bhadri VA, Beck D, Thoms JA, Yakob NA, Wong JW, et al. Opposing regulation of BIM and BCL2 controls glucocorticoid-induced apoptosis of pediatric acute lymphoblastic leukemia cells. Blood. 2015;125(2):273-83.
9. Abrams MT, Robertson NM, Yoon K, Wickstrom E. Inhibition of glucocorticoid-induced apoptosis by targeting the major splice variants of BIM mRNA with small interfering RNA and short hairpin RNA. J Biol Chem. 2004;279(53):55809-17.
10. Hall CP, Reynolds CP, Kang MH. Modulation of Glucocorticoid Resistance in Pediatric T-cell Acute Lymphoblastic Leukemia by Increasing BIM Expression with the PI3K/mTOR Inhibitor BEZ235. Clin Cancer Res. 2016;22(3):621-32.
11. Ley R, Balmanno K, Hadfield K, Weston C, Cook SJ. Activation of the ERK1/2 signaling pathway promotes phosphorylation and proteasome-dependent degradation of the BH3-only protein, Bim. J Biol Chem. 2003;278(21):18811-6.
12. Wang Z, Malone MH, He H, McColl KS, Distelhorst CW. Microarray analysis uncovers the induction of the proapoptotic BH3-only protein Bim in multiple models of glucocorticoid-induced apoptosis. J Biol Chem. 2003;278(26):23861-7.
13. Wang C, Youle RJ. The role of mitochondria in apoptosis*. Annu Rev Genet. 2009;43:95-118.
14. Willis SN, Fletcher JI, Kaufmann T, van Delft MF, Chen L, Czabotar PE, et al. Apoptosis initiated when BH3 ligands engage multiple Bcl-2 homologs, not Bax or Bak. Science. 2007;315(5813):856-9.
15. Gavathiotis E, Suzuki M, Davis ML, Pitter K, Bird GH, Katz SG, et al. BAX activation is initiated at a novel interaction site. Nature. 2008;455(7216):1076-81.
16. Piovan E, Yu J, Tosello V, Herranz D, Ambesi-Impiombato A, Da Silva AC, et al. Direct reversal of glucocorticoid resistance by AKT inhibition in acute lymphoblastic leukemia. Cancer Cell. 2013;24(6):766-76.

17. Bachmann PS, Gorman R, Papa RA, Bardell JE, Ford J, Kees UR, et al. Divergent mechanisms of glucocorticoid resistance in experimental models of pediatric acute lymphoblastic leukemia. Cancer Res. 2007;67(9):4482-90.
18. Bachmann PS, Piazza RG, Janes ME, Wong NC, Davies C, Mogavero A, et al. Epigenetic silencing of BIM in glucocorticoid poor-responsive pediatric acute lymphoblastic leukemia, and its reversal by histone deacetylase inhibition. Blood. 2010;116(16):3013-22.
19. Singh A, Ye M, Bucur O, Zhu S, Tanya Santos M, Rabinovitz I, et al. Protein phosphatase 2A reactivates FOXO3a through a dynamic interplay with 14-3-3 and AKT. Mol Biol Cell. 2010;21(6):1140-52.
20. Yang JY, Zong CS, Xia W, Yamaguchi H, Ding Q, Xie X, et al. ERK promotes tumorigenesis by inhibiting FOXO3a via MDM2-mediated degradation. Nat Cell Biol. 2008;10(2):138-48.
21. Lu J, Quearry B, Harada H. p38-MAP kinase activation followed by BIM induction is essential for glucocorticoid-induced apoptosis in lymphoblastic leukemia cells. FEBS letters. 2006;580(14):3539-44.
22. Hubner A, Barrett T, Flavell RA, Davis RJ. Multisite phosphorylation regulates Bim stability and apoptotic activity. Mol Cell. 2008;30(4):415-25.
23. Leung KT, Li KK, Sun SS, Chan PK, Ooi VE, Chiu LC. Activation of the JNK pathway promotes phosphorylation and degradation of BimEL--a novel mechanism of chemoresistance in T-cell acute lymphoblastic leukemia. Carcinogenesis. 2008;29(3):544-51.
24. Lei K, Davis RJ. JNK phosphorylation of Bim-related members of the Bcl2 family induces Bax-dependent apoptosis. Proc Natl Acad Sci U S A. 2003;100(5):2432-7.
25. Barata JT, Silva A, Brandao JG, Nadler LM, Cardoso AA, Boussiotis VA. Activation of PI3K is indispensable for interleukin 7-mediated viability, proliferation, glucose use, and growth of T cell acute lymphoblastic leukemia cells. J Exp Med. 2004;200(5):659-69.
26. Ribeiro D, Melao A, van Boxtel R, Santos CI, Silva A, Silva MC, et al. STAT5 is essential for IL-7-mediated viability, growth, and proliferation of T-cell acute lymphoblastic leukemia cells. Blood Adv. 2018;2(17):2199-213.
27. Silva A, Laranjeira AB, Martins LR, Cardoso BA, Demengeot J, Yunes JA, et al. IL-7 contributes to the progression of human T-cell acute lymphoblastic leukemias. Cancer Res. 2011;71(14):4780-9.
28. Li Y, Buijs-Gladdines JG, Cante-Barrett K, Stubbs AP, Vroegindeweij EM, Smits WK, et al. IL-7 Receptor Mutations and Steroid Resistance in Pediatric T cell Acute Lymphoblastic Leukemia: A Genome Sequencing Study. PLoS Med. 2016;13(12):e1002200.
29. Delgado-Martin C, Meyer LK, Huang BJ, Shimano KA, Zinter MS, Nguyen JV, et al. JAK/STAT pathway inhibition overcomes IL7-induced glucocorticoid resistance in a subset of human T-cell acute lymphoblastic leukemias. Leukemia. 2017;31(12):2568-76.
30. Meyer LK, Huang BJ, Delgado-Martin C, Roy RP, Hechmer A, Wandler AM, et al. Glucocorticoids paradoxically facilitate steroid resistance in T-cell acute lymphoblastic leukemias and thymocytes. J Clin Invest. 2019.
31. Barata JT, Durum SK, Seddon B. Flip the coin: IL-7 and IL-7R in health and disease. Nat Immunol. 2019;20(12):1584-93.
32. Erlacher M, Michalak EM, Kelly PN, Labi V, Niederegger H, Coultas L, et al. BH3-only proteins Puma and Bim are rate-limiting for gamma-radiation- and glucocorticoid-induced apoptosis of lymphoid cells in vivo. Blood. 2005;106(13):4131-8.
33. Jing D, Huang Y, Liu X, Sia KCS, Zhang JC, Tai X, et al. Lymphocyte-Specific Chromatin Accessibility Pre-determines Glucocorticoid Resistance in Acute Lymphoblastic Leukemia. Cancer Cell. 2018;34(6):906-21 e8.
34. Cheng EH, Wei MC, Weiler S, Flavell RA, Mak TW, Lindsten T, et al. BCL-2, BCL-X(L) sequester BH3 domain-only molecules preventing BAX- and BAK-mediated mitochondrial apoptosis. Mol Cell. 2001;8(3):705-11.

35. Puthalakath H, Huang DC, O'Reilly LA, King SM, Strasser A. The proapoptotic activity of the Bcl-2 family member Bim is regulated by interaction with the dynein motor complex. Mol Cell. 1999;3(3):287-96.
36. Gomez-Bougie P, Bataille R, Amiot M. Endogenous association of Bim BH3-only protein with Mcl-1, Bcl-xL and Bcl-2 on mitochondria in human B cells. Eur J Immunol. 2005;35(3):971-6.
37. Korfi K, Smith M, Swan J, Somervaille TC, Dhomen N, Marais R. BIM mediates synergistic killing of B-cell acute lymphoblastic leukemia cells by BCL-2 and MEK inhibitors. Cell Death Dis. 2016;7:e2177.
38. Maude SL, Dolai S, Delgado-Martin C, Vincent T, Robbins A, Selvanathan A, et al. Efficacy of JAK/STAT pathway inhibition in murine xenograft models of early T-cell precursor (ETP) acute lymphoblastic leukemia. Blood. 2015;125(11):1759-67.
39. Gianfelici V, Chiaretti S, Demeyer S, Di Giacomo F, Messina M, La Starza R, et al. RNA sequencing unravels the genetics of refractory/relapsed T-cell acute lymphoblastic leukemia. Prognostic and therapeutic implications. Haematologica. 2016;101(8):941-50.
40. Trinquand A, Tanguy-Schmidt A, Ben Abdelali R, Lambert J, Beldjord K, Lengline E, et al. Toward a NOTCH1/FBXW7/RAS/PTEN-based oncogenetic risk classification of adult T-cell acute lymphoblastic leukemia: a Group for Research in Adult Acute Lymphoblastic Leukemia study. J Clin Oncol. 2013;31(34):4333-42.
41. Richter-Pechanska P, Kunz JB, Hof J, Zimmermann M, Rausch T, Bandapalli OR, et al. Identification of a genetically defined ultra-high-risk group in relapsed pediatric T-lymphoblastic leukemia. Blood Cancer J. 2017;7(2):e523.
42. Harada H, Quearry B, Ruiz-Vela A, Korsmeyer SJ. Survival factor-induced extracellular signal-regulated kinase phosphorylates BIM, inhibiting its association with BAX and proapoptotic activity. Proc Natl Acad Sci U S A. 2004;101(43):15313-7.
43. Biswas SC, Greene LA. Nerve growth factor (NGF) down-regulates the Bcl-2 homology 3 (BH3) domain-only protein Bim and suppresses its proapoptotic activity by phosphorylation. J Biol Chem. 2002;277(51):49511-6.
44. Moustafa-Kamal M, Gamache I, Lu Y, Li S, Teodoro JG. BimEL is phosphorylated at mitosis by Aurora A and targeted for degradation by betaTrCP1. Cell Death Differ. 2013;20(10):1393-403.
45. Gilley R, Lochhead PA, Balmanno K, Oxley D, Clark J, Cook SJ. CDK1, not ERK1/2 or ERK5, is required for mitotic phosphorylation of BIMEL. Cell Signal. 2012;24(1):170-80.
46. Bhadri VA, Cowley MJ, Kaplan W, Trahair TN, Lock RB. Evaluation of the NOD/SCID xenograft model for glucocorticoid-regulated gene expression in childhood B-cell precursor acute lymphoblastic leukemia. BMC Genomics. 2011;12:565.
47. Verbeke D, Gielen O, Jacobs K, Boeckx N, De Keersmaecker K, Maertens J, et al. Ruxolitinib Synergizes With Dexamethasone for the Treatment of T-cell Acute Lymphoblastic Leukemia. Hemasphere. 2019;3(6):e310.
48. Greenfield G, McPherson S, Mills K, McMullin MF. The ruxolitinib effect: understanding how molecular pathogenesis and epigenetic dysregulation impact therapeutic efficacy in myeloproliferative neoplasms. J Transl Med. 2018;16(1):360.
49. Irving J, Matheson E, Minto L, Blair H, Case M, Halsey C, et al. Ras pathway mutations are prevalent in relapsed childhood acute lymphoblastic leukemia and confer sensitivity to MEK inhibition. Blood. 2014;124(23):3420-30.
50. Matheson EC, Thomas H, Case M, Blair H, Jackson RK, Masic D, et al. Glucocorticoids and selumetinib are highly synergistic in RAS pathway mutated childhood acute lymphoblastic leukemia through upregulation of BIM. Haematologica. 2019.
51. Jones CL, Gearheart CM, Fosmire S, Delgado-Martin C, Evensen NA, Bride K, et al. MAPK signaling cascades mediate distinct glucocorticoid resistance mechanisms in pediatric leukemia. Blood. 2015;126(19):2202-12.

A

PDX name	AUC Prednisolone (-IL7)	Prednisolone (+IL7)	Ratio
6206Rel	100.70	66.24	0.66
5716	142.80	105.80	0.74
1946	260.40	206.10	0.79
1950	181.70	148.00	0.81
L861	107.90	100.30	0.93
6953Dx	102.60	95.97	0.94
335	140.10	133.00	0.95
3977	221.60	211.90	0.96
L9H60	220.60	212.70	0.96
1643Dx	134.50	130.00	0.97
COG17Dx	124.10	122.40	0.99
257	143.30	143.50	1.00
14643Rel	248.10	249.30	1.00
8148Rel	167.20	168.40	1.01
3920	149.70	150.80	1.01
COG17Rel	296.10	304.60	1.03
1179	211.00	217.20	1.03
6953Rel	123.70	130.00	1.05
8711Rel	149.80	158.20	1.06
COG5Rel	177.10	188.20	1.06
719	199.10	212.90	1.07
9175	83.62	90.36	1.08
419	122.40	136.00	1.11
6206Dx	167.70	187.10	1.12
8173Rel	159.80	179.40	1.12
Z3143	272.40	316.40	1.16
8711Dx	130.50	155.80	1.19
4564Rel	73.20	90.38	1.23
11936Dx	111.30	139.10	1.25
531	112.00	140.90	1.26
COG5Dx	83.04	108.10	1.30
V9577	223.80	303.10	1.35
11451Dx	211.80	299.70	1.42
2229	143.40	208.00	1.45
913	186.90	288.10	1.54
11936Rel	112.30	173.40	1.54
8148Dx	129.80	202.00	1.56
634	321.60	536.80	1.67
2322	110.50	189.70	1.72
5676	280.50	495.80	1.77
V10138	80.36	143.20	1.78
11451Rel	146.50	262.30	1.79
1949	92.65	178.60	1.93
Z1808	126.60	291.90	2.31
4564Dx	93.88	236.70	2.52
540	197.30	1007.00	5.10

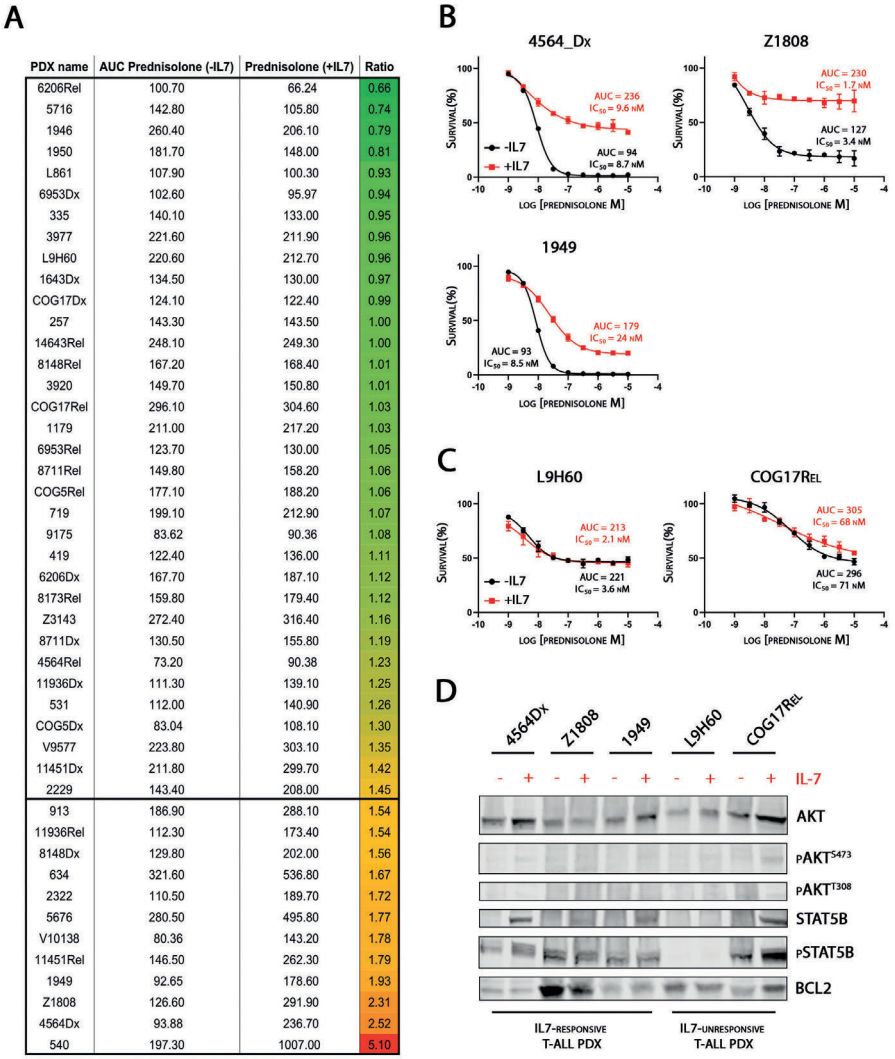

Supplemental Figure 1. *(**A**) Cell toxicity screening of 46 T-ALL PDX samples in IL7 treated and untreated condition. Area Under the Curve (AUC) values represent steroid response (range 3.16nM-31.6µM prednisolone). Samples that demonstrated >1.5 fold increase in prednisolone AUC in presence of IL7 were assigned to the 'IL7-responsive' group. In our analysis, AUC values exceeding 400 were corrected to this maximum AUC in a 5-log dynamic concentration range of prednisolone. (**B**) Western blot of selected T-ALL PDX samples to study downstream STA5B and AKT pathway activation. (**C**) Steroid sensitivity screen of three selected (and representative) IL7-responsive PDX samples, that demonstrated a >1.5 fold increase in prednisolone AUC in IL7-treated condition. (**D**) Steroid sensitivity screen of two selected (and representative) IL7-independent steroid resistant PDX samples with an AUC exceeding 200.*

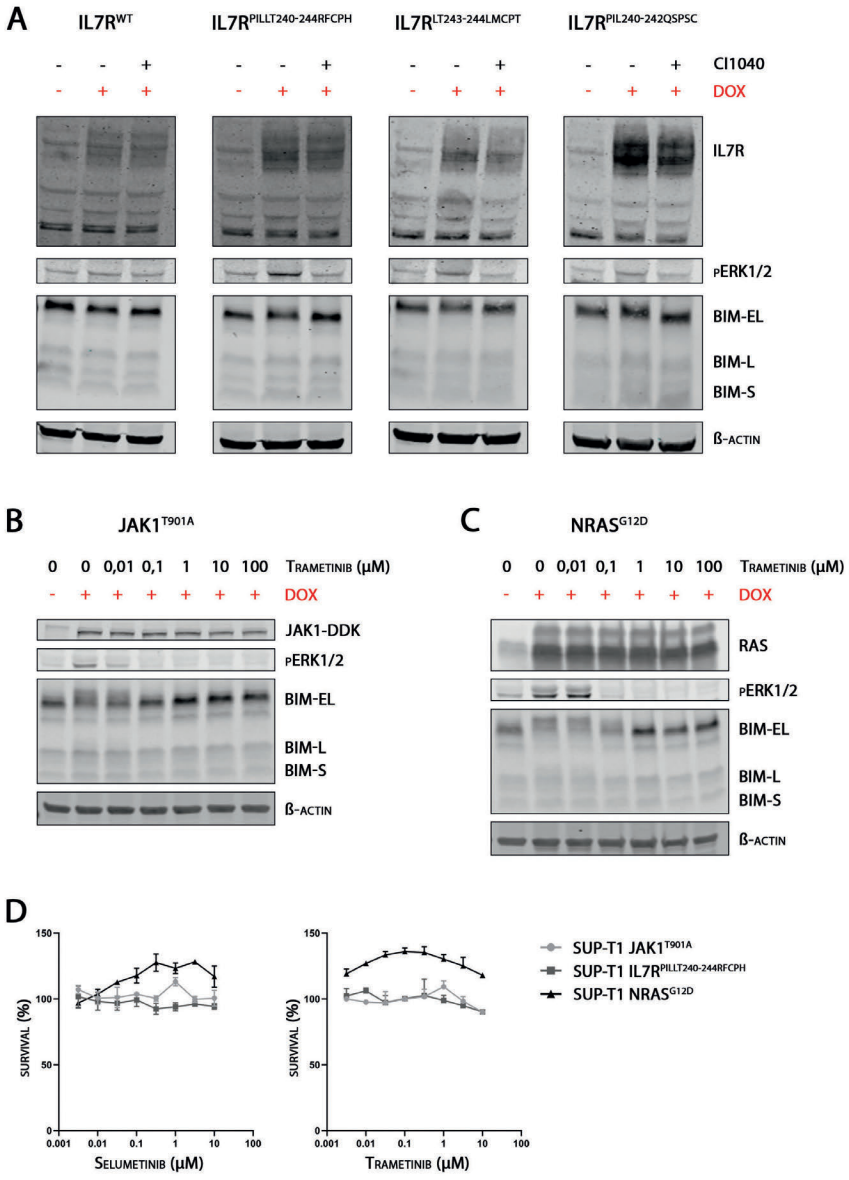

Supplemental Figure 2. *(**A**) Western blot of wild-type and cysteine-mutant IL7Rα cells that were induced (second lane and third lane in each individual blot, +DOX) and treated with 2µM of MEK inhibitor CI1040 (third lane only). (**B-C**) Protein phosphorylation of ERK and BIM at increasing concentration of MEK inhibitor trametinib (range 0-100µM) in JAK1^{T901A} and NRAS^{G12D} overexpressing cells. (**D**) Four-day ATP-light cell viability screen with selumetinib and trametinib (range 0.0032-10µM) in JAK1^{T901A}, NRAS^{G12D} and IL7R$^{PILLT240-244RFCPH}$ derivate cell lines.*

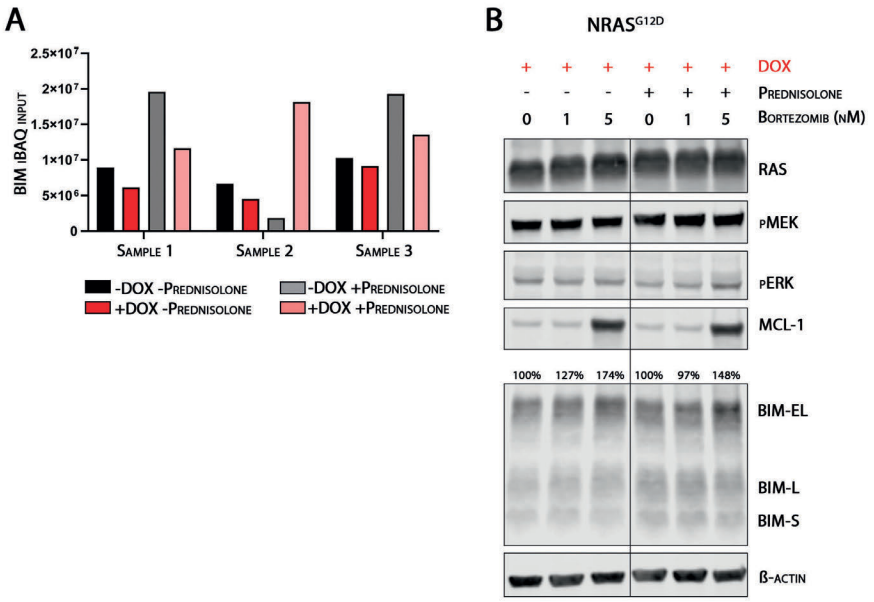

Supplemental Figure 3. *(**A**) BIM iBAQ values of three individual NRAS^{G12D} overexpressing cell samples +/- a one day doxycycline-induction in the absence or presence of prednisolone (250 µg/ml) as measured by mass spectrometry (adapted from* **supplemental table 1***). (**B**) Western blot of NRAS^{G12D} overexpressing SUPT-1 cells treated with prednisolone (250 µg/ml) and/or bortezomib (0, 1 or 5nM) overnight. BIM-EL band intensity was scanned, whereas lane 1 serves as reference for lane 2 and 3 and lane 4 serves as reference for lane 5 and 6.*

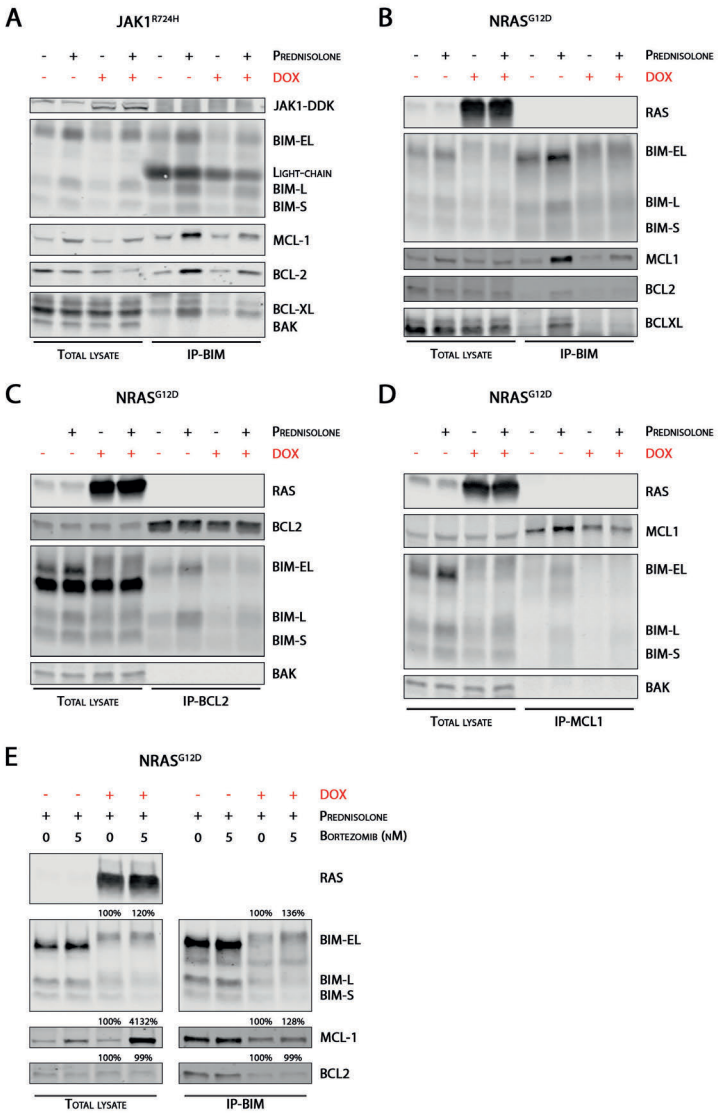

Supplemental Figure 4. *(**A-B**) BIM-immunoprecipitation of JAK1^{R724H} and NRAS^{G12D} mutant cells. Lane 1-4: total lysate of induced and non-induced cells incubated overnight in the absence or presence of 250 µg/ml prednisolone. Lane 5-6: BIM-immunoprecipitation of corresponding samples, studying differences in the binding of BIM to anti-apoptotic BCL-2 family members (MCL-1, BCL-2 and BCL-XL). (**C-D**) Reversed immunoprecipitation of BCL-2 and MCL-1 respectively in NRAS^{G12D} overexpressing cells. (**E**) Western blot and BIM-immunoprecipitation of NRAS^{G12D} overexpressing SUPT-1 cells treated with prednisolone (250 µg/ml) overnight. Lane 2 and 4 lysates were also treated with 5nM bortezomib simultaneous of prednisolone treatment. BIM-EL band intensity of doxycycline-induced cells was scanned, whereas the BIM-EL abundance of bortezomib untreated*

samples was taken as reference.

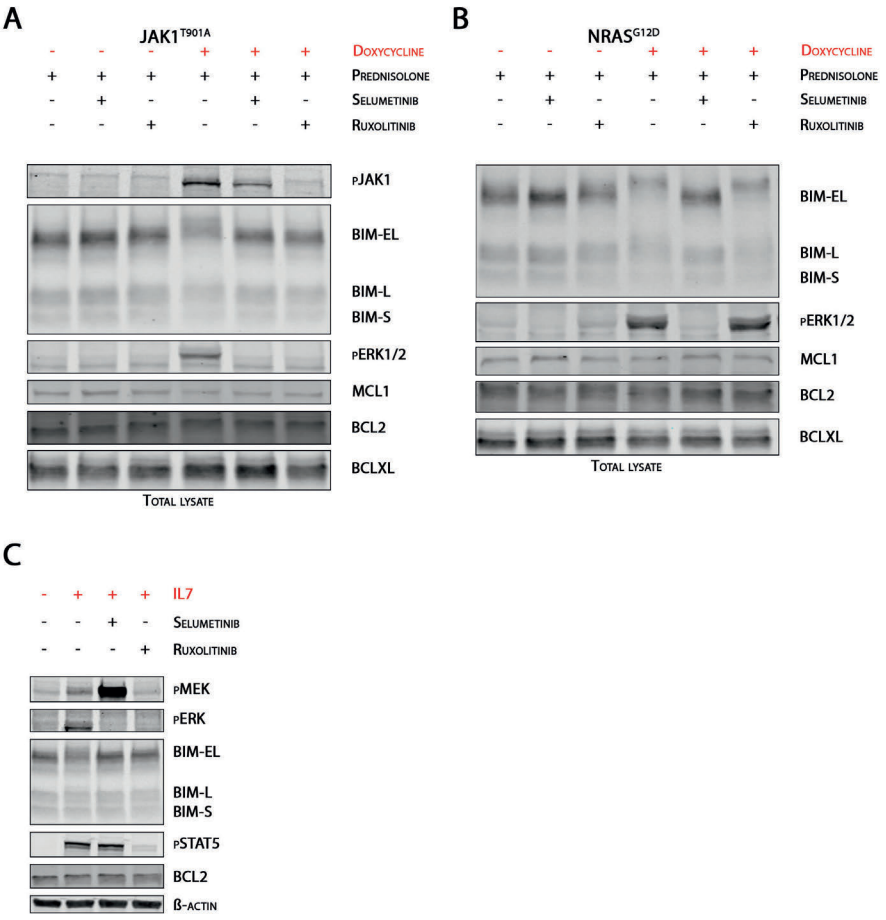

Supplemental Figure 5. *(***A-B***) Total lysates of BIM-immunopricipitation JAK1^{T901A} NRAS^{G12D} mutant cells. In addition to doxycycline-induction and prednisolone treatment (250 µg/ml prednisolone), samples were treated with either 2µM ruxolitinib or 10µM selumetinib. (***C***) Western blot of IL7-induced signaling of PDX Z1808, treated with either 2µM ruxolitinib or 10µM selumetinib.*

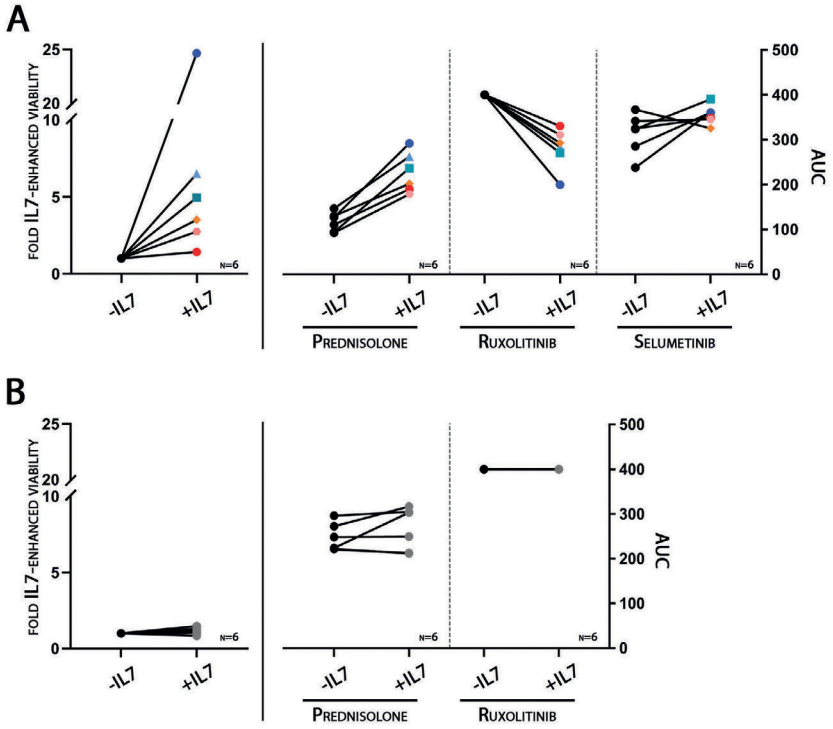

Supplemental Figure 6. *(***A***) IL7-enhanced viability of six untreated 'IL7-dependent steroid resistant' PDX samples (left), and the cell viability of these samples when treated with prednisolone, ruxolitinib or selumetib in the presence or absence of IL7. 'IL7-dependent steroid resistant' PDX samples were defined by an increase in prednisolone AUC by >1.5 fold in the presence of IL7 with a minimal AUC of 175 in the presence of IL7. Fold IL7-enhanced viability was defined by the relative increase in cell viability in the presence of IL7 relative to viability in the absence of IL7 (normalized to 1, supplemental table 2). Each individual sample is illustrated by matching colors and symbol. (***B***) IL7-enhanced viability (left) and drug-treated cell viability represented in AUC (right) in six 'non-IL7-dependent steroid resistant' PDX samples. 'Non-IL7-dependent steroid resistant' PDX samples were defined by a lack of significant (e.g. 1.5 fold) change in prednisolone AUC in the presence of IL7, but with a minimal AUC of 200 in either condition.*

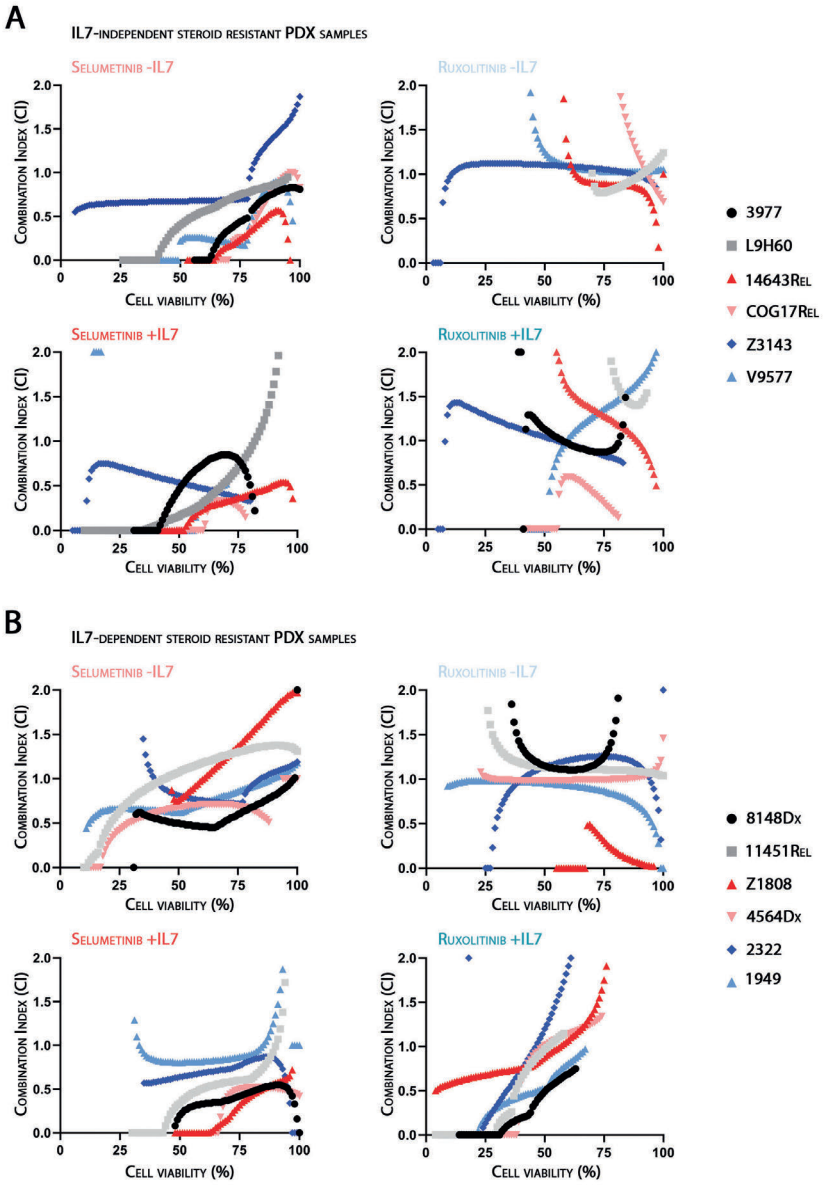

Supplemental Figure 7. *Combination index (CI) range of (***A***) six 'IL7-independent steroid resistant' PDX samples or (***B***) six 'IL7-dependent steroid resistant' PDX samples, treated with prednisolone and selumetinib (left) or prednisolone and ruxolitinib (right) in the absence (top) or presence (bottom) of IL7. Combination treatment was performed according to the previously described SynergyFinder method (supplemental materials and methods). CI values of the complete therapeutic window are illustrated, which was demarcated by the minimal cell viability when treated with prednisolone and selumetinib or ruxolitinib, and the maximal cell viability at the highest concentration of selumetinib or ruxolitinib.*

Supplemental Table 1. iBAQ values of qualitative unbiased mass spectrometry analysis of triplicate BIM-immunoprecipitations in SUPT-1 NRAS G12D overexpressing cells. *NODOX= -doxycycline -prednisolone condition. DOX = +doxycycline -prednisolone condition. PRED = -doxycycline +prednisolone condition. DOXPRED = +doxycycline +prednisolone condition. iBAQ_BIM_corrected = iBAQ values corrected for BIM iBAQ input value (iBAQ protein/iBAQ BIM); correcting for technical differences and potential proteasomal degradation.*

Online link to Table S1: https://tinyurl.com/Chap4-SupTable1-Jordy-vd-Zwet

Supplemental Table 2. Proliferation of IL7 treated T-ALL patient PDX cells. *Light green samples represent IL7-independent steroid resistant PDX cells, dark green samples represent IL7-dependent steroid resistant PDX cells.*

Online link to Table S2: https://tinyurl.com/Chap4-SuppTable2-Jordy-vd-Zwet

Supplemental Table 3. IC50 values of prednisolone, selumetinib and ruxolitinib used for the SynergyScreen of T-ALL PDX cells. *Light green samples represent IL7-independent steroid resistant PDX cells, dark green samples represent IL7-dependent steroid resistant PDX cells. When an IC50 could not be determined due to significant insensitivity to selumetinib or ruxolitinib, a fixed concentration of 0.32 or 1µM was used in the SynergScreen (indicated by ** or *** for selumetinib or ruxolitinib respectively).*

Online link to Table S3: https://tinyurl.com/Chap4-SuppTable3-Jordy-vd-Zwet

SUPPLEMENTAL MATERIALS AND METHODS

Gateway cloning of lentiviral expression vectors and virus production

Gateway multi-site recombination (Invitrogen) was used to simultaneously clone multiple DNA fragments into the lentiviral pLEGO-iC2 destination vector (Addgene). Inserted DNA fragments consisted of a 3rd generation doxycycline-inducible promoter (Clontech), human cDNA sequence (no stop-codon), protein-tag (DDK, T2A *(Thosea asigna* virus 2A peptide)-mTagBFP, or none), WPRE and a constitutive pSFFV promoter for a TETon-T2A-puromycin resistance cassette. HEK293T cells were transfected with the pLEGO derivative lentiviral expression vector DNA and pMD2.G (VSV-G), pMDLg/pRRE, and pRSV-REV support vectors (Addgene) using X-tremeGene HP DNA Transfection reagent (Roche). Transfection was performed in DMEM medium supplemented with 10% (v/v) heat-inactivated fetal calf serum (FCS), 1x Glutamax, 1% (v/v) penicillin/streptomycin, and 0.25 µg/ml Fungizone. Following transfection, lentivirus particles were produced and collected in serum-free Opti-MEM1 (Thermo Fisher Scientific) for 48 hours, filtered through a 0.45 µM filter (Sartorius) and concentrated by centrifugation using VIVASPIN 20 concentration columns (Sartorius).

Generation of cell lines

Lentiviral transduction was applied to obtain SUPT-1 cell lines containing various different expression vectors. After transduction, cells were cultured in RPMI-1640 medium (Gibco) supplemented with 1x Glutamax, 10% heat-inactivated fetal bovine serum (Gibco), 2% pencillin/streptomycin (Gibco) and 0,4% Fungizone (Gibco). Transduction efficiency was further enriched by selection in medium containing 1-2 µg/mL puromycin. Transduction efficiency was determined by flow cytometry by staining for intracellular DDK, mTagBFP signals or CD127 expression. Expression of the cloned human cDNA insert and/or DDK was induced by doxycycline (0.5 µg/ml) for 16 to 24 hours.

Cytotoxicity assays

SUPT-1 cells were plated at a concentration of $0{,}2x10^6$ cells/mL in RPMI-1640 medium supplemented with puromycin, as described above, in the presence or absence of prednisolone. Viability after four days was measured by methylthiazolyldiphenyl-tetrazolium bromide (MTT, Sigma Aldrich). Cytotoxicity screen of PDX samples was performed as previously described (1) in the presence or absence of 25 ng/ml IL7 (R&D Systems) in RPMI-1640 medium (Gibco) supplemented with 1x Glutamax, 20% heat-inactivated fetal bovine serum (Gibco), 2% pencillin/streptomycin (Gibco) and 0,4% Fungizone (Gibco). PDX cells were plated at a concentration of $1x10^6$ cells/ml, and viability after four days was measured by ATPlite 1Step (Perkin Elmer, Groningen, The Netherlands).

Cytotoxicity combination screen (SynergyFinderTM)

PDX cells were plated at a concentration of $1x10^6$ cells/ml, and viability after four days was measured by ATPlite 1Step (Perkin Elmer, Groningen, The Netherlands). The SynergyFinder™ screen was performed as previously described (1, 2). For each individual sample, the IC_{50} value was determined for prednisolone, selumetinib and ruxolitinib. Next, cells were treated in a 1:1 ratio with prednisolone and selumetinib or ruxolitinib, with individual drug concentrations ranging from 0.01 to 10 times its IC_{50} (*e.g.*, 0.01, 0.032, 0.10, 0.32, 1.0, 3.16 or 10 times IC_{50}). When an IC_{50} could not be determined due to significant insensitivity to selumetinib or ruxolitinib, a fixed concentration of 0.32 or 1µM was used respectively *versus* a 0.01 - 10 times IC_{50} range of prednisolone (**Supplemental table 3**). By non-linear regression analysis, the 7-point viability curve was converted to a slim-fitted curve (red and blue curves in the example below). The therapeutic window per treatment per sample was demarcated by the minimal cell viability in the combination treatment, and the maximal cell viability at the highest concentration of prednisolone or selumetinib/ruxolitinib (colored area, 'fraction affected'). For the fraction affected, the combination index was calculated per percent viability (**Supplementary Figure 6**). The average of all these combination index values was taken as an overall synergy score per individual sample (CI^{AV}, **Figure 5c**). Two examples are illustrated below. Left: single compound treatment (prednisolone and selumetinib or ruxolitinib) and the combination treatment (red or blue lines). Based on all three curves, the fraction affect was determined and used to calculate the combination index per percent viability (each dot represents a CI value).

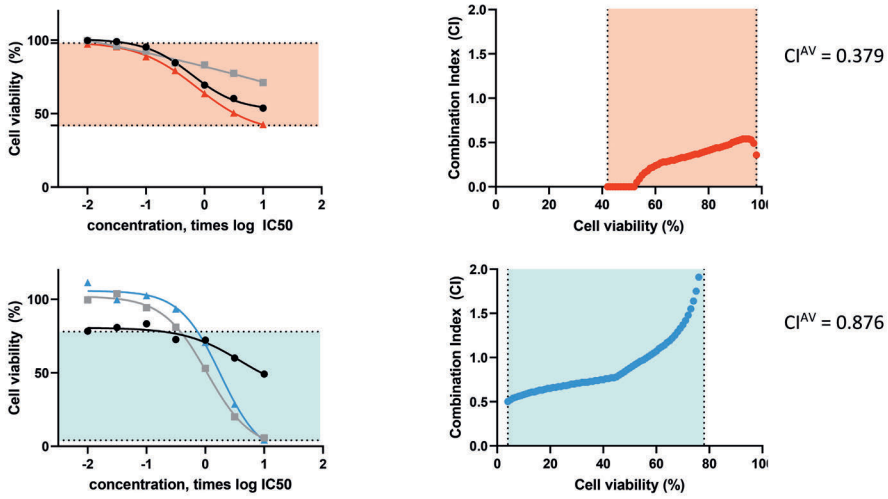

Immunoblot analysis

Cell pellets were lysed using KLB (kinase lysis buffer) lysis buffer and 25-50 µg of protein was loaded on BioRad Mini-Protean® TGX™ any-kd precast gels unless specified

elsewhere. KLB lysis buffer consists of 25mM Tris (pH 7.4), 150mM NaCl, 5mM EDTA, 1% Triton X-100, 10% mM glycerol, 10mM sodium-pyrophosphate, 1mM sodium-orthovanadate and 10mM glycerolphosphate, and was supplemented with 2mM DTT, 1mM PMSF, 1% aprotinin, 10mM sodium-fluoride, and sodium-pervanadate (86% orthovanadate (50mM) and 14% H_2O_2 (30%)). In cells treated with lambda phosphatase (NEB P0753S, Bioke), phosphatase inhibitors (EDTA, sodium-pyrophosphate, sodium-orthovanadate, glycerolphosphate, sodium-fluoride and sodium-pervanadate) within the KLB lysis buffer are diluted. Explicitly, cell lysates were treated with lambda phosphatase *ex-vivo* in the lysis buffer. Protein was then transferred on the 0.2 µm nitrocellulose membrane using the Trans-Blot® Turbo™ Transfer System (BioRad). Primary antibodies used for Western blot protein detection are: DKDDDDK Tag antibody (#2368), phospho-ERK (#4370), phospho-MEK (#9121), BCLXL (#2764), MCL1 (#4572 and #sc12756), BAK (#12105); Abcam BIM (#ab32158), β-Actin (#ab6276); R&D Systems IL7R alpha/CD127 (#MAB306), all from Cell Signaling, BCL2 (#sc-130308; Santa Cruz Biotechnology) and RAS (#05-516; Merck Millipore). Following primary antibody incubation, blots were thoroughly washed and stained with IRDye fluorescent secondary antibodies (LI-COR). Fluorescent signals were measured with the Odyssey-CLx Imaging System (LI-COR).

RNA isolation, cDNA synthesis and quantitative real-time reverse-transcription PCR (RTQ-PCR)

RNA was isolated with TRIzol reagent (Thermo Fisher Scientific) according to the guidelines of the manufacturer with minor modifications as described before (3). RNA was denaturated for 5' at 70 °C, and reverse transcribed into cDNA using a mix of random hexamers (2.5µM, Life Technologies) and OligodT primers (20nM, Life Technologies). The RT-reaction was performed in a mixture containing 0.2mM dNTPs (Promega), 200U Moloney murine leukemia virus reverse transcriptase (Promega) and 25U RNAsin (Promega). Conditions for the RT-reaction were 37°C for 45 minutes and 42 °C for 15 minutes followed by an enzyme inactivation step at 94 °C for 5 minutes. RTQ-PCR reactions were performed by using the DyNAmo HS SYBR Green qPCR Kit (Thermo Fisher Scientific) under 1X conditions, supplemented with 4mM $MgCl_2$ (Thermo Fisher Scientific), 3,75pmol forward and reverse primers, 10ng cDNA and dH_2O in a total volume of 12.5 µL using the CFX384 Touch-Time PCR Detection System (Biorad). Expression level of *BIM* was quantified relative to the expression level of the endogenous housekeeping gene glyceraldehyde-3-phosphatedehydrogenase (GAPDH). Conditions for the RTQ-PCR-reaction were 95 °C for 10 minutes, followed by 40 cycles of 95 °C for 10 seconds and 60 °C for 1 minute, followed by a dissociation step (60-94) for melting temperature analysis. Expression levels were calculated as percentage of GAPDH expression using the equation: $relative\ expression\ = 2^{\Delta Ct} * 100\%; where\ \Delta Ct = Ct_{GAPDH} - Ct_{gene}.$ Primers used are: *GAPDH* Fw primer 5'-GTCGGAGTCAACGGATT-3', *GAPDH* Rev primer 5'-AAGCTTCCCGTTCTCAG-3'; *BIM* Fw primer 5'-GCGCCAGAGATATGGAT-3', *BIM* Rev primer 5'-CGCAAAGAACCTGTCAAT-3'.

Mass spectometry

Doxycycline-induced and non-induced SUPT-1 $NRAS^{G12D}$ cell lysates were cultured in the presence or absence of 250 µg/ml prednisolone for 24 hours. BIM-immunoprecipitation was performed as described in the method section of the manuscript. For mass spectrometry, these IP products of SUPT-1 $NRAS^{G12D}$ were cleaned using S-Trap (Protifi) prior to LC-MS/MS analysis. Elution of the beads was performed under reducing conditions. Samples were heated for 10 minutes at 95 °C and allowed to cool down before alkylation using 100µL IAA (10 mg/mL) in 10% SDS for 30 minutes in the dark. The samples were spun down for 8 minutes at 13,000 x g before addition of 10 µL 12% phosphoric acid. After addition of 1.5 mL S-Trap binding buffer (90% MeOH, 100mM TEAB, pH 7.1), the protein mixture was added in steps of 190 µL to the S-Trap Mini Spin Column(Protifi) and spun down at 4,000 x g. Proteins were bound to the protein filter and the flow-through was discarded. The trapped proteins were washed three times using 150 µL S-Trap binding buffer. Proteins were digested using 0.75µg trypsin (Promega) in digestion buffer (50mM AMBIC) for 1 hour at 47 °C. Peptides were eluted in multiple steps by centrifugation at 4,000 x g using the following buffers sequentially: 40 µL 50mM AMBIC, 40 µL 0.2% FA and 35 µL 50%ACN/0.2% FA. Eluates were combined, dried down and stored at -20 °C until LC-MS/MS analysis.

LC-MS/MS analysis

Dried peptides were reconstituted in 50 µL 2% FA of which 6 µL was analyzed by LC-MS/MS using an Agilent 1290 system coupled to a Q-exactive HF-X (Thermo Scientific). Peptides were loaded onto a trap column (100µm inner diameter and 2 cm length, packed with ReproSil-Pur 120 C18-AQ 3 µm resin material) with a flowrate of 5 µL/min in loading solvent A (0.1% FA in HPLC grade water). Peptides were separated on an analytical column (75µm inner diameter and 50 cm length, packed with Poroshell 120 EC-C18 2.7 µm) by increasing the concentration of buffer B (80% ACN/0.1%FA) from 8% to 32% during a 2 hour gradient. Peptides were ionized using electrospray operating at 1.9kV. The Q-Exactive HF-X was operating in data-dependent acquisition mode, using the following settings for full scan mode: a scan range of 375-1600 m/z, AGC target of 3e6 and a resolution of 60,000 and maximum injection time 50 msec. The MS2 scan settings were as follows: resolution of 30,000, AGC target of 1e5, loop count of 12 and maximum injection time 120msec. Peptide fragmentation was achieved using normalized collision energy of 27. The dynamic exclusion was set to 16 seconds and the isolation window was 1.4m/z.

MS data processing and analysis

Raw MS data files were searched using MaxQuant software (v1.6.7.0). MS/MS spectra were searched using Andromeda against a reviewed human database (Uniprot, March 2017). Trypsin was used as digestive enzyme and up to two missed cleavages were allowed. Oxidation (M) and acetylation (N-terminus) were set as variable modifications, carbamidomethyl (C) was set as fixed modification. Filtering was performed at 1% false

discovery rate (FDR) at both the PSM and protein level. Mass tolerance was set to 20ppm for MS/MS. iBAQ quantification was performed.

Data was analyzed using Perseus (v.1.6.10.0). The iBAQ values of the proteinGroups.txt file were loaded into Perseus. Potential contaminants, peptides only identified by site and reversed sequences were filtered out. iBAQ values for corresponding proteins were corrected for BIM protein abundancy of each individual sample (e.g. protein iBAQ/BIM iBAQ). Proteins that bound to IgG or antibody control IP-experiments were excluded from further analysis.

***In vitro* phosphorylation assay**

The experimental set up was adapted from (4). Briefly, human active (MEK-activated) recombinant ERK1 (R&D systems, Cat nr 1879-KS-01; Lot nr 1534614) and human recombinant BIM-L (R&D systems, Cat nr: 1325-BL-050; Lot nr HUM0718101) were diluted in kinase reaction buffer (20mM HEPES pH 7.4, 10mM DTT, 100µM EGTA, 10mM $MgCl_2$) in a 1:3 kinase : substrate weight ratio (150ng ERK1 and 450ng BIM, respectively) in the presence or absence of 100µM ATP. Samples were incubated in a thermomixer at 37° for 1 hour with gentle shaking. After 1 hour the reaction was stopped by adding 4x Laemmli buffer containing 200mM DTT. Samples were denatured for 5 minutes at 95° and one third of the total reaction (corresponding to 50ng ERK1 and 150ng BIM) was loaded on gel for SDS-PAGE and western blotting. Antibodies used for staining were Abcam BIM (#ab32158) and ERK (CST, L34F12).

REFERENCES

1. Li Y, Buijs-Gladdines JG, Cante-Barrett K, Stubbs AP, Vroegindeweij EM, Smits WK, et al. IL-7 Receptor Mutations and Steroid Resistance in Pediatric T cell Acute Lymphoblastic Leukemia: A Genome Sequencing Study. PLoS Med. 2016;13(12):e1002200.
2. Uitdehaag JC, de Roos JA, van Doornmalen AM, Prinsen MB, Spijkers-Hagelstein JA, de Vetter JR, et al. Selective Targeting of CTNBB1-, KRAS- or MYC-Driven Cell Growth by Combinations of Existing Drugs. PLoS One. 2015;10(5):e0125021.
3. Van Vlierberghe P, van Grotel M, Beverloo HB, Lee C, Helgason T, Buijs-Gladdines J, et al. The cryptic chromosomal deletion del(11)(p12p13) as a new activation mechanism of LMO2 in pediatric T-cell acute lymphoblastic leukemia. Blood. 2006;108(10):3520-9.
4. Fiesel FC, Hudec R, Springer W. Non-radioactive in vitro PINK1 Kinase Assays Using Ubiquitin or Parkin as Substrate. Bio Protoc. 2016;6(19).

5

Targeting steroid resistance by combined MEK-inhibitor and BH3-mimetic treatment in pediatric T-cell acute lymphoblastic leukemia

Jordy C.G. van der Zwet[1], Vera Poort[1], Valentina Cordo'[1], Jessica G.C.A.M. Buijs-Gladdines[1], Kim Bodaar[2], Willem K. Smits[1], Alejandro Gutierrez[2] and Jules P.P. Meijerink[1]

[1]Princess Máxima Center for Pediatric Oncology, Utrecht, the Netherlands

[2]Boston Children's Hospital, Harvard Medical School, Boston, MA, USA

ABSTRACT

Resistance to steroid treatment is frequently observed in pediatric T-cell acute lymphoblastic (T-ALL) and predicts for inferior outcome. Physiological or mutational activation of the IL7R signaling cascade can facilitate steroid resistance. Activation of the IL7R leads to activation of the downstream MAPK-ERK, PI3K-AKT and STAT5 signaling pathways. Steroid-induced expression of pro-apoptotic *BIM* is essential to induce apoptosis in lymphoblasts treated with synthetic glucocorticoids like prednisolone. BIM binds and neutralizes anti-apoptotic Bcl2-protein family members, of which some can be upregulated downstream of the STAT5B or PI3K-AKT pathways. Activation of the MAPK pathway provokes steroid resistance by phosphorylation, which inactivates pro-apoptotic BIM. MEK-inhibitors were shown effective to restore a steroid-sensitive phenotype. Here, we studied whether BH3-mimetic compounds directed towards BCL2 (ABT-199) or MCL1 (S63845 or AZD5991) would synergistically enhance steroid sensitivity when combined with the MEK-inhibitor selumetinib. Whereas selumetinib synergizes with prednisolone treatment in both IL7-independent and IL7-dependent steroid resistant T-ALL patient cells, the ABT-199 BH3-mimetic only synergized with steroid treatment in IL7-dependent steroid resistant T-ALL cells. The triple combination prednisolone/selumetinib/ABT-199 but not the combination steroid/selumetinib/AZD5991 was strongly synergistic in both IL7-independent and IL7-dependent steroid resistant T-ALL PDX cells. However, addition of ABT-199 to combined prednisolone/selumetinib treatment did not further enhance the mitochondrial priming of MAPK-ERK activated SUPT-1 T-ALL cells compared to prednisolone/selumetinib treatment only as determined by BH3-profiling analysis. Our work concludes that the dynamic balance between pro- (BIM) and anti-apoptotic (BCL2, BCL-XL and MCL1) proteins is an important determinant for steroid responsiveness, for which the preservation of the pro-apoptotic BIM response by MEK-inhibition seems generally superior to enhance steroid responsiveness than inhibition of anti-apoptotic molecules.

INTRODUCTION

Pediatric T-cell acute lymphoblastic leukemia (T-ALL) is a high-risk hematological malignancy characterized by the malignant expansion of immature T-cells. Due to improved risk-stratification and intensive chemotherapeutic treatment regimens, including high dose synthetic steroid treatment, 5-year overall survival rates up to 81% are currently achieved for T-ALL (1, 2). However, resistance to steroid treatment is related to inferior outcome, indicating that novel treatment strategies are required for patients with steroid resistant leukemia (3, 4). Steroid treatment activates the glucocorticoid receptor (NR3C1) and triggers its cytoplasmic to nuclear translocation, where it serves as a transcription factor at glucocorticoid responding elements (GREs) (5). Of its transcriptional target genes, upregulation of *BIM* seems most pivotal to promote steroid-induced cell death. The BH3-only pro-apoptotic BIM protein directs the apoptotic balance by interaction with anti-apoptotic Bcl2-protein family members BCL2, BCLXL and MCL1 (6-8). Steroid-induced upregulation of BIM alters this apoptotic balance, and promotes the initiation of mitochondrial apoptosis via the BAK and BAX executioner proteins (9).

Events that inactivate BIM – including phosphorylation of the steroid receptor (NR3C1) at Ser^{134}, the epigenetic silencing of *BIM* or inactivating phosphorylation of BIM – are identified as mechanisms that contribute to steroid resistance in T-ALL patient cells and/or patient-derived xenograft (PDX) samples (10-14). We recently demonstrated that phosphorylation of BIM-EL and BIM-L isoforms by active MAPK-ERK signaling specifically impairs its binding and neutralization of anti-apoptotic Bcl2-family proteins, which therefore drives steroid resistance (14). Since the MAPK-ERK pathway is activated by interleukin-7 (IL7) or IL7-receptor (IL7R) signaling pathway mutations (i.e. in ~25% and ~35% of T-ALL patients respectively), this pathway reflects an important contributor to steroid resistance in T-ALL (14). We demonstrated that MEK-inhibitors restore a steroid sensitive phenotype by preventing ERK-dependent phosphorylation of steroid-induced BIM (14, 15). Due to the importance of BIM to neutralize the anti-apoptotic molecules BCL2, BCL-XL and MCL1 in maintaining a steroid sensitive phenotype, it is tempting to speculate that therapeutic inhibition of these anti-apoptotic Bcl-2 protein family members using BH3-mimetics could further improve the steroid responsiveness of MEK-inhibitor treated T-ALL cells.

Treatment with BH3-mimetics, that bind and neutralize anti-apoptotic BCL2 protein family members, have emerged as a promising strategy to treat multiple cancer types (16). Their effectiveness in hematological malignancies was first highlighted in chronic lymphocytic leukemia (CLL), a disease characterized by high *BCL2* expression (17). By means of BH3-profiling, a dependency on BCL2 is also identified in early thymus progenitor-ALL (ETP-ALL), a T-ALL entity that is characterized by high BCL2 protein expression (18-20). Both protein expression and mitochondrial-dependency gradually

change towards BCL-XL at more advanced T-cell developmental stages and T-ALL subtypes (19). This change in BCL2 to BCL-XL dependency from ETP-ALL to more mature T-cell developmental stages correlates with the sensitivity to BCL2-inhibitor venetoclax (ABT-199) or the BCL2/BCL-XL-inhibitor navitoclax (ABT-293) treatment respectively (18, 19). Recent clinical reports showed promising results for venetoclax treatment with or without navitoclax in pediatric and adult T-ALL (21, 22). Currently, two pediatric T-ALL phase 1 trials are active for venetoclax (NCT03236857) or venetoclax combined with navitoclax (NCT03181126).

In contrast to BCL2 and BCL-XL, MCL1 protein levels in leukemic blasts are reported to be comparable to healthy peripheral blood cells (23). Moreover, *MCL1* mRNA expression levels are lowest in acute leukemia compared to other cancer types (Broad Institute Cancer Cell Line Encyclopedia). Nevertheless, T-ALL cell lines and a T-ALL zebrafish model responded well to MCL1-inhibition (24, 25). For *MLL*-rearranged infant ALL patients, it was demonstrated that high MCL1 levels predict for steroid resistance (26). In line with this, we previously demonstrated that MCL1 itself is upregulated by steroid treatment, possibly by acting as a direct target gene of NR3C1 (14). MCL1 inhibitors AZD5991 and AMG176 have already been proven as effective drugs in melanoma and AML models (24, 27) and MCL1-inhibition has been demonstrated to relieve venetoclax-resistance in various hematological malignancies (28-30). Venetoclax treatment results in increased MCL1 protein expression in T-ALL cell lines, possibly as a compensatory mechanism, which could explain the synergistic effect for combined MCL1 inhibitor S63845 and venetoclax treatment in T-ALL cell lines and a T-ALL zebrafish model (25). These studies stress the potential of MCL1 inhibition in T-ALL, which has been translated into a clinical trial for MCL1-inhibitor AZD5991 for relapsed/refractory hematologic malignancies (NCT03218683) (27).

Both physiological interleukin-7 (IL-7) induced signaling and activating IL7R pathway mutations in T-ALL blasts have been associated with steroid resistance and facilitate the inactivation of pro-apoptotic BIM, as well as the upregulation of anti-apoptotic molecules such as BCL2 and BCL-XL (14, 15, 31, 32). Additionally, high expression of *BCL2* was previously associated with a slow early treatment response (31). For this reason, we aimed to investigate whether combined MEK-inhibitor and BH3 mimetic treatment could synergistically enhance steroid responsiveness in IL7R signaling active and steroid-resistant T-ALL cells.

METHOD AND MATERIALS

Generation and culturing of cell lines

Cell lines were generated as previously described (14, 33). SUPT-1 cells were cultured in RPMI-1640 medium (Gibco) supplemented with 1x Glutamax, 10% heat-inactivated fetal bovine serum (Gibco), 2% penicillin/streptomycin (Gibco) and 0,4% Fungizone (Gibco).

Transduction efficiency of SUPT-1 was enriched by selection in medium containing 1-2 µg/mL puromycin. T-ALL PDX cells were cultured in RPMI-1640 medium (Gibco) supplemented with 1x Glutamax, 20% heat-inactivated fetal bovine serum (Gibco), 2% pencillin/streptomycin (Gibco) and 0,4% Fungizone (Gibco), in the absence or presence of 25 ng/ml IL7 (R&D Systems).

Cell toxicity screens for PDX cells

Cell toxicity screens for double inhibition were performed as previously described (14). For the triple inhibition, we treated cells with prednisolone, selumetinib and either ABT-199 or AZD5991 in a 1:1:1 ratio. For this, the IC_{50} of each compound for each individual PDX sample was determined. Next, a compound mixture with all three compounds in a 1:1:1 ratio with 1/3 of each drug IC_{50} was generated (i.e. 1/3xIC_{50} prednisolone + 1/3xIC_{50} selumetinib + 1/3xIC_{50} BH3-mimetic). Cells were treated with this mixture in a 7-point toxicity screen, with drug concentrations ranging from 0.01 to 10 times its $IC50_{50}$ (*e.g.*., 0.01, 0.032, 0.10, 0.32, 1.0, 3.16 or 10 times IC_{50}) in equal ratios. Cell viability was measured after four days by ATPlite 1 Step (Perkin Elmer, Groningen, The Netherlands).

Immunoblot analysis and BIM-immunoprecipitation

Immunoblot analysis and BIM-immunoprecipitation of SUPT-1 cells treated with prednisolone (62,5ug/ml), selumetinib (1uM), ABT-199 (1uM) and/or S63845 (100nM) was performed as previously described (14). Primary antibodies used for Western blot protein detection are: phospho-ERK (#4370), BCLXL (#2764), MCL1 (#4572 and #sc12756), Abcam BIM (#ab32158), β-Actin (#ab6276); BCL2 (#sc-130308; Santa Cruz Biotechnology) and RAS (#05-516; Merck Millipore). Primary antibody used for immunoprecipitation is Abcam BIM (#ab32158), primary antibody for Western Blot protein detection of immunoprecipitated-BIM is BIM (#2933; Cell Signaling). IRDye fluorescent secondary antibodies were used (LI-COR). Fluorescent signals were measured with the Odyssey-CLx Imaging System (LI-COR).

Annexin V staining

SUPT-1 cells were treated with prednisolone (62,5ug/ml), selumetinib (1uM), ABT-199 (1uM) and/or S63845 (100nM) for 16 hours. After treatment, cells were washed with PBS buffer, and resuspended in Annexin V binding buffer (Invitrogen, cat# V13246). Subsequently, AnnexinV antibody (Biolegend cat# 640920, dilution 1:20) was added and incubated at room temperature for 15 minutes. After incubation, AnnexinV-APC positivity was measured by flowcytometry (ZE5 cell analyzer, Bio Rad).

iBH3-profiling of cell lines

Intracellular BH3 profiling was performed by flow cytometry to assess the effects of the hBIM BH3 peptide (Acetyl-MRPEIWIAQELRRIGDEFNA-Amide, rapid depolarization when BAX/BAK are functional), or PUMA2A mutant control peptide (Acetyl -EQWAREIGAQARRMAADLNA- Amide, no depolarization) on cytochrome c release, a

surrogate measurement for mitochondrial outer membrane permeabilization (MOMP). Alamethicin was used as a positive internal control for maximal BAX/BAK independent MOMP. Doxycycline-induced and non-doxycycline induced SUPT-1 cells were treated for with prednisolone (62,5ug/ml), selumetinib (1uM), venetoclax (1uM) and/or S63845 (100nM) for 20 hours. After incubation, 1 million SUPT-1 cells per condition were harvested, washed once with PBS, and subsequently resuspended in 1ml room-temperature DTEB buffer (135 mM trehalose, 50 mM KCl, 20 mM EDTA, 20 mM EGTA, 5 mM succinate, 0.1% BSA, 10 mM HEPES-KOH. Final pH 7.5). Per condition 8 FACS tubes (3xhBIM, 4xPUMA2A, 1x20uM Alamethicine) were prepared with 100µl DTEB buffer containing 0.002% (w/v) digitonin and optimized concentrations of the peptides (to achieve cytochrome c release between 20-60% in the vehicle sample, SUPT-1 5µM). 100,000 cells were added to the FACS tubes and incubated for exactly 40 minutes at 20°C. Cells were fixed by the addition of 60µl 8% paraformaldehyde (in PBS) for 15 minutes. Subsequently, 40µl Cytochrome C staining (1:40 anti-cytochrome C antibody, AF647 (BD Biosciences, San Jose, CA #558709) in staining buffer (20% FBS, 10% BSA, 1% Saponin, 3 mM Sodium Azide in PBS) was added to all tubes except one PUMA2A FMO control (add buffer without antibody). Cells were incubated overnight at 4°C and acquired with the ZE5 cell analyzer (Bio Rad) and analyzed with FlowJo software (Version 10, Treestar, Ashland, OR, USA). The median fluorescence intensity (MFI) of the cytochrome c stain in single alive cells was used to calculate Cytochrome c release as described below and graphed normalized to the -doxycycline vehicle condition. Only experiments in which the Alamethicin internal positive control showed an expected 80% release in all conditions were used for analysis.

Cytochrome c release = 1 - (hBIM- avgFMO) / (avgPUMA2A – avgFMO) *.
*avgFMO = all conditions, avgPUMA2A = triplicates within treatment condition.

RESULTS

MEK inhibitors combined with BCL2- or MCL1- inhibitors reinforce the pro-apoptotic capacity of BIM in MAPK-ERK activated cells

High MEK-ERK activity by IL7-induced or aberrant IL7R signaling due to activating mutations in signaling molecules importantly contribute to steroid resistance in T-ALL patients. This results in the phosphorylation and therefore inactivation of pro-apoptotic BIM, an important and direct target gene of the steroid receptor NR3C1 (14). Phosphorylated BIM is unable to bind and to neutralize anti-apoptotic family members including BCL2, BCL-XL and MCL1. Treatment with MEK-inhibitors block phosphorylation of BIM, which secures neutralization of anti-apoptotic BCL2, BCLXL and MCL1 molecules and restores a steroid responsive phenotype of T-ALL cells (14). We therefore hypothesized that inclusion of BH3-mimetics in steroid/MEK-inhibitor

combination treatment will further neutralize anti-apoptotic molecules and improve steroid responsiveness.

To test this hypothesis, we used our doxycycline-inducible SUPT-1 $NRAS^{G12D}$ cell line model that strongly activates MEK-ERK signaling upon doxycycline exposure (+dox). Whereas non-induced SUPT-1 or P12-Ichikawa $NRAS^{G12D}$ cells remain steroid sensitive, $NRAS^{G12D}$ induced cells become highly resistant to steroid treatment (14, 15). We first treated these SUPT-1 cells with prednisolone in the presence or absence of the MEK-inhibitor selumetinib, the BCL2-specific BH3-mimetic ABT-199, the MCL1-specific BH3-mimetic S63845 or their combinations. In the absence (-dox) or presence (+dox) of $NRAS^{G12D}$ expression, total protein lysates were collected for all these conditions. $NRAS^{G12}$ expression highly activated MAPK-ERK signaling, which resulted in the strong phosphorylation of BIM-EL and BIM-L isoforms (**Figure 1A**, lanes 7, 11 and 12), and was effectively abolished by the MEK-inhibitor selumetinib (lane 8). Treatment with ABT-199 (BCL2) or S63845 (MCL1) led to increased MCL1 protein levels (lanes 3-6 and 9-12), possibly due to a compensatory mechanism upon BCL2 inhibition or stabilization of the MCL1 protein respectively.

To investigate the effects of these compounds and their combinations on the function of steroid-induced BIM in interacting and neutralizing anti-apoptotic molecules MCL1, BCL2 and BCL-XL, we performed immunoprecipitation experiments. For non-induced SUPT-1 $NRAS^{G12D}$ cells, steroid-induced BIM efficiently bound to these anti-apoptotic molecules (**Figure 1B**, lane 1), which was slightly increased upon MEK-inhibitor treatment (lane 2). ABT-199 (lanes 3 and 5) or S63845 (lanes 4 and 6) treatment readily impaired binding of BCL2 or MCL1 to BIM, respectively. For doxycycline-induced and steroid-exposed SUPT-1 $NRAS^{G12D}$ cells (lane 7), we observed an impaired binding of BIM to all 3 anti-apoptotic molecules. Selumetinib treatment effectively blocked phosphorylation of BIM and restored the binding of BIM to BCL2, BCL-XL and MCL1 (lane 8). Whereas the combined steroid treatment with the BCL2 mimetic ABT-199 or the MCL1 mimetic S63845 compounds resulted in slightly increased binding of BIM to MCL1 or BCL2 (lanes 9-10), respectively, addition of selumetinib treatment strongly enhanced the binding of BIM to MCL1 (lane 11) or BCL2 (lane 12). From this, we conclude that the addition of a BH3-mimetic to combined steroid-selumetinib treatment can further potentiate the binding and neutralization of (non BH3-mimetic targeted) anti-apoptotic molecules by pro-apoptotic BIM.

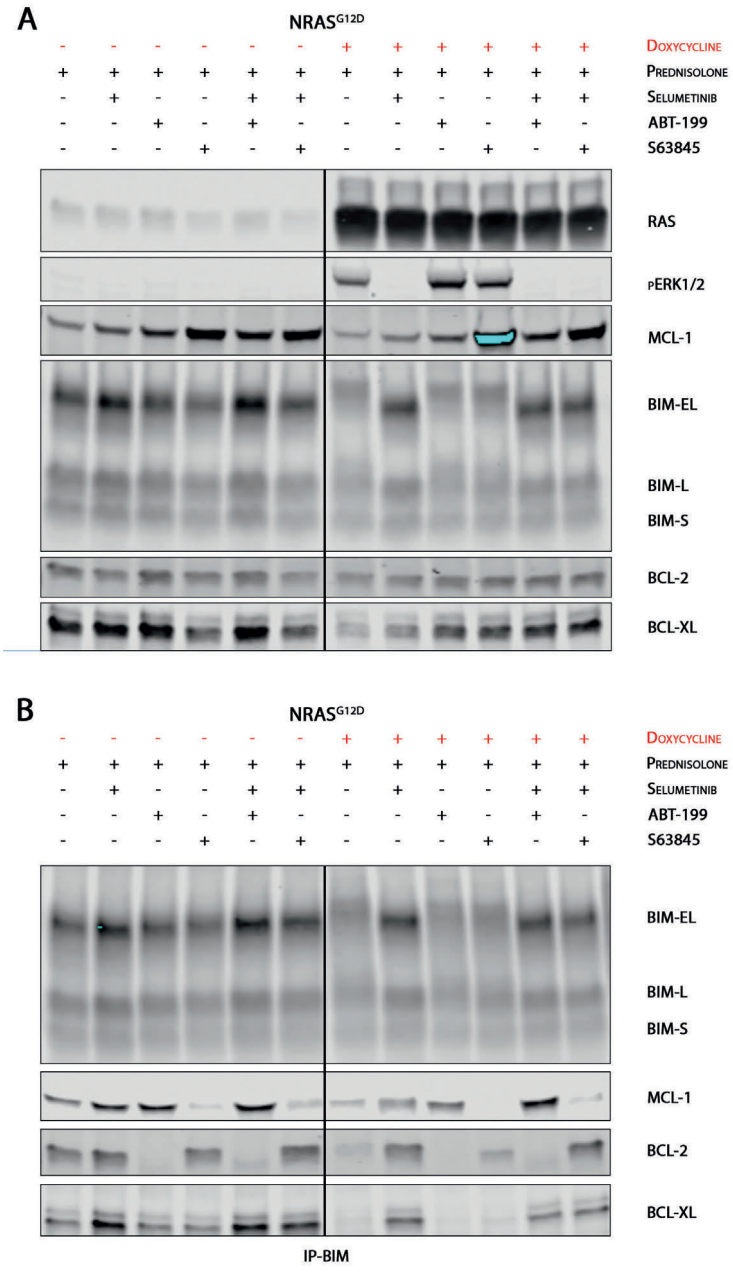

Figure 1. *(***A***). Immunoblot analysis of NRAS^{G12D} overexpressing SUPT-1 cells. Lanes 1-6 represent protein lysates of cells that do not express the lentiviral vector, and lanes 7-12 represent lysates of doxycycline-induced NRAS^{G12D} cells. Cells were treated with prednisolone (62,5µg/ml), selumetinib (1µM), ABT-199 (1µM) and/or S63845 (100nM) for 16 hours. (***B***) BIM-immunoprecipitation of corresponding cell lysates.*

MEK-inhibitor and BH3-mimetics treatment synergize in steroid-induced cell death

To test if combined selumetinib and BH3-mimetic treatment would increase steroid-induced cell death, we measured the induction of steroid-induced apoptosis by measuring the percentage of AnnexinV^{+} cells. For this, we used doxycycline-inducible SUPT-1 NRAS^{WT} cells, that activate MEK-ERK signaling and phosphorylate BIM upon exposure to doxycycline (not shown). Non-induced SUPT-1 NRAS^{G12D} cells were sensitive towards steroid treatment, and over 76 percent of cells died following a 72 hours treatment with 62,5µg/ml of prednisolone (**Figure 2**). Single selumetinib, ABT-199 or S63845 treatment or the combined selumetinib/BH3-mimetic treatment did not increase cell death. As demonstrated before (14), induction of NRAS^{WT} (+dox) significantly reduced the sensitivity towards prednisolone-induced cell death as compared to the non-induced (-dox) control condition (white bars, p=0.0002). This steroid resistance could be significantly prevented by selumetinib treatment (red bar, p=0.0005). Combined ABT-199 or S63845 treatment with prednisolone also enhanced steroid sensitivity (dark grey bars). Moreover, 'triple therapy' (prednisolone, selumetinib and ABT-199 or S63845) enhanced steroid-induced apoptosis compared to prednisolone/selumetinib treated cells. Therefore, this screen demonstrates that both MEK-inhibitors and BH3-mimetics augment steroid-induced cell death in MAPK-ERK activated T-ALL cells, and that triple treatment with fixed drug concentrations induces more cell death than prednisolone/selumetinib or prednisolone/BH3-mimetic duo treatment.

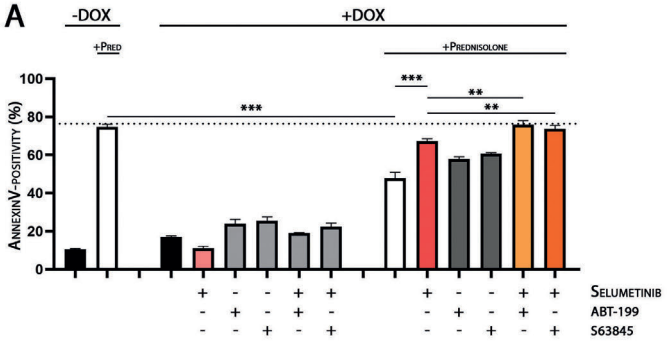

Figure 2. *Annexin V-staining of NRAS^{WT} overexpressing SUPT-1 cells as measured by flowcytometry. Y-axis represent Annexin V positivity. Cells were treated with prednisolone (62,5µg/ml), selumetinib (1µM), ABT-199 (1µM) and/or S63845 (100nM) for 16 hours. Statistical differences were calculated with an unpaired t-test (*p<0.05, **p<0.01, ***p<0.001, ****p<0.0001).*

MEK-inhibition restores the apoptotic priming of BIM-phosphorylated T-ALL cells

To study if BH3-mimetics combined with steroid/MEK-inhibitor treatment enhances a pro-apoptotic mitochondrial state, we performed BH3-profiling for SUPT-1 $NRAS^{WT}$ cells under all treatment conditions as mentioned above. This BH3-profiling assay quantifies the primed apoptotic state of mitochondria in cells by measuring the cytochrome-c release as a functional read-out for BAK/BAX-executed cell death (34). High mitochondrial priming indicates that cells are closer towards mitochondrial outer membrane permeabilization (MOMP), and thus BAX/BAK-executed cell death. Doxycycline-induction of $NRAS^{WT}$, which drives a MAPK-ERK dependent phosphorylation of BIM, lowered the baseline apoptotic priming of SUPT-1 cells as measured by the decreased cytochrome-c release (black bars, **Figure 3A-B**). In the presence of steroids, the apoptotic priming of $NRAS^{WT}$-induced (+dox) cells was enhanced, though lower compared to non-induced control cells, representing steroid resistance (white bars). Neither ABT-199 (**Figure 3A**) nor S63845 (**Figure 3B**) alone influenced the mitochondrial priming of non-induced or $NRAS^{WT}$-induced SUPT-1 cells (light-green and light-yellow bars; **Figure 3A** and **Figure 3B,** respectively), possibly through the upregulation of other anti-apoptotic proteins as compensatory mechanism as previously observed (**Figure 1A**). Moreover, both BH3-mimetics combined with steroid treatment did not further raise mitochondrial priming in non-induced nor in $NRAS^{WT}$-induced cells (dark green and dark yellow bars, **Figures 3A and B**). In contrast, single selumetinib treatment enhanced the primed apoptotic state of $NRAS^{WT}$ expressing cells, which reflects its ability to restore non-phosphorylated BIM levels (light red versus black bars, **Figures 3C-D**). Furthermore, selumetinib treatment enhanced the apoptotic priming of steroid-treated cells (dark red versus white bars, **Figures 3C-D**), which is in line with the previously observed synergy between selumetinib and prednisolone (14). Addition of ABT-199 or S63845 to the selumetinib/prednisolone combination treatment did not further raise the mitochondrial priming of these cells (**Figures 3C and D**). Based on these results, we conclude that the MEK-inhibitor selumetinib – but not BCL2 or MCL1 BH3-mimetics nor their combinations – enhances the mitochondrial apoptotic priming of MAPK-ERK-activated T-ALL cells during steroid treatment.

BH3-mimetics do not antagonize the synergy between MEK-inhibitors and steroid treatment

Next, we measured the *in-vitro* therapeutic response of BH3-mimetics and the MEK-inhibitor selumetinib in a cohort of 46 T-ALL PDX samples. Since S63845 is currently not clinically approved, we tested the sensitivity of the clinically relevant MCL1-inhibitor AZD5991 instead (27). The cytotoxic effects of the compounds were defined by their 'Area Under the Curve' (AUC), and a maximum AUC of 400 indicated complete drug resistance. Most PDX samples already demonstrated responsiveness towards single selumetinib or single anti-BCL2- or anti-MCL1 BH3 mimetic treatment (**Figure 4A, Supplemental Figure 1**).

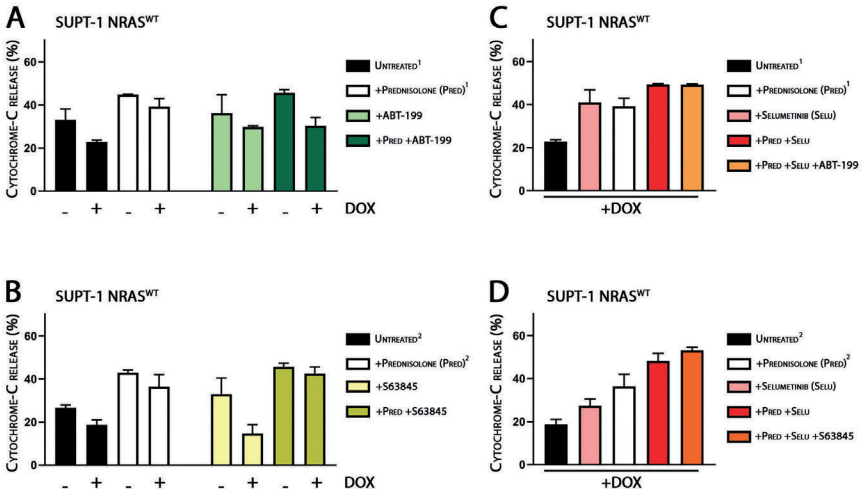

Figure 3. *BH3-profiling of NRAS^{WT} overexpressing SUPT-1 cells. Doxycycline-induced and non-doxycycline induced SUPT-1 cells were treated for with prednisolone (62,5ug/ml), selumetinib (1uM), ABT-199 (1uM) and/or S63845 (100nM) for 20 hours. (***A***) BH3-profiling of prednisolone and ABT-199 treated SUPT-1 cells (doxycycline-induced and non-induced). (***B***) BH3-profiling of prednisolone and S63845 treated SUPT-1 cells (doxycycline-induced and non-induced). (***C***) BH3-profiling of prednisolone, selumetinib and ABT-199 treated doxycycline-induced SUPT-1 cells. (***D***) BH3-profiling of prednisolone, selumetinib and S3845 treated doxycycline-induced SUPT-1 cells. SD bars represent technical triplicates, results are representative for biological triplicate experiments.*

From this cohort, we selected 6 PDX models that were resistant to steroid treatment in the absence of IL7 ('IL7-independent steroid resistance'). In addition, we selected 6 PDX models that became resistant to prednisolone only in the presence of IL-7 ('IL7-dependent steroid resistance') (**Supplemental Figure 1**). The latter also demonstrated decreased sensitivity towards the BCL2 directed BH3-mimetic ABT-199 but not to selumetinib or AZD5991 in the presence of IL-7 (**Figure 4B, Supplemental Figure 1**). For the IL7-independent steroid resistant T-ALL PDX samples, we previously demonstrated that combined selumetinib and steroid treatment was highly synergistic with 5 out of 6 samples having a combination index (CI) below 0.5 (14). In contrast, ABT-199 or AZD5991 did not synergize with steroid treatment in these PDX models (**Figure 4C**). For IL7-dependent steroid resistant PDX cells, we observed a clear synergy for selumetinib or ABT-199 in combination with prednisolone treatment, but only a mild synergy for AZD5991 combined with prednisolone (**Figure 4D**). The synergy between ABT-199 and prednisolone may be explained by IL7-induced STAT5 activation in these samples (**Supplemental Figure 2**).

Last, we studied synergy in 'triple treated' cells (i.e. prednisolone, selumetinib and ABT-199 or AZD5991 treatment) (**Figure 4C-D**; right part, and **Supplemental Figure 3**).

For prednisolone/selumetinib/ABT-199 treatment, we observed clear synergy in all PDX samples tested. Since triple treated cells were treated in a 1:1:1 drug ratio (i.e. 1/3 of the compounds IC_{50}, or 0.01 to 10 times its IC_{50} in equal ratios, **Supplemental Figure 3**), this indicated that the observed synergy was achieved at lower drug concentrations. The level of synergy was comparable to the synergy achieved by selumetinib/prednisolone duo treatment. Thus, ABT-199 does not impair the synergy between selumetinib and prednisolone and can therefore be safely combined with selumetinib/prednisolone treatment. For AZD5991 triple treatment, synergy was observed only in IL7-dependent steroid resistant samples. These observations likely extend to combination treatment with other MEK-inhibitors, since the cytotoxic effect of the MEK-inhibitor trametinib seems to be stronger than selumetinib mono-treatment (Wilcoxon test $p<0.0001$ for both IC50 and AUC; **Supplemental Figure 4**).

DICUSSION

Despite major improvements in the outcome of pediatric leukemia over the last decades, the prognosis of pediatric T-ALL is still inferior over the outcome of BCP-ALL patients (2). Various new treatment strategies have emerged for T-ALL (35), with certain compounds specifically focusing on improving or restoring steroid responsiveness of otherwise steroid-resistant leukemias. As the IL7R signaling cascade and its downstream pathways can influence the steroid response, deciphering underlying resistance mechanisms may point to compounds that can improve steroid responsiveness. In this respect, we recently identified that the downstream MAPK-ERK pathway – that is activated by physiological IL7 signaling or by activating mutations in the IL7R signaling pathway – is an important contributor to steroid resistance in T-ALL. MAPK-ERK activation results in the phosphorylation and inactivation of the steroid-induced pro-apoptotic molecule BIM. Steroid-induced expression of BIM is essential for lymphoid cells to undergo apoptosis following steroid treatment. MEK-inhibitors were shown to effectively re-sensitize MAPK-ERK activated and steroid resistant T-ALL cells towards steroid treatment (14, 15).

In the current study, we measured the mitochondrial apoptotic primed state of cells, determined by the balance between pro- and anti-apoptotic Bcl2-family proteins. Whereas steroid treatment increases mitochondrial priming, simultaneous MAPK-ERK activation decreases this priming due to the phosphorylation and inactivation of pro-apoptotic BIM, an important steroid receptor (NR3C1) transcriptional target gene. By means of BH3-profilling, the MEK-inhibitor selumetinib effectively restores the apoptotic priming state of MAPK-ERK activated T-ALL cells and thereby restores a steroid-sensitive phenotype. In contrast, BH3-mimetics directed to anti-apoptotic molecules BCL2 (ABT-199; venetoclax) or MCL1 (S63845) did not enhance the priming of MAPK-ERK activated cells, possibly due to compensatory mechanisms whereby other anti-apoptotic family members are activated upon inhibition of a specific Bcl-2 protein family member.

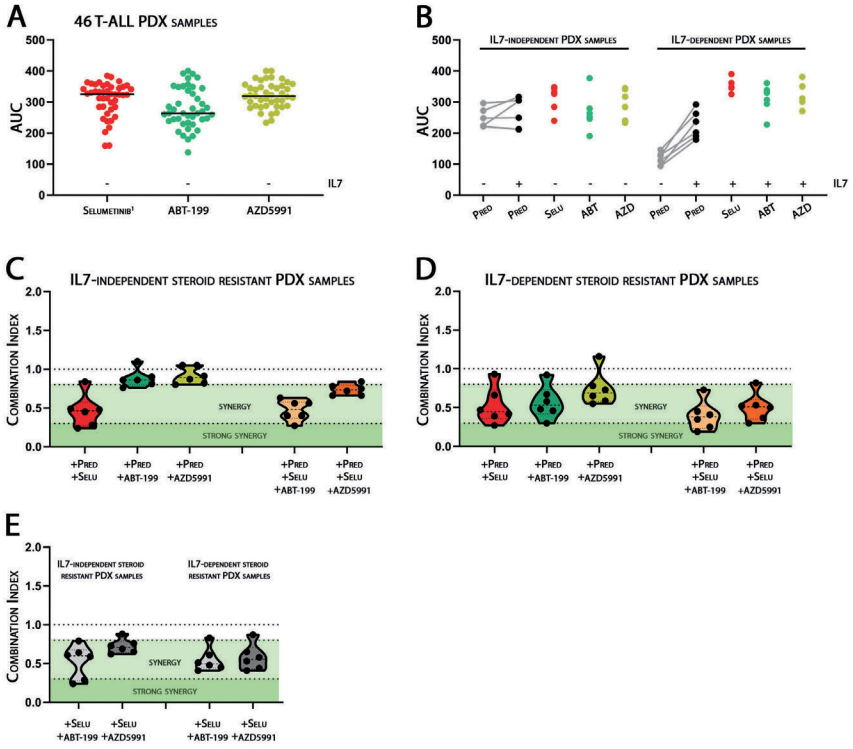

Figure 4. *(***A***) Cell toxicity screening of 46 T-ALL PDX samples for selumetinib (MEK-inhibitor; (14)), ABT-199 (BCL2-directed BH3-mimetic) and AZD5991 (MCL1-directed BH3-mimetic). Cell viability is illustrated by AUC, whereas an AUC of 400 represent the maximum AUC in a 4-log dynamic concentration range of each specific inhibitor. (***B***) AUC of T-ALL PDX samples treated with prednisolone, selumetinib, ABT-199 or AZD5991 in the presence or absence of IL7. 'IL7-dependent steroid resistant' PDX samples were defined by an increase in prednisolone AUC by >1.5 fold in the presence of IL7 with a minimal AUC of 175 in the presence of IL7 (14). (***C-D***) The combination index (CI) of T-ALL PDX samples, treated with prednisolone and selumetinib (red), prednisolone and ABT-199 (green), prednisolone and AZD5991 (yellow), or triple combination (prednisolone/selumetinib/BH3-mimetic; light or dark orange). PDX cells were treated with prednisolone and a BH3-mimetic in a 1:1 ratio (i.e. 1/2 of the compounds IC_{50}, or 0.01 to 10 times its IC_{50} in equal ratios). The synergy value of each sample illustrated is an average CI score, calculated over the complete therapeutic window of the combination treatment Synergy was defined by a CI between 0.3 and 0.8, whereas strong synergy was defined by a CI <0.3. (***E***) The combination index (CI) of T-ALL PDX samples treated with selumetinib and ABT-199 (light gray) or selumetinib and AZD5991 (dark gray). Synergy was defined by a CI between 0.3 and 0.8, whereas strong synergy was defined by a CI <0.3.*

Therefore, restoring the BIM response seems more efficient to restore steroid responsiveness in MAPK-activated T-ALL cells than inhibition of anti-apoptotic molecules. However, additional research is required to study if this also accounts for leukemias that highly activate anti-apoptotic molecules downstream of STAT5B signaling in T-ALL or leukemias with low MAPK-ERK pathway activity.

Upon treatment with the anti-MCL1 BH3-mimetic S63845, we observed a dramatic increase in MCL1 expression, which likely represented protein stabilization of inhibitor bound MCL1 that may prevent proteasomal degradation. Moreover, upregulation of MCL1 protein levels have also been described as an ABT-199 resistance mechanism (28, 29). Addition of selumetinib to prednisolone/S63845 treatment reduced MCL1 expression in our SUPT-1 cell line model, indicating that inhibition of ERK is involved in the stabilization of MCL1 (36, 37). Simultaneous or intermittent treatment of MEK-inhibitors with BH3-mimetics have already been demonstrated to be effective in various melanoma, solid- and hematological cancer cell lines and PDX models (38-42). In the majority of our T-ALL PDX samples, we also observed synergy between selumetinib and ABT-199 or S63845. More research is required to explore the biological rationale for combined MEK-inhibitor and BH3 mimetic treatment in T -ALL and other malignancies.

ABT-199 is reported to be mainly effective in malignancies and cell lines with high BCL2 expression or BCL2 dependency (18, 19). We observed that addition of ABT-199 to selumetinib treatment only mildly enhanced steroid-induced cell death in SUPT-1 cells, despite our observations that ABT-199 did not alter the mitochondrial apoptotic priming of these cells. In contrast, we observed clear synergy between prednisolone/ABT-199 and prednisolone/selumetinib/ABT-199 in IL7-dependent steroid resistant PDX samples. This indicates that addition of ABT-199 to prednisolone/selumetinib treatment could be beneficial for a subset of T-ALL patients. More research is required to identify which biological characteristics underly our observed synergy; for example, if these samples highly express BCL2 or depend on BCL2 expression for their survival. In line with this, the effects of ABT-199 on mitochondrial priming may be bigger in T-ALL cell lines with a more immature and BCL2 dependent phenotype than SUPT-1 cells (19).

Triple inhibition with prednisolone, selumetinib and a BH3-mimetic (and in particular ABT-199) was as synergistic as selumetinib/prednisolone duo inhibition in T-ALL PDX samples, although achieved at lower drug concentrations. This suggests that triple treatment allows for dose-reduction of all compounds used. More research is required to study if triple treatment indeed allows for dose-reduction in T-ALL patient treatment regimens without decreasing cytotoxic efficacy. Moreover, functional screenings like BH3-profiling or measurement of *BCL2* expression may be required as a biomarker to identify these T-ALL patients that may benefit from ABT-199 treatment in future treatment regimens.

Acknowledgements. This study was sponsored by grants of the foundation “Kinderen Kankervrij”; KiKa-219 (JvdZ), KiKa-92 and KiKa-295 (WKS), KiKa-335 (VP) and KWF-2016-10335 (VC).

Contribution of authors. JvdZ designed study, performed research and wrote manuscript. VP, VC, JBG, KB, WS, and AG performed research. JM designed and supervised the study and wrote manuscript.

Disclosures. None.

REFERENCES

1. Pieters R, de Groot-Kruseman H, Van der Velden V, Fiocco M, van den Berg H, de Bont E, et al. Successful Therapy Reduction and Intensification for Childhood Acute Lymphoblastic Leukemia Based on Minimal Residual Disease Monitoring: Study ALL10 From the Dutch Childhood Oncology Group. J Clin Oncol. 2016;34(22):2591-601.
2. Reedijk AMJ, Coebergh JWW, de Groot-Kruseman HA, van der Sluis IM, Kremer LC, Karim-Kos HE, et al. Progress against childhood and adolescent acute lymphoblastic leukaemia in the Netherlands, 1990-2015. Leukemia. 2020.
3. Riehm H, Reiter A, Schrappe M, Berthold F, Dopfer R, Gerein V, et al. [Corticosteroid-dependent reduction of leukocyte count in blood as a prognostic factor in acute lymphoblastic leukemia in childhood (therapy study ALL-BFM 83)]. Klinische Padiatrie. 1987;199(3):151-60.
4. Lauten M, Moricke A, Beier R, Zimmermann M, Stanulla M, Meissner B, et al. Prediction of outcome by early bone marrow response in childhood acute lymphoblastic leukemia treated in the ALL-BFM 95 trial: differential effects in precursor B-cell and T-cell leukemia. Haematologica. 2012;97(7):1048-56.
5. Weikum ER, Knuesel MT, Ortlund EA, Yamamoto KR. Glucocorticoid receptor control of transcription: precision and plasticity via allostery. Nat Rev Mol Cell Biol. 2017;18(3):159-74.
6. Willis SN, Fletcher JI, Kaufmann T, van Delft MF, Chen L, Czabotar PE, et al. Apoptosis initiated when BH3 ligands engage multiple Bcl-2 homologs, not Bax or Bak. Science. 2007;315(5813):856-9.
7. O'Connor L, Strasser A, O'Reilly LA, Hausmann G, Adams JM, Cory S, et al. Bim: a novel member of the Bcl-2 family that promotes apoptosis. EMBO J. 1998;17(2):384-95.
8. Chen L, Willis SN, Wei A, Smith BJ, Fletcher JI, Hinds MG, et al. Differential targeting of prosurvival Bcl-2 proteins by their BH3-only ligands allows complementary apoptotic function. Mol Cell. 2005;17(3):393-403.
9. Youle RJ, Strasser A. The BCL-2 protein family: opposing activities that mediate cell death. Nat Rev Mol Cell Biol. 2008;9(1):47-59.
10. Bachmann PS, Gorman R, Papa RA, Bardell JE, Ford J, Kees UR, et al. Divergent mechanisms of glucocorticoid resistance in experimental models of pediatric acute lymphoblastic leukemia. Cancer Res. 2007;67(9):4482-90.
11. Jing D, Bhadri VA, Beck D, Thoms JA, Yakob NA, Wong JW, et al. Opposing regulation of BIM and BCL2 controls glucocorticoid-induced apoptosis of pediatric acute lymphoblastic leukemia cells. Blood. 2015;125(2):273-83.
12. Jing D, Huang Y, Liu X, Sia KCS, Zhang JC, Tai X, et al. Lymphocyte-Specific Chromatin Accessibility Pre-determines Glucocorticoid Resistance in Acute Lymphoblastic Leukemia. Cancer Cell. 2018;34(6):906-21 e8.
13. Bachmann PS, Piazza RG, Janes ME, Wong NC, Davies C, Mogavero A, et al. Epigenetic silencing of BIM in glucocorticoid poor-responsive pediatric acute lymphoblastic leukemia, and its reversal by histone deacetylase inhibition. Blood. 2010;116(16):3013-22.
14. van der Zwet JCG, Buijs-Gladdines J, Cordo V, Debets DO, Smits WK, Chen Z, et al. MAPK-ERK is a central pathway in T-cell acute lymphoblastic leukemia that drives steroid resistance. Leukemia. 2021.
15. Li Y, Buijs-Gladdines JG, Cante-Barrett K, Stubbs AP, Vroegindeweij EM, Smits WK, et al. IL-7 Receptor Mutations and Steroid Resistance in Pediatric T cell Acute Lymphoblastic Leukemia: A Genome Sequencing Study. PLoS Med. 2016;13(12):e1002200.
16. Lessene G, Czabotar PE, Colman PM. BCL-2 family antagonists for cancer therapy. Nat Rev Drug Discov. 2008;7(12):989-1000.

17. Roberts AW, Davids MS, Pagel JM, Kahl BS, Puvvada SD, Gerecitano JF, et al. Targeting BCL2 with Venetoclax in Relapsed Chronic Lymphocytic Leukemia. N Engl J Med. 2016;374(4):311-22.
18. Peirs S, Matthijssens F, Goossens S, Van de Walle I, Ruggero K, de Bock CE, et al. ABT-199 mediated inhibition of BCL-2 as a novel therapeutic strategy in T-cell acute lymphoblastic leukemia. Blood. 2014;124(25):3738-47.
19. Chonghaile TN, Roderick JE, Glenfield C, Ryan J, Sallan SE, Silverman LB, et al. Maturation stage of T-cell acute lymphoblastic leukemia determines BCL-2 versus BCL-XL dependence and sensitivity to ABT-199. Cancer Discov. 2014;4(9):1074-87.
20. Gala JL, Vermylen C, Cornu G, Ferrant A, Michaux JL, Philippe M, et al. High expression of bcl-2 is the rule in acute lymphoblastic leukemia, except in Burkitt subtype at presentation, and is not correlated with the prognosis. Ann Hematol. 1994;69(1):17-24.
21. Lacayo NJ, Pullarkat VA, Stock W, Jabbour E, Bajel A, Rubnitz J, et al. Safety and Efficacy of Venetoclax in Combination with Navitoclax in Adult and Pediatric Relapsed/Refractory Acute Lymphoblastic Leukemia and Lymphoblastic Lymphoma. Blood. 2019;134(Supplement_1):285-.
22. Starza RL, Cambò B, Pierini A, Bornhauser B, Montanaro A, Bourquin J-P, et al. Venetoclax and Bortezomib in Relapsed/Refractory Early T-Cell Precursor Acute Lymphoblastic Leukemia. JCO Precision Oncology. 2019(3):1-6.
23. Salomons GS, Smets LA, Verwijs-Janssen M, Hart AA, Haarman EG, Kaspers GJ, et al. Bcl-2 family members in childhood acute lymphoblastic leukemia: relationships with features at presentation, in vitro and in vivo drug response and long-term clinical outcome. Leukemia. 1999;13(10):1574-80.
24. Caenepeel S, Brown SP, Belmontes B, Moody G, Keegan KS, Chui D, et al. AMG 176, a Selective MCL1 Inhibitor, Is Effective in Hematologic Cancer Models Alone and in Combination with Established Therapies. Cancer Discov. 2018;8(12):1582-97.
25. Li Z, He S, Look AT. The MCL1-specific inhibitor S63845 acts synergistically with venetoclax/ABT-199 to induce apoptosis in T-cell acute lymphoblastic leukemia cells. Leukemia. 2019;33(1):262-6.
26. Stam RW, Den Boer ML, Schneider P, de Boer J, Hagelstein J, Valsecchi MG, et al. Association of high-level MCL-1 expression with in vitro and in vivo prednisone resistance in MLL-rearranged infant acute lymphoblastic leukemia. Blood. 2010;115(5):1018-25.
27. Tron AE, Belmonte MA, Adam A, Aquila BM, Boise LH, Chiarparin E, et al. Discovery of Mcl-1-specific inhibitor AZD5991 and preclinical activity in multiple myeloma and acute myeloid leukemia. Nat Commun. 2018;9(1):5341.
28. Choudhary GS, Al-Harbi S, Mazumder S, Hill BT, Smith MR, Bodo J, et al. MCL-1 and BCL-xL-dependent resistance to the BCL-2 inhibitor ABT-199 can be overcome by preventing PI3K/AKT/mTOR activation in lymphoid malignancies. Cell Death Dis. 2015;6:e1593.
29. Ramsey HE, Fischer MA, Lee T, Gorska AE, Arrate MP, Fuller L, et al. A Novel MCL1 Inhibitor Combined with Venetoclax Rescues Venetoclax-Resistant Acute Myelogenous Leukemia. Cancer Discov. 2018;8(12):1566-81.
30. Phillips DC, Xiao Y, Lam LT, Litvinovich E, Roberts-Rapp L, Souers AJ, et al. Loss in MCL-1 function sensitizes non-Hodgkin's lymphoma cell lines to the BCL-2-selective inhibitor venetoclax (ABT-199). Blood Cancer J. 2016;6:e403.
31. Meyer LK, Huang BJ, Delgado-Martin C, Roy RP, Hechmer A, Wandler AM, et al. Glucocorticoids paradoxically facilitate steroid resistance in T cell acute lymphoblastic leukemias and thymocytes. J Clin Invest. 2020;130(2):863-76.
32. Delgado-Martin C, Meyer LK, Huang BJ, Shimano KA, Zinter MS, Nguyen JV, et al. JAK/STAT pathway inhibition overcomes IL7-induced glucocorticoid resistance in a subset of human T-cell acute lymphoblastic leukemias. Leukemia. 2017;31(12):2568-76.

33. Cante-Barrett K, Mendes RD, Smits WK, van Helsdingen-van Wijk YM, Pieters R, Meijerink JP. Lentiviral gene transfer into human and murine hematopoietic stem cells: size matters. BMC Res Notes. 2016;9:312.
34. Certo M, Del Gaizo Moore V, Nishino M, Wei G, Korsmeyer S, Armstrong SA, et al. Mitochondria primed by death signals determine cellular addiction to antiapoptotic BCL-2 family members. Cancer Cell. 2006;9(5):351-65.
35. Cordo' V, van der Zwet JCG, Canté-Barrett K, Pieters R, Meijerink JPP. T-cell Acute Lymphoblastic Leukemia: A Roadmap to Targeted Therapies. Blood Cancer Discovery. 2021;2(1):19-31.
36. Domina AM, Vrana JA, Gregory MA, Hann SR, Craig RW. MCL1 is phosphorylated in the PEST region and stabilized upon ERK activation in viable cells, and at additional sites with cytotoxic okadaic acid or taxol. Oncogene. 2004;23(31):5301-15.
37. Yeh YY, Chen R, Hessler J, Mahoney E, Lehman AM, Heerema NA, et al. Up-regulation of CDK9 kinase activity and Mcl-1 stability contributes to the acquired resistance to cyclin-dependent kinase inhibitors in leukemia. Oncotarget. 2015;6(5):2667-79.
38. Sale MJ, Cook SJ. The BH3 mimetic ABT-263 synergizes with the MEK1/2 inhibitor selumetinib/AZD6244 to promote BIM-dependent tumour cell death and inhibit acquired resistance. Biochem J. 2013;450(2):285-94.
39. Sale MJ, Minihane E, Monks NR, Gilley R, Richards FM, Schifferli KP, et al. Targeting melanoma's MCL1 bias unleashes the apoptotic potential of BRAF and ERK1/2 pathway inhibitors. Nat Commun. 2019;10(1):5167.
40. Nangia V, Siddiqui FM, Caenepeel S, Timonina D, Bilton SJ, Phan N, et al. Exploiting MCL1 Dependency with Combination MEK + MCL1 Inhibitors Leads to Induction of Apoptosis and Tumor Regression in KRAS-Mutant Non-Small Cell Lung Cancer. Cancer Discov. 2018;8(12):1598-613.
41. Han L, Zhang Q, Dail M, Shi C, Cavazos A, Ruvolo VR, et al. Concomitant targeting of BCL2 with venetoclax and MAPK signaling with cobimetinib in acute myeloid leukemia models. Haematologica. 2019.
42. Konopleva M, Milella M, Ruvolo P, Watts JC, Ricciardi MR, Korchin B, et al. MEK inhibition enhances ABT-737-induced leukemia cell apoptosis via prevention of ERK-activated MCL-1 induction and modulation of MCL-1/BIM complex. Leukemia. 2012;26(4):778-87.

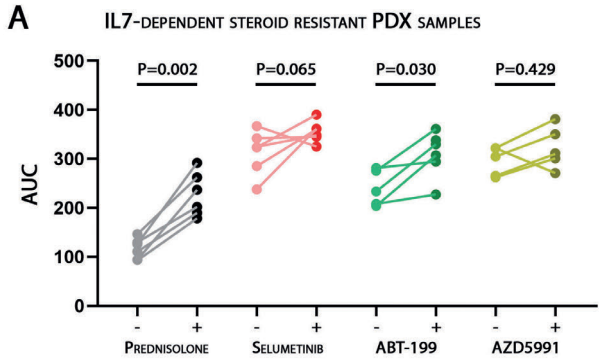

Supplemental Figure 1. *AUC of six 'IL7-dependent steroid resistant' T-ALL PDX samples treated with prednisolone, selumetinib, ABT-199 or AZD5991 in the presence or absence of IL7. Statistical differences were calculated with the Mann-Withney test.*

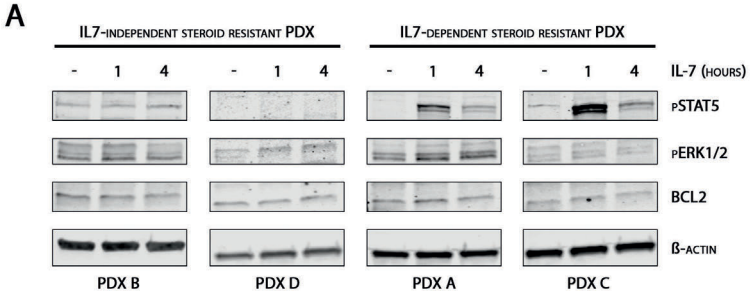

Supplemental Figure 2. *Immunoblot analysis of four PDX samples (two IL7-indendent and two IL7-dependnet steroid resistant PDX samples) treated with IL-7 for 0, 1 or 4 hours.*

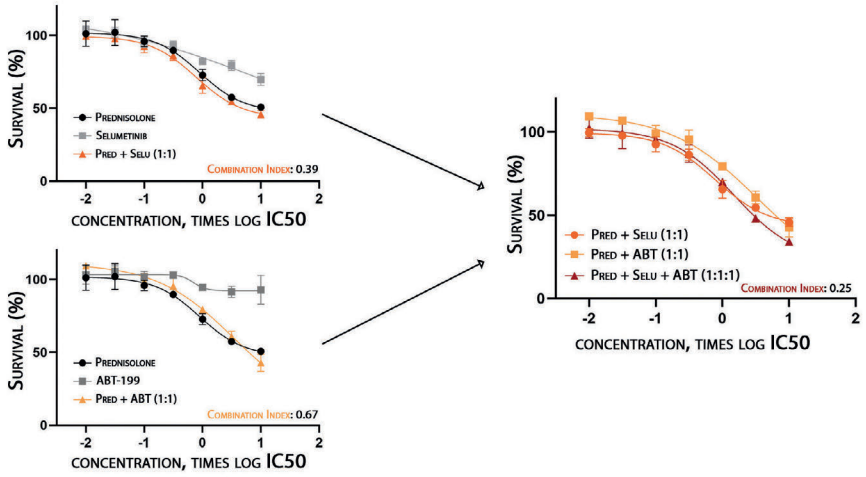

Supplemental Figure 3. *Representative example of an analyzed T-ALL PDX sample by the SynergyFinder™ with duo (1:1 drug ratio) and triple (1:1:1 drug ratio) treatment (14).*

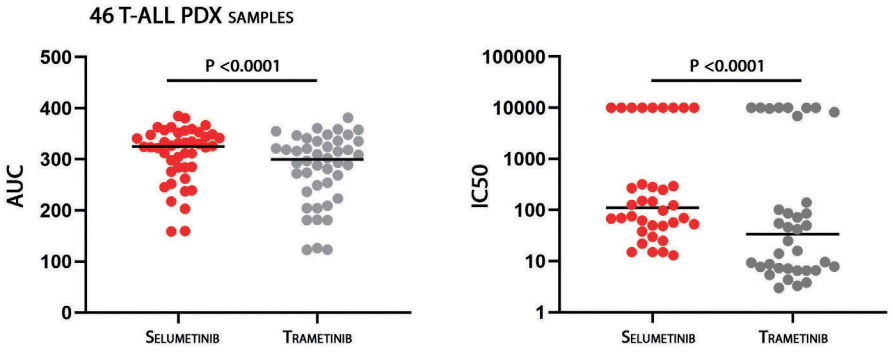

Supplemental Figure 4. *Cell toxicity screening of 46 T-ALL PDX samples for selumetinib or trametinib. Left: cell viability illustrated by AUC, whereas an AUC of 400 represent the maximum AUC in a 4-log dynamic concentration range of each specific inhibitor. Right: corresponding IC50 values of treated PDX samples. Statistical differences were calculated with the Wilcoxon test (*p<0.05, **p<0.01, ***p<0.001, ****p<0.0001).*

6

STAT5 does not drive steroid resistance in T-cell acute lymphoblastic leukemia despite the activation of *BCL2* and *BCLXL* following glucocorticoid treatment

Jordy C.G. van der Zwet[1], Valentina Cordo'[1], Jessica G.C.A.M. Buijs-Gladdines[1], Rico Hagelaar[1], Willem K. Smits[1], Eric Vroegindeweij[1], Laura T.M. Graus[1], Vera Poort[1], Marloes Nulle[1], Rob Pieters[1] and Jules P.P. Meijerink[1*]

[1]Princess Máxima Center for Pediatric Oncology, Utrecht, the Netherlands

ABSTRACT

Physiologic and pathogenic IL7-receptor (IL7R) induced signaling provokes glucocorticoid resistance in a subset of pediatric T-cell acute lymphoblastic leukemia (T-ALL) patients. Activation of downstream STAT5 has been suggested to cause steroid resistance through upregulation of anti-apoptotic *BCL2*, one of its downstream target genes. Here, we demonstrate that isolated STAT5 signaling in various T-ALL cell models is insufficient to raise cellular steroid resistance despite its capacity to upregulate BCL2 and BCL-XL. Upregulation of anti-apoptotic *BCL2* and *BCLXL* in STAT5-activated T-ALL cells is particularly enhanced upon glucocorticoid treatment. We demonstrate that the enhanced expression of these anti-apoptotic molecules is facilitated by direct interaction between NR3C1 and activated STAT5 molecules at STAT5-regulatory sites. In contrast, STAT5 occupancy at glucocorticoid response elements (GREs) does not affect the expression of NR3C1 target genes. Strong upregulation of BIM, a NR3C1 pro-apoptotic target gene, upon prednisolone treatment can counterbalance STAT5-induced BCL2 and BCL-XL expression downstream of IL7-induced or pathogenic IL7R signaling. This explains why isolated STAT5 activation does not directly impair the steroid response. Our study suggests that STAT5 activation only contributes to steroid resistance in combination with cellular defects or alternative signaling routes that disable the pro-apoptotic and steroid-induced BIM response.

Key points

1. Activation of the STAT5 pathway does not raise steroid resistance despite enhanced expression of BCL2 and BCLXL following steroid treatment.

2. The glucocorticoid receptor (NRC1) is an essential STAT5 co-regulator to activate canonical STAT5 target genes including *BCL2* and *BCLXL*.

INTRODUCTION

Synthetic steroids remain a vital cornerstone drug in the treatment of pediatric T-cell acute lymphoblastic leukemia (T-ALL). Upon binding with steroids, the glucocorticoid receptor (NR3C1) dimerizes and migrates to the nucleus where it functions as a transcription factor and regulates the expression of multiple steroid-response genes, including the pro-apoptotic gene *BIM* (1-3). Resistance to steroid treatment predicts for inferior outcome and therefore remains a major clinical problem for T-ALL (4, 5). An important signaling pathway that interferes with steroid sensitivity is the interleukin-7 receptor (IL7R) pathway. Both physiological IL7-signaling or the presence of activating mutations in various IL7R signaling molecules have been linked to steroid resistance in T-ALL patients (6, 7).

Recently, the mechanisms underlying IL7R-dependent survival and/or steroid resistance have been studied. IL7R signaling results in downstream activation of the PI3K-AKT and STAT5 pathways, but also activates MAPK-ERK signaling (6, 8-12). For these individual downstream signaling pathways, different mechanisms have been identified that may contribute to steroid resistance (**Figure 1**). Activation of the PI3K-AKT pathway activation is reported to drive phosphorylation of NR3C1, which blocks its migration to the nucleus (13). Additionally, PI3K-AKT signaling can upregulate various anti-apoptotic proteins including BCLXL and MCL1 (6). AKT can also inhibit transcription of the important glucocorticoid receptor target gene *BIM* via an inhibitory phosphorylation of the FOXO3A transcription factor (14). Epigenetic silencing of the *BIM* locus, as found in some ALL patient-derived xenograft models, has also been proposed as an important steroid-resistance mechanism (15, 16).

IL7R signaling mutations, found in approximately 35% of pediatric T-ALL patients, or physiological IL7 signaling activates downstream MAPK-ERK signaling (6, 7, 12). Activated ERK phosphorylates BIM-L and BIM-EL proteins, which therefore lose their potential to bind and neutralize anti-apoptotic BCL2 protein family members including BCL2, BCLXL and MCL1, hence resulting in steroid resistance (12). MEK-inhibitors, and to a limited extent the JAK-inhibitor ruxolitinib, showed synergy with steroid treatment by restoring functional BIM levels, thereby representing promising targeted compounds to overcome steroid resistance in T-ALL (6, 12).

Activation of the glucocorticoid receptor NR3C1 facilitates transcriptional upregulation of glucocorticoid target genes, including *BIM* and *IL7R* (17). Recently, it was shown that by upregulating IL7Rα, steroid treatment could paradoxically induce steroid resistance (18), since enhanced IL7-induced signaling activates STAT5 and consequentially enhances the expression of the pro-survival gene *BCL2* (18) and the *PIM1* kinase gene (19). Thus far, upregulation of BCL2 is regarded as the driving mechanism for IL7-induced survival and steroid resistance (7, 17, 18, 20, 21).

Here, we explore the significance of STAT5 signaling downstream of physiological or mutant IL7R signaling in relation to steroid resistance in pediatric T-ALL. We studied whether induced expression of the constitutively active N642H STAT5 mutant can activate BCL2 and drive steroid resistance.

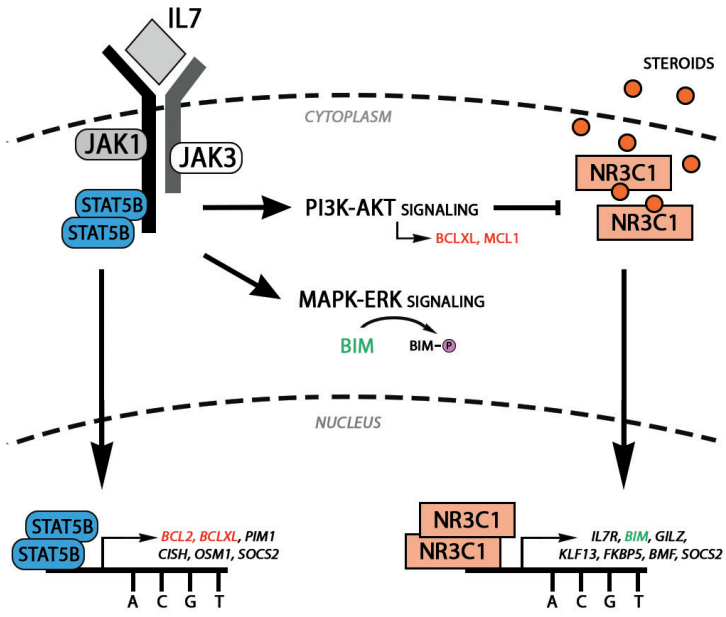

Figure 1. Schematic overview of IL7-receptor- and steroid-induced signaling. *In the presence of IL-7, IL7Rα (left) and IL7Rγ (right) subunits heterodimerize, allowing transphosphorylation of JAK1 and JAK3 kinases and phosphorylation of IL7Rα as a docking site for STAT5. As a result, downstream PI3K-AKT, MAPK-ERK and STAT5 signaling pathways are activated. Activated STAT5 migrates to the nucleus as a homodimer to regulate the transcription of canonical STAT5 target genes, including anti-apoptotic BCL2 and BCLXL. Activated PI3K-AKT signaling upregulates anti-apoptotic BCLXL and MCL1 and can regulate the nuclear translocation of the activated glucocorticoid receptor (NR3C1). Activated MAPK-ERK signaling phosphorylates and therefore inactivates pro-apoptotic BIM. Upon exposure to steroids, NR3C1 migrates to the nucleus as a homodimer and induces the expression of NR3C1 target genes (including pro-apoptotic BIM) at glucocorticoid response element (GRE) sites.*

MATERIAL AND METHODS

Generation of cell lines

Gateway cloning (Invitrogen) and lentiviral transduction of SUPT-1 cell lines with wild type or mutant IL7R or STAT5 constructs were performed as previously described (22) . SUPT-1 and CCRF-CEM cells were cultured in RPMI-1640 medium (Gibco) supplemented with 1x Glutamax, 10% heat-inactivated fetal bovine serum (Gibco), 2% pencillin/streptomycin (Gibco) and 0,4% Fungizone (Gibco). Media for SUPT-1 cells was supplemented with 1-2 µg/mL puromycin for purification of doxycycline-inducible cells.

Cell preparation and cytotoxicity assays

For quantitative real-time reverse-transcription PCR (RTQ-PCR), immunoblot analysis and cytotoxicity assays, SUPT-1 and CCRF-CEM cells were plated in RPMI-1640 medium as described above. For activation of IL7R signaling, medium of CCRF-CEM cells was supplemented with 10 ng/ml IL7 (R&D systems). For RTQ-PCR and immunoblot analysis experiments, cells were plated at a concentration of $1x10^6$ cells/mL overnight. For cytotoxicity assays, cells were plated at a concentration of $0,2x10^6$ cells/mL, and cell viability was determined after four days by methylthiazolyldiphenyl-tetrazolium bromide (MTT, Sigma Aldrich).

Immunoblot analysis

Cell pellets of treated cell suspensions were lysed using KLB (kinase lysis buffer) lysis buffer, and protein eluates were loaded on BioRad Mini-Protean® TGX™ any-kd precast gels (12). Protein transfer to 0.2 µm nitrocellulose membranes was performed using the Trans-Blot® Turbo™ Transfer System (BioRad). Primary antibodies used for immunoblot analysis were: phospho-ERK (#4370; Cell Signaling Technologies (CST)), phospho-MEK (#9121; CST), BCLXL (#2764; CST), MCL1 (#4572; CST, and #sc-12756; Santa Cruz Biotechnology (sc)), BIM (#ab32158; Abcam (ab)), β-Actin (#ab6276; ab); IL7R alpha/CD127 (#MAB306; R&D), BCL2 (#sc-130308; sc), RAS (#05-516; Merck Millipore), AKT (#9272; CST), pAKT-T308 (#9275; CST), pAKT-473 (#9271; CST), NR3C1 (#12041; CST), NR3C1 (#sc-1003; sc), STAT5 (#94205; CST), STAT5 (#sc-835; sc) and pSTAT5 (#9351; CST). IRDye fluorescent secondary antibodies (LI-COR) were used for fluorescent signal detection on the Odyssey-CLx Imaging System (LI-COR).

Immunoprecipitation (IP)

Immunoprecipitation was performed as previously described (12). Antibodies were linked to Dynabeads (Thermo Fisher Scientific) and crosslinked to BS^3 (2,5mM). The total lysate protein eluate of each designated sample was mixed with the Dynabeads-antibody suspension and incubated overnight at 4 degrees. Afterwards, the antibody-bound proteins were eluted from the Dynabeats-antibody-antigen complexes and visualized by immunoblot analysis. Antibodies used for immunoprecipitation: BIM (C34C5 #2933, CST), NR3C1 (#12041; CST).

Quantitative real-time reverse-transcription PCR (RTQ-PCR)
Isolation of RNA, cDNA synthesis and RTQ-PCR reactions were performed as previously described (22, 23). The expression of NR3C1 or STAT5 target genes were calculated using the delta CT (dCT) method as percentage of GADPH expression. Fold expression change was calculated relative to the non-doxycycline-induced (-dox), non-prednisolone treated (-pred) condition. Primers used: *GAPDH* Fw primer 5'-GTCGGAGTCAACGGATT-3', *GAPDH* Rev primer 5'-AAGCTTCCCGTTCTCAG-3'; *BIM* Fw primer 5'-GCGCCAGAGATATGGAT-3', *BIM* Rev primer 5'-CGCAAAGAACCTGTCAAT-3'; *IL7R* Fw primer 5'-AGTAAATGCAAAGCACCCTGAG-3', *IL7R* Rev primer 5'-TAAATGGGGCTTAAGCTCTGAC-3'; *SOCS2* Fw primer 5'- GGGAGCTCGGTCAGAC-3', *SOCS2* Rev primer 5'- CCAGCTGATGTTTTAACAGAT-3'; *PIM1* Fw primer 5'-GATCCTGCTGTATGATATGGT-3', *PIM1* Rev primer 5'- GAAGGTTGGCCTATCTGAT-3'; *CISH* Fw primer 5'- CCAGCCCAGACAGAGAG-3', *CISH* Rev primer 5'- TGGAGTCGGCATACTCA-3'; *OSM1* Fw primer 5'- AGCTGCTCGAAAGAGTACC-3', *OSM1* Rev primer 5'-AAGTCGGCCAGTCTGTG-3'; *BCL2* Fw primer 5'- TCGGTGGGGTCATGT-3', *BCL2* Rev primer 5'- GGGCCAAACTGAGCA-3'; *BC2L1* (BCLXL) Fw primer 5'- CCCAGGGACAGCATATC-3', *BCL2L1* (BCLXL) Rev primer 5'- GCTGCATTGTTCCCATAG-3'; *MCL1* Fw primer 5'-CGCCAAGGACACAAAG-3', *MCL1* Rev primer 5'- AAGGCACCAAAAGAAATG-3'.

Chromatin-immunoprecipitation sequencing (ChIP-seq)
Doxycycline-induced $STAT5^{WT}$ and $STAT5B^{N642H}$ SUPT-1 cells were cultured with or without 250µg/ml prednisolone for 16 hours. After incubation, $20x10^6$ cells were fixed and chromatin-immunoprecipitation (ChIP) was performed according to the manufacturer's instructions (Simple ChIP Enzymatic Chromatin IP Kit, #9003, CST). Water bath sonification was performed for seven cycles (30 seconds on 30 seconds off), and DNA fragment size was validated by electrophoresis. Antibodies used during for ChIP: STAT5 (CST, D206U) and NR3C1 NR3C1 (#sc-1003; sc). DNA library preparation was performed using the NEBNext Ultra II DNA Library Prep kit (New England Biolabs #E7103) with an additional 0,52X beads purification step. DNA eluates were sequenced using the Illumina NextSeq500 platform of the Utrecht Sequence facility (USEQ).

ChIP-seq data processing and visualization
Raw reads were aligned to the CRCh38 human genome, using BWA (24) with default settings. Narrowpeak calling with default settings from MACS2 (25) was used for peak calling. BamCoverage from deeptools (26) was used to normalize input signal for figures, using reads per genomic content (RPGC) method. Peaks were visualized using IGV (27). Bedtools (28) was used to select unique and overlapping peaks for STAT5/NR3C1. These are visualized using plotheatmap function from deeptools. Meme-chip was used for detecting motifs within regions of 50bps up or down of the summit of NR3C1 or STAT5 peak summits (101bp window), using default settings (29).

Data availability

Affymetrix U133 Plus2 microarray data for the 117 patients as previously published (30), was normalized using Robust Multichip Average (RMA), using Affy package (31). Micoarray data is available at http://www.ncbi.nlm.nih.gov/geo/ under accession number GSE26713. A selection of STAT5 target genes were visualized using R package pheatmap (pheatmap: Pretty Heatmaps, R package version 1.0.12). IL7R mutations, as detected in Li et al (6), are denoted at the top. ChIPseq files are available at Gene Expression Omnibus under GEO series accession number: GSE171976, https://www.ncbi.nlm.nih.gov/geo/query/acc.cgi?acc=GSE171976.

RESULTS

Activation of STAT5 target genes does not predict for steroid resistance in T-ALL.

To study the significance of STAT5 activation in relation to steroid resistance in pediatric T-ALL, we investigated the expression of STAT5 target genes (*e.g., BCL2*, *BCL2L1 (BCLXL)*, *PIM1*, *CISH*, *OSM1* and *SOCS2*) in our historic microarray dataset for 117 treatment-naïve pediatric T-ALL patient samples (30). The leukemia subtype and the IL7R signaling pathway mutational status of these patients, as previously determined (6, 30), are displayed (**Figure 2a)**. Cluster analysis based on the expression of STAT5 target genes separated T-ALL patients into two major clusters, with cluster B representing patients with high expression of STAT5 target genes. In relation to leukemic subtype, cluster B was significantly enriched for *TLX3*-rearranged leukemias ($p<0.0001$), whereas *TLX1-/NKX2-1*- rearranged patients or *TAL1/2* and *LMO1/2*-rearranged T-ALL patients were strongly associated with cluster A ($p=0.0126$ and $p<0.0001$ respectively, **Figure 2b**). Moreover, activating IL7R signaling mutations in *IL7R*, *JAK1*, *JAK3* and/or *STAT5B* genes were also strongly associated with STAT5 transcriptional activity ($p<0.0001$) (**Figure 2c**), in line with previous observations that these mutations are also associated with *TLX3*-rearranged patients (6, 30, 32). This result highlights the contribution of *IL7R*, *JAK1*, *JAK3* and/or *STAT5B* mutations to activate STAT5 in T-ALL. In relation to *ex-vivo* prednisolone cytotoxic response levels, as determined for 84 out of these 117 T-ALL patient samples, we observed that the prednisolone LC50 values were comparable for patients with high or low STAT5 transcriptional activity (**Figure 2d**). This suggests that the predicted STAT5-activity alone does not predict for sensitivity to steroid treatment at diagnosis, either by having no immediate impact on steroid sensitivity or due to the presence of alternative resistance mechanisms.

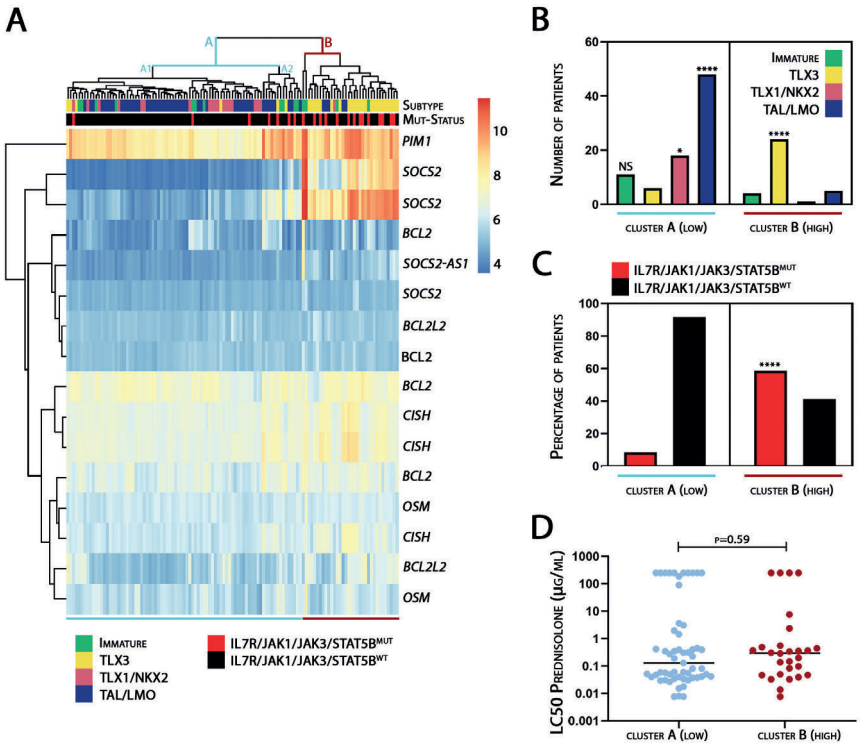

Figure 2. **STAT5 transcriptional activity in pediatric T-ALL patients does not predict for steroid resistance**. **(A)** *Unsupervised clustering of STAT5 target gene expression of 117 treatment-naïve pediatric T-ALL patients using Affymetrix U133 Plus2 microarrays. The leukemic subtype and IL7R-pahtway mutational status for these patients has been previously determined. Cluster B represents patients with the highest STAT5 transcriptional activity. (B) Representation of the four major leukemic T-ALL subtypes in both STAT5 transcriptional clusters. Statistical differences calculated by Chi-square test; *p<0.05, **p<0.01, ***p<0.001, ****p<0.0001.* **(C)** *IL7R/JAK1/JAK3/STAT5B mutation status of primary patient blasts related to STAT5 transcriptional clusters. Statistical differences calculated by Chi-square test; *p<0.05, **p<0.01, ***p<0.001, ****p<0.0001.* **(D)** *Statistical analysis of in-vitro prednisolone sensitivity of patients in low versus high STAT5 transcriptional clusters (Mann-Whitney-test).*

STAT5 activation does not drive steroid resistance in IL7R-mutant cell lines.

To further explore the relation between the STAT5-regulated transcriptional program and steroid resistance, we generated SUPT-1 or P12-Ichikawa derivative lines that can be induced to express wild type IL7Ra (IL7R^{WT}) or cysteine-mutant IL7Rα molecules (IL7R$^{PILT240\text{-}244RFCPH}$ or IL7R$^{PIL240\text{-}242QSPSC}$) following exposure to doxycycline. We previously demonstrated that induced expression of cysteine-mutant IL7Rα molecules, in contrast to wild type IL7Rα, provoked steroid resistance in otherwise steroid-sensitive T-ALL SUPT-1 cells (12). Overexpression of mutant IL7Rα resulted in STAT5 phosphorylation and

thus STAT5 activation, while no effect was seen upon wild type IL7Rα overexpression (**Figure 3a**). Examining the activation of STAT5 target genes, both mutant IL7Rα molecules strongly induced BCL2 and BCLXL protein expression, but only in the presence of prednisolone. As *BCL2* has been described as a STAT5 target gene, elevated BCL2 (and BCLXL) expression is in line with active STAT5B signaling in both IL7R mutant lines. To further validate this concept, we studied the expression of *BCL2* and *BCLXL* and various other STAT5 target genes such as *PIM1* and *CISH* in SUPT-1 cells expressing $IL7R^{WT}$ or a cysteine-mutant IL7R variant. Expression of these STAT5 target genes was also studied in the presence of prednisolone with or without targeted JAK1/2- (ruxolitinib), MEK- (selumetinib) and/or AKT- (MK2206) inhibitors (**Figure 3b)**. Again, steroid treatment of IL7R-mutant overexpressing cells led to a nearly two-fold increase in *BCL2* and *BCLXL* expression (**Figure 3c**). As expected, the JAK-inhibitor ruxolitinib effectively blocked downstream STAT5B, MAPK-ERK and AKT pathways (**Supplemental Figure 1**), and also blocked steroid-dependent upregulation of *BCL2*, *BCLXL*, *CISH* and *PIM1* (**Figure 3c**). Treatment with the MEK-inhibitor selumetinib or the AKT-inhibitor MK2206, nor their combination could block transcriptional upregulation of these genes. Similar results were obtained in the context of IL7-induced signaling in the T-ALL cell line CCRF-CEM, indicating that this reflects a general mechanism in T-ALL cells (**Supplemental Figure 2a-b**).

Unexpectedly, whereas expression of both mutant IL7R isoforms strongly raised steroid resistance, this effect seemed independent of upregulation of pro-survival proteins BCL2 and BCL-XL via STAT5; while the JAK-inhibitor ruxolitinib inhibits upregulation of BCL2 and BCL-XL and reverts steroid resistance in this model, both AKT- or combined MEK- and AKT- inhibitor treatment also sensitized SUP-T1 cells for prednisolone treatment (**Figure 3d**) regardless of the STAT5-driven BCL2 and BCLXL hyper-induction (**Figure 3c**). Similar findings were observed for T-ALL CCRF-CEM cells, where these inhibitors reverted IL7-induced steroid resistance independently of the expression levels of BCL2 and BCL-XL via STAT5 (**Supplemental Figure 2b-c**). Therefore, we conclude that STAT5 activation and consequent upregulation of BCL2 and BCLXL do not have a direct negative impact on steroid sensitivity (**Figure 2d**).

$STAT5^{N624H}$-induced SUPT1 cells remain steroid sensitive despite enhanced *BCL2* and *BCLXL* levels

To further exclude a direct role of active STAT5 signaling in relation to steroid resistance, we generated doxycycline-inducible SUPT-1 and P12-Ichikawa derivative lines that express wild type STAT5B ($STAT5^{WT}$) or the constitutively active mutant isoform $STAT5^{N642H}$ (**Figure 4a**). Expression of $STAT5B^{N642H}$, but not $STAT5^{WT}$, led to activated STAT5B signaling without affecting the MAPK-ERK or PI3K-AKT signaling pathways (**Figure 4a, Supplemental Figure 3a**) (6, 33-37). In line with these results, expression of $STAT5B^{WT}$ was ineffective to activate the expression of downstream target genes, while $STAT5B^{N642H}$ induced the expression of canonical STAT5 target genes (**Figure 4b, Supplemental Figure 3b**).

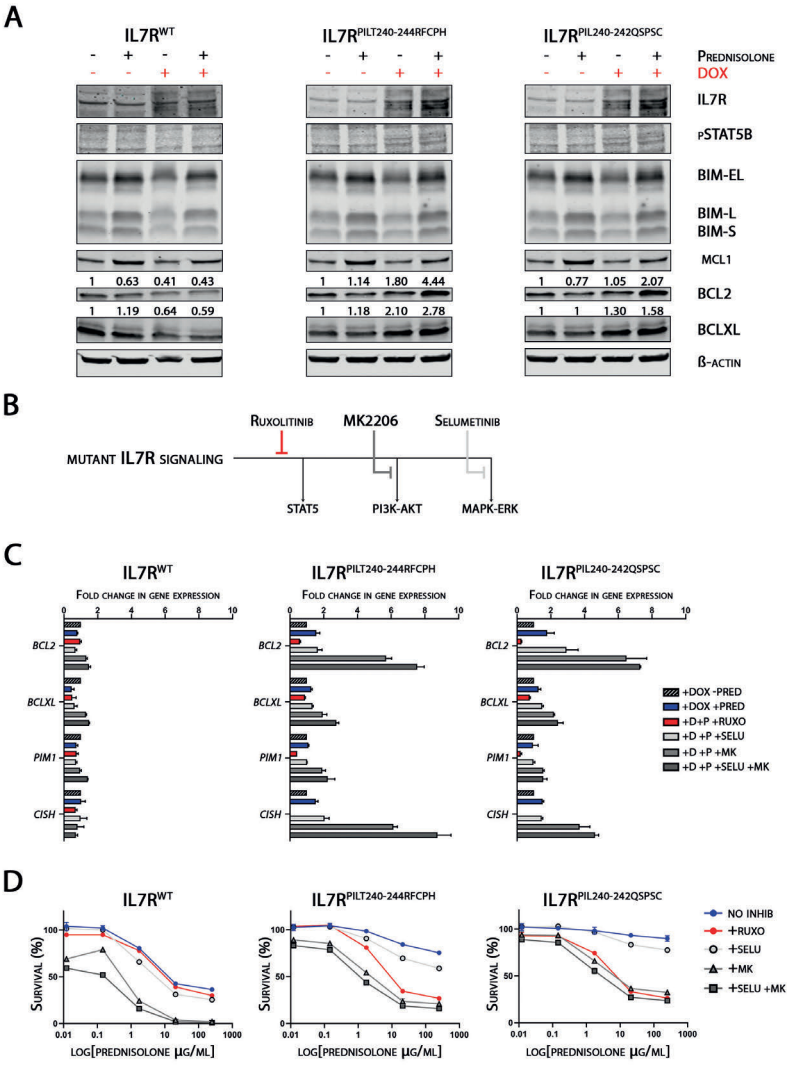

Figure 3. Steroid treatment and inhibition of MAPK-ERK and PI3K-AKT signaling enhance the expression of STAT5 target genes in mutant IL7R cell lines. (A) *Ligand-independent STAT5B pathway activation in wild-type and cysteine-mutant IL7R overexpressing SUPT-1 cell lines. Protein band intensity for BCL2 and BCLXL represented relative to -dox-pred condition.* **(B)** *Graphic representation of* **Supplemental Figure 1***: selective inhibition of IL7R^{MUT} activated pathways by ruxolitinib (1µM, JAK1/2-inhibitor), selumetinib (1µM, MEK-inhibitor) and MK2206 (0,5µM AKT-inhibitor).* **(C)** *Expression of STAT5B target genes in wild-type and mutant IL7R overexpressing SUPT-1 cells. Cells were treated with targeted inhibitors for 30 minutes before doxycycline-induction. Steroid exposed cells were treated with prednisolone (250µg/ml) for 16 hours.* **(D)** *Steroid sensitivity of wild-type and mutant IL7R overexpressing SUPT-1 cells in the absence or presence of targeted inhibitors. Steroid sensitivity was determined by a 4-day MTT read-out. Representative data of a biological duplicate.*

Moreover, the expression of STAT5 target genes was further boosted in STAT5^{N642H} cells upon steroid treatment, and was most prominent for *BCL2* and *BCLXL* compared to other classical STAT5 target genes such as *PIM1*, *CISH* and *OSM1* (**Figure 4b**). Despite upregulation of both anti-apoptotic molecules upon induction of STAT5^{N642H}, the cytotoxic steroid response did not change for SUPT-1 or P12-Ichikawa cells (**Figure 4c-d**). This again demonstrates that STAT5 signaling alone does not provoke steroid resistance despite enhanced upregulation of anti-apoptotic BCL2 and BCLXL.

NR3C1-STAT5B co-binding enhances the expression of canonical STAT5 target genes

The enhanced STAT5 transcriptional activity during steroid treatment has previously been attributed to the steroid-induced transcriptional upregulation of *IL7Ra* by NR3C1, which can further enhance STAT5 activation and subsequently the upregulation of *BCL2* in the presence of IL7 (18). As the induction of *BCL2* and *IL7Ra* also occurs in parallel in IL7-exposed and inhibitor-treated CCRF-CEM cells (**Supplemental Figures 2b and 4a**), an alternative hypothesis could be that NR3C1 and STAT5B act in a single transcriptional complex and co-regulate an identical set of target genes. To explore this possibility, we performed NR3C1 co-immunoprecipitation experiments using SUPT-1 STAT5B^{WT} and STAT5B^{N642H} cells and identified that NR3C1 and STAT5B could indeed physically interact (**Figure 5a**). This interaction seemed independent of the phosphorylation status of STAT5B, as both (unphosphorylated) wild type STAT5 and (phosphorylated) mutant STAT5B bound NR3C1 to equal extends following steroid exposure. To explore whether (mutant) STAT5 and NR3C1 could bind to the same transcriptional regulatory regions, we performed chromatin-immunoprecipitation sequencing (ChIP-seq) for NR3C1 and STAT5. While wild type STAT5 was expressed in a non-phosphorylated, transcriptionally inactive form, we observed that it could still bind to many regulatory sites that were also bound by the phosphorylated and constitutively active STAT5B^{N642H} isoform (**Figure 5b**). While binding of STAT5B^{WT} or STAT5B^{N642H} to regulatory sites was independent of steroid exposure, NR3C1 only bound to DNA upon prednisolone treatment, which was expected based on its nuclear translocation upon interaction with steroids (1). We identified genomic regions that were predominantly bound by either STAT5B or NR3C1, denoted as STAT5 or NR3C1 unique binding sites. Interestingly, many genomic regions were bound by both STAT5B and NR3C1 upon steroid exposure, suggesting that STAT5B and NR3C1 can co-regulate a common set of target genes. Motif analysis for NR3C1 and NR3C1/STAT5 binding sites revealed significant enrichment of classical glucocorticoid response element (GRE) motifs (38) and STAT5 motifs, but not at binding sites that were uniquely bound by STAT5 (**Figure 5c and Supplemental Table 1**).

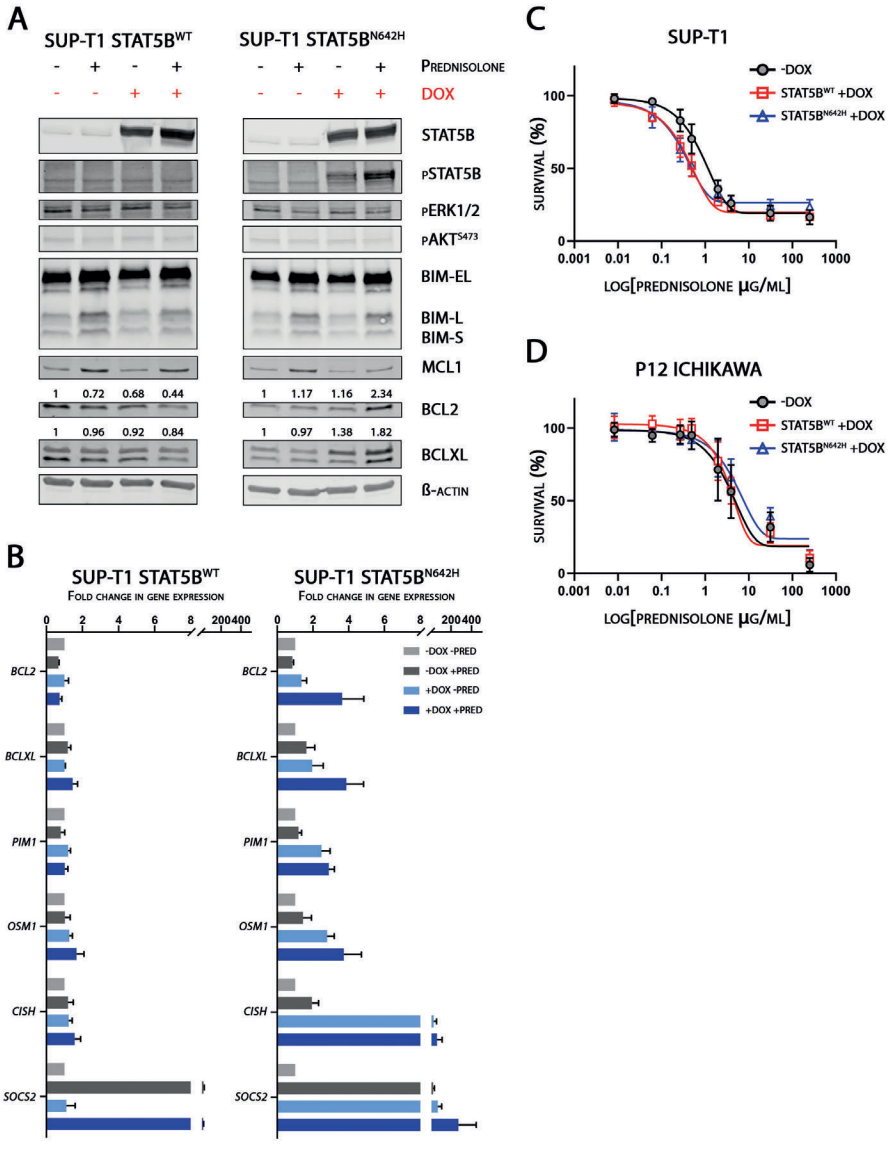

Figure 4. Overexpression of STAT5B^{N642H} does not provoke steroid resistance despite enhanced expression of anti-apoptotic molecules upon steroid treatment. (A) *Activation of STAT5B signaling and expression of anti-apoptotic Bcl2 family proteins in STAT5B wild-type and mutant overexpressing SUPT-1 cells. Protein band intensity for BCL2 and BCLXL represented relative to -dox-pred condition.* **(B)** *Expression STAT5 target genes in STAT5B^{WT} and STAT5B^{N642H} overexpressing cells in the absence and presence of prednisolone treatment (16 hours, 250µg/ml). Data of biological triplicates with SD indicated.* **(C)** *Steroid sensitivity of wild-type and mutant STAT5B overexpressing SUPT-1 and P12 ICHIKAWA cell lines. Steroid sensitivity was determined by a 4-day MTT read-out. Data of biological triplicates with SD indicated.*

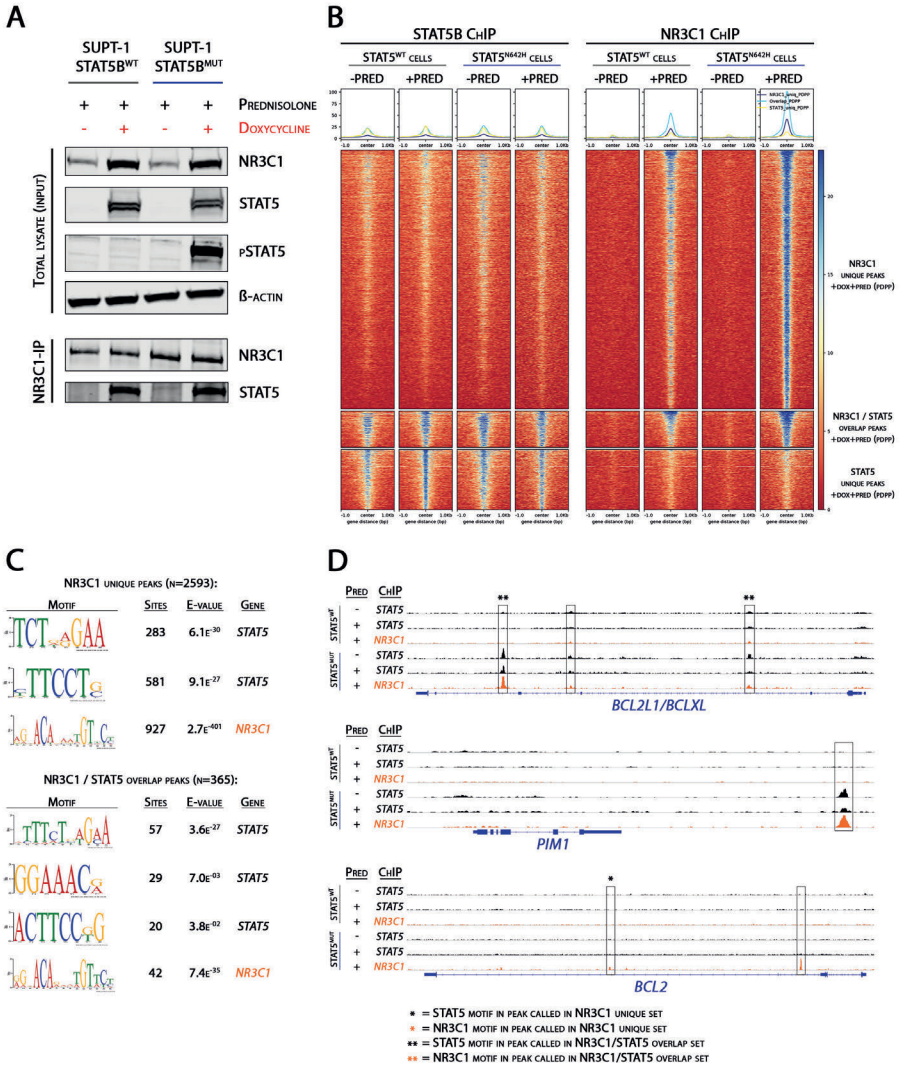

Figure 5. NR3C1 co-regulates the expression of transcriptional STAT5 target genes by co-binding at STAT5 regulated genes. (A) *Immunoblot analysis of NR3C1-immunoprecipitation in STAT5B^{WT} and STAT5B^{N642H} SUPT-1 cells. Steroid exposed cells were treated with prednisolone (250µg/ml) for 16 hours. (***B***) RPGC normalized centered heat map of unique and overlapping NR3C1 and STAT5 chromatin-immunoprecipitation sequencing (ChIP-seq) binding peaks of doxycycline-induced STAT5B^{WT} and STAT5B^{N642H} SUPT-1 cells with (+dox+pred) or without (+dox-pred) prednisolone treatment (16 hours, 250µg/ml).* **(C)** *MEME-ChIP motif analysis of NR3C1 and STAT5 motifs significantly enriched in NR3C1/STAT5 unique or overlapping peak sets.* **(D)** *ChIP-seq identified binding of NR3C1 and STAT5 transcription factors at STAT5 target genes BCL2, BCLXL and PIM1.*

We then specifically studied co-occupancy of STAT5 and NR3C1 at the regulatory sites of selected STAT5 target genes (**Figure 5d, Supplemental Figure 4b**). For *BCLXL* and *PIM1*, we identified STAT5 regulatory sites that were bound by $STAT5B^{N642H}$ but not by wild type STAT5B, indicating that binding of STAT5 at these regulatory sites is dependent on STAT5 phosphorylation. Interestingly, we found that NR3C1 could also bind to these sites upon steroid exposure in mutant STAT5 cells. For the *BCL2* locus, two NR3C1 peaks were identified and bound by NR3C1 only in $STAT5^{N642H}$ cells, with one site harboring a STAT5 binding motif. We did not identify GREs at any of the NR3C1-bound sites in *BCLXL*, *PIM* or *BCL2*, suggesting that NR3C1 may be recruited to these binding sites by binding to STAT5B rather than physical binding to DNA. Combined, these data revealed that NR3C1 can interact with STAT5B and bind in or near STAT5-bound genomic sites, even in the absence of a conserved GRE binding motif. Binding of STAT5 to various 'canonical STAT5 target genes' seems dependent on its active (phosphorylated) form, which enables recruitment of NR3C1 to these sites following steroid exposure to further boosts the expression of these target genes.

In a reciprocal manner, ChIP-seq analysis identified STAT5 binding near NR3C1-binding sites that lack conserved STAT5 binding motifs. Examination of various NR3C1 target genes including *BIM, KLF13*, *FKBP5* and *GILZ* and the newly proposed NR3C1 target genes *BMF* and *MCL1* revealed various NR3C1 binding sites that harbor conserved GRE sequences in *BIM*, *KLF13* and *FKBP5* (**Figure 6a-b, Supplemental Figure 5a-b**). Remarkably, binding of $STAT5^{WT}$ and $STAT5^{N624H}$ was observed at GRE sites of *KLF13* and *FKBP5* that were not flanked by conserved STAT5 binding sequences. This suggests that STAT5 molecules can be recruited to these sites by (direct) interaction with NR3C1, independently of their activation (phosphorylation) state. The significance of STAT5 binding at these sites remains unknown, as the expression of NR3C1 target genes, including *BIM,* following steroid exposure remained unaffected upon co-incubation with JAK1/2-, MEK-, AKT- or combined MEK-AKT inhibitors (**Figure 6c**).

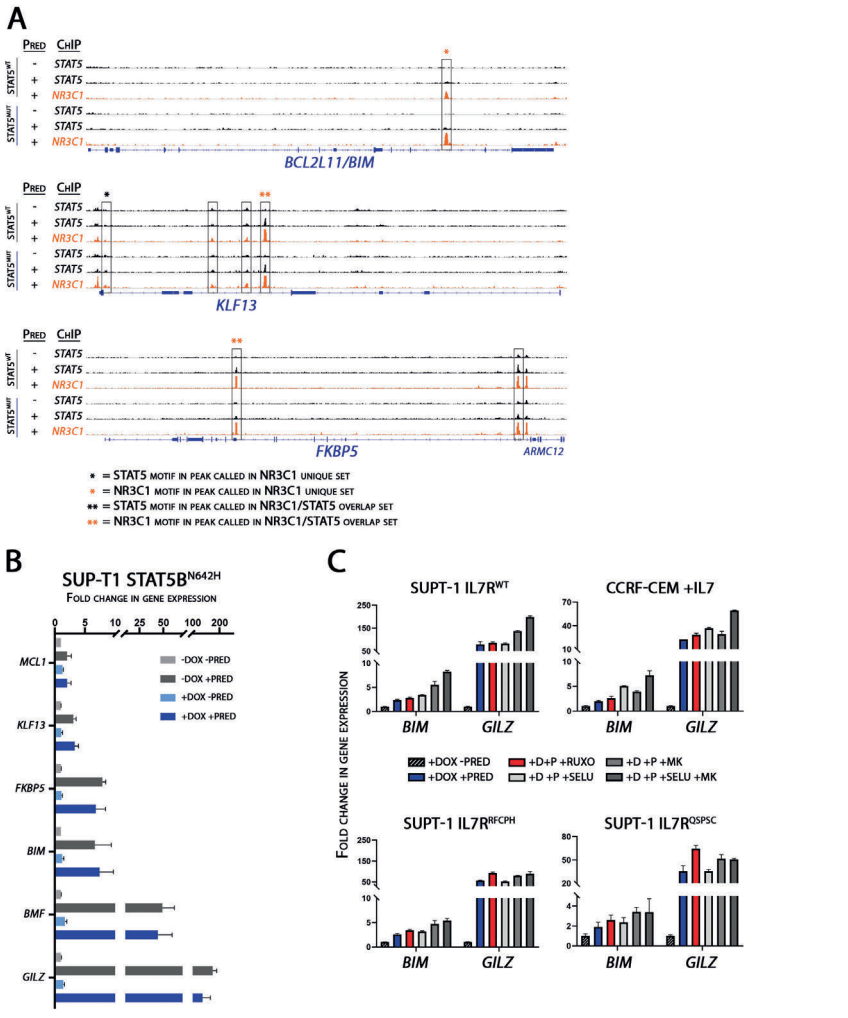

Figure 6. Intact NR3C1 transcriptional activity outbalances steroid-dependent enhanced expression of anti-apoptotic molecules. (A) *ChIP-seq identified binding of NR3C1 and STAT5 transcription factors at GREs of NR3C1 target genes BIM, FKBP5 and KLF13.* **(B)** *Gene expression of NR3C1 target genes (MCL1, KLF13, FKBP5, BIM, BMF and GILZ) in mutant STAT5 overexpressing SUPT-1 cells in the absence or presence of overnight steroid treatment (250µg/ml). Data of biological triplicate with SD indicated.* **(C)** *Immunoblot analysis of BIM-immunoprecipitation in STAT5B^{N642H} SUPT-1 cells (left: total lysate, right: BIM-IP). The protein abundancy of BCL2, BCLXL and BIM was quantified, and the expression in -doxycycline +prednisolone treated cells was taken as reference.* **(D)** *Gene expression of NR3C1 target genes (BIM and GILZ) in wild-type and mutant IL7R overexpressing SUPT-1 cells in the absence and presence of targeted inhibitors. Cells were treated with targeted inhibitors 30 minutes before doxycycline-induction. Steroid exposed cells were treated with prednisolone (250ug/ml) for 16 hours.*

NR3C1 induction of BIM overrides the anti-apoptotic effects of BCL2 and BCL-XL in STAT5B^{N642H} cells

We then explored if the pro-apoptotic steroid response (upregulation of pro-apoptotic BIM via NR3C1) could effectively counter-balance the strong upregulation of anti-apoptotic BCL2 and BCLXL molecules downstream of activated STAT5 during steroid treatment. For this, we performed BIM-immunoprecipitation experiments in non-induced or doxycycline-induced STAT5B^{N642H} SUP-T1 cells that were exposed to prednisolone treatment. As shown in **Figure 7**, steroid treatment led to increased expression of BIM in its active and unphosphorylated form (total lysate, lanes 2 and 4). In line with previous results (12), active BIM strongly bound to BCL2, BCLXL and MCL1 (IP, lane 2). Steroid treatment again enhanced the expression BCL2 and BCLXL in doxycycline-induced STAT5B^{N642H} cells (total lysate, lane 4). However, immunoprecipitated BIM could effectively bind the upregulated BCL2 and BCLXL, despite their increased expression (IP, lane 4). Since STAT5^{N642H} overexpression in SUPT-1 cells does not confer steroid resistance (**Figure 4c-d**), BIM seems to counter the STAT5/NR3C1 driven anti-apoptotic hyper-induction of BCL2 and BCLXL and therefore preserves a sensitive steroid response. Therefore, our study highlights that steroid sensitivity is not solely defined by the upregulation of anti-apoptotic proteins, but is regulated by a tight balance between anti- and pro-apoptotic molecules.

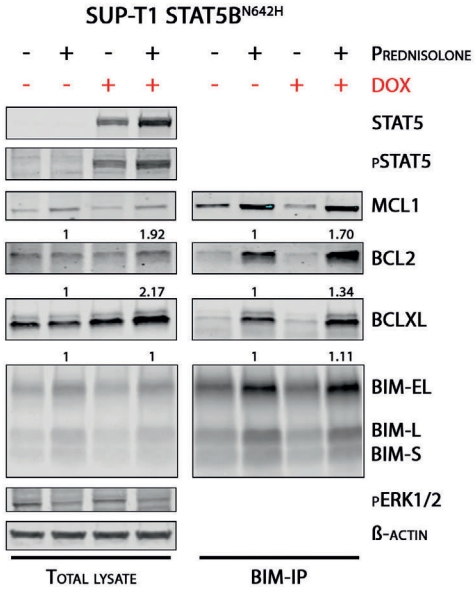

Figure 7. Steroid-induced BIM expression counterbalances STAT5/NR3C1-regulated hyper-induction of BCL2 and BCLXL. *BIM immunoprecipitation of STAT5^{N642H} overexpressing SUPT-1 cells. Steroid exposed cells were treated with prednisolone (250µg/ml) for 16 hours.*

DISCUSSION

Resistance to synthetic steroids remains a problem in the treatment of pediatric ALL. Aberrant activation of the IL7R signaling cascade is frequently observed in T-ALL, either due to production of IL7 by stromal cells in the leukemia microenvironment (7) or by activating mutations in the IL7R signaling pathway (6, 12). Activation of the IL7R pathway has been strongly related to steroid resistance via various pro-survival mechanisms downstream of PI3K-AKT, JAK-STAT and MAPK-ERK signaling pathways. Understanding these resistance mechanisms is of utmost importance, as it may reveal new therapeutic strategies to revert steroid resistance using targeted agents.

In the last decade, various steroid resistance mechanisms that are linked to the IL7R pathway have been uncovered. Interestingly, many of these mechanisms involve the inactivation or activation of pro- (*e.g.,* BIM, BMF) and anti-apoptotic Bcl-2 family members (*e.g.,* BCL2, BCLXL, MCL1), respectively. In healthy lymphocytes, steroid-induced upregulation of BIM is sufficient to neutralize anti-apoptotic Bcl-2 family members, to antagonize their function and to effectuate cellular apoptosis during early T-cell selection processes (39, 40). Overexpression of BCL2 in healthy thymocytes has been demonstrated to outbalance pro-apoptotic BIM, resulting in the abnormal survival and cellular resistance to steroid-induced cell death (41-44). Similarly, upregulation of *BCL2* downstream of STAT5 has been proposed to drive IL7-induced steroid resistance in T-ALL patient samples (7, 18). Here, we demonstrate that upregulation of *BCL2* and *BCLXL* by STAT5 is not sufficient to induce steroid resistance in various T-ALL cellular models.

Previously, we demonstrated that aberrant activation of the MEK-ERK signaling pathway is one of the major drivers of steroid resistance in IL7R, JAK1 and RAS mutant cells, since activated ERK phosphorylates and inactivates pro-apoptotic BIM (12). MEK-inhibitors (and to a lesser extend the JAK-inhibitor ruxolitinib) can re-sensitize IL7-induced or IL7R signaling mutant T-ALL patient cells towards steroid treatment. Other studies also revealed the importance pro-apoptotic BIM, since epigenetic silencing of *BIM* also results in steroid resistance in T-ALL (15, 16).

Our current study suggests that the anti-apoptotic response of activated STAT5 signaling on itself is insufficient to drive steroid resistance. In fact, combined MEK- and AKT-inhibition in mutant-IL7R T-ALL cell models resensitized these cells towards steroid treatment, despite elevated *BCL2* and *BCLXL* expression levels by activated STAT5. The NR3C1-induced expression of BIM seems sufficient to counteract STAT5-induced BCL2 and BCLXL levels through direct binding. Activation of STAT5 may contribute to steroid resistance when the steroid-induced pro-apoptotic BIM response is disabled by (epi-)genetic changes or by MAPK-ERK and PI3K-AKT signaling events (12-16). This is also supported by our observation that active STAT5 signaling, as measured by the

expression of various downstream target genes in primary T-ALL patient cells, is not associated with steroid resistance in T-ALL patients.

This study further reveals that enhanced expression of *BCL2* and other STAT5-regulated genes following steroid exposure reflect a common mechanism in different STAT5 activated T-ALL models. Whereas regulatory sites of many genes can be bound by both inactive (non-phosphorylated) $STAT5^{WT}$ and constitutively active (phosphorylated) $STAT5^{N642H}$, various canonical STAT5 target genes were only bound by active STAT5. Remarkably, NR3C1 is also recruited to these sites upon steroid treatment, which points to important direct co-regulation of NR3C1 in the induction of STAT5 target genes. Although we only analyzed a limited set of genes in more detail, we observed that NR3C1 can be recruited to these sites in the absence of GRE sequences, confirming that NR3C1 can act as a transcriptional co-factor. In combination with our IP results, we suggest that this co-occupancy is caused by direct binding between NR3C1 and STAT5, rather than genomic binding of NR3C1 and STAT5 at overlapping sites. In line with this, we also observed that STAT5 can be recruited to NR3C1-bound target genes irrespective of its activation state. Various of these sites did not contain STAT5 binding motifs, again implying that STAT5 directly binds to NR3C1 rather than binding directly to specific DNA sequences. In contrast to the expression of STAT5-target genes, binding of STAT5 at NR3C1-bound target genes does not further enhance the relative expression of NR3C1 downstream target genes, and the expression of these genes also remained unaffected by ruxolitinib treatment.

Co-binding of STAT5 with NR3C1 has previously been reported to occur during glucocorticoid-induced signaling in T-cells, mammary and hepatocyte epithelial cells (45-48). Apart from acting as an transcription factor, STAT5 is known to regulate chromatin accessibility of the TCRγ-locus or immunoglobulin heavy-chain (49, 50), and induces epigenetic changes at EZH2- and SUZ12-binding sites in $STAT5B^{N642H}$ mutated cells (37). Therefore, STAT5-dependent chromatin remodeling might render (certain) gene sites accessible for NR3C1. This would give an alternative explanation why certain STAT5-target gene sites are only bound by NR3C1 in SUPT-1 cells that overexpress the constitutively active mutant STAT5 molecule.

Our results warrant more detailed research in the mechanisms of STAT5 and NR3C1 cooperation in STAT5-induced and NR3C1/steroid-induced signaling. The complexity of STAT5 regulated transcription is exemplified by the interaction of STAT5 with the transcription factor TLX1 in T-ALL cases that harbor a NUP214-ABL1 fusion. Co-binding of these transcription factors drive the expression of *BCL2* and *MYC* in these leukemias (51). STAT5 therefore seems to act as a versatile transcription factor that can interact with various transcription factors to promote the transcription of STAT5-regulated genes. In fact, TLX1 and STAT5 are predominantly found at the same enhancer sites in *NUP214-ABL1*-positive leukemias, and BET protein inhibitors diminish the expression

of *BCL2* and *MYC*. Moreover, deacetylase inhibitors can also inhibit STAT5-mediated transcription by relocating BET proteins (52). These and our data highlight the plasticity of STAT5 as a transcription factor, and its ability to induce local or broad epigenetic changes in leukemia.

In conclusion, we identified that NR3C1 can directly co-regulate the expression of STAT5 target genes including *BCL2* and *BCLXL*, without influencing the steroid response. We demonstrated that STAT5-regulated expression of *BCL2* and *BCLXL* can be counterbalanced by the upregulation of the pro-apoptotic and steroid response gene *BIM*. Therefore, in the absence of other BIM inactivating mechanisms by aberrant IL7 signaling, STAT5 activation itself is insufficient to provoke steroid resistance in T-ALL.

Acknowledgements. This study was sponsored by grants of the foundation “Kinderen Kankervrij”; KiKa-219 (JvdZ), KiKa-92 and KiKa-295 (WKS), KiKa-335 (VP), KiKa-244 (EV) and KWF-2016-10335 (VC).

Contribution of authors. JvdZ designed study, performed research, and wrote manuscript. JBG, RH, WKS, EV, LG, MN, and VP performed research. RP and VC provided critical input and wrote manuscript. JM designed and supervised the study and wrote manuscript.

Disclosures. None.

REFERENCES

1. Weikum ER, Knuesel MT, Ortlund EA, Yamamoto KR. Glucocorticoid receptor control of transcription: precision and plasticity via allostery. Nat Rev Mol Cell Biol. 2017;18(3):159-74.
2. Wang Z, Malone MH, He H, McColl KS, Distelhorst CW. Microarray analysis uncovers the induction of the proapoptotic BH3-only protein Bim in multiple models of glucocorticoid-induced apoptosis. J Biol Chem. 2003;278(26):23861-7.
3. Jing D, Bhadri VA, Beck D, Thoms JA, Yakob NA, Wong JW, et al. Opposing regulation of BIM and BCL2 controls glucocorticoid-induced apoptosis of pediatric acute lymphoblastic leukemia cells. Blood. 2015;125(2):273-83.
4. Lauten M, Moricke A, Beier R, Zimmermann M, Stanulla M, Meissner B, et al. Prediction of outcome by early bone marrow response in childhood acute lymphoblastic leukemia treated in the ALL-BFM 95 trial: differential effects in precursor B-cell and T-cell leukemia. Haematologica. 2012;97(7):1048-56.
5. Kaspers GJ, Pieters R, Van Zantwijk CH, Van Wering ER, Van Der Does-Van Den Berg A, Veerman AJ. Prednisolone resistance in childhood acute lymphoblastic leukemia: vitro-vivo correlations and cross-resistance to other drugs. Blood. 1998;92(1):259-66.
6. Li Y, Buijs-Gladdines JG, Cante-Barrett K, Stubbs AP, Vroegindeweij EM, Smits WK, et al. IL-7 Receptor Mutations and Steroid Resistance in Pediatric T cell Acute Lymphoblastic Leukemia: A Genome Sequencing Study. PLoS Med. 2016;13(12):e1002200.
7. Delgado-Martin C, Meyer LK, Huang BJ, Shimano KA, Zinter MS, Nguyen JV, et al. JAK/STAT pathway inhibition overcomes IL7-induced glucocorticoid resistance in a subset of human T-cell acute lymphoblastic leukemias. Leukemia. 2017;31(12):2568-76.
8. Oliveira ML, Akkapeddi P, Ribeiro D, Melao A, Barata JT. IL-7R-mediated signaling in T-cell acute lymphoblastic leukemia: An update. Adv Biol Regul. 2019;71:88-96.
9. Barata JT, Silva A, Brandao JG, Nadler LM, Cardoso AA, Boussiotis VA. Activation of PI3K is indispensable for interleukin 7-mediated viability, proliferation, glucose use, and growth of T cell acute lymphoblastic leukemia cells. J Exp Med. 2004;200(5):659-69.
10. Zenatti PP, Ribeiro D, Li W, Zuurbier L, Silva MC, Paganin M, et al. Oncogenic IL7R gain-of-function mutations in childhood T-cell acute lymphoblastic leukemia. Nat Genet. 2011;43(10):932-9.
11. Cante-Barrett K, Spijkers-Hagelstein JA, Buijs-Gladdines JG, Uitdehaag JC, Smits WK, van der Zwet J, et al. MEK and PI3K-AKT inhibitors synergistically block activated IL7 receptor signaling in T-cell acute lymphoblastic leukemia. Leukemia. 2016;30(9):1832-43.
12. van der Zwet JCG, Buijs-Gladdines J, Cordo V, Debets DO, Smits WK, Chen Z, et al. MAPK-ERK is a central pathway in T-cell acute lymphoblastic leukemia that drives steroid resistance. Leukemia. 2021.
13. Piovan E, Yu J, Tosello V, Herranz D, Ambesi-Impiombato A, Da Silva AC, et al. Direct reversal of glucocorticoid resistance by AKT inhibition in acute lymphoblastic leukemia. Cancer Cell. 2013;24(6):766-76.
14. Xie M, Yang A, Ma J, Wu M, Xu H, Wu K, et al. Akt2 mediates glucocorticoid resistance in lymphoid malignancies through FoxO3a/Bim axis and serves as a direct target for resistance reversal. Cell Death Dis. 2019;9(10):1013.
15. Bachmann PS, Gorman R, Papa RA, Bardell JE, Ford J, Kees UR, et al. Divergent mechanisms of glucocorticoid resistance in experimental models of pediatric acute lymphoblastic leukemia. Cancer Res. 2007;67(9):4482-90.
16. Bachmann PS, Piazza RG, Janes ME, Wong NC, Davies C, Mogavero A, et al. Epigenetic silencing of BIM in glucocorticoid poor-responsive pediatric acute lymphoblastic leukemia, and its reversal by histone deacetylase inhibition. Blood. 2010;116(16):3013-22.

17. Franchimont D, Galon J, Vacchio MS, Fan S, Visconti R, Frucht DM, et al. Positive effects of glucocorticoids on T cell function by up-regulation of IL-7 receptor alpha. J Immunol. 2002;168(5):2212-8.
18. Meyer LK, Huang BJ, Delgado-Martin C, Roy RP, Hechmer A, Wandler AM, et al. Glucocorticoids paradoxically facilitate steroid resistance in T cell acute lymphoblastic leukemias and thymocytes. J Clin Invest. 2020;130(2):863-76.
19. De Smedt R, Morscio J, Reunes L, Roels J, Bardelli V, Lintermans B, et al. Targeting cytokine- and therapy-induced PIM1 activation in preclinical models of T-cell acute lymphoblastic leukemia and lymphoma. Blood. 2020;135(19):1685-95.
20. Ribeiro D, Melao A, van Boxtel R, Santos CI, Silva A, Silva MC, et al. STAT5 is essential for IL-7-mediated viability, growth, and proliferation of T-cell acute lymphoblastic leukemia cells. Blood Adv. 2018;2(17):2199-213.
21. Maude SL, Dolai S, Delgado-Martin C, Vincent T, Robbins A, Selvanathan A, et al. Efficacy of JAK/STAT pathway inhibition in murine xenograft models of early T-cell precursor (ETP) acute lymphoblastic leukemia. Blood. 2015;125(11):1759-67.
22. Cante-Barrett K, Mendes RD, Smits WK, van Helsdingen-van Wijk YM, Pieters R, Meijerink JP. Lentiviral gene transfer into human and murine hematopoietic stem cells: size matters. BMC Res Notes. 2016;9:312.
23. Meijerink J, Mandigers C, van de Locht L, Tonnissen E, Goodsaid F, Raemaekers J. A novel method to compensate for different amplification efficiencies between patient DNA samples in quantitative real-time PCR. J Mol Diagn. 2001;3(2):55-61.
24. Li H, Durbin R. Fast and accurate short read alignment with Burrows-Wheeler transform. Bioinformatics. 2009;25(14):1754-60.
25. Zhang Y, Liu T, Meyer CA, Eeckhoute J, Johnson DS, Bernstein BE, et al. Model-based analysis of ChIP-Seq (MACS). Genome Biol. 2008;9(9):R137.
26. Ramirez F, Ryan DP, Gruning B, Bhardwaj V, Kilpert F, Richter AS, et al. deepTools2: a next generation web server for deep-sequencing data analysis. Nucleic Acids Res. 2016;44(W1):W160-5.
27. Robinson JT, Thorvaldsdottir H, Winckler W, Guttman M, Lander ES, Getz G, et al. Integrative genomics viewer. Nat Biotechnol. 2011;29(1):24-6.
28. Quinlan AR, Hall IM. BEDTools: a flexible suite of utilities for comparing genomic features. Bioinformatics. 2010;26(6):841-2.
29. Machanick P, Bailey TL. MEME-ChIP: motif analysis of large DNA datasets. Bioinformatics. 2011;27(12):1696-7.
30. Homminga I, Pieters R, Langerak AW, de Rooi JJ, Stubbs A, Verstegen M, et al. Integrated Transcript and Genome Analyses Reveal NKX2-1 and MEF2C as Potential Oncogenes in T Cell Acute Lymphoblastic Leukemia. Cancer Cell. 2011;19(4):484-97.
31. Gautier L, Cope L, Bolstad BM, Irizarry RA. affy--analysis of Affymetrix GeneChip data at the probe level. Bioinformatics. 2004;20(3):307-15.
32. Liu Y, Easton J, Shao Y, Maciaszek J, Wang Z, Wilkinson MR, et al. The genomic landscape of pediatric and young adult T-lineage acute lymphoblastic leukemia. Nat Genet. 2017;49(8):1211-8.
33. de Araujo ED, Erdogan F, Neubauer HA, Meneksedag-Erol D, Manaswiyoungkul P, Eram MS, et al. Structural and functional consequences of the STAT5B(N642H) driver mutation. Nat Commun. 2019;10(1):2517.
34. Govaerts I, Jacobs K, Vandepoel R, Cools J. JAK/STAT Pathway Mutations in T-ALL, Including the STAT5B N642H Mutation, are Sensitive to JAK1/JAK3 Inhibitors. Hemasphere. 2019;3(6):e313.

35. Kontro M, Kuusanmaki H, Eldfors S, Burmeister T, Andersson EI, Bruserud O, et al. Novel activating STAT5B mutations as putative drivers of T-cell acute lymphoblastic leukemia. Leukemia. 2014;28(8):1738-42.
36. Bandapalli OR, Schuessele S, Kunz JB, Rausch T, Stutz AM, Tal N, et al. The activating STAT5B N642H mutation is a common abnormality in pediatric T-cell acute lymphoblastic leukemia and confers a higher risk of relapse. Haematologica. 2014;99(10):e188-92.
37. Pham HTT, Maurer B, Prchal-Murphy M, Grausenburger R, Grundschober E, Javaheri T, et al. STAT5BN642H is a driver mutation for T cell neoplasia. J Clin Invest. 2018;128(1):387-401.
38. Strahle U, Klock G, Schutz G. A DNA sequence of 15 base pairs is sufficient to mediate both glucocorticoid and progesterone induction of gene expression. Proc Natl Acad Sci U S A. 1987;84(22):7871-5.
39. Willis SN, Fletcher JI, Kaufmann T, van Delft MF, Chen L, Czabotar PE, et al. Apoptosis initiated when BH3 ligands engage multiple Bcl-2 homologs, not Bax or Bak. Science. 2007;315(5813):856-9.
40. Strasser A. The role of BH3-only proteins in the immune system. Nat Rev Immunol. 2005;5(3):189-200.
41. Gratiot-Deans J, Merino R, Nunez G, Turka LA. Bcl-2 expression during T-cell development: early loss and late return occur at specific stages of commitment to differentiation and survival. Proc Natl Acad Sci U S A. 1994;91(22):10685-9.
42. Siegel RM, Katsumata M, Miyashita T, Louie DC, Greene MI, Reed JC. Inhibition of thymocyte apoptosis and negative antigenic selection in bcl-2 transgenic mice. Proc Natl Acad Sci U S A. 1992;89(15):7003-7.
43. Sentman CL, Shutter JR, Hockenbery D, Kanagawa O, Korsmeyer SJ. bcl-2 inhibits multiple forms of apoptosis but not negative selection in thymocytes. Cell. 1991;67(5):879-88.
44. Wojciechowski S, Tripathi P, Bourdeau T, Acero L, Grimes HL, Katz JD, et al. Bim/Bcl-2 balance is critical for maintaining naive and memory T cell homeostasis. J Exp Med. 2007;204(7):1665-75.
45. Stocklin E, Wissler M, Gouilleux F, Groner B. Functional interactions between Stat5 and the glucocorticoid receptor. Nature. 1996;383(6602):726-8.
46. Stoecklin E, Wissler M, Moriggl R, Groner B. Specific DNA binding of Stat5, but not of glucocorticoid receptor, is required for their functional cooperation in the regulation of gene transcription. Mol Cell Biol. 1997;17(11):6708-16.
47. Mueller KM, Themanns M, Friedbichler K, Kornfeld JW, Esterbauer H, Tuckermann JP, et al. Hepatic growth hormone and glucocorticoid receptor signaling in body growth, steatosis and metabolic liver cancer development. Mol Cell Endocrinol. 2012;361(1-2):1-11.
48. Petta I, Dejager L, Ballegeer M, Lievens S, Tavernier J, De Bosscher K, et al. The Interactome of the Glucocorticoid Receptor and Its Influence on the Actions of Glucocorticoids in Combatting Inflammatory and Infectious Diseases. Microbiol Mol Biol Rev. 2016;80(2):495-522.
49. Ye SK, Agata Y, Lee HC, Kurooka H, Kitamura T, Shimizu A, et al. The IL-7 receptor controls the accessibility of the TCRgamma locus by Stat5 and histone acetylation. Immunity. 2001;15(5):813-23.
50. Bertolino E, Reddy K, Medina KL, Parganas E, Ihle J, Singh H. Regulation of interleukin 7-dependent immunoglobulin heavy-chain variable gene rearrangements by transcription factor STAT5. Nat Immunol. 2005;6(8):836-43.
51. Vanden Bempt M, Demeyer S, Broux M, De Bie J, Bornschein S, Mentens N, et al. Cooperative Enhancer Activation by TLX1 and STAT5 Drives Development of NUP214-ABL1/TLX1-Positive T Cell Acute Lymphoblastic Leukemia. Cancer Cell. 2018;34(2):271-85 e7.
52. Pinz S, Unser S, Buob D, Fischer P, Jobst B, Rascle A. Deacetylase inhibitors repress STAT5-mediated transcription by interfering with bromodomain and extra-terminal (BET) protein function. Nucleic Acids Res. 2015;43(7):3524-45.

Supplemental Table 1. *Peak details of ChIP motif analysis of NR3C1 and STAT5 motifs significantly enriched in NR3C1/STAT5 unique or overlapping peak sets.*

Link:
https://tinyurl.com/Chap6-SuppTable1-Jordy-vd-Zwet

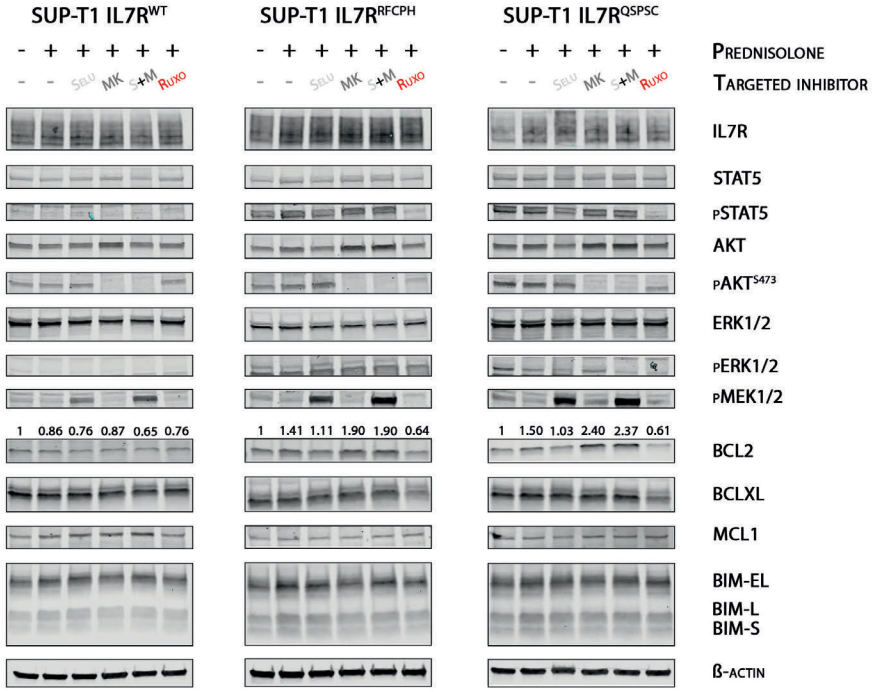

Supplemental Figure 1. *Immunoblot analysis of wild type and mutant IL7R overexpressing cells treated with prednisolone, ruxolitinib (1µM, JAK1/2-inhibitor), selumetinib (1µM, MEK-inhibitor) and/or MK2206 (0,5µM AKT-inhibitor). Cells were treated with targeted inhibitors 30 minutes before doxycycline-induction. Steroid exposed cells were treated with prednisolone (250µg/ml) for 16 hours.*

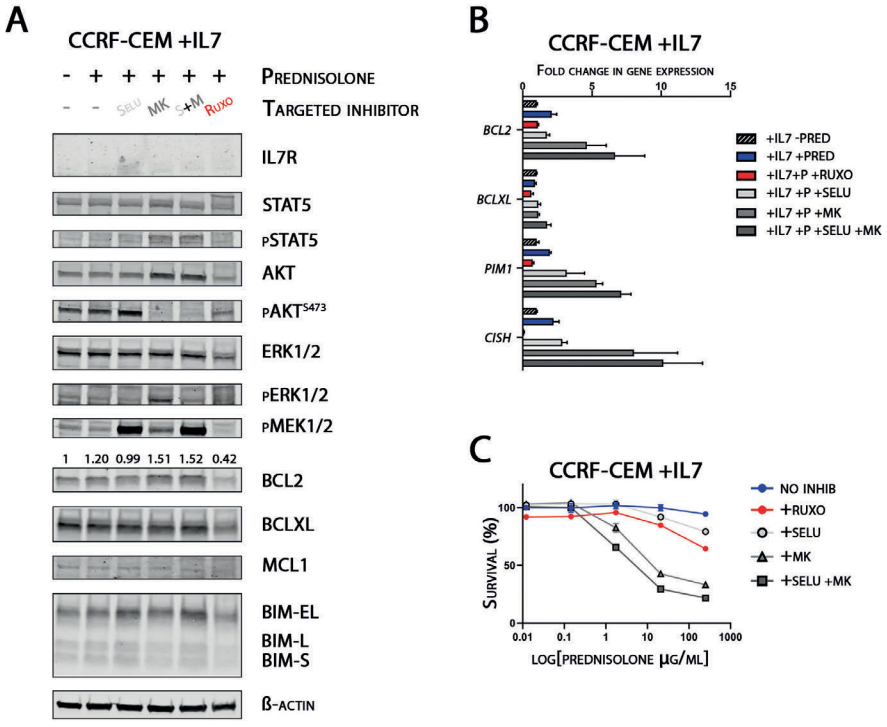

Supplemental Figure 2. (A) *Immunoblot analysis of CCRF-CEM cells co-cultured with IL7. Cells were treated with targeted inhibitors (ruxolitinib (1µM, JAK1/2-inhibitor), selumetinib (1µM, MEK-inhibitor) and/or MK2206 (0,5µM AKT-inhibitor)) 30 minutes before doxycycline-induction. Steroid exposed cells were treated with prednisolone (250µg/ml) for 16 hours.* **(B)** *Corresponding expression of STAT5B target genes of these CCRF-CEM cells.* **(C)** *Steroid sensitivity of CCRF-CEM cells in the absence or presence of targeted inhibitors. Steroid sensitivity was determined by a 4-day MTT read-out. Representative data of biological duplicate.*

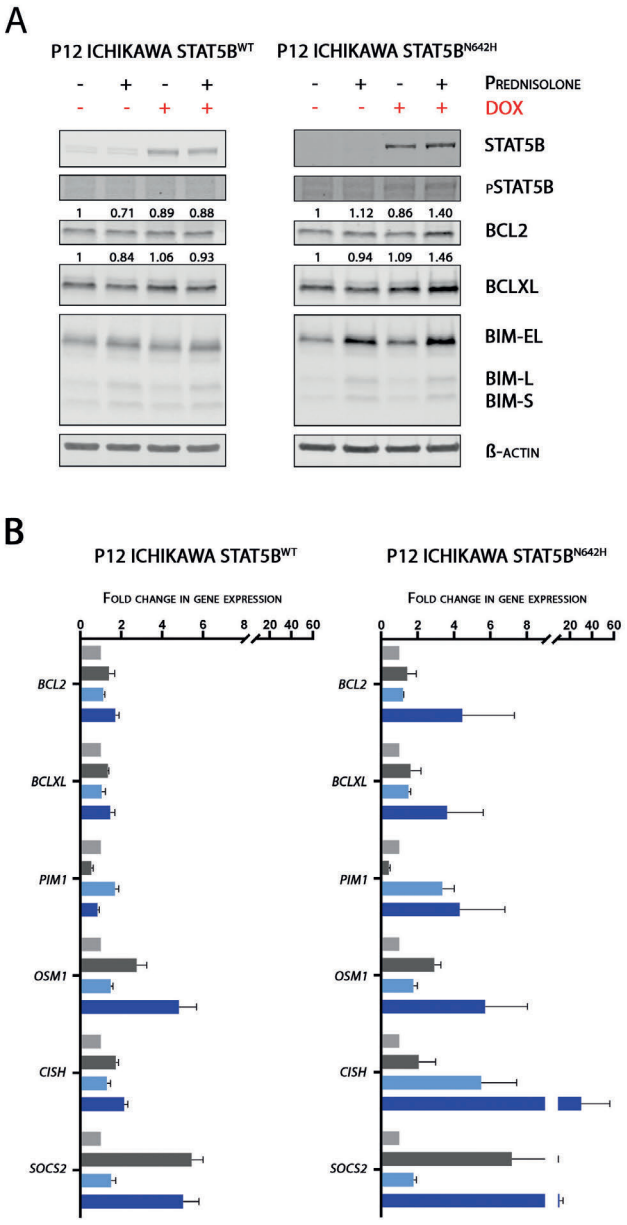

Supplemental Figure 3. (A) *Activation of STAT5B signaling and expression of anti-apoptotic Bcl2 family proteins in STAT5B wild-type and mutant overexpressing P12 ICHIKAWA cells. Protein band intensity for BCL2 and BCLXL represented relative to -dox-pred condition.* **(B)** *Expression STAT5 target genes in STAT5BWT and STAT5BN642H overexpressing P12 ICHIKAWA cells in the absence or presence of prednisolone treatment (250µg/ml) for 16 hours. Data of biological triplicate with SD indicated.*

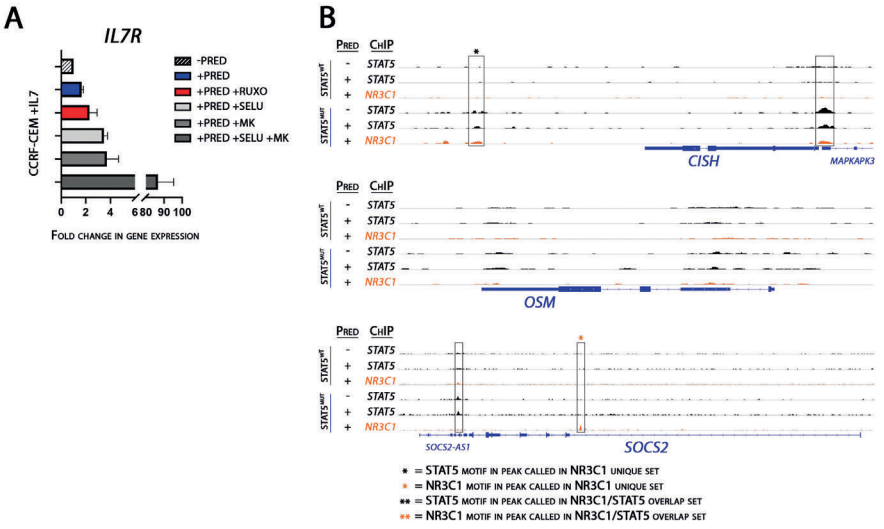

Supplemental Figure 4. (A) *Expression of IL7R in CCRF-CEM cells exposed to IL7. Cells were treated with targeted inhibitors 30 minutes before IL7 exposure. Steroid exposed cells were treated with prednisolone (250µg/ml) for 16 hours.* **(B)** *ChIP-seq identified binding of NR3C1 and STAT5 transcription factors at STAT5 target genes OSM, CISH and SOCS2.*

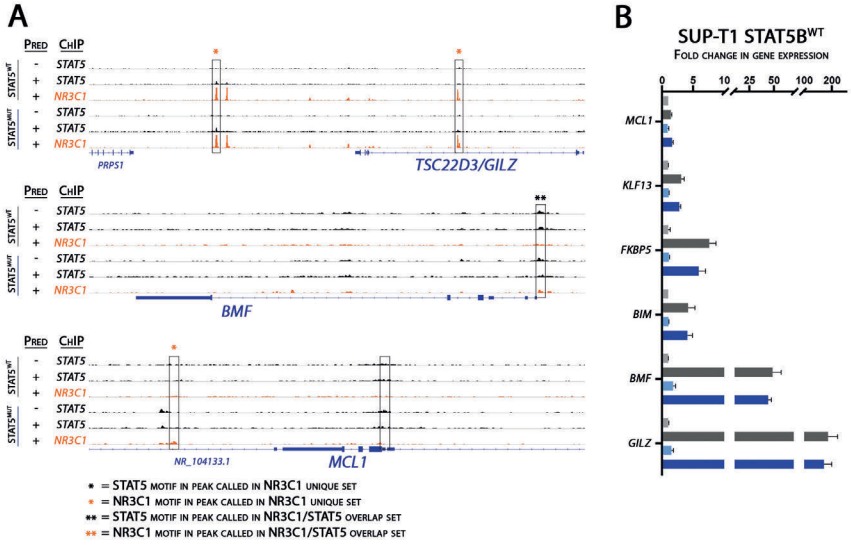

Supplemental Figure 5. (A) *ChIP-seq identified binding of NR3C1 and STAT5 transcription factors at NR3C1 target genes BMF, GILZ and MCL1.* **(B)** *Gene expression of NR3C1 target genes (MCL1, KLF13, FKBP5, BIM, BMF and GILZ) in wild type STAT5 overexpressing SUPT-1 cells in the absence or presence of overnight steroid treatment (250µg/ml).*

Supplemental Table 1. *Peak details of NR3C1 and STAT5 ChIP.*

Online link to Table S1: https://tinyurl.com/Chap6-SuppTable1-Jordy-vd-Zwet

7

The biological and clinical impact of the AKT E17K mutation in T-cell acute lymphoblastic leukemia

Jordy C.G. van der Zwet[1], Izabella Mollova[1], Jessica G.C.A.M Buijs-Gladdines[1], Laura Graus[1], Willem K. Smits[1], Frank L. Bos[1], Anne C. Rios[1] and Jules P.P. Meijerink[1].

[1]Princess Máxima Center for Pediatric Oncology, Utrecht, the Netherlands

ABSTRACT

Aberrant PI3K-AKT pathway activation due to activating IL7R mutations or other genetic aberrations is observed in over 40% of T-cell acute lymphoblastic leukemia (T-ALL) patients and has been associated to steroid resistance in T-ALL patients. Here, we demonstrate that overexpression of AKT^{WT} induces severe resistance to prednisolone treatment in SUPT-1 cells. Surprisingly, the activating AKT^{E17K} mutant only slightly impairs steroid sensitivity. We investigated the differences in the activation mechanisms between AKT^{WT} and AKT^{E17K}, and observed that AKT^{E17K} is predominantly located at the inner side of the plasma membrane, while AKT^{WT} has a patchy localization throughout the cell. Moreover, AKT^{E17K} is predominantly phosphorylated at T308 compared to S473 phosphorylation in contrast to AKT^{WT} cells. This suggests that mutations in the plecktrin homology (PH)-domain can drive an open AKT configuration and membrane binding independent from the requirement for S473 phosphorylation. We did not observe differences in the phosphorylation of downstream AKT substrates including GSK3A/B and FOXO3A between AKT^{WT} and AKT^{E17K} cells. ATP-competitive AKT inhibitors enhanced steroid-induced cell death in AKT^{WT} and AKT^{E17K} cells. As expected, AKT^{E17K} seemed less affected by allosteric inhibitors compared to AKT^{WT} cells, and these inhibitors only synergized with steroid treatment in AKT^{WT} cells. Combined, this study highlights differences in AKT^{WT} and AKT^{E17K} activation mechanisms and that this affects steroid responsiveness in T-ALL.

INTRODUCTION

Activation of the IL-7 receptor (IL7R) signaling pathway has been thoroughly studied in the context of normal T-cell development and leukemogenesis. IL-7-induced homodimerization of the IL7Rα and -γc chains activates downstream signaling pathways that promote the differentiation and proliferation of early T cells (1). In T-cell acute lymphoblastic leukemia (T-ALL), activating mutations in the IL7R signaling cascade (in IL7Ra, JAK1, JAK3, STAT5B, N/K RAS and AKT) contribute to leukemogenesis by aberrantly activating downstream JAK-STAT, MAPK-ERK and PI3K-AKT pathways (2, 3). These mutations are associated with decreased event-free survival and most cause steroid resistance (3). In addition, T-ALL blasts also increase steroid resistance in the presence of interleukin-7 (IL-7) (4). As synthetic steroids are cornerstone drugs in upfront ALL treatment regimens, and patients with poor steroid response have an inferior outcome. Therefore, it is critical to understand how aberrant IL7R signaling interferes with steroid sensitivity to develop adequate intervention strategies.

Ligand-induced IL7R signaling activates PI3K at the plasma membrane, which converts phosphoinositide PIP2 into PIP3 to recruit AKT from the cytosol to the plasma membrane (5, 6). At the plasma membrane, engagement and binding of PI3K-generated phospholipids with the N-terminal PH-domain of AKT relieves AKT from its inactive and closed conformation. The open and active AKT conformation allows phosphorylation of AKT at T308 ($pAKT^{308}$) in the activation loop by PDK1 and at the C-terminal S473 residue ($pAKT^{473}$) by mTORC2 (7-9). Phospholipid-independent activation of AKT is effectuated by C-terminal phosphorylation of S473 and/or S477/T479 sites (10, 11). Phosphorylated S473 interacts with the linker of the PH-domain, subsequently relieving autoinhibition of the PH-domain and exposing the activation loop to PDK1-dependent phosphorylation of T308 (10). Activated and phosphorylated AKT further drives phosphorylation of numerous AKT downstream substrates that results in their activation or inhibition (10). AKT substrates that directly or indirectly affect cell growth or cell death include Forkhead Box O (FOXO) transcription factors, CREB, IKK, BAD, GSK3 and mTORC1 (12-15).

Aberrant PI3K-AKT pathway activation is frequently observed in T-ALL due to activating mutations in *PI3K or AKT* itself, or due to loss-of-function mutations of the phosphatase PTEN that normally acts as a negative regulator of PI3K (2, 3, 16-19). Specific PI3K-AKT activating aberrations are predominantly found in *TAL1*- or *LMO2*-rearranged patients (18, 19), and PTEN inactivating events predict for inferior outcome (16, 18, 20, 21). High PI3K-AKT pathway activity in T-ALL has been identified as a cause for steroid resistance (3, 22, 23) and a few mechanisms have been suggested to effectuate PI3K-AKT-induced steroid resistance, including the upregulation of anti-apoptotic MCL1 and BCL-XL (20, 24), phosphorylation of the transcription factor FOXO3a to subsequently inhibit the transcription of pro-apoptotic *BIM* (25), or phosphorylation of the glucocorticoid receptor (NR3C1) at S104 that impairs nuclear translocation of NR3C1 upon steroid

binding and therefore impairs the activation of its downstream target genes (including *BIM*) (26). As a result, PI3K-AKT signaling can influence the balance between pro-apoptotic (e.g. BIM) and anti-apoptotic (e.g. MCL1, BCL-XL) Bcl-2 family proteins.

Transforming AKT^{E17K} mutations are found in around 2-3% of pediatric T-ALL patients (2, 16). The E17K mutation, located in the PH-domain of AKT, disables the auto-inhibition of the PH-domain by abrogating the interaction between Glu17 and Lys14 (27). Consequently, AKT^{E17K} can enhance the interaction with D5-phosphorylated phosphoinositides to enhance its binding to the inner side of the cell membrane in NIH 3T3 cells (27). AKT^{E17K} behaves as a transforming mutation in IL3-dependent BaF3 cells that facilitates ligand-independent growth in contrast to wild type AKT (AKT^{WT}) (2). However, overexpression of AKT^{WT} but not AKT^{E17K} was shown to confer strong steroid resistance in steroid-sensitive SUPT-1 and P12 Ichikawa cells (2, 3). These seemingly contradicting results point to important differences in downstream regulated pathways or processes that are important for proliferation (by AKT^{E17K}) and steroid resistance (by AKT^{WT}). We therefore aimed to uncover mechanistic differences in AKT^{E17K} and AKT^{WT} induced signaling explanatory for differences in cell survival and steroid responsiveness.

MATERIALS AND METHODS

Generation cell lines and culturing conditions for SUPT-1 cells
Lentiviral transduction of SUPT-1 cell lines was performed as previously described (28). Transduced cells were cultured in RPMI-1640 medium (Gibco) supplemented with 1x Glutamax, 10% heat-inactivated fetal bovine serum (Gibco), 2% pencillin/streptomycin (Gibco), 0,4% Fungizone (Gibco) and 1-2 µg/mL puromycin. Expression of the cloned human cDNA insert was induced by doxycycline (0.5 µg/ml) for at least 16 hours, or as indicated differently.

Cell toxicity screens SUPT-1 and PDX cells
SUPT-1 cell toxicity screens were performed by a 4-day methylthiazolyldiphenyl-tetrazolium bromide (MTT, Sigma Aldrich) assay as previously described (chapter 3). For dual compound screens, Bliss synergy was calculated with R package: 'synergyfinder' (29). Cytotoxicity screen of PDX samples was performed as previously described (3, 28). PDX cells were cultured in RPMI-1640 medium (Gibco) supplemented with 1x Glutamax, 20% heat-inactivated fetal bovine serum (Gibco), 2% pencillin/streptomycin (Gibco) and 0,4% Fungizone (Gibco). Cell viability after four days was measured by ATPlite 1Step (Perkin Elmer, Groningen, The Netherlands).

Immunoblot analysis and protein cell fractionation
Protein isolation and immunoblot analysis was performed as previously described (chapter 3). Cytoplasmic and nuclear protein fractions were isolated using the Active Motif Nuclear Complex Co-IP kit (Active Motif®) according to the manufacturer's

procedures. To the hypotonic and digestion buffers, additional HALT protease/phosphatase inhibitor (1:200) (Thermo Fisher Scientific) was added. Antibodies used for immunoblot analysis: AKT (CST, 9272S), pAKT-308 (CST, 9275S), pAKT-473 (CST, 9271S), GSK3 (CST, 5676P), pGSK3-S21/9 (CST, 9331S), MCL1 (Santa Cruz, sc-12756), BCL2 (Santa Cruz, sc-130308), BCLXL (CST, 2764S), BIM (abcam, ab32158), B-actin (abcam, ab6276), NR3C1 (Santa Cruz, sc-1003), pNR3C1-S134 (Millipore Q2668259), FOXO3a (CST, 12829S) and pFOXO3a (CST, 13129S).

Intracellular staining and flowcytometry

Doxycycline-induced cells were washed with Automax Pro Running buffer (MACS Buffer, Miltenyi Biotec) and fixed in 2-4% formaldehyde/Phosphate-buffered Saline (PBS, Thermo Fisher Scientific) for 10 minutes at 37°C, followed by 1 minute incubation on ice. Subsequently, cells were centrifuged and permeabilized in cold (4°C) 90% methanol for 30 minutes on ice. Afterwards, cells were subjected to primary antibody incubation for 1 hour at room temperature (RT). After multiple washing steps, cells were incubated with an IRDye fluorescently labelled secondary antibody (LI-COR®) for 30 minutes at RT. Finally, cells were washed, and fluorescence was measured on the CytoFLEX S flow cytometer (Beckman Coulter). Data was analyzed using FlowJo® software. Antibodies used for flowcytometry: AKT (CST, 9272S), pAKT-308 (CST, 9275S), pAKT-473 (CST, 9271S).

Confocal imaging

Fixation and permeabilization of doxycycline-induced SUPT-1 cells were performed as described above. Cells were stained for AKT (CST #9272) for 1 hour at RT. After thorough washing, cells were stained with a fluorescent secondary antibody (AF 488) for 1 hour in the dark at RT. Cells were again washed and resuspended in Automax Pro Running buffer. Last, DAPI (1:500, Thermo Fisher Scientific, AF 358/461) was added to the suspension. After a 10-minute incubation at RT, cells were directly plated on poly-L-lysine (Sigma Aldrich) coated cover glass and imaged using the Leica Confocal SP8 Microscope. Images were analyzed using the Fiji imaging software.

Quantitative real-time reverse-transcription PCR (RTQ-PCR)

RNA isolation, cDNA synthesis and quantitative real-time reverse-transcription PCR was performed as previously described (chapter 3). Primer sequences for *GAPDH*, *BIM*, *BCL2*, *MCL1* and *BCLXL* were previously described (chapter 3, and reference 3 in this chapter). Other primer sequences: *FasL* forward 5'-CCACCCCCTGAAAAAA-3', *FasL* reverse 5'-GATCCTGGGGATACTTAGAGT-3', *TRAIL* forward 5'-TGCTCCTGCAGTCTCTCT-3', *TRAIL* reverse 5'-CAGGGGCTGTTCATACTCT-3', *p15* forward 5'-GATCCCAACGGAGTCAA-3', *p15* reverse 5'- AGGTACCCTGCAACGT-3', *p19* forward 5'- GCTGCTGGAGGAGGTT-3', *p19* reverse 5'- GCTGCGTCATGGACTG-3', $p21^{CIP1}$ forward 5'- CCGGCTGATCTTCTCC-3', $p21^{CIP1}$ reverse 5'- AAATGCCCAGCACTCTTA-3', $p27^{KIP1}$ forward 5'-GCCTGGCCTCAGAAGA-3' and $p27^{KIP1}$ reverse 5'- AGAGGCAGATCATTTAAGAGTG-3'.

RESULTS

The steroid-responsive AKT^{E17K} mutation demonstrates enhances membrane localization

We first validated previous observed findings in relation to steroid responsiveness for T-ALL cells that express AKT^{E17K} and AKT^{WT} (3)). For this, we generated new doxycycline-inducible BFP-tagged AKT^{WT} and AKT^{E17K} SUPT-1 cell lines. As non-induced derivative SUPT-1 cells remained equally sensitive to steroid treatment compared to parental SUPT-1 cells (data not shown), induction of AKT^{WT} expression by addition of doxycycline strongly raised steroid resistance (**Figure 1a**). In line with previous observations (20),overexpression of AKT^{E17K} only slightly raised steroid resistance (**Figure 1b**). To explore the underlying mechanisms of steroid resistance, we studied if AKT overexpression would affect the steroid-induced upregulation of pro-apoptotic *BIM.* Treatment with prednisolone significantly induced *BIM* expression, independent of overexpression of AKT^{WT} or AKT^{E17K} (**Figure 1c-d**). We also did not observe differences in the transcriptional levels of anti-apoptotic *BCL2, BCLXL* and *MCL1* genes among doxycycline-induced AKT^{WT} and AKT^{E17K} SUPT-1 cells compared to non-induced cells (**Figure 1c-d**). Therefore, we conclude that differences in steroid sensitivity between AKT^{WT} and AKT^{E17K} SUPT-1 cells was not caused by an altered transcriptional response of pro- and/or anti-apoptotic molecules.

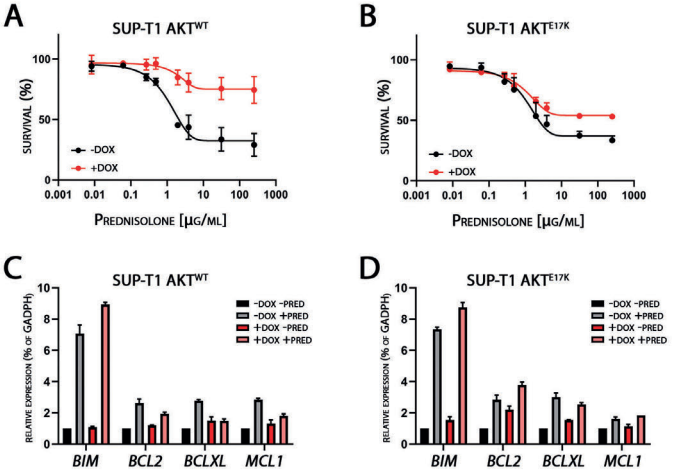

Figure 1. **(A-B)** *Cell toxicity screening of doxycycline-induced AKT^{WT} (A) and AKT^{E17K} (B) SUPT-1 cell lines (n=3). The non-induced counterparts are used as a negative control and represent the steroid sensitivity of SUPT-1 cells. Cells were treated with prednisolone (range 0.00822 – 250 µg/ml) for four days. (***C-D***). Relative expression of pro-apoptotic BIM, and anti-apoptotic BCL2, BCLXL and MCL1 genes in AKT^{WT} (C) and AKT^{E17K} (D) cells. Expression was normalized to GAPDH expression. The expression of non-induced cells that were not treated with prednisolone was used as baseline (relative expression=1). RT-QPCR was performed on both doxycycline-induced and non-induced samples that were treated overnight with prednisolone (250 µg/ml) (n=2).*

The E17K mutation impacts cellular localization and phospho-activation of AKT

Since the mutated AKT^{E17K} protein shows increased recruitment to the membrane in NIH 3T3 cells (27), we hypothesized that the cellular localization of AKT is important to induce steroid resistance. To study if the AKT^{E17K} mutation demonstrated enhanced membranal localization in our T-ALL SUPT-1 model, we performed immunofluorescence confocal imaging on AKT^{WT} and AKT^{E17K} overexpressing cell lines. Whereas overexpressed AKT^{WT} localized throughout the cell, AKT^{E17K} was predominantly recruited to the inner side of the outer cell membrane (**Figure 2a**). This was further investigated by studying the expression of total AKT protein and phosphorylated AKT isoforms (T308 and S473) using flowcytometry. Induction of AKT^{WT} or AKT^{E17K} was accompanied with enhanced phosphorylation of both S473 and T308 (**Figure 2b**, pAKT^{473} and pAKT^{308} for non-induced cells are not shown). Interestingly, phosphorylation of kinase domain activation marker T308 is more prominent than S473 phosphorylation for AKT^{E17K} cells than for AKT^{WT} (**Figure 2b**).

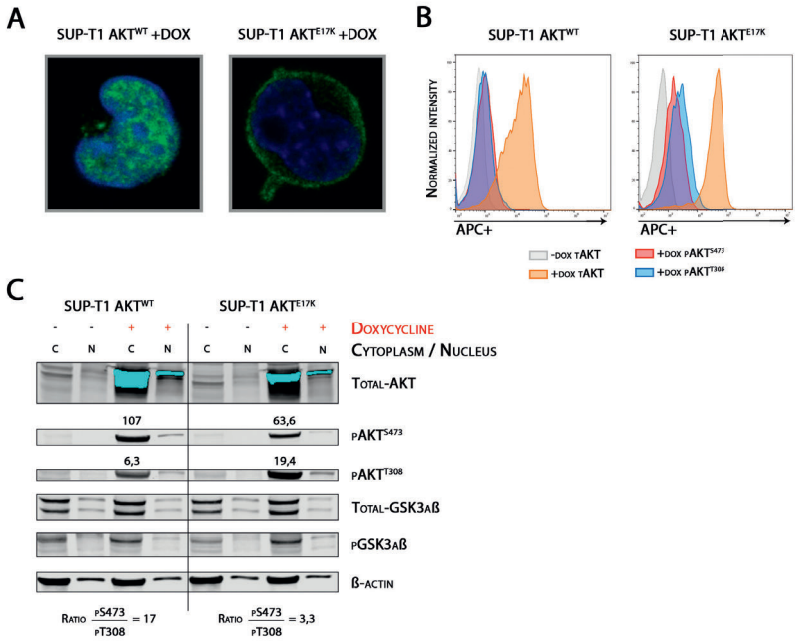

Figure 2. (A) *Confocal imaging of doxycycline-induced AKT^{WT} (left) and AKT^{E17K} (right) SUPT-1 cells. Intracellular staining for AKT is visualized in green, and DAPI (blue) staining was performed to visualize the cell nucleus.* **(B)** *Flowcytometry of intracellular stained doxycycline-induced AKT^{WT} (left) and AKT^{E17K} (right) SUPT-1 cells. Fluorescence of total AKT is illustrated in orange, phosphorylation of S473 in red and phosphorylation of the T308 phospho-site in blue. The fluorescence of non-doxycycline-induced cells stained for total-AKT was illustrated as negative control (grey).* **(C)** *Immunoblot analysis of cytoplasmic and nuclear cell fractions of doxycycline-induced AKT^{WT} (left) and AKT^{E17K} (right) SUPT-1 cells. The band intensities of pAKT^{S473} and pAKT^{T308} were quantified, and the ratio between pS473/pT308 was calculated.*

This was further confirmed by performing immunoblot analysis on cellular fractions for AKT^{WT} and AKT^{E17K} expressing SUPT-1 cells (**Figure 2c**), which also demonstrated that S473 phosphorylation was more prominent over T308 phosphorylation in AKT^{WT} cells. The S473/S308 phosphorylation ratios for AKT^{E17K} and AKT^{WT} cells were 3,3 versus 17, respectively. This suggested that these cell lines have different AKT activation mechanisms that may be related to differences in cellular localization. The different S473/S308 phosphorylation ratios did not alter the kinase activity of AKT as GSK3 phosphorylation levels of the AKT substrate was similar in AKT^{WT} and AKT^{E17K} cells. To summarize, the transforming AKT^{E17K} mutant molecule is preferentially localized at the inner cell membrane, enriches T308 phosphorylation relative to S473 phosphorylation, but is equally effective to phosphorylate downstream substrates such as GSK3 as AKT^{WT} cells.

NR3C1 and FOXO3a phosphorylation is similar between AKT^{WT} and AKT^{E17K} overexpressing cells

To study if AKT^{WT} could selectively modulate the function of downstream substrates that are involved in steroid-induced cell death compared to AKT^{E17K}, we performed immunoblot analysis on total cell lysates from AKT^{WT} and AKT^{E17K} cells at several time points following doxycycline-induction (**Figure 3a**). Again we observed that AKT^{E17K} has relatively abundant phosphorylation of T308, while AKT^{WT} molecules have relative higher levels of S473 phosphorylation compared to T308 phosphorylation. We observed no differences in the levels of phospho-MCL1, which can be phosphorylated by activated PI3K-AKT signaling. Phosphorylation of NR3C1 by AKT at S134 results in enhanced cytoplasmic retention and steroid resistance (26). However, we did not observe higher S134 phosphorylation following induction in AKT^{WT} cells compared to AKT^{E17K} E17K cells. This is in line with our observations that the expression of NR3C1 target gene *BIM* remains unaffected upon steroid treatment in both lines (**Figure 1c-d**). We also did not observe differences in the phosphorylation of FOXO3a, and the expression of various FOXO3a regulated genes including p15, p19, $p21^{CIP1}$, $p27^{KIP1}$, FasL and TRAIL was similar for non-induced and induced AKT^{WT}- and AKT^{E17K}-expressing SUPT-1 cells (**Figure 3b**). Therefore, we conclude that the difference in steroid sensitivity between AKT^{WT} and AKT^{E17K} cells could not be explained by differences in phosphorylation levels of pronounced AKT targets such as GSK3A/B, FOXO3a, MCL1 and NR3C1 substrates.

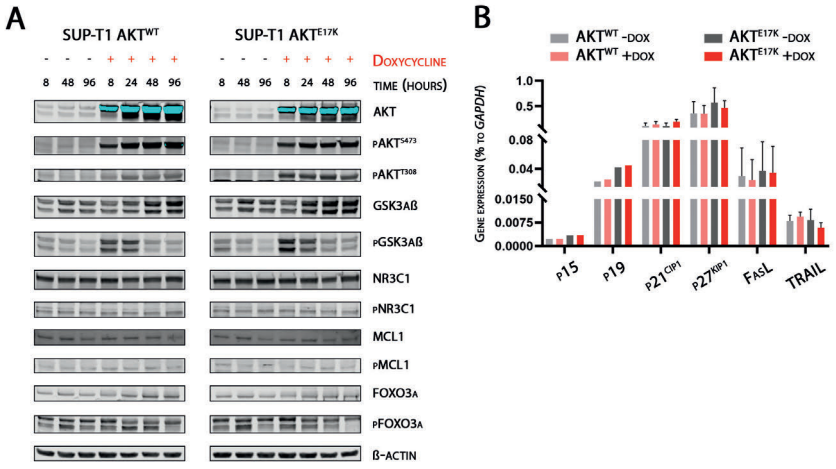

Figure 3. (A) *Immunoblot analysis of time-dependent doxycycline-induced AKT^{WT} (left) and AKT^{E17K} (right) SUPT-1 cells. The protein abundancy and phosphorylation of downstream GSK3, NR3C1 and MCL1 substrates were illustrated.* **(B)** *Relative expression of FOXO3a target genes p15 and p19 (n=1), p21^{CIP1}, p27^{KIP1}, FasL and TRAIL (n=3/4) in AKT^{WT} and AKT^{E17K} SUPT-1 cells. The expression of these genes was normalized and visualized relative to GAPDH expression.*

AKT^{E17K} is relative resistant to allosteric AKT-inhibitors

We then tested the capacity of allosteric and ATP-competitive AKT-inhibitors to abolish the activity of AKT^{WT} or AKT^{E17K}. In both cell lines, dose-dependent inhibition of GSK3 phosphorylation was observed upon treatment with the allosteric inhibitor MK2206 or the ATP-competitive inhibitor AZD5363/Capivasertib (**Figure 4a-b**). While higher concentrations of MK2206 resulted in a gradual decrease in AKT phosphorylation at T308, this was not observed for the ATP-competitive AZD5363 inhibitor. In contrast, AZD5363 treatment even seems to enhance phosphorylation of T308 in AKT^{WT} cells. Enhanced phosphorylation of the activating T308 phospho-site by AZD5363 treatment has been previously reported, but does not affect kinase activity since downstream PI3K-AKT signaling is effectively inhibited by AZD5363 despite enriched T308 phosphorylation (30). We found that AKT^{E17K} overexpressing cells were relatively resistant to MK2206 treatment, but remained equally sensitive to AZD5363 as AKT-induced cells (**Figure 4c**). The open configuration of AKT^{E17K} and its binding to the plasma membrane may result in the decreased sensitivity towards allosteric AKT inhibition.

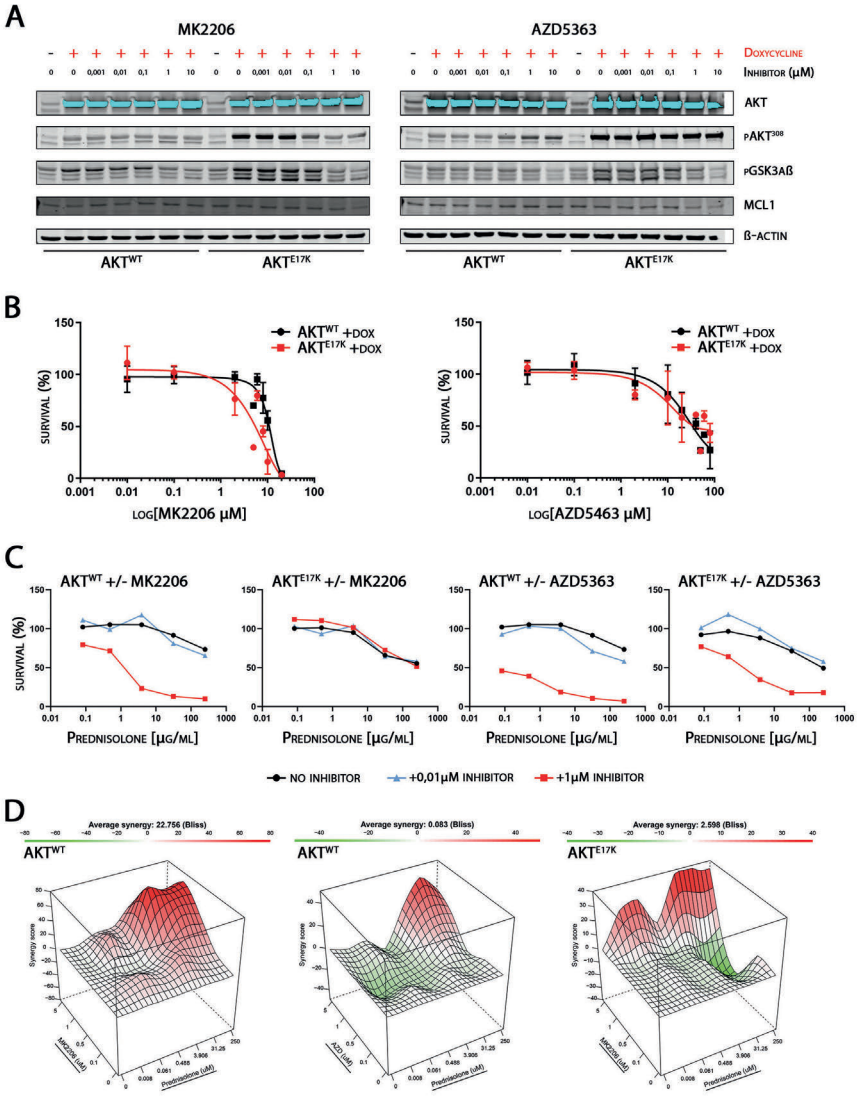

Figure 4. (A) *Immunoblot analysis of AKT^{WT} and AKT^{E17K} SUPT-1 cells treated with increasing concentrations of the allosteric AKT-inhibitor MK2206 (left) or ATP-competitive AKT-inhibitor AZD5363 (right).* **(B)** *Cell toxicity screening of doxycycline-induced AKT^{WT} and AKT^{E17K} SUPT-1 cell lines. Cells were treated with MK2206 (range 0.01-20 μM) or AZD5363 (range 0.01-80 μM) for four days (n=3).* **(C)** *Dual cell toxicity screening of doxycycline-induced AKT^{WT} (top) and AKT^{E17K} (bottom) SUPT-1 cell lines between prednisolone and a fixed concentration of AKT-inhibitor (MK2206 or AZD5363). Prednisolone treatment range: 0.00822 – 250 μg/ml.* **(D)** *Dual cell toxicity (matrix) screening and Bliss Synergy score of doxycycline-induced AKT^{WT} (top) and AKT^{E17K} (bottom) SUPT-1 cell lines. Six-point prednisolone treatment range: 0.00822 – 250 μg/ml. Four-point MK2206 or AZD5363 range: 0.1-5μM.*

We then assessed whether these AKT-inhibitors could revert AKT-induced steroid resistance. Whereas the ATP-competitive inhibitor AZD5363 improved the steroid-sensitivities of both wild type and mutant AKT-induced cells, 1μM of the allosteric inhibitor MK2206 only enhanced steroid-induced cell death in AKT^{WT}- but not in AKT^{E17K} SUPT-1 cells (**Figure 4d**). MK2206 strongly synergized with prednisolone treatment in cytotoxicity assays using AKT^{WT} cells but not for AKT^{E17K} cells (**Figure 4e**). Therefore, the AKT^{E17K} mutant isoform is less sensitive to allosteric AKT-inhibitors than AKT^{WT} cells while remaining equally sensitive to ATP-competitive AKT inhibitors. However, when testing two allosteric- (MK2206 and ARQ092/Miransertib) and two ATP-competitive- (Capivasertib and GDC0068/Ipatasertib) AKT-inhibitors on 44 T-ALL PDX samples, allosteric inhibitors were superior based on IC_{50} concentrations (**Figure 5**).

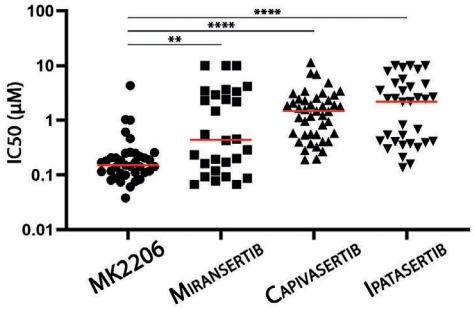

Figure 5. *Survival of 44 T-ALL PDX samples treated with a 4-log range of allosteric AKT-inhibitor (MK2206, Miransertib) or ATP-competitive (AZD5363/Capivasertib, Ipatasertib) AKT-inhibitor treatment. Cell viability is illustrated by IC_{50}. Significance was calculated using the two-tailed Wilcoxon test. P<0.01=**. P<0.0001=****.*

DISCUSSION

The PI3K-AKT pathway is frequently activated in T-ALL patient samples downstream of ligand-receptor signaling or by activating mutations in the IL7R signaling pathway (3, 31). Furthermore, genetic aberrations affecting *PTEN*, *PI3K* or *AKT* also strongly activate PI3K-AKT signaling in over 45% of T-ALL patients (2, 16). In this study, we demonstrate that overexpression of AKT^{WT} confers steroid resistance in otherwise steroid-sensitive SUPT-1 cells. This is in line with previous observations that active PI3K-AKT signaling can reduce steroid-induced cell death (22, 23, 32). We here demonstrate that PI3K-AKT pathway activation by the activating AKT^{E17K} mutation only slightly affects steroid sensitivity in contrast to AKT. Interestingly, overexpression of AKT^{E17K} but not AKT^{WT} can drive IL3-independent transformation of BaF3 cells (2). This points to differences in downstream signaling for wild type and mutant AKT.

AKT can be activated upon docking to PIP3 phospholipids in the plasma membrane, which is mediated by multiple residues of the AKT pleckstrin homology (PH)-domain including Lys14, Arg25, Tyr38, Arg48, Arg86, Thr21 and Arg23 (33, 34). This results in a conformational change that relieves AKT from an inactive state, partially by abrogation of the interaction between Lys14 and Glu17. However, Lys17 (AKT^{E17K}) also disrupts the interaction with Lys14, thereby relieving the kinase from its auto-inhibitory and closed conformation in the absence of phosphoinositides (27)(**Figure 6**). We demonstrate AKT^{E17K} cells are predominantly located at the inner side of the plasma membrane in SUPT-1 cells, while AKT^{WT} is spread throughout the cells. It is reported that cytoplasmic AKT can also interact with cytoplasmic endomembranes and therefore has the potential to phosphorylate compartmentally localized downstream AKT substrates (35). We therefore speculate that differences in cellular localization and subsequent activation or inhibition of downstream substrates at specific cellular compartments are involved in the difference in steroid responsiveness. More extensive, cellular department differentiating, research is required to study this hypothesis.

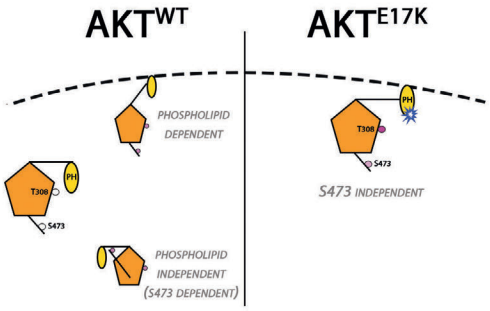

Figure 6. *Schematic overview of AKT^{WT} and AKT^{E17K} activation mechanisms. Orange: AKT kinase domain. Yellow: AKT PH-domain. White eclipses: unphosphorylated phospho-sites (T308 and S473). Purple eclipses: phosphorylated phospho-sites (T308 and S473). Purple intensity reflects relative magnitude of phosphorylation.*

In addition to phospholipid-dependent AKT activation, AKT can also be activated by C-tail phosphorylation. Phosphorylation of the S473 residue seems vital in this activation mechanism of AKT^{WT}, as phospho-S473 can interact with the PH-domain linker to potentiate phosphorylation of T308 in the activation loop by PDK1 (10, 11). Therefore, C-tail phosphorylation seems to precede T308 phosphorylation in phospho-lipid independent AKT activation mechanisms. While AKT^{WT} and AKT^{E17K} are both phosphorylated at T308 and S473, we observed that AKT^{E17K} cells had relative high levels of T308 phosphorylation compared to S473 phosphorylation. Considering this predominant T308 phosphorylation in AKT^{E17K} SUPT-1 cells, our data suggest

that mutant-dependent disruption of the PH-kinase domain interface makes S473 phosphorylation dispensable for AKT activation (**Figure 6**).

Our study demonstrates that AKT^{E17K} overexpressing cells do not provoke strong steroid resistance in contrast to AKT^{WT} cells. However, we show that these differences in steroid sensitivity could not be explained by big differences in the activation or abundancy of downstream MCL1, NR3C1 and FOXO3a targets. However, other downstream substrates might be differently regulated by mutant and wild type AKT, or their regulation is selectively regulated in specific cellular compartments (i.e. only at the membrane, liposomes or nucleus). Therefore, more extended, unbiased transcriptional and proteomics approaches are required to identify transcriptional or signaling differences between AKT^{WT} and AKT^{E17K} regulated signaling respectively.

Allosteric kinase inhibitors bind regulatory sites outside the ATP-binding pocket, and therefore selectively keep AKT in an inactive, closed conformation (36). An intact PH-kinase domain interface is essential for the binding of allosteric AKT-inhibitors to AKT, since these inhibitors interact with the PH-domain to lock the kinase in an inactive conformation (37-40). The allosteric AKT-inhibitor MK2206 seems promising for future clinical trials, and a phase I trial for pediatric refractory malignancies has already been completed (NCT01231919) (41). Importantly, MK2206 indeed interacts with multiple residues located in the PH domain (40). These interactions seemed impeded by the PH-open AKT^{E17K} kinase conformation, since AKT^{E17K} SUPT-1 cells decreased their sensitivity towards MK2206 treatment. The K17 allosteric interface was also demonstrated to hinder the binding of other allosteric AKT inhibitors (42). In our study, the decreased sensitivity to MK2206 of AKT^{E17K} cells prevented potential synergy with steroid treatment, while AZD5363 could further increase steroid sensitivity of AKT^{E17K} cells. However, as AKT^{E17K} cells are still responsive for steroid treatment, it seems unlikely that glucocorticoid treatment will not lead to the selection of AKT^{E17K} mutated cells during leukemia treatment. Therefore, we reason that the presence of the AKT^{E17K} mutation at clonal or subclonal level has no clinical consequence, and should not impact the choice for an allosteric or ATP-competitive inhibitor to treat PI3K-AKT activated leukemias. Combined with our previous observations that MK2206 synergizes with prednisolone in primary T-ALL patient blasts (3), we conclude that MK2206 serves as a promising compound for future personalized basket-trials to treat PI3K-AKT activated leukemias.

Acknowledgements. This study was sponsored by grants of the foundation “Kinderen Kankervrij”; KiKa-219 (JvdZ), KiKa-92 and KiKa-295 (WKS).

Contribution of authors. JvdZ designed study, performed research and wrote manuscript. IM, JBG, VC, LG, WKS, FB and AR performed research. JM designed and supervised the study and wrote manuscript.

Disclosures. None.

REFERENCES

1. Jiang Q, Li WQ, Aiello FB, Mazzucchelli R, Asefa B, Khaled AR, et al. Cell biology of IL-7, a key lymphotrophin. Cytokine Growth Factor Rev. 2005;16(4-5):513-33.
2. Cante-Barrett K, Spijkers-Hagelstein JA, Buijs-Gladdines JG, Uitdehaag JC, Smits WK, van der Zwet J, et al. MEK and PI3K-AKT inhibitors synergistically block activated IL7 receptor signaling in T-cell acute lymphoblastic leukemia. Leukemia. 2016;30(9):1832-43.
3. Li Y, Buijs-Gladdines JG, Cante-Barrett K, Stubbs AP, Vroegindeweij EM, Smits WK, et al. IL-7 Receptor Mutations and Steroid Resistance in Pediatric T cell Acute Lymphoblastic Leukemia: A Genome Sequencing Study. PLoS Med. 2016;13(12):e1002200.
4. Delgado-Martin C, Meyer LK, Huang BJ, Shimano KA, Zinter MS, Nguyen JV, et al. JAK/STAT pathway inhibition overcomes IL7-induced glucocorticoid resistance in a subset of human T-cell acute lymphoblastic leukemias. Leukemia. 2017;31(12):2568-76.
5. James SR, Downes CP, Gigg R, Grove SJ, Holmes AB, Alessi DR. Specific binding of the Akt-1 protein kinase to phosphatidylinositol 3,4,5-trisphosphate without subsequent activation. Biochem J. 1996;315 (Pt 3):709-13.
6. Stephens L, Anderson K, Stokoe D, Erdjument-Bromage H, Painter GF, Holmes AB, et al. Protein kinase B kinases that mediate phosphatidylinositol 3,4,5-trisphosphate-dependent activation of protein kinase B. Science. 1998;279(5351):710-4.
7. Ebner M, Lucic I, Leonard TA, Yudushkin I. PI(3,4,5)P3 Engagement Restricts Akt Activity to Cellular Membranes. Mol Cell. 2017;65(3):416-31 e6.
8. Sarbassov DD, Guertin DA, Ali SM, Sabatini DM. Phosphorylation and regulation of Akt/PKB by the rictor-mTOR complex. Science. 2005;307(5712):1098-101.
9. Alessi DR, James SR, Downes CP, Holmes AB, Gaffney PR, Reese CB, et al. Characterization of a 3-phosphoinositide-dependent protein kinase which phosphorylates and activates protein kinase Balpha. Curr Biol. 1997;7(4):261-9.
10. Chu N, Salguero AL, Liu AZ, Chen Z, Dempsey DR, Ficarro SB, et al. Akt Kinase Activation Mechanisms Revealed Using Protein Semisynthesis. Cell. 2018;174(4):897-907 e14.
11. Liu P, Begley M, Michowski W, Inuzuka H, Ginzberg M, Gao D, et al. Cell-cycle-regulated activation of Akt kinase by phosphorylation at its carboxyl terminus. Nature. 2014;508(7497):541-5.
12. Manning BD, Toker A. AKT/PKB Signaling: Navigating the Network. Cell. 2017;169(3):381-405.
13. Du K, Montminy M. CREB is a regulatory target for the protein kinase Akt/PKB. J Biol Chem. 1998;273(49):32377-9.
14. Zha J, Harada H, Yang E, Jockel J, Korsmeyer SJ. Serine phosphorylation of death agonist BAD in response to survival factor results in binding to 14-3-3 not BCL-X(L). Cell. 1996;87(4):619-28.
15. Romashkova JA, Makarov SS. NF-kappaB is a target of AKT in anti-apoptotic PDGF signalling. Nature. 1999;401(6748):86-90.
16. Gutierrez A, Sanda T, Grebliunaite R, Carracedo A, Salmena L, Ahn Y, et al. High frequency of PTEN, PI3K, and AKT abnormalities in T-cell acute lymphoblastic leukemia. Blood. 2009;114(3):647-50.
17. Seki M, Kimura S, Isobe T, Yoshida K, Ueno H, Nakajima-Takagi Y, et al. Recurrent SPI1 (PU.1) fusions in high-risk pediatric T cell acute lymphoblastic leukemia. Nat Genet. 2017;49(8):1274-81.
18. Zuurbier L, Petricoin EF, 3rd, Vuerhard MJ, Calvert V, Kooi C, Buijs-Gladdines JG, et al. The significance of PTEN and AKT aberrations in pediatric T-cell acute lymphoblastic leukemia. Haematologica. 2012;97(9):1405-13.

19. Liu Y, Easton J, Shao Y, Maciaszek J, Wang Z, Wilkinson MR, et al. The genomic landscape of pediatric and young adult T-lineage acute lymphoblastic leukemia. Nat Genet. 2017;49(8):1211-8.
20. Mendes RD, Sarmento LM, Cante-Barrett K, Zuurbier L, Buijs-Gladdines JG, Povoa V, et al. PTEN microdeletions in T-cell acute lymphoblastic leukemia are caused by illegitimate RAG-mediated recombination events. Blood. 2014;124(4):567-78.
21. Trinquand A, Tanguy-Schmidt A, Ben Abdelali R, Lambert J, Beldjord K, Lengline E, et al. Toward a NOTCH1/FBXW7/RAS/PTEN-based oncogenetic risk classification of adult T-cell acute lymphoblastic leukemia: a Group for Research in Adult Acute Lymphoblastic Leukemia study. J Clin Oncol. 2013;31(34):4333-42.
22. Blackburn JS, Liu S, Wilder JL, Dobrinski KP, Lobbardi R, Moore FE, et al. Clonal evolution enhances leukemia-propagating cell frequency in T cell acute lymphoblastic leukemia through Akt/mTORC1 pathway activation. Cancer Cell. 2014;25(3):366-78.
23. Beesley AH, Firth MJ, Ford J, Weller RE, Freitas JR, Perera KU, et al. Glucocorticoid resistance in T-lineage acute lymphoblastic leukaemia is associated with a proliferative metabolism. Br J Cancer. 2009;100(12):1926-36.
24. Wei G, Twomey D, Lamb J, Schlis K, Agarwal J, Stam RW, et al. Gene expression-based chemical genomics identifies rapamycin as a modulator of MCL1 and glucocorticoid resistance. Cancer Cell. 2006;10(4):331-42.
25. Xie M, Yang A, Ma J, Wu M, Xu H, Wu K, et al. Akt2 mediates glucocorticoid resistance in lymphoid malignancies through FoxO3a/Bim axis and serves as a direct target for resistance reversal. Cell Death Dis. 2019;9(10):1013.
26. Piovan E, Yu J, Tosello V, Herranz D, Ambesi-Impiombato A, Da Silva AC, et al. Direct reversal of glucocorticoid resistance by AKT inhibition in acute lymphoblastic leukemia. Cancer Cell. 2013;24(6):766-76.
27. Carpten JD, Faber AL, Horn C, Donoho GP, Briggs SL, Robbins CM, et al. A transforming mutation in the pleckstrin homology domain of AKT1 in cancer. Nature. 2007;448(7152):439-44.
28. van der Zwet JCG, Buijs-Gladdines JGCAM, Cordo' V, Debets DO, Smits WK, Chen Z, et al. MAPK-ERK is a central pathway in T-cell acute lymphoblastic leukemia that drives steroid resistance. Leukemia. 2021.
29. He L, Kulesskiy E, Saarela J, Turunen L, Wennerberg K, Aittokallio T, et al. Methods for High-throughput Drug Combination Screening and Synergy Scoring. Methods Mol Biol. 2018;1711:351-98.
30. Davies BR, Greenwood H, Dudley P, Crafter C, Yu DH, Zhang J, et al. Preclinical pharmacology of AZD5363, an inhibitor of AKT: pharmacodynamics, antitumor activity, and correlation of monotherapy activity with genetic background. Mol Cancer Ther. 2012;11(4):873-87.
31. Barata JT, Silva A, Brandao JG, Nadler LM, Cardoso AA, Boussiotis VA. Activation of PI3K is indispensable for interleukin 7-mediated viability, proliferation, glucose use, and growth of T cell acute lymphoblastic leukemia cells. J Exp Med. 2004;200(5):659-69.
32. Bornhauser BC, Bonapace L, Lindholm D, Martinez R, Cario G, Schrappe M, et al. Low-dose arsenic trioxide sensitizes glucocorticoid-resistant acute lymphoblastic leukemia cells to dexamethasone via an Akt-dependent pathway. Blood. 2007;110(6):2084-91.
33. Rong SB, Hu Y, Enyedy I, Powis G, Meuillet EJ, Wu X, et al. Molecular modeling studies of the Akt PH domain and its interaction with phosphoinositides. J Med Chem. 2001;44(6):898-908.
34. Lucic I, Rathinaswamy MK, Truebestein L, Hamelin DJ, Burke JE, Leonard TA. Conformational sampling of membranes by Akt controls its activation and inactivation. Proc Natl Acad Sci U S A. 2018;115(17):E3940-E9.

35. Jethwa N, Chung GH, Lete MG, Alonso A, Byrne RD, Calleja V, et al. Endomembrane PtdIns(3,4,5)P3 activates the PI3K-Akt pathway. J Cell Sci. 2015;128(18):3456-65.
36. Lu X, Smaill JB, Ding K. New Promise and Opportunities for Allosteric Kinase Inhibitors. Angew Chem Int Ed Engl. 2020;59(33):13764-76.
37. Wu WI, Voegtli WC, Sturgis HL, Dizon FP, Vigers GP, Brandhuber BJ. Crystal structure of human AKT1 with an allosteric inhibitor reveals a new mode of kinase inhibition. PLoS One. 2010;5(9):e12913.
38. Calleja V, Laguerre M, Larijani B. 3-D structure and dynamics of protein kinase B-new mechanism for the allosteric regulation of an AGC kinase. J Chem Biol. 2009;2(1):11-25.
39. Barnett SF, Defeo-Jones D, Fu S, Hancock PJ, Haskell KM, Jones RE, et al. Identification and characterization of pleckstrin-homology-domain-dependent and isoenzyme-specific Akt inhibitors. Biochem J. 2005;385(Pt 2):399-408.
40. Rehan M, Beg MA, Parveen S, Damanhouri GA, Zaher GF. Computational insights into the inhibitory mechanism of human AKT1 by an orally active inhibitor, MK-2206. PLoS One. 2014;9(10):e109705.
41. Fouladi M, Perentesis JP, Phillips CL, Leary S, Reid JM, McGovern RM, et al. A phase I trial of MK-2206 in children with refractory malignancies: a Children's Oncology Group study. Pediatr Blood Cancer. 2014;61(7):1246-51.
42. Parikh C, Janakiraman V, Wu WI, Foo CK, Kljavin NM, Chaudhuri S, et al. Disruption of PH-kinase domain interactions leads to oncogenic activation of AKT in human cancers. Proc Natl Acad Sci U S A. 2012;109(47):19368-73.

8

Multi-omic approaches to improve outcome for T-cell acute lymphoblastic leukemia patients

Jordy C.G. van der Zwet[1], Valentina Cordo'[1], Kirsten Canté-Barrett[1] and Jules P.P. Meijerink[1]

[1]Princess Máxima Center for Pediatric Oncology, Utrecht, The Netherlands

Published in Advances in Biological Regulation, December 2019
doi: 10.1016/j.jbior.2019.100647, PMID: 31523030

ABSTRACT

In the last decade, tremendous progress in curative treatment has been made for T-ALL patients using high-intensive, risk-adapted multi-agent chemotherapy. Further treatment intensification to improve the cure rate is not feasible as it will increase the number of toxic deaths. Hence, about 20% of pediatric patients relapse and often die due to acquired therapy resistance. Personalized medicine is of utmost importance to further increase cure rates and is achieved by targeting specific initiation, maintenance or resistance mechanisms of the disease. Genomic sequencing has revealed mutations that characterize genetic subtypes of many cancers including T-ALL. However, leukemia may have various activated pathways that are not accompanied by the presence of mutations. Therefore, screening for mutations alone is not sufficient to identify all molecular targets and leukemic dependencies for therapeutic inhibition. We review the extent of the driving type A and the secondary type B genomic mutations in pediatric T-ALL that may be targeted by specific inhibitors. Additionally, we review the need for additional screening methods on the transcriptional and protein levels. An integrated 'multi-omic' screening will identify potential targets and biomarkers to establish significant progress in future individualized treatment of T-ALL patients.

Keywords: T-cell acute lymphoblastic leukemia, genomics, transcriptomics, proteomics, personalized medicine, interleukin-7 signaling

Abbreviations

T-ALL:	*T-cell acute lymphoblastic leukemia*
EGIL:	*European group of immunological characterization of leukemias*
CD:	*cluster of differentiation*
TCR:	*T-cell receptor*
ETP:	*early thymocyte progenitor*
INDEL:	*insertion/deletion*
IL-7R:	*interleukin-7 receptor*
MAPK:	*mitogen-activated protein kinase*
RTK:	*receptor tyrosine kinase*
RPPA:	*reverse-phase protein array*
IL-7:	*interleukin-7*

T-ALL SUBTYPES AND DRIVING ONCOGENES

T-cell acute lymphoblastic leukemia (T-ALL) is the malignant expansion of immature, arrested T-cells at various stages of thymocyte development. The European Group for the Immunological Characterization of Leukemias (EGIL) distinguished three T-ALL subtypes by virtue of their expression of Cluster of Differentation markers (CD-markers). These subtypes were denoted as early, cortical and mature T-ALL (1). The outcome of cortical T-ALL was found superior over the outcome of both other subtypes (2, 3).

The first T-ALL oncogenes were identified by resolving the translocations from T-cell receptor (TCR) gene enhancers or promotors to other chromosomes as a consequence of errors in VDJ recombination events. This led to the discovery of the *TAL1* oncogene for patients harboring the t(1;14)(p34;q11) translocation (4, 5), *LYL1* in a patient with a t(7;19)(q34;p13) translocation (6) and *TLX1/HOX11* in patients bearing t(10;14)(q24;q11) translocations (7-11). For *TAL1*, small deletions were identified in approximately 12-25% of pediatric patients that result in repositioning of the *TAL1* coding region behind the *STIL* gene promoter (12-14). Whereas *TAL1* abnormalities are predominantly associated with late cortical development (15), *TLX1*-rearranged patients mostly resemble early cortical thymocytes (16). Since these initial discoveries, extensive molecular and cytogenetic analyses have resolved many additional oncogenic rearrangements in nearly 80 percent of the T-ALL patients (**Table 1**) (17-24).

The first genome-wide gene expression analysis that distinguished the T-ALL subtype from other leukemic types was performed by the group of Eric Lander (25). Shortly after, the gene signatures of immature, early and late cortical T-cell developmental stages in T-ALL patient samples could be distinguished that were characterized by ectopic expression levels of oncogenic transcription factors including *LYL1*, *TLX1*/*HOX11* or *TAL1*, respectively (26). Whereas expression of *TLX1* and *TAL1* are driven by chromosomal rearrangements, *LYL1*-positive T-ALL patients are devoid of *LYL1* rearrangements. Some early cortical T-ALL patients express the *TLX1*-related gene *TLX3/HOX11L2* due to a cryptic (5;14)(q35;q32) chromosomal translocation in approximately 25 percent of pediatric T-ALL patients (26, 27). Later gene expression microarray studies distinguished at least four T-ALL groups, *i.e.* the immature, TLX, proliferative and TALLMO subtypes (28-30). Identification of additional oncogenes extended previous observations that each subtype was characterized by specific oncogenic rearrangements that facilitate specific blocks in T-cell development and drive T-ALL. Each genetic subtype is discussed below.

Immature subtype (ETP-ALL)

Immature T-ALL patients are characterized by high expression levels of *BCL2*, *LYL1*, *LMO2*, *HHEX* and *MEF2C,* reflecting activation of self-renewal genes that are also expressed in hematopoietic stem cells (29, 31). This profile matched with the immature

T-ALL entity that was identified based on its resemblance to normal early thymocyte progenitor cells (ETP) (32-34). This subtype was accordingly denoted ETP-ALL. In-depth molecular-cytogenetic analysis of immature/ETP-ALL patient samples revealed unique rearrangements of the *MEF2C* transcription factor in some patients while others contained *ETV6*-coupled fusions of the MEF2C co-factor NCOA2/TIFF (29, 35, 36). Rearrangements that affect other *MEF2C* transcriptional regulators—including *SPI1*, *NKX2.5* and a *RUNX1-AFF3* fusion product—have also been reported in ETP-ALL (**Table 1**) (29).

Since the introduction of next-generation sequencing, various additional fusions have been identified in ETP-ALL patients affecting *ETV6*, *KTM2A, RUNX1, ABL, MLLT10, NUP214* and *NUP98* (**Table 1**) (37-39). A Japanese study on 121 pediatric T-ALL cases identified recurrent *SPI1* (encoding PU.1) fusions including *STMN1-SPI1* and *TCF7-SPI1* fusions in ETP-ALL patients that highly expressed *MEF2C*, *HHEX*, *FLT3* and *cKIT* (40). In contrast to most other ETP-ALL patients (37), ETP-ALL cases bearing *SPI1* fusion products were characterized by recurrent activating *NOTCH1* mutations (40). Some ETP-ALL patients bear rearrangements that result in the activation of various members of the *HOXA* gene cluster (**Table 1,** *HOXA* act). Such *HOXA*-positive ETP-ALL patients were related to high intrinsic chemo-resistance and very poor outcome in the French GRAALL-2003 and -2005 studies (41, 42).

TLX subtype

Most patients that cluster in the TLX subtype are characterized by *TLX3* rearrangements (29). Whereas some patients express the γδ TCR, other TLX patients have a more immature phenotype that lack TCR surface expression suggesting that this disease entity is associated with early γδ lineage of development (43, 44). The TLX cluster also comprises patients with *HOXA*-activating events including *SET-NUP214*, *PICALM-MLLT10* or *MLL* fusion products (29, 38).

TLX3 rearrangements mostly reposition the *TLX3* oncogene from 5q35 in close proximity to the *BCL11B* enhancer at 14q32, thereby inactivating one functional allele of the *BCL11B* haplo-insufficient tumor suppressor gene (27, 45). BCL11B is a critical transcription factor that commits early developing thymocytes to the αβ lineage of T-cell development (46-48). *TLX3-BCL11B* rearrangements may therefore impair αβ differentiation potential and consequently drive differentiation towards the γδ lineage. Some TLX patients also inactivate the second, non-rearranged *BCL11B* allele that may further block αβ lineage commitment potential (49-51). TLX3 itself may also switch off the TCR αβ lineage program. As a strong repressor (52), TLX3 represses the *TRCA* enhancer in an ETS-dependent fashion thereby limiting *TCRA* recombination events (53). As a significant number of *TLX3*-rearranged cases express cytoplasmic TCRB (44), it cannot be ruled out that *TLX3-BCL11B* rearrangements may initially have occurred in αβ lineage cortical thymocytes that subsequently diverged towards the γδ lineage

as a consequence of BCL11B insufficiency and/or TLX3 expression (54). Some early studies reported an association of *TLX3* rearrangements with poor outcome (16, 26, 55-58), but no such association has been reported for patients treated on contemporary treatment protocols.

Proliferative subtype

T-ALL patients that express a proliferative gene signature are frequently characterized by *TLX1* or *NKX2-1* translocations (29). Historically, *TLX1* translocated patients have been associated with superior outcome compared to patients from other T-ALL subtypes (16, 59-61). *TLX1* translocation breakpoints mostly occur downstream of *TLX1*, coupling the *TCRB* enhancer downstream of *TLX1* in *TCRB*-translocated patients. However, in *TCRAD* translocated patients the *TLX1* genomic breaks are positioned upstream and positions *TLX1* behind promoters of *TCRAD* V-gene segments, possibly because the *TCRAD* enhancer is repressed by TLX1 similar to the repressor function of TLX3 (53). Various patients of the proliferative cluster contain translocations or inversions involving the *NKX2-1* or the homologous *NKX2-2* homeobox genes (29). In these patients, ectopic *NKX2-1/2-2* oncogene expression levels are driven as consequence of their close proximities to *TCRB* or *TCRAD* enhancers (29). The presence of recurrent *NKX2-1* aberrations in T-ALL has been confirmed in other studies (39, 62). Remarkably, most *TLX1*-rearranged patients also express low levels of *NKX2-1* in the absence of *NKX2-1* rearrangements implying direct regulation of *NKX2-1* by TLX1 (29).

TALLMO subtype

Patients with a TALLMO gene expression profile represent nearly half of all pediatric T-ALL patients (26, 28, 29, 38). Just as in normal hematopoietic erythroid precursors, TAL1 and TAL2 proteins form transcription complexes with E2A/HEB, RUNX1, GATA3, and MYB co-factors that are bridged by LMO1 or LMO2 in these T-ALL cells (63, 64). In addition to recurrent *TAL1* translocations or *SIL-TAL1* deletions that drive ectopic TAL1 expression, other TALLMO patients bear alternative *TCRB* or *TCRAD* rearrangements that ectopically drive *TAL2*, *LYL1*, *LMO1*, *LMO2* or *LMO3* oncogenes (6, 26, 28, 29, 65-71). Almost a quarter of all TALLMO patients harbor a combination of 2 different aberrations that affect both members of *TAL1* and *LMO2* gene families. In addition, small insertion/deletion (INDEL) mutations have recently been identified that create strong MYB binding sites in or upstream of *TAL1*, *LMO1* or *LMO2* loci in nearly 6 percent of pediatric/young adult T-ALL patients (38). Recruitment of MYB at these sites results in the assembly of a TAL1 super-enhancer complex that strongly drives oncogene expression (72-75).

Non-driver mutations in T-ALL

In addition to the driving oncogenes or oncogene fusion products that characterize the four predominant T-ALL subtypes and that are denoted type A aberrations (76), various other recurrent aberrations including point- or INDEL mutations, chromosomal gains and losses have been described for T-ALL (19, 20, 23, 24). These aberrations are not necessarily disease-initiating events as they mostly appear in leukemia subclones (76). These mutations were accordingly denoted as type B mutations. These mutations provide advantages for oncogenesis, disease progression, relapse, or induce therapy resistance. Historic research and recent next-generation sequencing studies have now revealed over 100 genes that are recurrently mutated, amplified or deleted in T-ALL (**Table 2)** (37-39, 77-80). The majority of these genetic alterations impact on cell cycle by inactivating cell cycle inhibitors or by loss of *Rb* (38), or ectopically activate signaling pathways that are important for T-cell development including NOTCH1 (81-85), cytokine signaling cascades (86-90) or their downstream pathways (91-95). Other mutations frequently involve (in)activation of transcriptional regulators, epigenetic reprogramming enzymes, components of ribosomes that affect protein translation, protein-modifying enzymes, or genes that are involved in the chromatin architecture and DNA looping, DNA repair or DNA synthesis. An overview of all mutations is listed in **Table 2**, along with the cellular processes they affect and notable associations.

While type B mutations occur in all T-ALL subtypes, ETP-ALL patients typically harbor the highest mutational load compared to the other subtypes (37, 78) and have been associated with an inferior steroid response (96). ETP-ALL is distinguished from other subtypes in the genetic landscape by the relative enrichment of specific type B events, which includes activating mutations in the tyrosine kinase receptor gene *FLT3*, mutations in the IL-7R (interleukin-7 receptor) signaling pathway (*i.e.* in *IL7R*, *JAK1* and/or *JAK3*) or recurrent 5q-deletions that affect the *NR3C1* gene locus (37, 97, 98). In contrast, ETP-ALL patients have a lower frequency of deletions affecting cell cycle regulators including *CDKN2A/B*, *CDKN1B* or *CDKN1C* and have lower incidences of NOTCH1-activating mutations (38, 40, 78). Although ETP-ALL was initially associated with extremely poor outcome (32, 90, 99-104), treatment intensification in contemporary risk-adapted treatment protocols has improved outcome for ETP-ALL patients and is now comparable to the outcome of other T-ALL patients (33, 105-107). The only exception is the *HOXA*-activated ETP-ALL group that still has a very poor outcome (41, 42). Other type B events that cluster with specific T-ALL subtypes include strong NOTCH1-activating mutations in *TLX3*-rearranged ALL, and activating *PIK3R1* or *PIK3CG* events, *PTEN*-inactivating mutations and inactivating *USP7* mutations in TALLMO subtype patients (**Table 2**). In contrast to NOTCH1-activating mutations, *PTEN*-inactivating events have been associated with poor outcome in various studies (78, 92, 95, 108-111) but not in the MRC UKALL2003 cohort (112).

Mutations in genes encoding various IL-7R signaling molecules (*i.e. IL7R*, *JAK1/3*, *STAT5B*, *N/KRAS* or *AKT*) have been found in nearly 35% of pediatric T-ALL patients and are associated with inferior event free survival (37-40, 78, 80, 88, 89, 93, 113-121). These pathway mutations are predominantly found in ETP-ALL and TLX subtypes and occur in a near mutually exclusive manner (78, 113). Moreover, JAK-STAT and RAS/PTEN alterations are often identified in chemorefractory patients, and identified in higher frequencies at disease relapse. Similar to mutations affecting *IL7R*, these mutations predict for very poor outcome of relapsed T-ALL (80, 122). One of the explanations for this is that aberrant IL-7R signaling results in increased cellular resistance towards steroid treatment (78).

COMBINED *OMIC*-BASED TARGETED THERAPIES: OPPORTUNITIES IN T-ALL

Contemporary multi-agent and risk-adapted protocols have boosted survival rates to approximately 80 percent, with the number of toxic deaths now almost equaling the number of patients that relapse (123). This proves that further treatment intensification is not feasible and there is an urgent need for targeted compounds in individualized treatment protocols for high-risk T-ALL patients. Given our profound understanding of pathogenic drivers and mutations in T-ALL, various targeted compounds could be implemented in the near future to improve outcome for refractory/relapsed T-ALL and may allow implementation in first-line treatment for high-risk T-ALL patients in the future.

Roughly 50% of all pediatric cancer patients present with a potentially druggable genetic event, with aberrations in NOTCH-, mitogen-activated protein kinase (MAPK)-, or receptor tyrosine kinase (RTK)-signaling and cell cycle control as potential targets for future T-ALL treatment regimens (124). The question remains whether introduction of single targeted compounds in current chemotherapy backbones will improve treatment outcome. In adult metastasized carcinoma patients genomics-directed treatment strategies only yielded minimal prognostic benefits (125-127). The effect of single targeted compound treatment might be disappointing in T-ALL since many of the targetable processes are the result of type B mutations that are frequently found at subclonal levels (128). Targeted inhibition should therefore not be expected to eradicate the complete leukemic burden. However, some subclonal mutations give rise to therapy resistance and could therefore still serve as essential targets for therapy. In the case of IL-7R pathway mutations, MEK and AKT are attractive targets for selective inhibitors that synergize with steroid treatment (78). Moreover, mutated subclones may actually reflect pathway dependency and/or drug sensitivity of the entire leukemic population. Therefore, the effect of combined treatment could extend beyond the elimination of mutated cells. For example, this has been implemented in the phase1/2 SeluDex trial in which dexamethasone treatment is given in combination with the MEK-inhibitor

Selumetinib for relapse or refractory RAS-mutant BCP-ALL (129) and is now open for relapsed/refractory T-ALL patients as well.

The observed benefit of combining targeted treatment with standard chemotherapeutics may extend beyond the treatment of patients that harbor specific (subclonal) mutations. Loh *et al*. demonstrated that in two out of three high risk-ALL cases no somatic mutations could be identified in tyrosine kinase-coding genes, despite their gene expression profiles that point to active kinase signaling (130). This indicates that patients with activated kinase signaling benefit from targeted therapy, especially those who lack druggable genetic targets. To decipher the full pathogenic program and to pinpoint novel biomarkers for both therapy and prognosis, an integrated approach that combines data on the genomic, transcriptomic and proteomic level may be required to identify additional druggable targets (131). This so-called 'multi-omic' approach could reveal other tumor targets, and therefore provides an opportunity to increase the detail and complexity of basket-trials for small numbers of patients or for individualized patient treatment programs (132) (**Figure 1**). Refinement of treatment strategies, as a direct consequence of this advanced screening approach, could consequently improve outcome. Since for most hematological malignancies sufficient patient material can be obtained at diagnosis, testing on these three levels indeed seems feasible for T-ALL. In the next two paragraphs, we will highlight the current progress and application of transcriptome sequencing and proteomics in ALL.

Integration of transcriptome sequencing

In the last few years, great technological advances in sequencing have been applied not only to DNA analysis but to RNA as well. RNA-sequencing of the leukemia transcriptome has a prominent role in the identification of novel splice variants and fusion transcripts that drive or sustain tumorigenesis. As mentioned before, RNA-sequencing studies have led to the discovery of various novel and cryptic fusion transcripts in T-ALL (39, 122, 133) and T-lymphoblastic lymphoma patients (134) that had not been identified earlier by genome sequencing or molecular-cytogenetic tests. The Total XVII protocol (NTC03117751) for the treatment of ALL at the St. Jude children's hospital integrates information from RNA sequencing with RT-PCR or FISH to detect potential druggable fusions at diagnosis that are then used for therapy stratification. While the pipeline for fusion detection from RNA-seq data will give results already at day 15 of the induction therapy, additional whole-genome sequencing information is available only at later stages of the treatment (135).

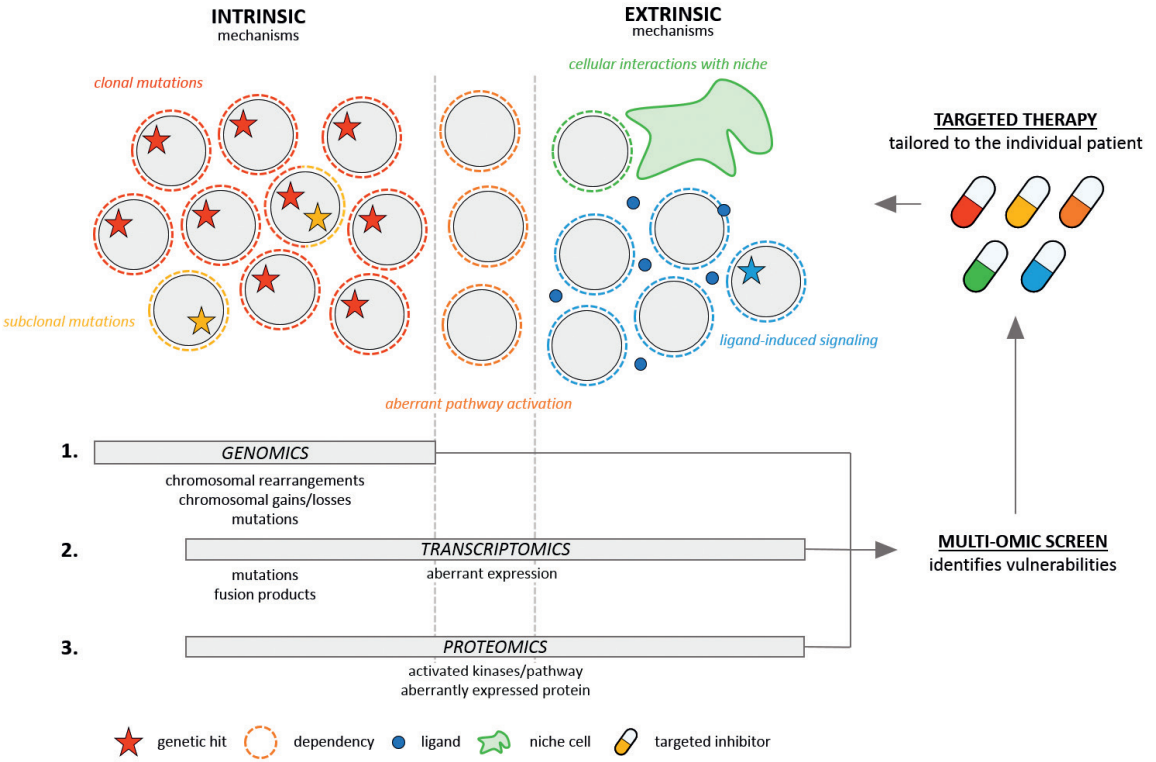

Figure 1. *Intrinsic mechanisms (e.g. by genetic hits (stars)), extrinsic mechanisms (e.g. by interaction with niche (green) or ligand-induced (blue)) and aberrant pathway activation with unknown cause (orange) involved in disease initiation, maintenance or drug resistance that may be observed in leukemic blasts. Integration of genomics, transcriptomics and proteomics identifies the vulnerabilities caused by these pathogenic events. As a result, it allows for the precise use of targeted compounds that (in combination with standard chemotherapeutics) can enhance treatment effectiveness and ultimately may improve survival.*

Cancer cells rely on altered mechanisms of signal transduction that boost cell cycle progression and proliferation (136). When pathological pathway activation is not predicted by genomic aberrations, different approaches like transcriptome sequencing will be required to identify the *Achilles' heel* of the disease. Quantitative measurement of pathway activity inferred from target gene mRNA levels have been developed for various signaling pathways, *e.g.* the Oncosignal platform by Philips Healthcare, and provides a molecular phenotype of the tumor (137-140). It generates an automated and reliable quantitative readout of specific pathways that are highly activated in malignant cells that can support the choice of relevant small-molecule inhibitors. Furthermore, it can potentially predict therapy resistance due to the activation of compensatory/ escape mechanisms.

Integration of proteomics

An additional way to discover novel oncogenic dependencies or identify new biomarkers is to analyze the cancer proteome. Mass spectrometry-based global proteomic analyses have been pivotal in the identification of changes in protein expression as well as in post-translational modifications, in particular phosphorylation (141, 142). These changes at the phospho-protein level reflect altered signal transduction that cannot be detected at the DNA or RNA level. Protein kinases are one of the major effectors of signal transduction. Nevertheless, direct quantification of activity levels of kinases has been challenging and requires *a priori* knowledge of the enzyme of interest. In the past decade, an increasing interest in post-translational modifications and their role in cancer led to development of workflows for the identification of alterations in protein phosphorylation levels as functional readout for enzyme hyper-activity. High-throughput phospho-proteome data can therefore provide direct information on pathway signaling.

In 2013, Casado *et al.* demonstrated that kinase activity inferred from analysis of global phospho-proteome data of different hematological cancer cell lines correlates with differential drug responses (143). Phospho-proteomic analyses have also been applied to the identification of putative therapy response biomarkers in ALL (reviewed in (144, 145)). In T-ALL, the phospho-proteomic studies investigating signal transduction have been limited to either a kinome microarray system—identifying differentially phosphorylated peptides for pediatric B-ALL versus T-ALL samples (146)—or by using Reverse-Phase Protein Array (RPPA) that identified hyper-activation of the mTOR/STAT3 and LCK/calcineurin axes in pediatric ETP-ALL (147). Based on the latter study, the authors suggested LCK hyper-activity as possible resistance factor for steroid treatment in T-ALL (148). Both kinome array and RPPA are valuable tools but can only detect changes in a subset of pre-defined proteins and therefore do not allow for screening of the entire (phospho)proteome. Unbiased mass spectrometry-based phospho-proteomic studies dedicated to T-ALL are necessary to unravel specific pathological signaling pathways and escape mechanisms. The identification and the degree of

pathway activation with subsequent downstream effects will provide a rationale for therapy stratification and will lead to the identification of novel disease specific- or individualized biomarkers (149).

Functional screening into practice: IL-7R-signaling and steroid resistance

IL-7R pathway activation by interleukin-7 (IL-7) even in the absence of IL-7R pathway mutations has also been shown to confer steroid resistance in T-ALL patients (96, 150). This indicates that pathway activation (and subsequent drug responsiveness) can depend on the availability of growth factors, and may provide an underlying mechanism for increased therapy resistance for local, niche embedded leukemia cells. For patients that present with this so called 'IL-7 dependent steroid resistance' (150), pathway inhibition by combined MEK or AKT inhibition with steroid treatment to restore steroid sensitivity may be equally effective as for patients that harbor IL-7R pathway mutations. Increase in the phosphorylation of STAT5 or the activation of downstream STAT5 target genes following IL-7 stimulation are important biomarkers to identify these patients for whom integration of phospho-proteomics and transcriptomics at diagnosis is needed.

Both proteomic and transcriptomic analyses have identified novel treatment targets or biomarkers that represent pathway activation downstream of the IL-7R before. For example, phospho-proteomic profiling of JAK3 mutated leukemia cells—that signal downstream of the IL-7R but do not impair steroid sensitivity in contrast to JAK1 mutations (78)—identified non-JAK-STAT druggable targets that were affected by mutant JAK3 signaling (151). Combined pathway inhibition of these targets with Ruxolitinib or Tofacitinib (JAK-inhibitors) worked synergistically *in vitro* and *in vivo* (151), indicating that proteomic profiling serves as a powerful tool to improve personalized medicine. Additionally, transcriptional and epigenetic research identified that the STAT5B^{N642H} mutation—which leads to strong STAT5B pathway activation—increases its binding at regions that are also bound by epigenetic regulators such as EZH2 and SUZ12 (118, 119, 152). STAT5B^{N642H} expressing T-cells showed a higher expression level and activity of the EZH2 target gene Aurora kinase B (Aurkb), yielding sensitivity for treatment with a specific Aurora Kinase B inhibitor (AT9283) (152). High *PIM1* expression downstream of STAT5 signaling has also been identified by transcriptional analysis, and PIM1 inhibition was demonstrated effective in (IL-7 mediated) JAK-STAT activated leukemias (153-155).

The observations for JAK3 and STAT5 illustrate that pathway activation and dependency, as measured by proteomic and transcriptomic approaches, predict sensitivity to selective inhibitors and may improve outcome by optimization of personalized medicine. Additionally, screening at multiple levels provides additional biomarkers that can be used for targeted therapy regardless of signaling mutations. For example, RNA sequencing could reveal significant *PIM1* overexpression (in the absence of *JAK* or *STAT5B* mutations as determined by genomic screening) and could therefore provide a rationale for treatment with a selective PIM1-inhibitor for individual patients. As another

example, phospho-proteomic results that point to activation of the AKT pathway in a T-ALL patient vouches for combination treatment with an AKT-inhibitor. Thus, 'multi-omics' screening approaches will excel the choice of targets to inhibit in personalized medicine. It will help clinicians to individualize treatment and optimize basket-trials in refractory/relapsed T-ALL patients. Moreover, a multi-omics functional screening with subsequent therapeutic consequences at the start of treatment might prevent (early) relapse, therefore significantly increasing the survival rate of T-ALL patients.

CONCLUDING REMARKS

Given our profound understanding of genomic aberrations in T-ALL, we can now successfully identify oncogenic driving lesions in nearly 80% of T-ALL patients (**Table 1**). Additionally, patients frequently present with non-driver mutations at the subclonal level for which some relate to inferior outcome or therapy resistance (**Table 2**). At present, the majority of small-molecule inhibitors that could be applied in clinical trials target these subclonal mutations and may offer therapeutic effect if the mutation in the subclone is indicative for a vulnerability of the total leukemic population. Genomic screening in T-ALL should therefore not only focus on driving events, but also on identifying genetic aberrations for which a selective inhibitor combined with standard chemotherapeutics drugs can lead to a maximal treatment response. Integration of genomic sequencing, RNA sequencing and phospho-proteomics in a 'multi-omics' functional screening will uncover the complete *Achilles' heel* of the leukemia, allowing great improvement of personalized medicine and eventually patient outcome as a result of the precise use of targeted compounds (**Figure 1**).

Acknowledgements. This research did not receive any specific grants from funding agencies in the public, commercial, or non-profit sectors.

Contribution of authors. JvdZ, VC, KCB and JM wrote the manuscript.

Disclosures. None.

Table 1. Oncogene rearrangements in T-ALL.

Oncogene activation	Enhancer/promoters	Incidence (%)	Associated subtype	Ref
TAL1, *TAL2*, *LYL1*	*TCRB (enh), TCRAD (enh), STIL (promoter), TCF7***, Myb-Enh mut.	27, <1, <1	TALLMO	(4-6, 12, 13, 75, 156-158)
LMO1, *LMO2*, *LMO3*	*TCRB (enh), TCRAD (enh), MBNL1, STAG2,* Myb-Enh mut., 11q13 deletion	5, 12, <1	TALLMO	(72, 73, 156, 159, 160)
TLX1	*TCRB (enh), TCRAD (V-gene promoter), DDX30***	5	Proliferative	(7-11)
NKX2-1, *NKX2-2*	*TCRAD (enh), TCRB (enh)*	5	Proliferative	(29)
TLX3	*BCL11B (enh), TCRB (enh), TCRAD (V-gene promoter), CAPSL*	21	TLX	(26, 27, 43, 161, 162)
HOXA9/A10	*TCRB (enh)*	<2	TLX/ ETP-ALL	(28, 163-165)
MEF2C	*PITX2*	<2	ETP-ALL	(29)
SP1	*BCL11B (enh)*	<1	ETP-ALL	(29)
*LMO2***	*BCL11B (enh)*	<1	ETP-ALL	
NKX2.5	*BCL11B(enh), TCRAD (enh)*	<1	ETP-ALL	(29, 166, 167)
LCK	*TCRB (enh)*	<1	unknown	
MYB	*TCRB (enh), duplications*	<2	unknown	(168-170)
CCND2	*TCRB (enh)*	<1	unknown	(171)

Oncogenic fusions	Partner gene	Incidence	Associated subtype	Ref
PICALM (*HOXA* act.)	*MLLT10*	3	TLX/ ETP-ALL	(29, 172)
KTM2A (*HOXA* act.)	*MLLT1*, *ENL*, *MLLT10*, *MLLT4*, *MLLT6, CT45A4*	<2	TLX/ ETP-ALL	(38, 173)
SET (*HOXA* act.)	*NUP214*	2	TLX/ ETP-ALL	(29, 30, 174)
SPI1	*STMN1, TCF7*	<1	ETP-ALL (post-ETP)	(40)
RUNX1	*AFF3*, *EVX*	<1	ETP-ALL	(29, 37)
ABL1	*BCR*, *EML1*, *ZMIZ1*, *NUP214 (episomal), SLC9A3R1, ETV6, MBNL1, ZBTB16**	<1	ETP-ALL/*TALLMO	(29, 38, 39, 175-185)
ETV6	*JAK2, NCOA2, INO80D, ABL1, CTNNB1*	<1	ETP-ALL	(37, 38)
MLLT10 (*HOXA* act.)	*PICALM, XPO1, NAP1L1, DDX3X, KTM2A, FAM17A1, CAPS2, HNRNPH1*		TLX/ ETP-ALL	(29, 37-39, 186)
NUP214	*ABL1 (episomal)*, *SET, SQSTM1*	6	ETP-ALL	(37)
NUP98	*RAP1GDS1, CCDC28A, LNP1, PSIP1, DDX10, VRK1*	<2	ETP-ALL	(38, 39)

**ABL1-ZBTB16* rearrangements found in 2 TALLMO patients; **unpublished unique rearrangement

Table 2. Mutations in cellular pathways or processes in T-ALL.

Process/ Pathway	Genes	Associations	Therapeutic compounds	Ref
Cell cycle	*CDKN2A/B, CDKN1B, CDKN1C, CCND3, RB*	Low in ETP-ALL	CDK4/6 inhibitors	(28, 38-40, 78, 80, 92, 171)
NOTCH signaling	*NOTCH1, FBXW7*	GPR, favorable	NOTCH inhibitors	(38-40, 78, 80-85, 186-190)
IL7R-JAK-STAT	*IL7Ra, JAK1, JAK3, PTPN2, STAT5B*	Steroid resistance	JAK, MEK or PIM1 inhibitors	(37-40, 78, 80, 88, 89, 113-119, 150, 189, 191-194)
RAS-MEK-ERK	*N/K-RAS, NF1, PTPN11, BRAF*	Steroid resistance	MEK-inhibitors	(37-40, 78, 80, 93, 113, 114, 120)
PI3K-AKT	*PIK3R1, PIK3CA, PIK3CD, AKT*	Poor	AKT or mTOR inhibitor	(38, 40, 78, 92, 113)
PTEN	*PTEN*	Poor, therapy failure, relapse	PI3K, AKT or mTOR inhibitors	(38-40, 91, 92, 95, 108, 109, 111, 112, 114, 191, 195-197)
Receptors and kinases	*ABL1, ALK, cKIT, FLT3, FAT1, ECT2L, SH2B3*	x	ABL-class tyrosine kinase inhibitors	(37, 38, 40, 77, 78, 80, 86, 87, 97, 198, 199)
Transcription factors	*RUNX1, ETV6, BCL11B, WT1, PHF6, TCF7, LEF1, CTNNB1, GATA3, IKZF1, MYC, MYB, CREBBP, MLLT10*	x	BET inhibitors	(29, 37-40, 49, 50, 52, 78, 80, 168, 169, 200-203)
Transcription co-factors	*EP300, MED12, SMARCA4, ATRX, CNOT1, CNOT3, CNOT6*	x	x	(38-40, 78, 80, 204)
Polycomb complex	*EED, SUZ12, EZH2, ASXL1*	x	x	(37, 39, 40, 80, 200, 205)
Epigenetic enzymes	*KDM6A, SETD2, KMT2A, KMT2D, KMT2C, DNMT3A, IDH1, IDH2*	x	HDAC or methyltransferase inhibitors	(37-40, 77, 78, 103, 198, 200)
Ribosomes	*RPL5, RPL0, RPL22, del6q*	x	ABT-199	(38-40, 78, 204, 206-209)
Protein stability	*USP7, USP9X*	x	Bortezomib	(38-40, 80, 200)
Chromatine remodeling	*CTCF*	x	x	(38-40, 80)
DNA repair	*P53, P53BP1, ATM, MSH2, MSH6, PMS2*	x	x	(38-40, 78, 80, 93)
Adhesion	*DNM2*	x	x	(37-40, 78, 80, 198, 210, 211)
Steroid receptor	*NR3C1*	x	x	(78, 98)
Therapy resistance	*NT5C2*	Only observed in relapse	x	(40, 80, 212)
Apoptosis	BCL2 protein expression*	ETP-ALL	ABT-199, ABT-737	(78, 213-216)

** No mutations for BCL2 have been reported*

REFERENCES

1. Bene MC, Castoldi G, Knapp W, Ludwig WD, Matutes E, Orfao A, et al. Proposals for the immunological classification of acute leukemias. European Group for the Immunological Characterization of Leukemias (EGIL). Leukemia. 1995;9(10):1783-6.
2. Pui CH, Behm FG, Crist WM. Clinical and biologic relevance of immunologic marker studies in childhood acute lymphoblastic leukemia. Blood. 1993;82(2):343-62.
3. Niehues T, Kapaun P, Harms DO, Burdach S, Kramm C, Korholz D, et al. A classification based on T cell selection-related phenotypes identifies a subgroup of childhood T-ALL with favorable outcome in the COALL studies. Leukemia. 1999;13(4):614-7.
4. Begley CG, Aplan PD, Davey MP, Nakahara K, Tchorz K, Kurtzberg J, et al. Chromosomal translocation in a human leukemic stem-cell line disrupts the T-cell antigen receptor delta-chain diversity region and results in a previously unreported fusion transcript. Proc Natl Acad Sci U S A. 1989;86(6):2031-5.
5. Finger LR, Kagan J, Christopher G, Kurtzberg J, Hershfield MS, Nowell PC, et al. Involvement of the TCL5 gene on human chromosome 1 in T-cell leukemia and melanoma. Proc Natl Acad Sci U S A. 1989;86(13):5039-43.
6. Mellentin JD, Smith SD, Cleary ML. lyl-1, a novel gene altered by chromosomal translocation in T cell leukemia, codes for a protein with a helix-loop-helix DNA binding motif. Cell. 1989;58(1):77-83.
7. Dube ID, Kamel-Reid S, Yuan CC, Lu M, Wu X, Corpus G, et al. A novel human homeobox gene lies at the chromosome 10 breakpoint in lymphoid neoplasias with chromosomal translocation t(10;14). Blood. 1991;78(11):2996-3003.
8. Hatano M, Roberts CW, Minden M, Crist WM, Korsmeyer SJ. Deregulation of a homeobox gene, HOX11, by the t(10;14) in T cell leukemia. Science. 1991;253(5015):79-82.
9. Kennedy MA, Gonzalez-Sarmiento R, Kees UR, Lampert F, Dear N, Boehm T, et al. HOX11, a homeobox-containing T-cell oncogene on human chromosome 10q24. Proc Natl Acad Sci U S A. 1991;88(20):8900-4.
10. Lu M, Gong ZY, Shen WF, Ho AD. The tcl-3 proto-oncogene altered by chromosomal translocation in T-cell leukemia codes for a homeobox protein. EMBO J. 1991;10(10):2905-10.
11. Dube ID, Raimondi SC, Pi D, Kalousek DK. A new translocation, t(10;14)(q24;q11), in T cell neoplasia. Blood. 1986;67(4):1181-4.
12. Brown L, Cheng JT, Chen Q, Siciliano MJ, Crist W, Buchanan G, et al. Site-specific recombination of the tal-1 gene is a common occurrence in human T cell leukemia. EMBO J. 1990;9(10):3343-51.
13. Bernard O, Lecointe N, Jonveaux P, Souyri M, Mauchauffe M, Berger R, et al. Two site-specific deletions and t(1;14) translocation restricted to human T-cell acute leukemias disrupt the 5' part of the tal-1 gene. Oncogene. 1991;6(8):1477-88.
14. Aplan PD, Lombardi DP, Ginsberg AM, Cossman J, Bertness VL, Kirsch IR. Disruption of the human SCL locus by "illegitimate" V-(D)-J recombinase activity. Science. 1990;250(4986):1426-9.
15. Macintyre EA, Smit L, Ritz J, Kirsch IR, Strominger JL. Disruption of the SCL locus in T-lymphoid malignancies correlates with commitment to the T-cell receptor alpha beta lineage. Blood. 1992;80(6):1511-20.
16. Cave H, Suciu S, Preudhomme C, Poppe B, Robert A, Uyttebroeck A, et al. Clinical significance of HOX11L2 expression linked to t(5;14)(q35;q32), of HOX11 expression, and of SIL-TAL fusion in childhood T-cell malignancies: results of EORTC studies 58881 and 58951. Blood. 2004;103(2):442-50.

17. Armstrong SA, Look AT. Molecular genetics of acute lymphoblastic leukemia. J Clin Oncol. 2005;23(26):6306-15.
18. Look AT. Oncogenic transcription factors in the human acute leukemias. Science. 1997;278(5340):1059-64.
19. Meijerink JP, den Boer ML, Pieters R. New genetic abnormalities and treatment response in acute lymphoblastic leukemia. Semin Hematol. 2009;46(1):16-23.
20. Belver L, Ferrando A. The genetics and mechanisms of T cell acute lymphoblastic leukaemia. Nat Rev Cancer. 2016;16(8):494-507.
21. Raimondi SC, Privitera E, Williams DL, Look AT, Behm F, Rivera GK, et al. New recurring chromosomal translocations in childhood acute lymphoblastic leukemia. Blood. 1991;77(9):2016-22.
22. Rubnitz JE, Look AT. Molecular genetics of childhood leukemias. J Pediatr Hematol Oncol. 1998;20(1):1-11.
23. Iacobucci I, Mullighan CG. Genetic Basis of Acute Lymphoblastic Leukemia. J Clin Oncol. 2017;35(9):975-83.
24. Van Vlierberghe P, Ferrando A. The molecular basis of T cell acute lymphoblastic leukemia. J Clin Invest. 2012;122(10):3398-406.
25. Golub TR, Slonim DK, Tamayo P, Huard C, Gaasenbeek M, Mesirov JP, et al. Molecular classification of cancer: class discovery and class prediction by gene expression monitoring. Science. 1999;286(5439):531-7.
26. Ferrando AA, Neuberg DS, Staunton J, Loh ML, Huard C, Raimondi SC, et al. Gene expression signatures define novel oncogenic pathways in T cell acute lymphoblastic leukemia. Cancer Cell. 2002;1(1):75-87.
27. Bernard OA, Busson-LeConiat M, Ballerini P, Mauchauffe M, Della Valle V, Monni R, et al. A new recurrent and specific cryptic translocation, t(5;14)(q35;q32), is associated with expression of the Hox11L2 gene in T acute lymphoblastic leukemia. Leukemia. 2001;15(10):1495-504.
28. Soulier J, Clappier E, Cayuela JM, Regnault A, Garcia-Peydro M, Dombret H, et al. HOXA genes are included in genetic and biologic networks defining human acute T-cell leukemia (T-ALL). Blood. 2005;106(1):274-86.
29. Homminga I, Pieters R, Langerak AW, de Rooi JJ, Stubbs A, Verstegen M, et al. Integrated transcript and genome analyses reveal NKX2-1 and MEF2C as potential oncogenes in T cell acute lymphoblastic leukemia. Cancer Cell. 2011;19(4):484-97.
30. Van Vlierberghe P, van Grotel M, Tchinda J, Lee C, Beverloo HB, van der Spek PJ, et al. The recurrent SET-NUP214 fusion as a new HOXA activation mechanism in pediatric T-cell acute lymphoblastic leukemia. Blood. 2008;111(9):4668-80.
31. McCormack MP, Young LF, Vasudevan S, de Graaf CA, Codrington R, Rabbitts TH, et al. The Lmo2 oncogene initiates leukemia in mice by inducing thymocyte self-renewal. Science. 2010;327(5967):879-83.
32. Coustan-Smith E, Mullighan CG, Onciu M, Behm FG, Raimondi SC, Pei D, et al. Early T-cell precursor leukaemia: a subtype of very high-risk acute lymphoblastic leukaemia. Lancet Oncol. 2009;10(2):147-56.
33. Zuurbier L, Gutierrez A, Mullighan CG, Cante-Barrett K, Gevaert AO, de Rooi J, et al. Immature MEF2C-dysregulated T-cell leukemia patients have an early T-cell precursor acute lymphoblastic leukemia gene signature and typically have non-rearranged T-cell receptors. Haematologica. 2014;99(1):94-102.
34. Bernt KM, Hunger SP, Neff T. The Functional Role of PRC2 in Early T-cell Precursor Acute Lymphoblastic Leukemia (ETP-ALL) - Mechanisms and Opportunities. Front Pediatr. 2016;4:49.

35. Nagel S, Meyer C, Quentmeier H, Kaufmann M, Drexler HG, MacLeod RA. MEF2C is activated by multiple mechanisms in a subset of T-acute lymphoblastic leukemia cell lines. Leukemia. 2008;22(3):600-7.
36. Strehl S, Nebral K, Konig M, Harbott J, Strobl H, Ratei R, et al. ETV6-NCOA2: a novel fusion gene in acute leukemia associated with coexpression of T-lymphoid and myeloid markers and frequent NOTCH1 mutations. Clin Cancer Res. 2008;14(4):977-83.
37. Zhang J, Ding L, Holmfeldt L, Wu G, Heatley SL, Payne-Turner D, et al. The genetic basis of early T-cell precursor acute lymphoblastic leukaemia. Nature. 2012;481(7380):157-63.
38. Liu Y, Easton J, Shao Y, Maciaszek J, Wang Z, Wilkinson MR, et al. The genomic landscape of pediatric and young adult T-lineage acute lymphoblastic leukemia. Nat Genet. 2017;49(8):1211-8.
39. Chen B, Jiang L, Zhong ML, Li JF, Li BS, Peng LJ, et al. Identification of fusion genes and characterization of transcriptome features in T-cell acute lymphoblastic leukemia. Proc Natl Acad Sci U S A. 2018;115(2):373-8.
40. Seki M, Kimura S, Isobe T, Yoshida K, Ueno H, Nakajima-Takagi Y, et al. Recurrent SPI1 (PU.1) fusions in high-risk pediatric T cell acute lymphoblastic leukemia. Nat Genet. 2017;49(8):1274-81.
41. Bond J, Machand T, Touzart A, Cieslak A, Trinquand A, Sutton L, et al. An early thymic progenitor phentotype predicts outcome exclusively in HOXA-overexpressing adult T-cell acute lymphoblastic leukemia: a group for research in adult acute lymphoblastic leukemia study. Haematologica. 2016;this issue.
42. Ben Abdelali R, Asnafi V, Petit A, Micol JB, Callens C, Villarese P, et al. The prognosis of CALM-AF10-positive adult T-cell acute lymphoblastic leukemias depends on the stage of maturation arrest. Haematologica. 2013;98(11):1711-7.
43. Berger R, Dastugue N, Busson M, Van Den Akker J, Perot C, Ballerini P, et al. t(5;14)/HOX11L2-positive T-cell acute lymphoblastic leukemia. A collaborative study of the Groupe Francais de Cytogenetique Hematologique (GFCH). Leukemia. 2003;17(9):1851-7.
44. van Grotel M, Meijerink JP, van Wering ER, Langerak AW, Beverloo HB, Buijs-Gladdines JG, et al. Prognostic significance of molecular-cytogenetic abnormalities in pediatric T-ALL is not explained by immunophenotypic differences. Leukemia. 2008;22(1):124-31.
45. Li L, Zhang JA, Dose M, Kueh HY, Mosadeghi R, Gounari F, et al. A far downstream enhancer for murine Bcl11b controls its T-cell specific expression. Blood. 2013;122(6):902-11.
46. Li L, Leid M, Rothenberg EV. An early T cell lineage commitment checkpoint dependent on the transcription factor Bcl11b. Science. 2010;329(5987):89-93.
47. Li P, Burke S, Wang J, Chen X, Ortiz M, Lee SC, et al. Reprogramming of T cells to natural killer-like cells upon Bcl11b deletion. Science. 2010;329(5987):85-9.
48. Yui MA, Feng N, Rothenberg EV. Fine-scale staging of T cell lineage commitment in adult mouse thymus. J Immunol. 2010;185(1):284-93.
49. De Keersmaecker K, Real PJ, Gatta GD, Palomero T, Sulis ML, Tosello V, et al. The TLX1 oncogene drives aneuploidy in T cell transformation. Nat Med. 2010;16(11):1321-7.
50. Gutierrez A, Kentsis A, Sanda T, Holmfeldt L, Chen SC, Zhang J, et al. The BCL11B tumor suppressor is mutated across the major molecular subtypes of T-cell acute lymphoblastic leukemia. Blood. 2011;118(15):4169-73.
51. Wakabayashi Y, Watanabe H, Inoue J, Takeda N, Sakata J, Mishima Y, et al. Bcl11b is required for differentiation and survival of alphabeta T lymphocytes. Nat Immunol. 2003;4(6):533-9.
52. Della Gatta G, Palomero T, Perez-Garcia A, Ambesi-Impiombato A, Bansal M, Carpenter ZW, et al. Reverse engineering of TLX oncogenic transcriptional networks identifies RUNX1 as tumor suppressor in T-ALL. Nat Med. 2012;18(3):436-40.

53. Dadi S, Le Noir S, Payet-Bornet D, Lhermitte L, Zacarias-Cabeza J, Bergeron J, et al. TLX homeodomain oncogenes mediate T cell maturation arrest in T-ALL via interaction with ETS1 and suppression of TCRalpha gene expression. Cancer Cell. 2012;21(4):563-76.
54. Asnafi V, Beldjord K, Libura M, Villarese P, Millien C, Ballerini P, et al. Age-related phenotypic and oncogenic differences in T-cell acute lymphoblastic leukemias may reflect thymic atrophy. Blood. 2004;104(13):4173-80.
55. Ballerini P, Blaise A, Busson-Le Coniat M, Su XY, Zucman-Rossi J, Adam M, et al. HOX11L2 expression defines a clinical subtype of pediatric T-ALL associated with poor prognosis. Blood. 2002;100(3):991-7.
56. Gottardo NG, Jacoby PA, Sather HN, Reaman GH, Baker DL, Kees UR. Significance of HOX11L2/TLX3 expression in children with T-cell acute lymphoblastic leukemia treated on Children's Cancer Group protocols. Leukemia. 2005;19(9):1705-8.
57. Mauvieux L, Leymarie V, Helias C, Perrusson N, Falkenrodt A, Lioure B, et al. High incidence of Hox11L2 expression in children with T-ALL. Leukemia. 2002;16(12):2417-22.
58. van Grotel M, Meijerink JP, Beverloo HB, Langerak AW, Buys-Gladdines JG, Schneider P, et al. The outcome of molecular-cytogenetic subgroups in pediatric T-cell acute lymphoblastic leukemia: a retrospective study of patients treated according to DCOG or COALL protocols. Haematologica. 2006;91(9):1212-21.
59. Ferrando AA, Neuberg DS, Dodge RK, Paietta E, Larson RA, Wiernik PH, et al. Prognostic importance of TLX1 (HOX11) oncogene expression in adults with T-cell acute lymphoblastic leukaemia. Lancet. 2004;363(9408):535-6.
60. Kees UR, Heerema NA, Kumar R, Watt PM, Baker DL, La MK, et al. Expression of HOX11 in childhood T-lineage acute lymphoblastic leukaemia can occur in the absence of cytogenetic aberration at 10q24: a study from the Children's Cancer Group (CCG). Leukemia. 2003;17(5):887-93.
61. Schneider NR, Carroll AJ, Shuster JJ, Pullen DJ, Link MP, Borowitz MJ, et al. New recurring cytogenetic abnormalities and association of blast cell karyotypes with prognosis in childhood T-cell acute lymphoblastic leukemia: a pediatric oncology group report of 343 cases. Blood. 2000;96(7):2543-9.
62. La Starza R, Lettieri A, Pierini V, Nofrini V, Gorello P, Songia S, et al. Linking genomic lesions with minimal residual disease improves prognostic stratification in children with T-cell acute lymphoblastic leukaemia. Leuk Res. 2013;37(8):928-35.
63. Hsu HL, Wadman I, Baer R. Formation of in vivo complexes between the TAL1 and E2A polypeptides of leukemic T cells. Proc Natl Acad Sci U S A. 1994;91(8):3181-5.
64. Porcher C, Chagraoui H, Kristiansen MS. SCL/TAL1: a multifaceted regulator from blood development to disease. Blood. 2017;129(15):2051-60.
65. Van Vlierberghe P, van Grotel M, Beverloo HB, Lee C, Helgason T, Buijs-Gladdines J, et al. The cryptic chromosomal deletion del(11)(p12p13) as a new activation mechanism of LMO2 in pediatric T-cell acute lymphoblastic leukemia. Blood. 2006;108(10):3520-9.
66. Homminga I, Vuerhard MJ, Langerak AW, Buijs-Gladdines J, Pieters R, Meijerink JP. Characterization of a pediatric T-cell acute lymphoblastic leukemia patient with simultaneous LYL1 and LMO2 rearrangements. Haematologica. 2012;97(2):258-61.
67. Simonis M, Klous P, Homminga I, Galjaard RJ, Rijkers EJ, Grosveld F, et al. High-resolution identification of balanced and complex chromosomal rearrangements by 4C technology. Nat Methods. 2009;6(11):837-42.
68. Hammond SM, Crable SC, Anderson KP. Negative regulatory elements are present in the human LMO2 oncogene and may contribute to its expression in leukemia. Leuk Res. 2005;29(1):89-97.

69. McGuire EA, Hockett RD, Pollock KM, Bartholdi MF, O'Brien SJ, Korsmeyer SJ. The t(11;14)(p15;q11) in a T-cell acute lymphoblastic leukemia cell line activates multiple transcripts, including Ttg-1, a gene encoding a potential zinc finger protein. Mol Cell Biol. 1989;9(5):2124-32.
70. Nam CH, Rabbitts TH. The role of LMO2 in development and in T cell leukemia after chromosomal translocation or retroviral insertion. Mol Ther. 2006;13(1):15-25.
71. Royer-Pokora B, Loos U, Ludwig WD. TTG-2, a new gene encoding a cysteine-rich protein with the LIM motif, is overexpressed in acute T-cell leukaemia with the t(11;14)(p13;q11). Oncogene. 1991;6(10):1887-93.
72. Li Z, Abraham BJ, Berezovskaya A, Farah N, Liu Y, Leon T, et al. APOBEC signature mutation generates an oncogenic enhancer that drives LMO1 expression in T-ALL. Leukemia. 2017.
73. Rahman S, Magnussen M, Leon TE, Farah N, Li Z, Abraham BJ, et al. Activation of the LMO2 oncogene through a somatically acquired neomorphic promoter in T-cell acute lymphoblastic leukemia. Blood. 2017.
74. Sengupta S, George RE. Super-Enhancer-Driven Transcriptional Dependencies in Cancer. Trends Cancer. 2017;3(4):269-81.
75. Mansour MR, Abraham BJ, Anders L, Berezovskaya A, Gutierrez A, Durbin AD, et al. Oncogene regulation. An oncogenic super-enhancer formed through somatic mutation of a noncoding intergenic element. Science. 2014;346(6215):1373-7.
76. Van Vlierberghe P, Pieters R, Beverloo HB, Meijerink JP. Molecular-genetic insights in paediatric T-cell acute lymphoblastic leukaemia. Br J Haematol. 2008;143(2):153-68.
77. Van Vlierberghe P, Ambesi-Impiombato A, Perez-Garcia A, Haydu JE, Rigo I, Hadler M, et al. ETV6 mutations in early immature human T cell leukemias. J Exp Med. 2011;208(13):2571-9.
78. Li Y, Buijs-Gladdines JG, Cante-Barrett K, Stubbs AP, Vroegindeweij EM, Smits WK, et al. IL-7 Receptor Mutations and Steroid Resistance in Pediatric T cell Acute Lymphoblastic Leukemia: A Genome Sequencing Study. PLoS Med. 2016;13(12):e1002200.
79. Kunz JB, Rausch T, Bandapalli OR, Eilers J, Pechanska P, Schuessele S, et al. Pediatric T-cell lymphoblastic leukemia evolves into relapse by clonal selection, acquisition of mutations and promoter hypomethylation. Haematologica. 2015;100(11):1442-50.
80. Richter-Pechanska P, Kunz JB, Hof J, Zimmermann M, Rausch T, Bandapalli OR, et al. Identification of a genetically defined ultra-high-risk group in relapsed pediatric T-lymphoblastic leukemia. Blood Cancer J. 2017;7(2):e523.
81. Weng AP, Ferrando AA, Lee W, Morris JPt, Silverman LB, Sanchez-Irizarry C, et al. Activating mutations of NOTCH1 in human T cell acute lymphoblastic leukemia. Science. 2004;306(5694):269-71.
82. Akhoondi S, Sun D, von der Lehr N, Apostolidou S, Klotz K, Maljukova A, et al. FBXW7/hCDC4 is a general tumor suppressor in human cancer. Cancer Res. 2007;67(19):9006-12.
83. Malyukova A, Dohda T, von der Lehr N, Akhoondi S, Corcoran M, Heyman M, et al. The tumor suppressor gene hCDC4 is frequently mutated in human T-cell acute lymphoblastic leukemia with functional consequences for Notch signaling. Cancer Res. 2007;67(12):5611-6.
84. O'Neil J, Grim J, Strack P, Rao S, Tibbitts D, Winter C, et al. FBW7 mutations in leukemic cells mediate NOTCH pathway activation and resistance to gamma-secretase inhibitors. J Exp Med. 2007;204(8):1813-24.
85. Thompson BJ, Buonamici S, Sulis ML, Palomero T, Vilimas T, Basso G, et al. The SCFFBW7 ubiquitin ligase complex as a tumor suppressor in T cell leukemia. J Exp Med. 2007;204(8):1825-35.
86. Paietta E, Ferrando AA, Neuberg D, Bennett JM, Racevskis J, Lazarus H, et al. Activating FLT3 mutations in CD117/KIT(+) T-cell acute lymphoblastic leukemias. Blood. 2004;104(2):558-60.

87. Van Vlierberghe P, Meijerink JP, Stam RW, van der Smissen W, van Wering ER, Beverloo HB, et al. Activating FLT3 mutations in CD4+/CD8- pediatric T-cell acute lymphoblastic leukemias. Blood. 2005;106(13):4414-5.
88. Shochat C, Tal N, Bandapalli OR, Palmi C, Ganmore I, te Kronnie G, et al. Gain-of-function mutations in interleukin-7 receptor-alpha (IL7R) in childhood acute lymphoblastic leukemias. J Exp Med. 2011;208(5):901-8.
89. Zenatti PP, Ribeiro D, Li W, Zuurbier L, Silva MC, Paganin M, et al. Oncogenic IL7R gain-of-function mutations in childhood T-cell acute lymphoblastic leukemia. Nat Genet. 2011;43(10):932-9.
90. Neumann M, Heesch S, Gokbuget N, Schwartz S, Schlee C, Benlasfer O, et al. Clinical and molecular characterization of early T-cell precursor leukemia: a high-risk subgroup in adult T-ALL with a high frequency of FLT3 mutations. Blood Cancer J. 2012;2(1):e55.
91. Palomero T, Sulis ML, Cortina M, Real PJ, Barnes K, Ciofani M, et al. Mutational loss of PTEN induces resistance to NOTCH1 inhibition in T-cell leukemia. Nat Med. 2007;13(10):1203-10.
92. Gutierrez A, Sanda T, Grebliunaite R, Carracedo A, Salmena L, Ahn Y, et al. High frequency of PTEN, PI3K, and AKT abnormalities in T-cell acute lymphoblastic leukemia. Blood. 2009;114(3):647-50.
93. Kawamura M, Ohnishi H, Guo SX, Sheng XM, Minegishi M, Hanada R, et al. Alterations of the p53, p21, p16, p15 and RAS genes in childhood T-cell acute lymphoblastic leukemia. Leuk Res. 1999;23(2):115-26.
94. Yamamoto T, Isomura M, Xu Y, Liang J, Yagasaki H, Kamachi Y, et al. PTPN11, RAS and FLT3 mutations in childhood acute lymphoblastic leukemia. Leuk Res. 2006;30(9):1085-9.
95. Mendes RD, Sarmento LM, Cante-Barrett K, Zuurbier L, Buijs-Gladdines JG, Povoa V, et al. PTEN microdeletions in T-cell acute lymphoblastic leukemia are caused by illegitimate RAG-mediated recombination events. Blood. 2014;124(4):567-78.
96. Maude SL, Dolai S, Delgado-Martin C, Vincent T, Robbins A, Selvanathan A, et al. Efficacy of JAK/STAT pathway inhibition in murine xenograft models of early T-cell precursor (ETP) acute lymphoblastic leukemia. Blood. 2015;125(11):1759-67.
97. Neumann M, Coskun E, Fransecky L, Mochmann LH, Bartram I, Sartangi NF, et al. FLT3 mutations in early T-cell precursor ALL characterize a stem cell like leukemia and imply the clinical use of tyrosine kinase inhibitors. PLoS One. 2013;8(1):e53190.
98. La Starza R, Barba G, Demeyer S, Pierini V, Di Giacomo D, Gianfelici V, et al. Deletions of the long arm of chromosome 5 define subgroups of T-cell acute lymphoblastic leukemia. Haematologica. 2016;101(8):951-8.
99. Gutierrez A, Dahlberg SE, Neuberg DS, Zhang J, Grebliunaite R, Sanda T, et al. Absence of Biallelic TCR{gamma} Deletion Predicts Early Treatment Failure in Pediatric T-Cell Acute Lymphoblastic Leukemia. J Clin Oncol. 2010;28(24):3816-23.
100. Inukai T, Kiyokawa N, Campana D, Coustan-Smith E, Kikuchi A, Kobayashi M, et al. Clinical significance of early T-cell precursor acute lymphoblastic leukaemia: results of the Tokyo Children's Cancer Study Group Study L99-15. Br J Haematol. 2012;156(3):358-65.
101. Ma M, Wang X, Tang J, Xue H, Chen J, Pan C, et al. Early T-cell precursor leukemia: a subtype of high risk childhood acute lymphoblastic leukemia. Front Med. 2012;6(4):416-20.
102. Allen A, Sireci A, Colovai A, Pinkney K, Sulis M, Bhagat G, et al. Early T-cell precursor leukemia/lymphoma in adults and children. Leuk Res. 2013;37(9):1027-34.
103. Van Vlierberghe P, Ambesi-Impiombato A, De Keersmaecker K, Hadler M, Paietta E, Tallman MS, et al. Prognostic relevance of integrated genetic profiling in adult T-cell acute lymphoblastic leukemia. Blood. 2013;122(1):74-82.
104. Yang YL, Hsiao CC, Chen HY, Lin KH, Jou ST, Chen JS, et al. Absence of biallelic TCRgamma deletion predicts induction failure and poorer outcomes in childhood T-cell acute lymphoblastic leukemia. Pediatr Blood Cancer. 2012;58(6):846-51.

105. Farah N, Kirkwood AA, Rahman S, Leon T, Jenkinson S, Gale RE, et al. Prognostic impact of the absence of biallelic deletion at the TRG locus for pediatric patients with T-cell acute lymphoblastic leukemia treated on the Medical Research Council UK Acute Lymphoblastic Leukemia 2003 trial. Haematologica. 2018;103(7):e288-e92.
106. Wood BL, Winter SS, Dunsmore KP, Devidas M, Chen S, Asselin BL, et al. T-lymphoblastic leukemia (T-ALL) showns excellent outcome, lack of significance of the early thymic precursor (ETP) immunophenotype, and validation of the prognostic value of end-induction minimal residual disease (MRD) in Children's Oncology Group (COG) study AALL0434. Blood. 2014;124(21):1.
107. Patrick K, Wade R, Goulden N, Mitchell C, Moorman AV, Rowntree C, et al. Outcome for children and young people with Early T-cell precursor acute lymphoblastic leukaemia treated on a contemporary protocol, UKALL 2003. Br J Haematol. 2014;166(3):421-4.
108. Zuurbier L, Petricoin EF, 3rd, Vuerhard MJ, Calvert V, Kooi C, Buijs-Gladdines JG, et al. The significance of PTEN and AKT aberrations in pediatric T-cell acute lymphoblastic leukemia. Haematologica. 2012;97(9):1405-13.
109. Trinquand A, Tanguy-Schmidt A, Ben Abdelali R, Lambert J, Beldjord K, Lengline E, et al. Toward a NOTCH1/FBXW7/RAS/PTEN-based oncogenetic risk classification of adult T-cell acute lymphoblastic leukemia: a Group for Research in Adult Acute Lymphoblastic Leukemia study. J Clin Oncol. 2013;31(34):4333-42.
110. Paganin M, Grillo MF, Silvestri D, Scapinello G, Buldini B, Cazzaniga G, et al. The presence of mutated and deleted PTEN is associated with an increased risk of relapse in childhood T cell acute lymphoblastic leukaemia treated with AIEOP-BFM ALL protocols. Br J Haematol. 2018;182(5):705-11.
111. Jotta PY, Ganazza MA, Silva A, Viana MB, da Silva MJ, Zambaldi LJ, et al. Negative prognostic impact of PTEN mutation in pediatric T-cell acute lymphoblastic leukemia. Leukemia. 2010;24(1):239-42.
112. Jenkinson S, Kirkwood AA, Goulden N, Vora A, Linch DC, Gale RE. Impact of PTEN abnormalities on outcome in pediatric patients with T-cell acute lymphoblastic leukemia treated on the MRC UKALL2003 trial. Leukemia. 2016;30(1):39-47.
113. Cante-Barrett K, Spijkers-Hagelstein JA, Buijs-Gladdines JG, Uitdehaag JC, Smits WK, van der Zwet J, et al. MEK and PI3K-AKT inhibitors synergistically block activated IL7 receptor signaling in T-cell acute lymphoblastic leukemia. Leukemia. 2016;30(9):1832-43.
114. Flex E, Petrangeli V, Stella L, Chiaretti S, Hornakova T, Knoops L, et al. Somatically acquired JAK1 mutations in adult acute lymphoblastic leukemia. J Exp Med. 2008;205(4):751-8.
115. Jeong EG, Kim MS, Nam HK, Min CK, Lee S, Chung YJ, et al. Somatic mutations of JAK1 and JAK3 in acute leukemias and solid cancers. Clin Cancer Res. 2008;14(12):3716-21.
116. Asnafi V, Le Noir S, Lhermitte L, Gardin C, Legrand F, Vallantin X, et al. JAK1 mutations are not frequent events in adult T-ALL: a GRAALL study. Br J Haematol. 2010;148(1):178-9.
117. Bains T, Heinrich MC, Loriaux MM, Beadling C, Nelson D, Warrick A, et al. Newly described activating JAK3 mutations in T-cell acute lymphoblastic leukemia. Leukemia. 2012;26(9):2144-6.
118. Kontro M, Kuusanmaki H, Eldfors S, Burmeister T, Andersson EI, Bruserud O, et al. Novel activating STAT5B mutations as putative drivers of T-cell acute lymphoblastic leukemia. Leukemia. 2014;28(8):1738-42.
119. Bandapalli OR, Schuessele S, Kunz JB, Rausch T, Stutz AM, Tal N, et al. The activating STAT5B N642H mutation is a common abnormality in pediatric T-cell acute lymphoblastic leukemia and confers a higher risk of relapse. Haematologica. 2014;99(10):e188-92.
120. Balgobind BV, Van Vlierberghe P, van den Ouweland AM, Beverloo HB, Terlouw-Kromosoeto JN, van Wering ER, et al. Leukemia-associated NF1 inactivation in patients with pediatric T-ALL and AML lacking evidence for neurofibromatosis. Blood. 2008;111(8):4322-8.

121. Oliveira ML, Akkapeddi P, Ribeiro D, Melao A, Barata JT. IL-7R-mediated signaling in T-cell acute lymphoblastic leukemia: An update. Adv Biol Regul. 2019;71:88-96.
122. Gianfelici V, Chiaretti S, Demeyer S, Di Giacomo F, Messina M, La Starza R, et al. RNA sequencing unravels the genetics of refractory/relapsed T-cell acute lymphoblastic leukemia. Prognostic and therapeutic implications. Haematologica. 2016;101(8):941-50.
123. Pieters R, de Groot-Kruseman H, Van der Velden V, Fiocco M, van den Berg H, de Bont E, et al. Successful Therapy Reduction and Intensification for Childhood Acute Lymphoblastic Leukemia Based on Minimal Residual Disease Monitoring: Study ALL10 From the Dutch Childhood Oncology Group. J Clin Oncol. 2016;34(22):2591-601.
124. Grobner SN, Worst BC, Weischenfeldt J, Buchhalter I, Kleinheinz K, Rudneva VA, et al. The landscape of genomic alterations across childhood cancers. Nature. 2018;555(7696):321-7.
125. Massard C, Michiels S, Ferte C, Le Deley MC, Lacroix L, Hollebecque A, et al. High-Throughput Genomics and Clinical Outcome in Hard-to-Treat Advanced Cancers: Results of the MOSCATO 01 Trial. Cancer Discov. 2017;7(6):586-95.
126. Marquart J, Chen EY, Prasad V. Estimation of the Percentage of US Patients With Cancer Who Benefit From Genome-Driven Oncology. JAMA Oncol. 2018;4(8):1093-8.
127. Le Tourneau C, Delord JP, Goncalves A, Gavoille C, Dubot C, Isambert N, et al. Molecularly targeted therapy based on tumour molecular profiling versus conventional therapy for advanced cancer (SHIVA): a multicentre, open-label, proof-of-concept, randomised, controlled phase 2 trial. Lancet Oncol. 2015;16(13):1324-34.
128. Ma X, Liu Y, Liu Y, Alexandrov LB, Edmonson MN, Gawad C, et al. Pan-cancer genome and transcriptome analyses of 1,699 paediatric leukaemias and solid tumours. Nature. 2018;555(7696):371-6.
129. Matheson EC, Thomas H, Case M, Blair H, Jackson RK, Masic D, et al. Glucocorticoids and selumetinib are highly synergistic in RAS pathway mutated childhood acute lymphoblastic leukemia through upregulation of BIM. Haematologica. 2019.
130. Loh ML, Zhang J, Harvey RC, Roberts K, Payne-Turner D, Kang H, et al. Tyrosine kinome sequencing of pediatric acute lymphoblastic leukemia: a report from the Children's Oncology Group TARGET Project. Blood. 2013;121(3):485-8.
131. Doll S, Gnad F, Mann M. The Case for Proteomics and Phospho-Proteomics in Personalized Cancer Medicine. Proteomics Clin Appl. 2019;13(2):e1800113.
132. Worst BC, van Tilburg CM, Balasubramanian GP, Fiesel P, Witt R, Freitag A, et al. Next-generation personalised medicine for high-risk paediatric cancer patients - The INFORM pilot study. Eur J Cancer. 2016;65:91-101.
133. Atak ZK, Gianfelici V, Hulselmans G, De Keersmaecker K, Devasia AG, Geerdens E, et al. Comprehensive analysis of transcriptome variation uncovers known and novel driver events in T-cell acute lymphoblastic leukemia. PLoS Genet. 2013;9(12):e1003997.
134. Lopez-Nieva P, Fernandez-Navarro P, Grana-Castro O, Andres-Leon E, Santos J, Villa-Morales M, et al. Detection of novel fusion-transcripts by RNA-Seq in T-cell lymphoblastic lymphoma. Sci Rep. 2019;9(1):5179.
135. Inaba H, Azzato EM, Mullighan CG. Integration of Next-Generation Sequencing to Treat Acute Lymphoblastic Leukemia with Targetable Lesions: The St. Jude Children's Research Hospital Approach. Front Pediatr. 2017;5:258.
136. Hanahan D, Weinberg RA. Hallmarks of cancer: the next generation. Cell. 2011;144(5):646-74.
137. van Ooijen H, Hornsveld M, Dam-de Veen C, Velter R, Dou M, Verhaegh W, et al. Assessment of Functional Phosphatidylinositol 3-Kinase Pathway Activity in Cancer Tissue Using Forkhead Box-O Target Gene Expression in a Knowledge-Based Computational Model. Am J Pathol. 2018;188(9):1956-72.

138. Stolpe AV, Holtzer L, van Ooijen H, de Inda MA, Verhaegh W. Enabling precision medicine by unravelling disease pathophysiology: quantifying signal transduction pathway activity across cell and tissue types. Sci Rep. 2019;9(1):1603.
139. van de Stolpe A. Quantitative Measurement of Functional Activity of the PI3K Signaling Pathway in Cancer. Cancers (Basel). 2019;11(3).
140. Verhaegh W, van Ooijen H, Inda MA, Hatzis P, Versteeg R, Smid M, et al. Selection of personalized patient therapy through the use of knowledge-based computational models that identify tumor-driving signal transduction pathways. Cancer Res. 2014;74(11):2936-45.
141. Jimenez CR, Verheul HM. Mass spectrometry-based proteomics: from cancer biology to protein biomarkers, drug targets, and clinical applications. Am Soc Clin Oncol Educ Book. 2014:e504-10.
142. Cutillas PR. Role of phosphoproteomics in the development of personalized cancer therapies. Proteomics Clin Appl. 2015;9(3-4):383-95.
143. Casado P, Alcolea MP, Iorio F, Rodriguez-Prados JC, Vanhaesebroeck B, Saez-Rodriguez J, et al. Phosphoproteomics data classify hematological cancer cell lines according to tumor type and sensitivity to kinase inhibitors. Genome Biol. 2013;14(4):R37.
144. Lopez Villar E, Wu D, Cho WC, Madero L, Wang X. Proteomics-based discovery of biomarkers for paediatric acute lymphoblastic leukaemia: challenges and opportunities. J Cell Mol Med. 2014;18(7):1239-46.
145. Lopez Villar E, Wang X, Madero L, Cho WC. Application of oncoproteomics to aberrant signalling networks in changing the treatment paradigm in acute lymphoblastic leukaemia. J Cell Mol Med. 2015;19(1):46-52.
146. van der Sligte NE, Scherpen FJ, Meeuwsen-de Boer TG, Lourens HJ, Ter Elst A, Diks SH, et al. Kinase activity profiling reveals active signal transduction pathways in pediatric acute lymphoblastic leukemia: a new approach for target discovery. Proteomics. 2015;15(7):1245-54.
147. Serafin V, Lissandron V, Buldini B, Bresolin S, Paganin M, Grillo F, et al. Phosphoproteomic analysis reveals hyperactivation of mTOR/STAT3 and LCK/Calcineurin axes in pediatric early T-cell precursor ALL. Leukemia. 2017;31(4):1007-11.
148. Serafin V, Capuzzo G, Milani G, Minuzzo SA, Pinazza M, Bortolozzi R, et al. Glucocorticoid resistance is reverted by LCK inhibition in pediatric T-cell acute lymphoblastic leukemia. Blood. 2017;130(25):2750-61.
149. Beekhof R, van Alphen C, Henneman AA, Knol JC, Pham TV, Rolfs F, et al. INKA, an integrative data analysis pipeline for phosphoproteomic inference of active kinases. Mol Syst Biol. 2019;15(4):e8250.
150. Delgado-Martin C, Meyer LK, Huang BJ, Shimano KA, Zinter MS, Nguyen JV, et al. JAK/STAT pathway inhibition overcomes IL7-induced glucocorticoid resistance in a subset of human T-cell acute lymphoblastic leukemias. Leukemia. 2017;31(12):2568-76.
151. Degryse S, de Bock CE, Demeyer S, Govaerts I, Bornschein S, Verbeke D, et al. Mutant JAK3 phosphoproteomic profiling predicts synergism between JAK3 inhibitors and MEK/BCL2 inhibitors for the treatment of T-cell acute lymphoblastic leukemia. Leukemia. 2018;32(3):788-800.
152. Pham HTT, Maurer B, Prchal-Murphy M, Grausenburger R, Grundschober E, Javaheri T, et al. STAT5BN642H is a driver mutation for T cell neoplasia. J Clin Invest. 2018;128(1):387-401.
153. De Smedt R, Peirs S, Morscio J, Matthijssens F, Roels J, Reunes L, et al. Pre-clinical evaluation of second generation PIM inhibitors for the treatment of T-cell acute lymphoblastic leukemia and lymphoma. Haematologica. 2019;104(1):e17-e20.
154. de Bock CE, Demeyer S, Degryse S, Verbeke D, Sweron B, Gielen O, et al. HOXA9 Cooperates with Activated JAK/STAT Signaling to Drive Leukemia Development. Cancer Discov. 2018;8(5):616-31.

155. Ribeiro D, Melao A, van Boxtel R, Santos CI, Silva A, Silva MC, et al. STAT5 is essential for IL-7-mediated viability, growth, and proliferation of T-cell acute lymphoblastic leukemia cells. Blood Adv. 2018;2(17):2199-213.
156. Meijerink JP. Genetic rearrangements in relation to immunophenotype and outcome in T-cell acute lymphoblastic leukaemia. Best Pract Res Clin Haematol. 2010;23(3):307-18.
157. Aplan PD, Lombardi DP, Reaman GH, Sather HN, Hammond GD, Kirsch IR. Involvement of the putative hematopoietic transcription factor SCL in T-cell acute lymphoblastic leukemia. Blood. 1992;79(5):1327-33.
158. Wang J, Jani-Sait SN, Escalon EA, Carroll AJ, de Jong PJ, Kirsch IR, et al. The t(14;21)(q11.2;q22) chromosomal translocation associated with T-cell acute lymphoblastic leukemia activates the BHLHB1 gene. Proc Natl Acad Sci U S A. 2000;97(7):3497-502.
159. Hu S, Qian M, Zhang H, Guo Y, Yang J, Zhao X, et al. Whole-genome noncoding sequence analysis in T-cell acute lymphoblastic leukemia identifies oncogene enhancer mutations. Blood. 129. United States2017. p. 3264-8.
160. Chen S, Nagel S, Schneider B, Kaufmann M, Meyer C, Zaborski M, et al. Novel non-TCR chromosome translocations t(3;11)(q25;p13) and t(X;11)(q25;p13) activating LMO2 by juxtaposition with MBNL1 and STAG2. Leukemia. 2011;25(10):1632-5.
161. Hansen-Hagge TE, Schafer M, Kiyoi H, Morris SW, Whitlock JA, Koch P, et al. Disruption of the RanBP17/Hox11L2 region by recombination with the TCRdelta locus in acute lymphoblastic leukemias with t(5;14)(q34;q11). Leukemia. 2002;16(11):2205-12.
162. Su XY, Busson M, Della Valle V, Ballerini P, Dastugue N, Talmant P, et al. Various types of rearrangements target TLX3 locus in T-cell acute lymphoblastic leukemia. Genes Chromosomes Cancer. 2004;41(3):243-9.
163. Bergeron J, Clappier E, Cauwelier B, Dastugue N, Millien C, Delabesse E, et al. HOXA cluster deregulation in T-ALL associated with both a TCRD-HOXA and a CALM-AF10 chromosomal translocation. Leukemia. 2006;20(6):1184-7.
164. Cauwelier B, Cave H, Gervais C, Lessard M, Barin C, Perot C, et al. Clinical, cytogenetic and molecular characteristics of 14 T-ALL patients carrying the TCRbeta-HOXA rearrangement: a study of the Groupe Francophone de Cytogenetique Hematologique. Leukemia. 2007;21(1):121-8.
165. Speleman F, Cauwelier B, Dastugue N, Cools J, Verhasselt B, Poppe B, et al. A new recurrent inversion, inv(7)(p15q34), leads to transcriptional activation of HOXA10 and HOXA11 in a subset of T-cell acute lymphoblastic leukemias. Leukemia. 2005;19(3):358-66.
166. Nagel S, Kaufmann M, Drexler HG, MacLeod RA. The cardiac homeobox gene NKX2-5 is deregulated by juxtaposition with BCL11B in pediatric T-ALL cell lines via a novel t(5;14)(q35.1;q32.2). Cancer Res. 2003;63(17):5329-34.
167. Przybylski GK, Dik WA, Grabarczyk P, Wanzeck J, Chudobska P, Jankowski K, et al. The effect of a novel recombination between the homeobox gene NKX2-5 and the TRD locus in T-cell acute lymphoblastic leukemia on activation of the NKX2-5 gene. Haematologica. 2006;91(3):317-21.
168. Clappier E, Cuccuini W, Kalota A, Crinquette A, Cayuela JM, Dik WA, et al. The C-MYB locus is involved in chromosomal translocation and genomic duplications in human T-cell acute leukemia (T-ALL) - the translocation defining a new T-ALL subtype in very young children. Blood. 2007;110(4):1251-61.
169. Lahortiga I, De Keersmaecker K, Van Vlierberghe P, Graux C, Cauwelier B, Lambert F, et al. Duplication of the MYB oncogene in T cell acute lymphoblastic leukemia. Nat Genet. 2007;39(5):593-5.
170. O'Neil J, Tchinda J, Gutierrez A, Moreau L, Maser RS, Wong KK, et al. Alu elements mediate MYB gene tandem duplication in human T-ALL. J Exp Med. 2007;204(13):3059-66.

171. Clappier E, Cuccuini W, Cayuela JM, Vecchione D, Baruchel A, Dombret H, et al. Cyclin D2 dysregulation by chromosomal translocations to TCR loci in T-cell acute lymphoblastic leukemias. Leukemia. 2006;20(1):82-6.
172. Dik WA, Brahim W, Braun C, Asnafi V, Dastugue N, Bernard OA, et al. CALM-AF10+ T-ALL expression profiles are characterized by overexpression of HOXA and BMI1 oncogenes. Leukemia. 2005;19(11):1948-57.
173. Ferrando AA, Armstrong SA, Neuberg DS, Sallan SE, Silverman LB, Korsmeyer SJ, et al. Gene expression signatures in MLL-rearranged T-lineage and B-precursor acute leukemias: dominance of HOX dysregulation. Blood. 2003;102(1):262-8.
174. Quentmeier H, Schneider B, Rohrs S, Romani J, Zaborski M, Macleod RA, et al. SET-NUP214 fusion in acute myeloid leukemia- and T-cell acute lymphoblastic leukemia-derived cell lines. J Hematol Oncol. 2009;2:3.
175. Barber KE, Martineau M, Harewood L, Stewart M, Cameron E, Strefford JC, et al. Amplification of the ABL gene in T-cell acute lymphoblastic leukemia. Leukemia. 2004;18(6):1153-6.
176. Bernasconi P, Calatroni S, Giardini I, Inzoli A, Castagnola C, Cavigliano PM, et al. ABL1 amplification in T-cell acute lymphoblastic leukemia. Cancer Genet Cytogenet. 2005;162(2):146-50.
177. Graux C, Cools J, Melotte C, Quentmeier H, Ferrando A, Levine R, et al. Fusion of NUP214 to ABL1 on amplified episomes in T-cell acute lymphoblastic leukemia. Nat Genet. 2004;36(10):1084-9.
178. Graux C, Stevens-Kroef M, Lafage M, Dastugue N, Harrison CJ, Mugneret F, et al. Heterogeneous patterns of amplification of the NUP214-ABL1 fusion gene in T-cell acute lymphoblastic leukemia. Leukemia. 2009;23(1):125-33.
179. Stergianou K, Fox C, Russell NH. Fusion of NUP214 to ABL1 on amplified episomes in T-ALL--implications for treatment. Leukemia. 2005;19(9):1680-1.
180. De Keersmaecker K, Graux C, Odero MD, Mentens N, Somers R, Maertens J, et al. Fusion of EML1 to ABL1 in T-cell acute lymphoblastic leukemia with cryptic t(9;14)(q34;q32). Blood. 2005;105(12):4849-52.
181. Van Limbergen H, Beverloo HB, van Drunen E, Janssens A, Hahlen K, Poppe B, et al. Molecular cytogenetic and clinical findings in ETV6/ABL1-positive leukemia. Genes Chromosomes Cancer. 2001;30(3):274-82.
182. Fabbiano F, Santoro A, Felice R, Catania P, Cannella S, Majolino I. bcr-abl rearrangement in adult T-lineage acute lymphoblastic leukemia. Haematologica. 1998;83(9):856-7.
183. Quentmeier H, Cools J, Macleod RA, Marynen P, Uphoff CC, Drexler HG. e6-a2 BCR-ABL1 fusion in T-cell acute lymphoblastic leukemia. Leukemia. 2005;19(2):295-6.
184. Colleoni GW, Yamamoto M, Kerbauy J, Serafim RC, Lindsey CJ, Costa FF, et al. BCR-ABL rearrangement in adult T-cell acute lymphoblastic leukemia. Am J Hematol. 1996;53(4):277-8.
185. De Braekeleer E, Douet-Guilbert N, Rowe D, Bown N, Morel F, Berthou C, et al. ABL1 fusion genes in hematological malignancies: a review. Eur J Haematol. 2011;86(5):361-71.
186. Bond J, Bergon A, Durand A, Tigaud I, Thomas X, Asnafi V, et al. Cryptic XPO1-MLLT10 translocation is associated with HOXA locus deregulation in T-ALL. Blood. 2014;124(19):3023-5.
187. Kox C, Zimmermann M, Stanulla M, Leible S, Schrappe M, Ludwig WD, et al. The favorable effect of activating NOTCH1 receptor mutations on long-term outcome in T-ALL patients treated on the ALL-BFM 2000 protocol can be separated from FBXW7 loss of function. Leukemia. 2010;24(12):2005-13.

188. Zuurbier L, Homminga I, Calvert V, te Winkel ML, Buijs-Gladdines JG, Kooi C, et al. NOTCH1 and/or FBXW7 mutations predict for initial good prednisone response but not for improved outcome in pediatric T-cell acute lymphoblastic leukemia patients treated on DCOG or COALL protocols. Leukemia. 2010;24(12):2014-22.
189. Asnafi V, Buzyn A, Le Noir S, Baleydier F, Simon A, Beldjord K, et al. NOTCH1/FBXW7 mutation identifies a large subgroup with favorable outcome in adult T-cell acute lymphoblastic leukemia (T-ALL): a Group for Research on Adult Acute Lymphoblastic Leukemia (GRAALL) study. Blood. 2009;113(17):3918-24.
190. Breit S, Stanulla M, Flohr T, Schrappe M, Ludwig WD, Tolle G, et al. Activating NOTCH1 mutations predict favorable early treatment response and long-term outcome in childhood precursor T-cell lymphoblastic leukemia. Blood. 2006;108(4):1151-7.
191. Bandapalli OR, Zimmermann M, Kox C, Stanulla M, Schrappe M, Ludwig WD, et al. NOTCH1 activation clinically antagonizes the unfavorable effect of PTEN inactivation in BFM-treated children with precursor T-cell acute lymphoblastic leukemia. Haematologica. 2013;98(6):928-36.
192. Kleppe M, Lahortiga I, El Chaar T, De Keersmaecker K, Mentens N, Graux C, et al. Deletion of the protein tyrosine phosphatase gene PTPN2 in T-cell acute lymphoblastic leukemia. Nat Genet. 2010;42(6):530-5.
193. Kleppe M, Soulier J, Asnafi V, Mentens N, Hornakova T, Knoops L, et al. PTPN2 negatively regulates oncogenic JAK1 in T-cell acute lymphoblastic leukemia. Blood. 2011;117(26):7090-8.
194. Melao A, Spit M, Cardoso BA, Barata JT. Optimal interleukin-7 receptor-mediated signaling, cell cycle progression and viability of T-cell acute lymphoblastic leukemia cells rely on casein kinase 2 activity. Haematologica. 2016;101(11):1368-79.
195. Szarzynska-Zawadzka B, Kunz JB, Sedek L, Kosmalska M, Zdon K, Biecek P, et al. PTEN abnormalities predict poor outcome in children with T-cell acute lymphoblastic leukemia treated according to ALL IC-BFM protocols. Am J Hematol. 2019;94(4):E93-E6.
196. Maser RS, Choudhury B, Campbell PJ, Feng B, Wong KK, Protopopov A, et al. Chromosomally unstable mouse tumours have genomic alterations similar to diverse human cancers. Nature. 2007;447(7147):966-71.
197. Silva A, Yunes JA, Cardoso BA, Martins LR, Jotta PY, Abecasis M, et al. PTEN posttranslational inactivation and hyperactivation of the PI3K/Akt pathway sustain primary T cell leukemia viability. J Clin Invest. 2008;118(11):3762-74.
198. Neumann M, Heesch S, Schlee C, Schwartz S, Gokbuget N, Hoelzer D, et al. Whole-exome sequencing in adult ETP-ALL reveals a high rate of DNMT3A mutations. Blood. 2013;121(23):4749-52.
199. Perez-Garcia A, Ambesi-Impiombato A, Hadler M, Rigo I, LeDuc CA, Kelly K, et al. Genetic loss of SH2B3 in acute lymphoblastic leukemia. Blood. 2013;122(14):2425-32.
200. Huether R, Dong L, Chen X, Wu G, Parker M, Wei L, et al. The landscape of somatic mutations in epigenetic regulators across 1,000 paediatric cancer genomes. Nat Commun. 2014;5:3630.
201. Van Vlierberghe P, Palomero T, Khiabanian H, Van der Meulen J, Castillo M, Van Roy N, et al. PHF6 mutations in T-cell acute lymphoblastic leukemia. Nat Genet. 2010;42(4):338-42.
202. Tosello V, Mansour MR, Barnes K, Paganin M, Sulis ML, Jenkinson S, et al. WT1 mutations in T-ALL. Blood. 2009;114(5):1038-45.
203. Gutierrez A, Sanda T, Ma W, Zhang J, Grebliunaite R, Dahlberg S, et al. Inactivation of LEF1 in T-cell acute lymphoblastic leukemia. Blood. 2010;115(14):2845-51.
204. De Keersmaecker K, Atak ZK, Li N, Vicente C, Patchett S, Girardi T, et al. Exome sequencing identifies mutation in CNOT3 and ribosomal genes RPL5 and RPL10 in T-cell acute lymphoblastic leukemia. Nat Genet. 2013;45(2):186-90.

205. Ntziachristos P, Tsirigos A, Van Vlierberghe P, Nedjic J, Trimarchi T, Flaherty MS, et al. Genetic inactivation of the polycomb repressive complex 2 in T cell acute lymphoblastic leukemia. Nat Med. 2012;18(2):298-301.
206. Girardi T, Vereecke S, Sulima SO, Khan Y, Fancello L, Briggs JW, et al. The T-cell leukemia-associated ribosomal RPL10 R98S mutation enhances JAK-STAT signaling. Leukemia. 2018;32(3):809-19.
207. Rao S, Lee SY, Gutierrez A, Perrigoue J, Thapa RJ, Tu Z, et al. Inactivation of ribosomal protein L22 promotes transformation by induction of the stemness factor, Lin28B. Blood. 2012;120(18):3764-73.
208. Gachet S, El-Chaar T, Avran D, Genesca E, Catez F, Quentin S, et al. Deletion 6q Drives T-cell Leukemia Progression by Ribosome Modulation. Cancer Discov. 2018;8(12):1614-31.
209. Kampen KR, Sulima SO, Verbelen B, Girardi T, Vereecke S, Fancello L, et al. Correction: The ribosomal RPL10 R98S mutation drives IRES-dependent BCL-2 translation in T-ALL. Leukemia. 2019;33(4):1055-62.
210. Ge Z, Li M, Zhao G, Xiao L, Gu Y, Zhou X, et al. Novel dynamin 2 mutations in adult T-cell acute lymphoblastic leukemia. Oncol Lett. 2016;12(4):2746-51.
211. Tremblay CS, Brown FC, Collett M, Saw J, Chiu SK, Sonderegger SE, et al. Loss-of-function mutations of Dynamin 2 promote T-ALL by enhancing IL-7 signalling. Leukemia. 2016;30(10):1993-2001.
212. Tzoneva G, Perez-Garcia A, Carpenter Z, Khiabanian H, Tosello V, Allegretta M, et al. Activating mutations in the NT5C2 nucleotidase gene drive chemotherapy resistance in relapsed ALL. Nat Med. 2013;19(3):368-71.
213. Chonghaile TN, Roderick JE, Glenfield C, Ryan J, Sallan SE, Silverman LB, et al. Maturation stage of T-cell acute lymphoblastic leukemia determines BCL-2 versus BCL-XL dependence and sensitivity to ABT-199. Cancer Discov. 2014;4(9):1074-87.
214. Kawashima-Goto S, Imamura T, Tomoyasu C, Yano M, Yoshida H, Fujiki A, et al. BCL2 Inhibitor (ABT-737): A Restorer of Prednisolone Sensitivity in Early T-Cell Precursor-Acute Lymphoblastic Leukemia with High MEF2C Expression? PLoS One. 2015;10(7):e0132926.
215. Peirs S, Matthijssens F, Goossens S, Van de Walle I, Ruggero K, de Bock CE, et al. ABT-199 mediated inhibition of BCL-2 as a novel therapeutic strategy in T-cell acute lymphoblastic leukemia. Blood. 2014;124(25):3738-47.
216. Suryani S, Carol H, Chonghaile TN, Frismantas V, Sarmah C, High L, et al. Cell and molecular determinants of in vivo efficacy of the BH3 mimetic ABT-263 against pediatric acute lymphoblastic leukemia xenografts. Clin Cancer Res. 2014;20(17):4520-31.

9

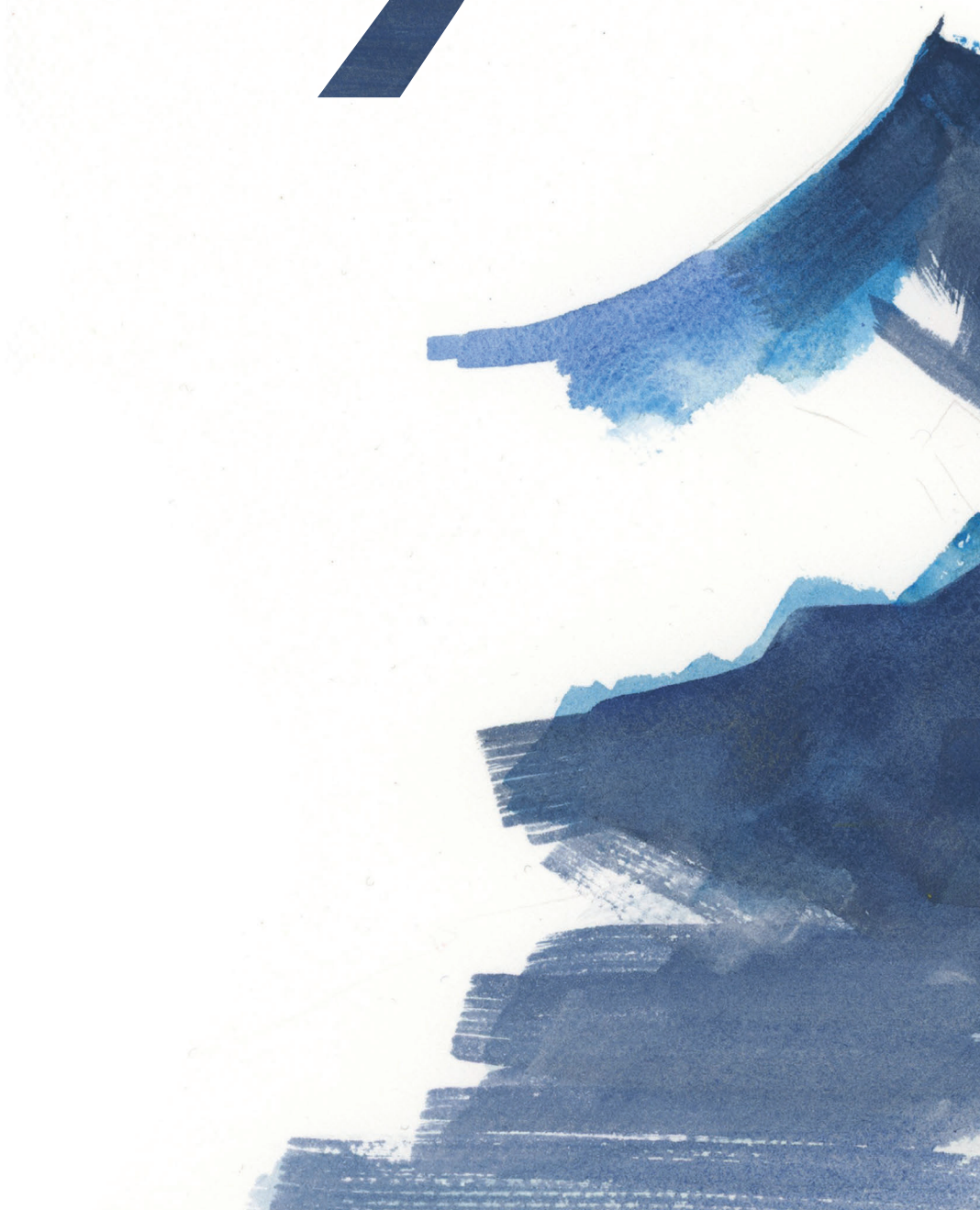

Summary, general discussion and future perspectives

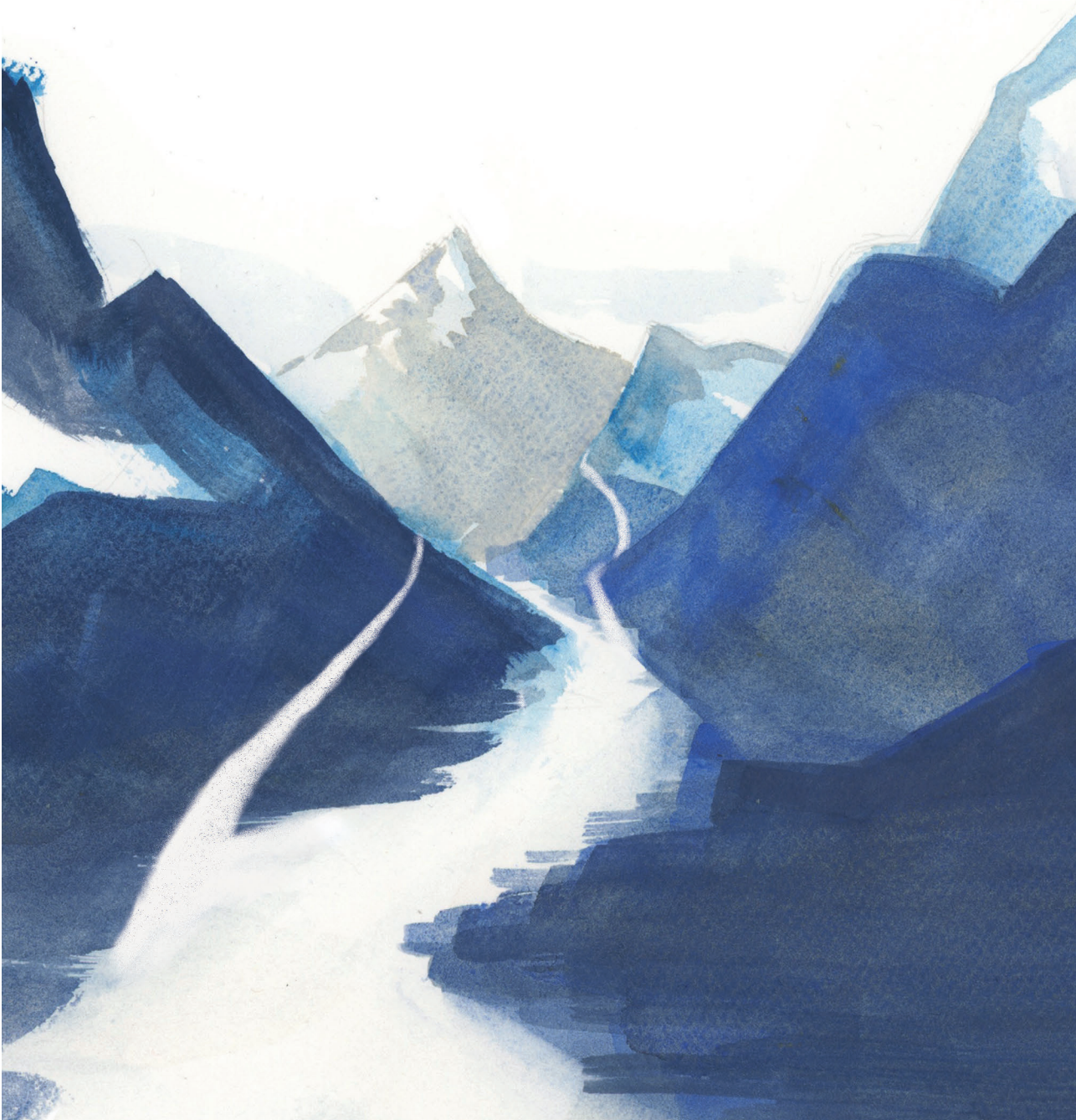

T-cell acute lymphoblastic leukemia (T-ALL) is a rare hematologic malignancy which yearly affects around 15-20 children in the Netherlands (SKION database). The malignant expansion of leukemic blasts in the bone marrow severely oppresses the development of healthy blood cells and is lethal when inadequately treated. Synthetic glucocorticoids (i.e. dexamethasone and prednisolone) are cornerstone drugs in the treatment regimens of pediatric ALL patients. The induction phase of the current Dutch Childhood Oncology Group (DCOG) ALL-11 protocol starts with 7 days of systemic treatment with high-dose prednisolone. Measuring the therapeutic effect of this first week of prednisolone treatment and the minimal residue disease (MRD) at day 33 and 79 of treatment has drastically improved risk-stratification and therefore the outcome of ALL patients (1). However, the overall and event-free survival for T-ALL patients has only slightly improved over the last two decades and is still inferior compared to B-cell precursor (BCP-) ALL patients (2, 3). Still, 1 out of 5 pediatric T-ALL patients succumb to relapse (2, 4, 5). Moreover, 34% of T-ALL patients are stratified to high-risk treatment arms compared to 6% of BCP-ALL patients (DCOG ALL-10 protocol) (1). This indicates that cellular mechanisms in malignant T-cells negatively impact early treatment response, requiring more intensive treatment. Therefore, novel and personalized treatment options are required to improve the outcome of this high-risk leukemia subtype.

Currently, over 40 novel targeted therapies have been tested in a clinical or pre-clinical setting for ALL. We reviewed these novel therapies in **chapter 2** of this thesis (6). Leukemic cells may become dependent on the aberrant activation of specific receptors or kinases, which generates a vulnerability that can be targeted with selective inhibitors. Importantly, some targeted inhibitors do not induce cell death as monotherapy, but can potentiate the anti-leukemic activity of contemporary chemotherapeutic compounds. This is of specific interest in diseases where drug resistance is often observed, like (relapsed) T-ALL. Moreover, these compounds may prevent the outgrowth of leukemic (sub)clones that give rise to relapsed disease later in life. Therefore, it is important to study the direct cytotoxic and cytostatic effects of novel compounds, but to also study their potential to synergize with other targeted compounds or contemporary chemotherapeutics that are currently used in ALL treatment regimens.

Resistance to steroid treatment is frequently observed in T-ALL and predicts for inferior outcome (5, 7, 8). This thesis therefore focused on the identification of inhibitors that could overcome steroid resistance and warrant a steroid-sensitive phenotype of leukemic T-ALL blasts. Synthetic glucocorticoids effectuate steroid-induced cell death via the activation of the glucocorticoid receptor (NR3C1). Activation of NR3C1 leads to its cytoplasmic-to-nuclear translocation, where it functions as a transcription factor and induces the transcription of genes that are vital for steroid-induced cell death. One of these target genes is the pro-apoptotic Bcl2-family member *BIM* (9). Steroid-induced activation of NR3C1 also induces the expression of *IL7R*. We studied the significance of recurrent *NR3C1* aberrations that are found in 7% of the T-ALL patients at disease

diagnosis in **chapter 3** (10)**.** We observed that *NR3C1* inactivating aberrations – including deletions, missense and nonsense mutations – relate to steroid resistance at disease diagnosis. However, in the REH cell line model which lacks a functional glucocorticoid receptor, the majority of our identified *NR3C1* missense mutations remained functional and induced robust steroid-induced cell death. Moreover, relative *NR3C1* mRNA expression in primary diagnostic T-ALL patient samples was not related to steroid sensitivity. These somewhat contradicting results indicate that steroid responsiveness at disease diagnosis is not solely defined by NR3C1, and that other aberrations may be more dominant in determining steroid responsiveness. However, the presence of *NR3C1* mutations may still synergize with these other aberrations at disease diagnosis and therefore contribute to steroid resistance.

In this thesis, we aimed to expose dominant mechanisms that drive steroid resistance and could be targeted with specific inhibitors. We therefore shifted our interest to other genetic aberrations that relate to steroid resistance. Recently, using whole-genome sequencing and target-exome sequencing in a cohort of 146 pediatric T-ALL patients (11), we found that mutations in the IL7R signaling pathway related to steroid resistance and inferior event-free survival. These mutations are found in nearly 35% of T-ALL patients, and include mutations of the IL-7 receptor (IL7R) alpha chain or downstream signaling proteins, including JAK1, JAK3, STAT5, AKT and RAS. Moreover, IL-7 can also provoke steroid resistance in T-ALL in the absence of these mutations (i.e. IL7-dependent steroid resistance) (12, 13).

IL7R signaling is important in normal T-cell development, since activation of the IL7R supports the survival of differentiating thymocytes at specific stages of T-cell development (14, 15). The IL7R signaling cascade roughly consists of three downstream signaling branches: the JAK-STAT pathway, the PI3K-AKT pathway and the MAPK-ERK pathway. Physiological activation of the IL7R by IL-7 in healthy T-cells activates downstream JAK-STAT and PI3K-AKT pathways. Moreover, IL-7 can also activate these pathways in T-ALL blasts (12, 13, 16, 17). In contrast, activation of the MAPK-ERK pathway by IL-7 in healthy T-cells and T-ALL patient blasts has not been reported before.

Thus far, STAT5 activation has been considered as the driving pathway for IL7-dependent steroid resistance (12, 13). STAT5 is activated (phosphorylated) upon binding to the activated IL7R (by IL-7), resulting in its homodimerization and migration to the nucleus to induce the expression of various target genes including anti-apoptotic *BCL2*, *BCLXL*, and *PIM1* (18). Steroid treatment induces the expression of *IL7R*, which results in enhanced activation of the STAT5 pathway in the presence of IL-7. As a result, the expression of anti-apoptotic proteins via STAT5 is enhanced by steroid treatment, resulting in steroid resistance (13, 19). Inhibition of JAK1/2 kinases by the small molecule inhibitor ruxolitinib has been demonstrated to abolish STAT5 pathway activation, and synergizes with dexamethasone in IL7-exposed CCRF-CEM cells and *in-vivo* T-ALL models

(12, 13, 20). This synergy has mainly been attributed to the decreased expression of anti-apoptotic *BCL2* by ruxolitinib. However, we hypothesized that inhibition of other signaling pathways downstream of IL7R/JAK such as the MAPK-ERK and the PI3K-AKT pathways may contribute to the observed enhanced steroid cytotoxic effect by ruxolitinib treatment. Therefore, we first studied the contribution of each of the IL7R downstream pathways in relation to steroid resistance in T-ALL.

Thus far, activation of MAPK-ERK signaling has been poorly studied in the context of aberrant IL7R signaling. Our group modeled various activating IL7R pathway mutations (including. *IL7Rα*, *JAK1* and *RAS* mutations) in steroid sensitive T-ALL SUPT-1 and P12 Ichikawa cell lines that resulted in high activation of the MAPK-ERK pathway and a steroid-resistant phenotype (11). Interestingly, these mutations also belong to a small set of mutations that predict for extreme poor outcome in relapsed T-ALL patients (21). Activation of the MAPK-ERK pathway may therefore play a vital role in steroid resistance and in the selective clonal selection of leukemic blasts during treatment. In **chapter 4**, we observed that activating mutations in *IL7R*, *JAK1* or *NRAS*, and activation of the IL7Rα by IL-7 activates MAPK-ERK signaling drive a steroid resistant phenotype. We found that activation of MAPK-ERK signaling resulted in the phosphorylation of pro-apoptotic BIM that rendered BIM unable to effectively bind and neutralize anti-apoptotic Bcl2-family member proteins including BCL2, BCLXL and MCL1. The balance between anti- and pro-apoptotic Bcl-2 family members therefore seems vital for the steroid responsiveness of leukemic blasts. MAPK-ERK pathway activation could effectively be abolished by treatment with MEK-inhibitors selumetinib and trametinib that avoided phosphorylation of BIM, and restored binding of BIM to anti-apoptotic proteins. Importantly, selumetinib was highly synergistic with steroid treatment in steroid resistant T-ALL PDX samples of which steroid resistance was dependent ('IL7-dependent') or independent ('IL7-independent') on the presence of IL-7. In contrast, the JAK1/2 inhibitor ruxolitinib only inhibited MAPK-ERK signaling if activation of this pathway was provoked by IL-7 or by mutations in *IL7R* or *JAK1* (that were denoted as 'upstream mutations'), but not by steroid resistance that was induced by downstream RAS mutations. Moreover, ruxolitinib was only synergistic with prednisolone in IL7-dependent steroid resistant PDX samples in the presence of IL-7, but not in IL7-independent steroid resistant PDX samples. Therefore, our study highlights the broader application of MEK-inhibitors over ruxolitinib to re-sensitize steroid-resistant T-ALL cells, and recommends MEK-inhibitors over ruxolitinib for patients with activating IL7R, JAK1 and RAS mutations or aberrant MAPK-ERK signaling in future basket-trials for T-ALL patients. These are import recommendations for the current phase I/II SeluDex trial (NCT03705507).

Chapter 4 concludes that preserving the function of pro-apoptotic BIM (i.e. by preventing or abolishing inhibitory phosphorylation) is crucial for effective steroid-induced cell death, suggesting that novel inhibitors that mimic the function of BIM (i.e. 'BH3-mimetics) seem promising in steroid-resistant T-ALL (22-25). In **chapter 5**, we therefore

studied the use of BH3-mimetics in combination with steroid treatment and/or MEK-inhibitors. When studying the interaction between pro- and anti-apoptotic molecules, we observed that BH3-mimetics indeed mimic the function of BIM by effectively binding and neutralizing the anti-apoptotic effects of BCL2, BCL-XL and MCL1 proteins. However, preventing phosphorylation of BIM by MEK-inhibitors was more effective in inducing cell death and restoring the apoptotic balance (as measured by BH3-profilling) than BH3-mimetics. Venetoclax, a BCL2-directed BH3-mimetic, was synergistic with steroid treatment in IL7-dependent steroid resistant T-ALL cells. Moreover, this compound synergized with MEK-inhibitor selumetinib and allowed dose-reduction of both compounds when administered as triple treatment with prednisolone. However, our work indicated that preserving the function of pro-apoptotic BIM (by MEK-inhibitors) seems more effective as therapy to restore a sensitive steroid response than inhibition of anti-apoptotic molecules (by BH3-mimetics) in general. Further research is required to study if combined MEK-inhibitor/BH3-mimetic therapy is more effective in *BCL2* overexpressing (T-cell) leukemias specifically. This is relevant for novel basket-trials, as venetoclax will be tested in combination with contemporary chemotherapeutics and other targeted compounds in *BCL2* overexpressing leukemias.

In **chapter 6**, we specifically studied the contribution of activated STAT5 signaling to steroid resistance. Activation of STAT5 in SUPT-1 cells only slightly activated the expression of anti-apoptotic *BCL2* and *BCLXL,* despite being reported as STAT5 direct target genes. In the presence of steroid treatment, the expression of BCL2 and BCLXL was strongly enhanced (hyper-induction) in these cells. Ruxolitinib abolished this hyper-induction of anti-apoptotic proteins and sensitized these cells for prednisolone treatment. However, combined AKT- and MEK-inhibition also sensitized these cells to steroid treatment, despite their controversial effect by even further enhancing the expression of *BCL2* and *BCLXL* in the presence of prednisolone. This suggested that STAT5- and steroid dependent hyper-induction of anti-apoptotic molecules does not drive steroid resistance *per se*. Indeed, overexpression of the activating $STAT5^{N642H}$ mutation does not provoke steroid resistance in SUPT-1 cells, despite high expression of anti-apoptotic *BCL2* and *BCLXL* by steroid treatment. We therefore hypothesized that the role of sole STAT5 pathway activation in steroid resistance is limited, and that the hyper-induction of BCL2 and BCLXL proteins is neutralized by the upregulation of steroid receptor target gene *BIM* following steroid exposure. In the case of BIM inactivating events, like absence of a functional NR3C1 receptor, phosphorylation by activated MAPK-ERK signaling (chapter 4) or transcriptional inhibition via AKT/FOXO3a (26), the upregulation of anti-apoptotic molecules is no longer counterbalanced by BIM resulting in steroid resistance. Thus, the interplay between all three IL7R downstream signaling pathways seems determinative for the steroid sensitivity of leukemic blasts.

In addition to studying novel treatment combinations for T-ALL patients, we also studied the molecular mechanisms induced by aberrant IL7R signaling and steroid treatment. In

chapter 6, we identified a novel mechanism in which steroid treatment enhances the transcription of canonical STAT5 target genes. Thus far, the steroid/STAT5-dependent hyper-induction of *BCL2* was demonstrated to be regulated via IL7R. Steroid treatment also enhances the expression of *IL7R* (as it is a direct NR3C1 transcriptional target gene), which enhances the abundancy of IL7R at the cell surface. In the presence of IL-7, this results in enhanced STAT5 signaling and thus the expression of *BCL2* (as a direct STAT5 transcriptional target gene). However, we identified that NR3C1 and STAT5 interact at regulatory STAT5 target gene sites in T-ALL, exposing an alternative and direct regulatory mechanism in which steroid treatment can enhance the expression of 'canonical' STAT5 regulated genes.

In **chapter 7**, we specifically studied the mechanistic differences between physiological and mutant AKT signaling. For this, we studied the transforming AKT^{E17K} mutation, which drives IL3-independent proliferation in IL3-dependent Ba/F3 cells while normal AKT does not (27, 28). Interestingly, we observed that the AKT^{E17K} mutation does not confer steroid resistance in contrast to wild type AKT. We demonstrated that AKT^{E17K} is predominantly localized at the inner cell membrane, while wild type AKT is located throughout the cell. Moreover, relieving AKT from its inhibitory conformation by the E17K mutation preempts C-tail phosphorylation of the kinase, resulting in an enhanced T308/S473 ratio in AKT^{E17K} versus AKT^{WT} cells. This supports recent reports in which the first step of AKT activation is accomplished by C-tail phosphorylation at S473 (29, 30). S473 phosphorylation seems indispensable if the PH-domain is already in an open conformation, which is the case for the AKT^{E17K} mutant molecule. Unfortunately, we could not identify which downstream substrates were affected by the altered cellular localization or activation mechanism of AKT^{E17K}. Therefore, more research is required to identify difference in downstream E17K versus wild type AKT signaling to understand why AKT^{E17K} cells do not provoke severe steroid resistance in T-ALL.

Chapter 4-7 uncovered important signaling mechanisms induced by aberrant IL7R signaling, of which some contribute to steroid resistance. By selectively studying the downstream branches of the IL7R signaling cascade individually, we carefully aimed to uncover new treatment strategies for pediatric T-ALL patients. This thesis recommends the use of MEK-inhibitors in future T-ALL treatment regimens. However, it may be challenging to integrate our findings in current treatment regimens, given the low prevalence of pediatric T-ALL and the relative beneficial outcome for pediatric ALL patients in general. The use of novel inhibitors should therefore be personalized to the biology of the leukemia. In **chapter 8**, we discussed our view on future diagnostic screenings to personalize and optimize the treatment of T-ALL patients (31). Recently, multiple genomic-directed treatment strategies for adults with metastasized carcinoma have been developed and studied (32-34). By tumor sequencing, targeted inhibitors were selected for individualized treatment. Unfortunately, these mutation-based treatment stratification programs only yielded minimal prognostic benefits. It remains

debatable to which extend sole genomic-based treatment strategies will improve T-ALL treatment regimens, since many mutations in T-ALL are frequently identified at a subclonal level and therefore may not represent a therapeutic target in all leukemia cells (35). For example; in the context of a subclonal $NRAS^{G12D}$ mutation, genomics-based treatment strategies may not identify this mutation as the driving and most preferred aberration to target, while disregarding the fact that this mutation may facilitate clonal selection by provoking steroid resistance. Consequently, MEK-inhibitors will not be advised as therapeutic strategy, even if these cells have to potency to facilitate disease relapse later in life. Moreover, some patients without classic MAPK-ERK activating mutations might also benefit from MEK-inhibitor treatment. We therefore believe that integration of genomics, transcriptomics and proteomics is crucial to fully understand which signaling events are active and important for the leukemia, allowing the most optimal personalized therapy recommendation.

In addition to the suggested *multi-omic* diagnostic screening, other functional screenings or biomarkers may also optimize personalized therapy or serve as a risk-stratification marker in the induction phase of therapy. As an example, increased mitochondrial priming which measures the capacity of the leukemia cells to undergo apoptosis upon treatment as measured using the BH3-profilling assay can predicts a superior clinical response to conventional chemotherapeutic agents in ALL (36). Priming-increasing agents, like BH3-mimetics, may therefore be used to treat leukemic blasts with low priming states (i.e. apoptosis resistance cells). More research is required to study if certain leukemic phenotypes – like high *BCL2* expression or the T-ALL ETP-subtype (characterized by high *BCL2* expression) – associate with low mitochondrial apoptotic priming, which would allow certain leukemic phenotypes to be used as biomarkers for personalized treatment. Based on the results of this thesis, we recommend the use of MEK-inhibitors in the treatment of T-ALL patients to maintain the pro-apoptotic function of BIM to effectuate steroid-induced cell death. Ideally, MEK-inhibitor treatment will be applied in the first week of systemic high-dose steroid treatment, to prevent the selection of leukemic blasts that evade steroid-induced cell death by phosphorylation of BIM. Unfortunately, we did not yet identify the phosphorylation site(s) of BIM that apparently is/are essential for the interaction of BIM with anti-apoptotic molecules. Further research is therefore required to identify the exact phosphorylation site(s), to which a diagnostic antibody staining can be developed in the future to identify potential steroid resistant patients that may benefit from combined MEK-inhibitor-steroid treatment.

Currently, novel inhibitors are mainly studied in the context of relapsed disease. For relapsed T-ALL, we suggest that basket trials should be constructed on a multi-omics stratification model. This thesis suggests that patients with a MAPK-ERK activating mutation (identified by genomic sequencing) – including *IL7R*, JAK1 and RAS mutations – should be eligible for MEK-inhibitor treatment in combination with steroid treatment.

Although not specifically studied in this thesis, BCL2 directed BH3-mimetics like venetoclax could be considered for patients with high *BCL2* expression (identified by transcriptomic sequencing, or ETP-ALL patients). Last, patients with blasts displaying high levels of MAPK-ERK pathway activation (or phosphorylation of BIM; identified by proteomic screens or immunoblot analysis) should also be eligible for MEK-inhibitor treatment. Sophisticated basket-trials will allow us to study the effect of novel inhibitors in a controlled setting. Importantly, since relapsed T-ALL is usually extreme chemo-resistant, promising results in relapsed T-ALL may even predict for bigger effects of this inhibitor in the setting of first-line treatment regimens. Hopefully, these trials will substantiate the potential use of combined MEK-inhibitor and steroid therapy in future (first-like) treatment regimens, to ultimately improve the outcome of pediatric T-ALL patients.

REFERENCES

1. Pieters R, de Groot-Kruseman H, Van der Velden V, Fiocco M, van den Berg H, de Bont E, et al. Successful Therapy Reduction and Intensification for Childhood Acute Lymphoblastic Leukemia Based on Minimal Residual Disease Monitoring: Study ALL10 From the Dutch Childhood Oncology Group. J Clin Oncol. 2016;34(22):2591-601.
2. Reedijk AMJ, Coebergh JWW, de Groot-Kruseman HA, van der Sluis IM, Kremer LC, Karim-Kos HE, et al. Progress against childhood and adolescent acute lymphoblastic leukaemia in the Netherlands, 1990-2015. Leukemia. 2020.
3. de Bruin O, Hagleitner MM, de Groot-Kruseman HA, Fiocco M, Karim-Kos HE, Pieters R. Outcome for Childhood T-cell Acute Lymphoblastic Leukemia (T-ALL) in the Netherlands: a Population-based study over 24-years Unpublished. 2021.
4. Conter V, Valsecchi MG, Parasole R, Putti MC, Locatelli F, Barisone E, et al. Childhood high-risk acute lymphoblastic leukemia in first remission: results after chemotherapy or transplant from the AIEOP ALL 2000 study. Blood. 2014;123(10):1470-8.
5. Lauten M, Moricke A, Beier R, Zimmermann M, Stanulla M, Meissner B, et al. Prediction of outcome by early bone marrow response in childhood acute lymphoblastic leukemia treated in the ALL-BFM 95 trial: differential effects in precursor B-cell and T-cell leukemia. Haematologica. 2012;97(7):1048-56.
6. Cordo' V, van der Zwet JCG, Canté-Barrett K, Pieters R, Meijerink JPP. T-cell Acute Lymphoblastic Leukemia: A Roadmap to Targeted Therapies. Blood Cancer Discovery. 2021;2(1):19-31.
7. Kaspers GJ, Pieters R, Van Zantwijk CH, Van Wering ER, Van Der Does-Van Den Berg A, Veerman AJ. Prednisolone resistance in childhood acute lymphoblastic leukemia: vitro-vivo correlations and cross-resistance to other drugs. Blood. 1998;92(1):259-66.
8. Lauten M, Stanulla M, Zimmermann M, Welte K, Riehm H, Schrappe M. Clinical outcome of patients with childhood acute lymphoblastic leukaemia and an initial leukaemic blood blast count of less than 1000 per microliter. Klinische Padiatrie. 2001;213(4):169-74.
9. Jing D, Bhadri VA, Beck D, Thoms JA, Yakob NA, Wong JW, et al. Opposing regulation of BIM and BCL2 controls glucocorticoid-induced apoptosis of pediatric acute lymphoblastic leukemia cells. Blood. 2015;125(2):273-83.
10. van der Zwet JCG, Smits W, Buijs-Gladdines J, Pieters R, Meijerink JPP. Recurrent NR3C1 Aberrations at First Diagnosis Relate to Steroid Resistance in Pediatric T-Cell Acute Lymphoblastic Leukemia Patients. Hemasphere. 2021;5(1):e513.
11. Li Y, Buijs-Gladdines JG, Cante-Barrett K, Stubbs AP, Vroegindeweij EM, Smits WK, et al. IL-7 Receptor Mutations and Steroid Resistance in Pediatric T cell Acute Lymphoblastic Leukemia: A Genome Sequencing Study. PLoS Med. 2016;13(12):e1002200.
12. Delgado-Martin C, Meyer LK, Huang BJ, Shimano KA, Zinter MS, Nguyen JV, et al. JAK/STAT pathway inhibition overcomes IL7-induced glucocorticoid resistance in a subset of human T-cell acute lymphoblastic leukemias. Leukemia. 2017;31(12):2568-76.
13. Meyer LK, Huang BJ, Delgado-Martin C, Roy RP, Hechmer A, Wandler AM, et al. Glucocorticoids paradoxically facilitate steroid resistance in T-cell acute lymphoblastic leukemias and thymocytes. J Clin Invest. 2019.
14. Jiang Q, Li WQ, Aiello FB, Mazzucchelli R, Asefa B, Khaled AR, et al. Cell biology of IL-7, a key lymphotrophin. Cytokine Growth Factor Rev. 2005;16(4-5):513-33.
15. Hong C, Luckey MA, Park JH. Intrathymic IL-7: the where, when, and why of IL-7 signaling during T cell development. Semin Immunol. 2012;24(3):151-8.

16. Barata JT, Silva A, Brandao JG, Nadler LM, Cardoso AA, Boussiotis VA. Activation of PI3K is indispensable for interleukin 7-mediated viability, proliferation, glucose use, and growth of T cell acute lymphoblastic leukemia cells. J Exp Med. 2004;200(5):659-69.
17. Ribeiro D, Melao A, van Boxtel R, Santos CI, Silva A, Silva MC, et al. STAT5 is essential for IL-7-mediated viability, growth, and proliferation of T-cell acute lymphoblastic leukemia cells. Blood Adv. 2018;2(17):2199-213.
18. Wingelhofer B, Neubauer HA, Valent P, Han X, Constantinescu SN, Gunning PT, et al. Implications of STAT3 and STAT5 signaling on gene regulation and chromatin remodeling in hematopoietic cancer. Leukemia. 2018;32(8):1713-26.
19. De Smedt R, Morscio J, Reunes L, Roels J, Bardelli V, Lintermans B, et al. Targeting cytokine- and therapy-induced PIM1 activation in preclinical models of T-cell acute lymphoblastic leukemia and lymphoma. Blood. 2020;135(19):1685-95.
20. Govaerts I, Jacobs K, Vandepoel R, Cools J. JAK/STAT Pathway Mutations in T-ALL, Including the STAT5B N642H Mutation, are Sensitive to JAK1/JAK3 Inhibitors. Hemasphere. 2019;3(6):e313.
21. Richter-Pechanska P, Kunz JB, Hof J, Zimmermann M, Rausch T, Bandapalli OR, et al. Identification of a genetically defined ultra-high-risk group in relapsed pediatric T-lymphoblastic leukemia. Blood Cancer J. 2017;7(2):e523.
22. Roberts AW, Davids MS, Pagel JM, Kahl BS, Puvvada SD, Gerecitano JF, et al. Targeting BCL2 with Venetoclax in Relapsed Chronic Lymphocytic Leukemia. N Engl J Med. 2016;374(4):311-22.
23. Chonghaile TN, Roderick JE, Glenfield C, Ryan J, Sallan SE, Silverman LB, et al. Maturation stage of T-cell acute lymphoblastic leukemia determines BCL-2 versus BCL-XL dependence and sensitivity to ABT-199. Cancer Discov. 2014;4(9):1074-87.
24. Karol SE, Alexander TB, Budhraja A, Pounds SB, Canavera K, Wang L, et al. Venetoclax in combination with cytarabine with or without idarubicin in children with relapsed or refractory acute myeloid leukaemia: a phase 1, dose-escalation study. Lancet Oncol. 2020;21(4):551-60.
25. Li Z, He S, Look AT. The MCL1-specific inhibitor S63845 acts synergistically with venetoclax/ABT-199 to induce apoptosis in T-cell acute lymphoblastic leukemia cells. Leukemia. 2019;33(1):262-6.
26. Xie M, Yang A, Ma J, Wu M, Xu H, Wu K, et al. Akt2 mediates glucocorticoid resistance in lymphoid malignancies through FoxO3a/Bim axis and serves as a direct target for resistance reversal. Cell Death Dis. 2019;9(10):1013.
27. Cante-Barrett K, Spijkers-Hagelstein JA, Buijs-Gladdines JG, Uitdehaag JC, Smits WK, van der Zwet J, et al. MEK and PI3K-AKT inhibitors synergistically block activated IL7 receptor signaling in T-cell acute lymphoblastic leukemia. Leukemia. 2016;30(9):1832-43.
28. Gutierrez A, Sanda T, Grebliunaite R, Carracedo A, Salmena L, Ahn Y, et al. High frequency of PTEN, PI3K, and AKT abnormalities in T-cell acute lymphoblastic leukemia. Blood. 2009;114(3):647-50.
29. Chu N, Salguero AL, Liu AZ, Chen Z, Dempsey DR, Ficarro SB, et al. Akt Kinase Activation Mechanisms Revealed Using Protein Semisynthesis. Cell. 2018;174(4):897-907 e14.
30. Liu P, Begley M, Michowski W, Inuzuka H, Ginzberg M, Gao D, et al. Cell-cycle-regulated activation of Akt kinase by phosphorylation at its carboxyl terminus. Nature. 2014;508(7497):541-5.
31. van der Zwet JCG, Cordo V, Cante-Barrett K, Meijerink JPP. Multi-omic approaches to improve outcome for T-cell acute lymphoblastic leukemia patients. Adv Biol Regul. 2019;74:100647.

32. Le Tourneau C, Delord JP, Goncalves A, Gavoille C, Dubot C, Isambert N, et al. Molecularly targeted therapy based on tumour molecular profiling versus conventional therapy for advanced cancer (SHIVA): a multicentre, open-label, proof-of-concept, randomised, controlled phase 2 trial. Lancet Oncol. 2015;16(13):1324-34.
33. Marquart J, Chen EY, Prasad V. Estimation of the Percentage of US Patients With Cancer Who Benefit From Genome-Driven Oncology. JAMA Oncol. 2018;4(8):1093-8.
34. Massard C, Michiels S, Ferte C, Le Deley MC, Lacroix L, Hollebecque A, et al. High-Throughput Genomics and Clinical Outcome in Hard-to-Treat Advanced Cancers: Results of the MOSCATO 01 Trial. Cancer Discov. 2017;7(6):586-95.
35. Ma X, Liu Y, Liu Y, Alexandrov LB, Edmonson MN, Gawad C, et al. Pan-cancer genome and transcriptome analyses of 1,699 paediatric leukaemias and solid tumours. Nature. 2018;555(7696):371-6.
36. Ni Chonghaile T, Sarosiek KA, Vo TT, Ryan JA, Tammareddi A, Moore Vdel G, et al. Pretreatment mitochondrial priming correlates with clinical response to cytotoxic chemotherapy. Science. 2011;334(6059):1129-33.

A

Nederlandse samenvatting
Curriculum Vitae
List of Publications
Acknowledgements

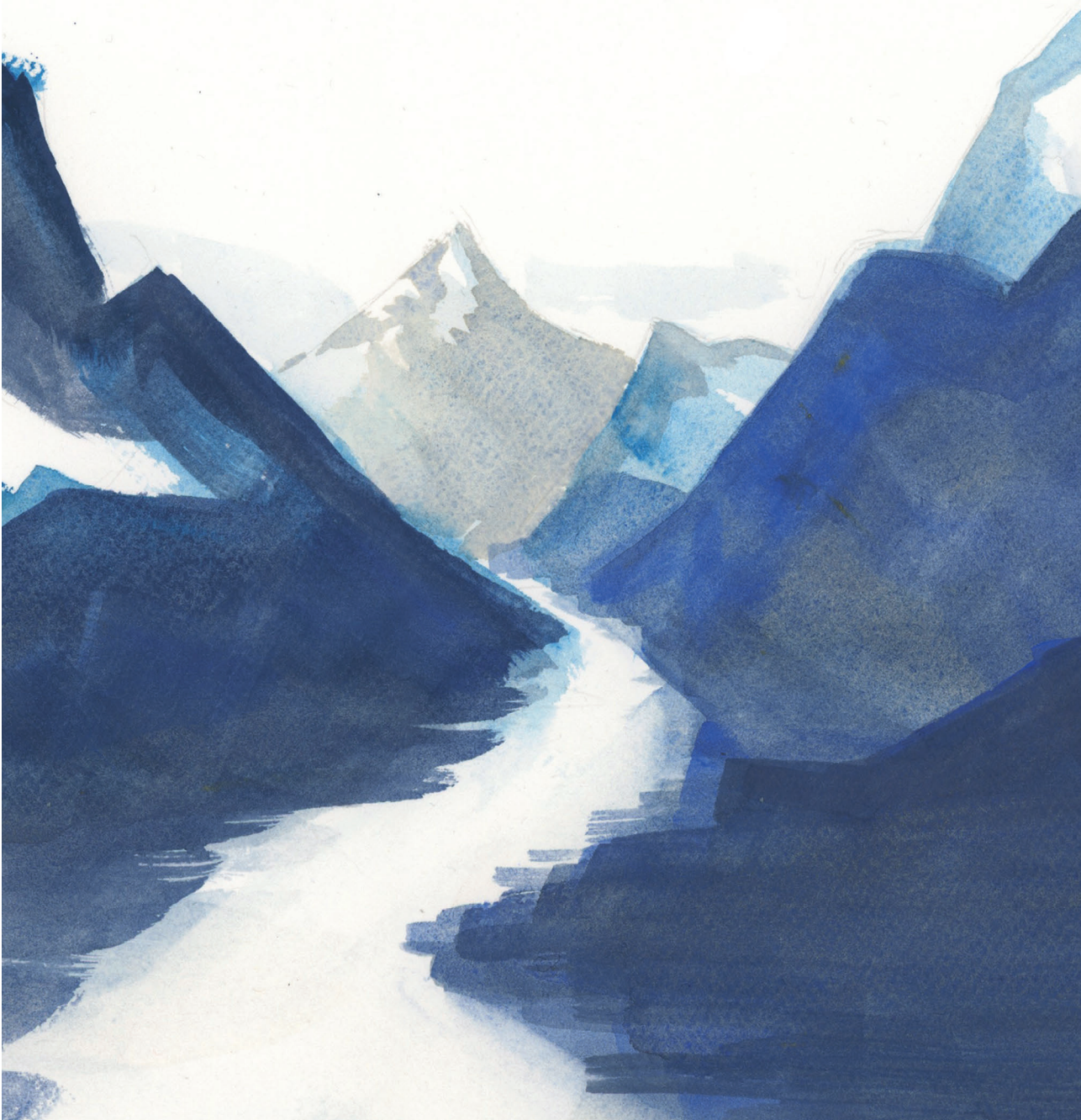

NEDERLANDSE SAMENVATTING

De productie van bloedcellen (hematopoëse) is een complex mechanisme wat zich grotendeels afspeelt in het beenmerg. Onder invloed van lokale omgevingsfactoren kunnen stamcellen zich ontwikkelen (differentiëren) naar rode bloedcellen, bloedplaatjes of witte bloedcellen. Lymfocyten, een type gespecialiseerde witte bloedcellen, spelen een cruciale rol in het verworven immuunsysteem. Tijdens de differentiatie van de hematopoëtische stamcel naar een volwassen lymfocyt kunnen (genetische) fouten in de cel ontstaan. Normaliter worden foutieve, onvolledig gedifferentieerde (immature) cellen door cellulaire verdedigingsmechanismen opgeruimd. Sommige foutieve cellen worden echter niet opgeruimd en/of beschikken over een overlevingsvoordeel. Als een immature foutieve lymfocyt de potentie krijgt tot ongecontroleerde groei, kan leukemie ontstaan.

Leukemie is de meest voorkomende kanker bij kinderen in Nederland. Leukemie bij kinderen ontstaat meestal door de kwaadaardige (maligne) expansie van immature foutieve lymfocyten (acute lymfatische leukemie; ALL), en betreft in 85% van de patiënten expansie van maligne B-lymfocyten (B-cel acute lymfatische leukemie; B-ALL) en in 15% van de patiënten expansie van maligne T-lymfocyten (T-cel acute lymfatische leukemie; T-ALL). Door de sterk verbeterde behandeling van kinderleukemie is de 5-jaars overleving van acute lymfatische leukemie hoger dan 90%. Helaas is de prognose van T-ALL minder goed dan de prognose van B-ALL en krijgt 1 op de 5 kinderen met T-ALL een terugval (recidief). Bij een T-ALL recidief zijn de leukemiecellen vaak erg ongevoelig voor chemotherapie (resistentie) en is de prognose daarom erg somber.

Als een hematopoëtische stamcel in het beenmerg differentieert naar een voorloper T-cel, migreert deze cel naar de thymus waar de cel door lokale omgevingssignalen uit kan groeien tot een volwassen T-cel. Een belangrijke omgevingsstof in de thymus is interleukine-7 (IL-7). Als de voorloper T-cel in contact komt met IL-7, bindt deze interleukine aan de interleukine-7 receptor (IL7R) op het buitenmembraan van de T-cel. Deze interactie activeert een specifieke signaalcascade in de T-cel, waarbij meerdere eiwitten in de cel geactiveerd worden. Deze eiwitten reguleren op hun beurt de expressie van genen in de celkern en stimuleren daarmee de overleving of groei van de zich ontwikkelende T-cel.

In immature leukemiecellen (lymfoblasten) van kinderen met T-ALL worden in bijna 35% van de patiënten mutaties gevonden in genen betrokken bij de IL7R signaalcascade. Dit betreft zowel mutaties van de IL7R als mutaties in eiwitten die normaal door de IL7R geactiveerd worden. Door deze mutaties heeft de lymfoblast geen omgevingssignaal meer nodig om (een gedeelte) van de IL7R cascade te activeren, met een overlevingsvoordeel als gevolg. Eerder toonde onze onderzoeksgroep aan dat T-ALL cellen met een mutatie in het IL7R pad minder gevoelig zijn voor steroïde

behandeling. Aangezien behandeling met hoge dosis synthetische steroïden essentieel is in de behandeling van kinderleukemie, beïnvloeden deze 'IL7R signaleringsmutaties' chemo-gevoeligheid en daarmee de prognose. Het doel van dit proefschrift is om te onderzoeken waarom mutaties in de IL7R signaleringscascade leukemiecellen resistent maken voor synthetische steroïden, zoals prednisolon en dexamethason. Daarnaast onderzochten we of nieuwe gerichte medicijnen IL7R-gedreven steroïde resistentie ongedaan kan maken of kan voorkomen.

Op dit moment worden meer dan 40 nieuwe therapieën en medicijnen onderzocht in een klinische of preklinische setting voor leukemie. **Hoofdstuk 2** geeft een overzicht over al deze nieuwe therapieën. Sommige van deze medicijnen werken niet goed als monotherapie, maar werken juist sterker als ze gecombineerd worden met andere (chemo)therapie zoals synthetische steroïden. Als gezonde of maligne lymfocyten in contact komen met steroïden zal de steroïdereceptor (NR3C1) van de T-cel de expressie van het gen *BIM* induceren. Het eiwit BIM reguleert de geprogrammeerde celdood (apoptose) van een cel door te binden aan anti-apoptotische eiwitten (BCL2, BCL-XL en MCL-1). Hiermee vangt BIM deze eiwitten weg bij de mitochondriële membranen van de cel. Bij een verhoogde expressie van BIM door steroïde behandeling vangt het pro-apoptotische eiwit BIM dus meer anti-apoptotische eiwitten weg, wat leidt tot mitochondrieel geïnduceerde celdood. In **hoofdstuk 3** onderzochten we of mutaties in de steroïdereceptor *NR3C1* invloed hebben op steroïde gevoeligheid. We vonden een relatie met genetische *NR3C1* afwijkingen en steroïde resistentie, waarbij meerdere gemuteerde NR3C1 varianten de expressie van *BIM* nog wel goed kon induceren in de aanwezigheid van prednisolon. Hoofdstuk 3 concludeert dat andere cellulaire mechanismen mogelijk dominanter zijn om steroïde gevoeligheid te reguleren.

In het vervolg van het onderzoek richten we ons op de drie individuele signaleringstakken van de IL7R signaleringscascade: het JAK-STAT pad, het PI3K-AKT pad en het MAPK-ERK pad. Deze paden worden aangezet bij activatie van de IL7R. Het MAPK-ERK pad is het minst bestudeerde signaleringspad van de IL7R cascade. In **hoofdstuk 4** vonden we dat dit pad echter een cruciale rol speelt in steroïde resistentie. Mutaties hoog in de IL7R cascade (zoals JAK1 en IL7R mutaties) en RAS mutaties zorgen voor sterke MAPK-ERK activatie. Geactiveerd ERK inactiveert pro-apoptosisch BIM middels fosforylatie van BIM. We vonden dat gefosforyleerd BIM niet meer goed kon binden aan anti-apoptotische eiwitten BCL2, BCL-XL en MCL-1, waardoor behandeling met steroïden minder apoptose induceerde. Door BIM inactiviteit te identificeren als mechanisme van steroïde resistentie ten gevolge van activatie van het MAPK-ERK pad, toonden we aan dat inhibitie van het MAPK-ERK pad door de MEK-inhibitor Selumetinib de functie van BIM weer kon herstellen. Nog belangrijker: Selumetinib werkte versterkend (synergistisch) in combinatie met synthetische steroïden om apoptose van T-ALL cellen te bewerkstelligen. De JAK1-inhibitor Ruxolitinib kon de inactivatie van BIM ook ongedaan maken, maar alleen indien het MAPK-ERK pad geactiveerd werd door IL7R

of JAK1 activatie. Daarom werkte Ruxolitinib alleen synergistisch met prednisolon in T-ALL cellen waarbij de steroïde resistentie afhankelijk was van de aanwezigheid van IL7.

In **hoofdstuk 5** onderzochten we de toepassing van 'BH3-mimetics', een nieuwe therapie die de functie van BIM nabootst en dus selectief kan binden aan BCL2, BCL-XL en/of MCL-1. De BH3-mimetic Venetoclax, die specifiek aan het anti-apoptotische eiwit BCL2 bindt, bleek ook synergistisch te werken met synthetische steroïden voor T-ALL cellen met IL7-afhankelijke steroïde resistentie. Synergie werd ook geobserveerd bij 'triple therapie' met Venetoclax, prednisolon en Selumetinib. Echter vonden we dat inhibitie van het MAPK-ERK pad, en daarmee behoud van de functie van pro-apoptotisch BIM, effectiever leek dan inhibitie van anti-apoptotiche eiwitten. Meer studies zijn nodig om te onderzoeken hoe BH3-mimetics effectief ingezet kunnen worden in de behandeling van kinderleukemie.

In **hoofdstuk 6** vonden we dat, in tegenstelling tot eerdere studies, de activatie van het JAK-STAT pad op zichzelf niet voldoende is om steroïde resistentie te induceren. Activatie van dit pad leidt tot opregulering van anti-apoptotisch BCL2 en BCLXL, waarbij de expressie van deze eiwitten zelfs hoger werd in de aanwezigheid van steroïden. We toonden aan dat de opregulering van anti-apoptotische eiwitten geantagoneerd werd door effectieve simultane opregulering van BIM. In de afwezigheid van BIM inhiberende gebeurtenissen, zoals fosforylatie door MAPK-ERK activatie, lijkt JAK-STAT pad activatie niet direct te leiden tot steroïde resistentie. Daarnaast vonden we een nieuw mechanisme waarin NR3C1 en STAT5 als transcriptiefactoren samenwerken om zo de expressie van STAT5 gereguleerde genen te reguleren.

Het laatste pad van de IL7R signaleringscascade, het PI3K-AKT pad, werd bestudeerd in **hoofdstuk 7**. Ondanks dat normale PI3K-AKT activatie leidt tot steroïde resistentie, zorgde de activerende AKT^{E17K} mutatie niet voor steroïde resistentie. Door de functionele verschillen tussen normaal (wild-type) AKT en mutant AKT te bestuderen, vonden we aanwijzingen dat de cellulaire lokalisatie en specifieke fosforylatie status van AKT de steroïde gevoeligheid van T-ALL cellen kan beïnvloeden. Meer onderzoek is nodig om te bestuderen hoe deze functionele verschillen exact leiden tot een verschil in steroïde gevoeligheid.

In hoofdstuk 4-7 vonden we verschillende mechanismen die de steroïde gevoeligheid kunnen beïnvloeden. **Hoofdstuk 8** discussieert over hoe 'diagnostische screeningsmiddelen' de behandeling van leukemie beter en gepersonaliseerd kunnen maken. Door te screenen voor activatie van specifieke signaalpaden die betrokken zijn bij chemo-resistentie, zoals MAPK-ERK pad activatie, kan een gepersonaliseerd behandelingsadvies gegeven worden zoals het toevoegen van een MEK-inhibitor. Screenen kan op drie niveaus: screenen naar belangrijke mutaties (genomics), screenen op (in)activatie van eiwitten van specifieke signaalpaden (proteomics) en screenen

van de transcriptie van genen betrokken bij celgroei of overleving (transcriptomics). De integratie van deze 'multi-omic' screeningsmiddelen in combinatie met nieuwe technieken, zoals BH3-profiling, kan de behandeling en daarmee prognose van kinderleukemie verder verbeteren.

Concluderend toont deze thesis dat het MAPK-ERK signaal pad, als onderdeel van de IL7R signaleringscascade, een essentiële rol speelt in steroïde resistentie in T-ALL. Inhibitie van dit pad lijkt de behandeling en daarmee prognose van T-ALL te kunnen verbeteren. Op basis van onze resultaten zouden MEK-inhibitors Selumetinib of Trametinib verkozen moeten worden boven de JAK1-inhibitor Ruxolitinib. Deze resultaten ondersteunen de inclusie van meer T-ALL patiënten in de SeluDex trial (NCT03705507) en ondersteunen het gebruik van MEK-inhibitors in nieuwe basket-trials voor T-ALL patiënten met IL7R signaleringsmutaties.

CURRICULUM VITAE

Jordy van der Zwet was born on the 21st of February in 1992 in Rotterdam, the Netherlands. After graduating secondary school at the Sint Laurens College in 2009, he started his medical training at the Erasmus University in Rotterdam. During his third year of medical school, he performed his minor internship in the pediatric oncology ward of the Sophia Children's Hospital in Rotterdam under the supervision of Dr. Auke Beishuizen. In 2015, he performed his masters research internship at the Dana-Farber Cancer Institute at Harvard Medical School, Boston, USA, under the supervision of Dr. David Weinstock and Nadja Kopp. During this internship, he studied the structural and oncogenic effects of JAK2 mutations in B-cell acute lymphoblastic leukemia (B-ALL) and the implication of the novel JAK2 inhibitor CHZ868. This internship was his first exposure to pre-clinical and fundamental research. The acquired interest in pediatric oncology and pre-clinical research motivated him to improve his knowledge in molecular science, cellular mechanisms and genetics. Therefore, upon his return from Boston, he worked as a student in the research group of Dr. Jules Meijerink and assisted in writing a grant proposal that was funded by the Stichting Kinderen Kankervrij (KiKa). Upon finalizing his clinical rotations in April 2016, he started his PhD study with the Meijerink Research Team in Rotterdam, and continued his research at the Princess Máxima Center for Pediatric Oncology in Utrecht when the team relocated. Since January 2021, he is working as a resident (ANIOS) in the Department of Pediatrics at the Franciscus Gasthuis & Vlietland Hospital in Rotterdam. This summer, he will start as a resident in training (AIOS) in Pediatrics at the Wilhelmina Kinderziekenhuis in Utrecht.

LIST OF PUBLICATIONS

Jordy C G van der Zwet, Jessica G C A M Buijs-Gladdines, Valentina Cordo', Donna O Debets, Willem K Smits, Zhongli Chen, Jelle Dylus, Guido J R Zaman, Maarten Altelaar, Koichi Oshima, Beat Bornhauser, Jean-Pierre Bourquin, Jan Cools, Adolfo A Ferrando, Josef Vormoor, Rob Pieters, Britta Vormoor, Jules P P Meijerink. MAPK-ERK is a central pathway in T-cell acute lymphoblastic leukemia that drives steroid resistance. **Leukemia** 2021 Dec;35(12):3394-3405.

Valentina Cordo', **Jordy C G van der Zwet**, Kirsten Canté-Barrett, Rob Pieters and Jules P P Meijerink. T-cell Acute Lymphoblastic Leukemia: A Roadmap to Targeted Therapies. **Blood Cancer Discovery** January 2021, BCD-20-0093.

Jordy C G van der Zwet, Willem Smits, Jessica G C A M Buijs-Gladdines, Rob Pieters, and Jules P P Meijerink. Recurrent *NR3C1* Aberrations at First Diagnosis Relate to Steroid Resistance in Pediatric T-Cell Acute Lymphoblastic Leukemia Patients. **HemaSphere** 2021 Jan; 5(1): e513.

Jordy C G van der Zwet, Valentina Cordo', Kirsten Canté-Barrett, Jules P P Meijerink. Multi-omic approaches to improve outcome for T-cell acute lymphoblastic leukemia patients. **Adv. Biol. Regul**. 2019 Dec;74:100647.

K Canté-Barrett, J A P Spijkers-Hagelstein, J G C A M Buijs-Gladdines, J C M Uitdehaag, W K Smits, **J van der Zwet**, R C Buijsman, G J R Zaman, R Pieters, J P P Meijerink. MEK and PI3K-AKT inhibitors synergistically block activated IL7 receptor signaling in T-cell acute lymphoblastic leukemia. **Leukemia** 2016 Sep;30(9):1832-43.

Shuo-Chieh Wu, Loretta S Li, Nadja Kopp, Joan Montero, Bjoern Chapuy, Akinori Yoda, Amanda L Christie, Huiyun Liu, Alexandra Christodoulou, Diederik van Bodegom, **Jordy van der Zwet**, Jacob V Layer, Trevor Tivey, Andrew A Lane, Jeremy A Ryan, Samuel Y Ng, Daniel J DeAngelo, Richard M Stone, David Steensma, Martha Wadleigh, Marian Harris, Emeline Mandon, Nicolas Ebel, Rita Andraos, Vincent Romanet, Arno Dölemeyer, Dario Sterker, Michael Zender, Scott J Rodig, Masato Murakami, Francesco Hofmann, Frank Kuo, Michael J Eck Lewis B Silverman, Stephen E Sallan, Anthony Letai, Fabienne Baffert, Eric Vangrevelinghe, Thomas Radimerski, Christoph Gaul, David M Weinstock. Activity of the Type II JAK2 Inhibitor CHZ868 in B Cell Acute Lymphoblastic Leukemia. **Cancer Cell** 2015 Jul 13;28(1):29-41.

ACKNOWLEDGEMENTS

Ondanks dat alleen mijn naam op de voorkant van deze thesis staat, is de weg naar – en de inhoud van – deze thesis echt het resultaat van **teamwork**. Daarom, aan iedereen die keihard gewerkt heeft aan dit onderzoek, kritisch heeft meegedacht, heeft meegeschreven, mijn enthousiaste verhalen en frustraties heeft aangehoord, morele support is geweest en mij door dik en dun gesteund heeft: dank jullie wel!

Prof. dr. R. Pieters, beste **Rob**, dank voor je supervisie en kritische feedback op de publicaties en deze thesis. Ik heb altijd erg veel bewondering gehad voor de totstandkoming van het Prinses Máxima Centrum en vond het een eer om zo vroeg in het bestaan al deel uit te mogen maken van dit prachtige centrum.

Dr. J.P.P. Meijerink, beste **Jules**, bedankt voor alle kansen die je mij hebt geboden in de afgelopen jaren. Door jouw begeleiding heb ik in een paar jaar tijd kunnen groeien van jonge dokter tot zelfstandige wetenschapper. Je hebt hart voor het vak en voor de mensen in je team, eigenschappen die ik altijd erg gewaardeerd heb. Je bent ontzettend enthousiast, gedreven en altijd kritisch op de kwaliteit van onderzoek. Eigenschappen die ik ook bij mijzelf herken en daarom soms voor pittige, maar ook inspiratievolle discussies zorgde. De kwaliteit van deze thesis is zonder twijfel het resultaat van jouw enorme betrokkenheid en de samenwerking die we hebben gehad. Ik kijk met ontzettend veel plezier terug naar de tijd die ik in je groep gewerkt heb!

Dank aan de leden van leescommissie: prof. dr. ir. Boudewijn M.T. Burgering, prof. dr. Monique L. den Boer, prof. dr. Jan Cools, prof. dr. H. Josef Vormoor en prof. dr. Eric F. Eldering. Daarnaast wil ik graag dr. Lotte E. van der Wagen en dr. Melanie Hagleitner bedanken voor het plaatsnemen in de grote commissie.

Lieve **Jessica**, ik heb ontzettend genoten van onze tijd samen in het lab. Niet alleen over werk, maar ook over de zaken ernaast konden we uren praten. We waren een ijzersterk team, stonden voor elkaar klaar en deelde zowel hoogte- als dieptepunten met een lach of een traan. Je was geduldig toen ik als ongetrainde kluns het lab in kwam, je ging altijd precies en correct te werk en je hebt een jaloersmakende werkdiscipline. Ik snap wel waarom ze een western blot machine naar jou vernoemd hebben. Zonder jou was deze thesis nooit zo mooi geworden. Stiekem hoort ook jouw naam op de voorkant. Onwijs bedankt voor alle mooie momenten die we met elkaar hebben meegemaakt! Ik ben ontzettend blij je aan mijn zijde te hebben als mijn paranimf.

Dear **Valentina**, you know how disappointed I initially was when you joined the group. ‘Great, now I’m still the dumbest around’. From there on our friendship grew stronger and we eventually became partners in crime in the lab. ‘No drama’ in the ML-1 with the stereo on max volume. I always valued your opinion and expertise, even when I

was mister *saputello* again. But to be honest, your western blots do look better now, *prego*. In tough times we helped each other out, keeping the spirits high, *morituri te salutant*. Thank you for all the amazing times we spend together! I'm glad to have you by my side as my paranymph.

Altijd kwam er gelach uit onze hoek van de kantoortuin en we droegen op meerdere vlakken ons steentje bij aan het centrum. De Meijerink borrels waren toch wel de beste en meest creatieve al zeg ik het zelf, van IKEA ballenbak tot chocolademelk met rum. Maar de pubquiz avond die ons PhD team voor alle PhD'ers organiseerde blijft toch een hoogtepunt. **Vera** en **Emma**, bedankt voor jullie gezelligheid en support deze jaren! Heel tof dat we met z'n 4'en (en team 'van Leeuwen') ook zoveel leuke dingen deden en doen, van borrels tot carnaval tot quarantaine Skype lunches. Als mensen mij direct vinden, dan kennen ze jullie overduidelijk nog niet. Vlijmscherp en gevat, vleugje sarcasme, ik heb er onwijs van genoten!

Met **Rico** op de linkerhand en **Eric** op de rechterhand was ik in het midden natuurlijk altijd de sjaak. Rico, sorry dat ik altijd commentaar had als jij weer 2 uur lang deed over het juiste kleurtje vinden voor een figuur. Hier bleek ik me achteraf voor de STAT5 paper ook schuldig aan te maken. Gelukkig heb ik je verder nooit gestalkt voor extra analyses terwijl je kinderen thuis aandacht nodig hadden. Eric, ontzettend droog en nuchter en altijd je snoep verstoppen voor de baas. Is dit het moment om te bekennen dat ik toch een significant deel van de 5 kilo emmer heb opgegeten?

'Moet er nog een PCR gedaan worden, dan vraag je **Wilco** toch even'? En zo geschiede. Altijd vrolijk, (bijna) niets was te veel, en stiekem onwijs gevat en grappig, bedankt! En **Kirsten**, als ervaren wetenschapper altijd bereid mee te denken en in voor gezelligheid. **Marloes** en **Mariska**, ook jullie bedankt voor al jullie input en werk aan de projecten. En natuurlijk de 2 briljante studenten die ik heb mogen begeleiden gedurende hun stages, **Isabella** en **Laura**.

Zowel binnen als buiten het centrum was men in voor samenwerkingen. **Annelienke**, één keer knipperen en opeens zat je in de celkweek in plaats van achter je computer voor de DexaDays. Gelukkig was het onwijs gezellig om ellendig veel klonen op te kweken en ik weet zeker dat die top publicatie er gaat komen. **Kim**, als je dan door corona toch niet meer terug kan naar Amerika, dan maar gezellig bij ons in het lab je een RSI pipetteren voor BH3 profiling toch? Dank voor het delen van al je kennis en hopelijk komen we elkaar in de kliniek weer snel tegen! Verder ook dank aan het team van **Anne Rios** voor hun hulp bij de fluorescentie microscopie experimenten, met speciale dank aan **Frank**. **Donna** en **Maarten**, dank voor jullie harde werk en bijdrage aan het phospho-BIM project middels de massaspectrometrie. En natuurlijk veel dank aan **Guido**, **Jelle** en **Martine**. Vele bezoeken en skype calls verder, maar het mega synergie experiment heeft zijn vruchten afgeworpen. Dank voor jullie geduld toen ik weer honderden vragen had

over de data en Excel files, en onwijs tof dat **NTRC** (Netherlands Translational Research Center) een bijdrage wilde leveren aan het drukken van deze thesis.

Behalve al het harde werk, was er in het Máxima genoeg ruimte voor plezier en gezelligheid. **Britt, Gawin, Miriam, Trisha en Willem,** team 'van Leeuwen', ik hoop dat we de feestjes nog lange tijd door zullen zetten! Discolamp huiskamer feestjes, emotionele carnaval sessies, zelf gebrouwen Duitse likeur afkraken, kilo's kalkoen eten met Friendsgiving en natuurlijk opscheppen over het mooie Rotterdam. Zomaar een reeks aan memorabele momenten.

The biggest benefit of starting at the Hubrecht Institute was by far the **Freezer Room**. We loved the room, our PIs slightly less. Mispronounced something: post-it. Insulted somebody: post-it. Asking critical questions to your student: post-it. Although we shared the room with many amazing colleagues, I shared the craziest times with **Patricia**, **Jiangyan** and **Zeljko**. A German, Chinese, Serbian and Dutchman stepped into a karaoke 'bar' or lasergame arena… And no, this isn't the start of a joke. Thank you for all the laughs and language lessons, although I'm pretty sure I won't impress locals with the acquired vocabulary.

Thanks to all the members of the PriMaPhD group: **Camilla**, **Eline**, **Elvin**, **Evelyn**, **Janna**, **Kaylee**, **Leiah**, **Loes**, **Lindy**, **Madeleine** and **Winnie**, and **Hans** for supervising us. I think we did an amazing job establishing a group that all PhD'ers of the Máxima could depend on. Thanks **Naomi** and **Karlijn**, the ASH 2019 detour crew. And thank you to so, so many other amazing PhD students and colleagues I've met throughout these years. En dank aan alle mensen die mij achter de schermen geholpen hebben in het PhD traject: **Sabine**, **Anna**, **Laurens**, **Frank** en **Jacqueline**.

En uiteraard dank aan de mensen die mijn interesse in preklinisch onderzoek vroeg aanwakkerde. **Auke**, voor het mentorschap vanaf de minor kinderoncologie, de begeleiding van mijn masteronderzoek en het faciliteren van een prachtige stage naar Boston. **David** and **Nadja**, thank you for the amazing opportunity and guidance at the Dana-Farber Cancer Institute. Nadja, who had to patience to guide a student who didn't even know what a PCR was. And look at this thesis now.

En dan de mensen die niet in het lab stonden, maar daarnaast ontzettend belangrijk voor me waren en dat nog steeds zijn. Het **WND kartel**, er is echt geen groep die in meer geuren en kleuren alle ups en downs van de afgelopen jaren meegekregen hebben. 'Komt 'ie weer hoor'. **Amy**, **Douwe**, **Kris**, **Merel** en **Peter**: onwijs bedankt voor al jullie support, ik kan me echt geen betere vriendengroep wensen. Geduldig en empathisch al mijn 'belachelijk succesvolle' en minder succesvolle verhalen aanhoren, om me vervolgens weer volledig met de grond gelijk te maken. De reflectie en relativering die

ik nodig heb gehad. Ik kan me alleen maar gelukkig prijzen dat jullie vanaf de zijlijn zo'n grote rol hebben gespeeld in mijn PhD rollercoaster. Maar hé: geluk dwing je af toch?

Ook dank aan alle familie leden en grootouders van de familie Janssen en Van der Zwet. Altijd geïnteresseerd in wat ik allemaal aan het doen ben, waar ik in de wereld dan ook ben. Speciale dank aan **Marnix**, jij weet dat het PhD traject soms echt wel pittig was voor me. Maar jij weet ook als enige wat voor lijdensweg we hebben doorstaan om de inspiratie van deze thesis cover vast te leggen. Ontzettend bijzonder hoe **Evelien Jagtman** dat moment heeft vormgegeven, waarbij het waanzinnige uitzicht op de Ama Dablam ook de inhoud van deze thesis reflecteert.

Er waren tijden, nog niet zo heel lang geleden, dat de woorden 'Jordy' en 'hockey' in één ademteug uitgesproken werden. Hockey is voor mij altijd de uitlaatklep geweest tijdens dit promotietraject. Dat ik tijdens mijn promotietraject hoofdcoach zou worden van Dames 1 en mijn eigen hockeybedrijf op zou zetten had ik vooraf ook niet bedacht. Maar waar een passie je wel niet toe kan zetten. **Sonja**, in 2010 voor het eerst met elkaar in de dug-out, en nu samen Highland Hockey, wat een ontzettend toffe reis. **Fieke**, als rebelse aanvoerder in MB1 waren we het gelukkig vaker oneens dan nu bij Highland, en ook wij hebben als coaches mooie tijden beleeft. En natuurlijk **Anouk**, van MD1 tot MC1 tot Dames 1. De mooiste hockeyjaren die ik heb gehad, ik ben onwijs blij die met jou beleefd te hebben. Altijd kon ik op je rekenen, met je sparren als dingen niet liepen en ik weer te veel ballen tegelijk aan het hooghouden was. Onwijs bedankt voor je warme en morele support gedurende deze jaren!

Ook in mijn opleiding ben ik genoeg mensen tegengekomen die mij op verschillende manieren gesteund of geïnspireerd hebben. Speciale dank aan **Clarissa**, **Femke**, **Laura**, **Lisa** en **Lisa**. En de tofste A+ co-groep: **Fenneke**, **Marwa**, **Michele**, **Mijke**, **Leoniek** en **Tim**.

En natuurlijk dank aan al mijn (oud-)collega's in het Franciscus. Het was behoorlijk schakelen na 5 jaar de kliniek uit te zijn geweest. Waar onderzoek eerst centraal stond, kwam ik opeens in een omgeving waar de woorden 'komt 'ie weer met z'n abracadabra onderzoek' naar m'n hoofd geslingerd werden. Speciale dank aan **Amy** en **Sarah**, 'door jullie tegengas ben ik gelukkig zo bescheiden gebleven'. En dank aan **Angelique**, **Alike**, **Nico** en **Gerdien** voor jullie mentorschap, supervisie en begeleiding richting de opleiding Kindergeneeskunde.

Lieve **mam** en **pap**, ontzettend bedankt voor al jullie geduld, support en lieve en bemoedigende woorden de afgelopen jaren. Jullie maakte het mogelijk dat ik naast het onderzoek nog zoveel andere leuke dingen kon doen. Altijd geïnteresseerd en betrokken bij het onderzoek, krantenkoppen en tv-fragmenten van het Máxima verzamelen, frequent langs de zijlijn op HBR en natuurlijk bij Highland Hockey. En mijn

lieve zus, **Yvette**. Het blijft bijzonder hoe mijn stage naar Boston onze band hechter heeft gemaakt. We delen dezelfde passie voor kinderen, al is het uit een hele andere hoek van expertise. Ook bij jou kan ik altijd mijn verhalen kwijt, of gaan we op stap voor leuke uitjes of festivals. Daarbij natuurlijk ook dank aan **Johan**, jullie kunnen natuurlijk altijd bij me aankloppen als de kleine er eindelijk is.